ENERGY CONSERVATION

ORNL/Sub/79-24712/2

Advanced Electric Heat Pump Component Development and Evaluation

Interim Report

S. E. Veyo

WESTINGHOUSE ELECTRIC CORPORATION
R&D Center
1310 Beulah Road
Pittsburgh, Pennsylvania 15235

Work performed for

OAK RIDGE NATIONAL LABORATORY
operated by
UNION CARBIDE CORPORATION
for the

U. S. DEPARTMENT OF ENERGY

OFFICE OF BUILDINGS ENERGY
RESEARCH AND DEVELOPMENT

NOTICE

This report was prepared as an account of work sponsored by an agency of the United States Government. Neither the United States Government nor any agency thereof, nor any of their employees, makes any warranty, expressed or implied, or assumes any legal liability or responsibility for any third party's use or the results of such use of any information, apparatus, product or process disclosed in this report or represents that its use by such third party would not infringe privately owned rights.

ORNL/Sub/79-24712/2

ADVANCED ELECTRIC HEAT PUMP COMPONENT DEVELOPMENT AND EVALUATION

Interim Report

S. E. Veyo, Manager
Heat Exchange Systems Research

September 10, 1982

Report Prepared by
Westinghouse Electric Corporation
R&D Center
1310 Beulah Road
Pittsburgh, Pennsylvania 15235

Under
Subcontract 86X-24712C

for

Oak Ridge National Laboratory
Oak Ridge, Tennessee 37830
operated by
UNION CARBIDE CORPORATION
for the
U.S. DEPARTMENT OF ENERGY
Under Contract No. W-7405-eng-26

ABSTRACT

This report for Tasks 3 and 4 under Contract 86X-24712C documents the Westinghouse effort to October, 1981 toward the development of an advanced electric heat pump 20 percent more efficient than the most efficient unit available in early 1979. The Westinghouse/DOE advanced heat pump will exceed the efficiency of a 1979 model high efficiency two-speed heat pump by 20 percent or more on an annual basis in all but the most southern regions of the continental United States. In colder regions, typified by Minneapolis or Pittsburgh, the estimated efficiency improvement is greater still. This performance is due in part to the development of a high efficiency reciprocating compressor with dual-capacity modulation by stroke change. The efficiency of this compressor exceeds the best currently available. Additional system improvement stems from the development of a microprocessor-based control system plus indoor and outdoor air movers that reduce air moving power by approximately half, relative to the state-of-the-art. Estimated system performance is given along with development details and measured performance for the major components (compressor, heat exchanger, fan, blower, motors).

TECHNICAL CONTRIBUTORS

J. C. Kastovich, Program Manager and Compressor Development Leader

S. E. Veyo, Team Leader - Technology Improvement

R. R. Young, Dual Stroke Compressor

W. A. English, Geared Compressor

R. W. Wolfe, Compressor Computer Analysis

T. J. Fagan, System Performance Analysis and Testing

K. H. Lee, Seasonal Performance Analysis

B. F. Habron, DOE Regulations

R. A. Lucheta, System Optimization

M. C. Chuang, Thermosiphon Heat Exchanger Analysis

N. M. Farukhi, Thermosiphon Heat Exchanger Analysis

T. Wright, Fan Development

D. Ariewitz, Blower Development

H. S. Kirschbaum, Motor Analysis

P. W. Kolody, Motor Analysis

R. Draper, Package Design, Heat Exchanger Analysis, Test Facilities

R. S. Lackey, Package Design, Prototype Design

J. A. Richard, Component Reliability

R. E. Fromson, Manufacturing Analysis

R. M. Hastings, Manufacturing Analysis

A. Meyerhoff, Manufacturing Analysis

F. J. Sisk, Consultant

P. T. Thayer, Consultant

R. G. Colclaser, Controls

R. A. Johnson, Controls

E. J. Phillips, Editing

TABLE OF CONTENTS

1. INTRODUCTION.....1-1

2. SUMMARY AND CONCLUSIONS.....2-1

2.1 System Design.....2-1

2.2 Estimated System Performance.....2-4

2.3 Estimated Seasonal Performance Comparisons.....2-6

2.4 Conclusions.....2-14

3. COMPONENT DEVELOPMENT.....3-1

3.1 Compressor Design and Development.....3-1

3.1.1 Dual Stroke Compressor Design.....3-2

3.1.2 Compressor Motor.....3-15

3.1.3 Dual-Stroke Compressor Performance.....3-23

3.1.4 Geared Two-Speed Compressor.....3-27

3.1.5 Evaluation.....3-33

3.1.6 Supporting Computer Analyses.....3-39

3.2 Heat Exchanger Design and Development.....3-40

3.2.1 Boiling Thermosiphon Evaporator.....3-42

3.2.2 Gravity Driven Condenser.....3-55

3.2.3 Evaluation.....3-63

3.2.4 Conclusions.....3-64

3.3 Air Mover Design and Development.....3-65

3.3.1 Outdoor Air Mover Development.....3-67

3.3.2 Indoor Air Mover.....3-91

3.3.3 Blower Motor.....3-112

3.3.4 Fan Motor.....3-117

3.3.5 Summary and Evaluation.....3-120

3.4 Advanced Heat Pump Controller.....3-122
3.4.1 Introduction.....3-122
3.4.2 Technical Discussions.....3-123
3.4.3 Summary.....3-140
3.5 Heat Pump Package Design and Development.....3-142
3.5.1 Outdoor Unit Package Design and Development.....3-144
3.5.2 Indoor Unit Package Design and Development.....3-164
3.6 Prototype Test Plan.....3-183
3.6.1 Thermodynamic Performance.....3-183
3.6.2 Noise Tests.....3-183

1. INTRODUCTION

The Westinghouse/DOE[1] heat pump research and development program has as its objective the development of a preproduction prototype, commercially and economically viable, advanced heat pump that can provide satisfactory performance with an annual energy efficiency at least 20 percent better than the most efficient units available in the marketplace in early 1979.[2]

The Westinghouse heat pump concept uses the well known vapor compression refrigeration cycle with R22 as the working fluid. To achieve the target efficiency, we have developed an improved reciprocating compressor with modulatable capacity, along with high efficiency air movers, a breadboard microprocessor-based control system, and highly effective heat exchangers. The relative proportions of the compressor, blower, fan, and heat exchangers are specified through system optimization to minimize annual ownership cost while providing comfort. The key to the potential commercial success of this system is the development of low cost compressor capacity modulation means.

This report documents the development path, expected performance, and design features of the Westinghouse/DOE advanced electric heat pump system and constitutive components.

---

1. Advanced Electric Residential Heat Pump Research and Development Program, Contract 86X-24712C.

2. DOE RFP P-2129-86, "Research, Development and Demonstration of an Advanced Electric Heat Pump," February 28, 1979, through Union Carbide Corporation, Nuclear Division.

2. SUMMARY AND CONCLUSIONS

2.1 System Design

An artist's sketch of the Westinghouse design for an advanced electric heat pump is shown in Figure 2.1-1. Air is ingested into the outdoor unit from all four sides and exhausted vertically upward. When the outdoor unit is elevated to provide 8 inches of clearance between the heat exchanger and ground, it occupies less than one cubic meter for a unit with approximately 4 tons maximum cooling capacity. The self-contained individually telescoping legs permit the unit to be elevated as much as two feet above the mounting surface and provide for easy installation on uneven terrain. In northern climates, an installation height of at least 15 inches is recommended in order to forestall snow blockage.

The heat exchanger within the outdoor unit is of the plate fin on tube design, three rows deep and has 13 rippled fins per inch. This heat exchanger is composed of four slab coils, with horizontal tubes. The face of the slab coils is oriented at an angle of 68° to the horizontal in order to facilitate water runoff. The bottom of each coil hangs completely free, thereby preventing the accumulation of ice between the coil and the unit structure. The two-speed outdoor air mover is of high-efficiency design and is constructed as a subassembly for insertion into the unit wrapper. The fan motor is designed for high reliability as well as high efficiency and uses trickle heating during cold weather fan-off situations in order to keep the motor interior dry and free turning.

It is worth noting that all coil surfaces are well protected from damage. During shipping, the telescopic legs retract completely into the unit, permitting a compact shipping carton.

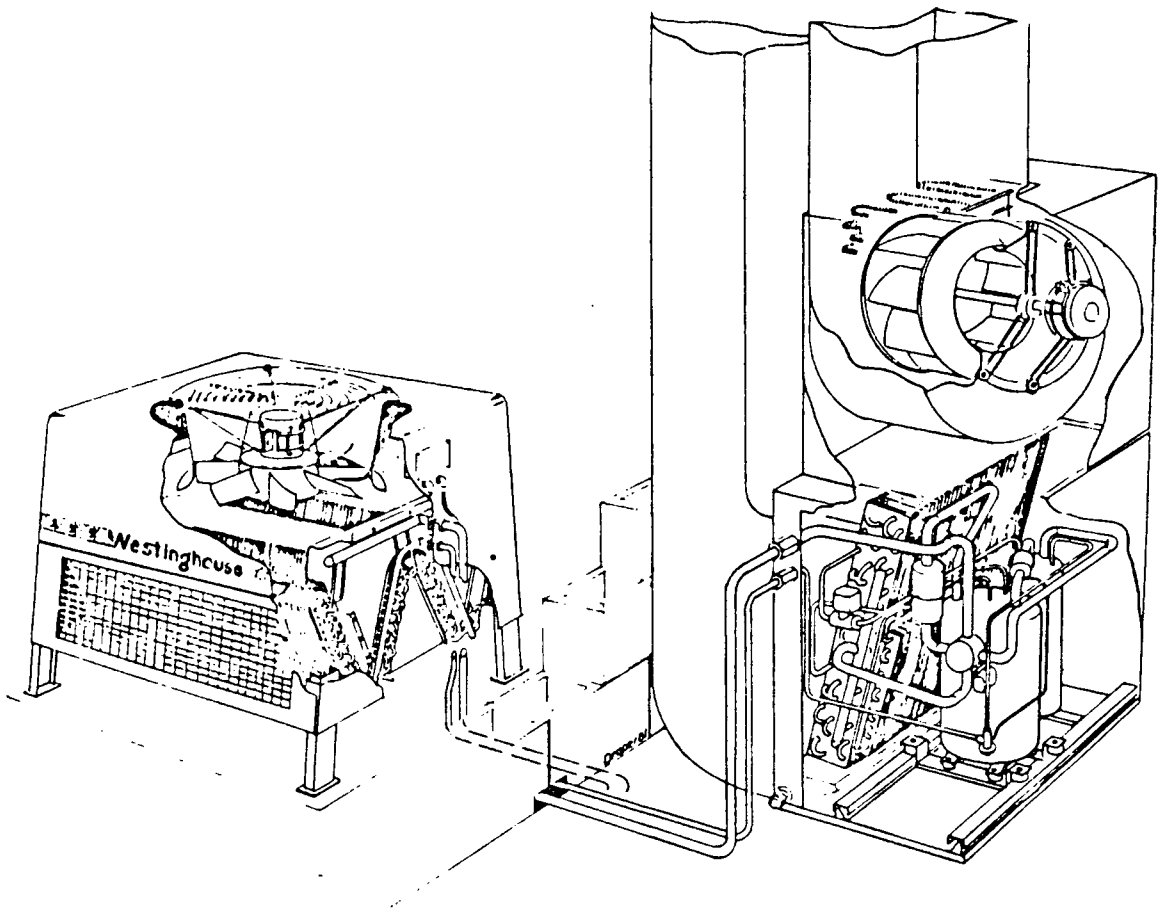

Figure 2.1-1 - Westinghouse-DOE advanced electric heat pump

The indoor unit is modular in four sections. The bottom module shown in Figure 2.1-1 contains the indoor refrigeration machine consisting of an advanced high efficiency dual-stroke compressor, a Hi-Re-Li R type suction line accumulator, a four-row, single slab, plate fin on tube-refrigerant to air heat exchanger, an electrically controlled bidirectional expansion device, the four-way refrigerant flow reversing valve, a suction line filter dryer, and an electrically operated solenoid valve to partition the indoor coil for low capacity operation. At installation, precharged refrigeration lines are connected between the indoor and outdoor unit to complete the refrigerant circuit. An access panel permits easy access to all servicable components. The compressor and accumulator are acoustically insulated and mounted to a subframe with acoustic isolator bushings. The subframe in turn is mounted to the module structure, using an additional set of acoustic bushings. If the compressor ever requires service, the parting of four refrigeration lines and the loosening of two clamps permits the compressor subframe to be pulled out on integral slides.

The air mover and controls module is shown stacked upon the refrigeration machine module. The air mover module contains the high efficiency two-speed blower with backwardly curved blades, plus a control box which contains all contactors and capacitors. An access panel provides for easy servicing of blower motor and control elements.

The microprocessor chassis box is mounted on a convenient side of the air mover module.

The uppermost module contains the resistance heat elements and the terminals for single-point power connection.

The indoor unit is 22.5 inches wide, 36 inches deep and 63 inches high. These dimensions permit closet mounting, with either side or bottom air entry. Air entry in the upflow mode can be accommodated from either side or from the bottom with minor manipulation of the blower subassembly and the air mover module housing. Horizontal air flow installation is easily accommodated by stacking the air mover

module alongside the refrigeration machine module. The resistance heat module is field modified to either a left- or right-handed configuration, as required.

The design of both indoor and outdoor units permits flexible installation in any climatic region with high performance, reliability, and ease of service.

2.2 Estimated System Performance

A Westinghoue proprietary computer code was used to generate system performance maps for the most recent version of the optimized Westinghouse/DOE dual-stroke heat pump. This system, which uses the MOD I dual-stroke compressor, has been designated configuration RDHPOV. The system has been optimized to minimize the annual cost of ownership per Btu of heat beneficially transported to and from the building. A fixed electricity cost of 4.97¢/kWh and a unit life of 15 years were assumed. Annual ownership costs include maintenance, amortization, and energy cost. The continuous parameters of optimization include indoor and outdoor coil face area and air flow and balance point. Discrete parameters such as heat exchanger row number are also considered. System RDHPOV, optimized for DOE region V, has a lower heating balance point of 17°F and an upper heating balance point of 32°F.

The estimated heating performance is shown in Figure 2.2-1. In the high capacity mode, the estimated capacity is 48,500 Btu/h at 47°F with a COP of 3.62, and 31,400 Btu/h at 17°F with a COP of 3.13. In the low capacity mode, a capacity of 28,700 Btu/h and a COP of 3.90 are estimated at 47°F, and a capacity of 14,800 Btu/h and a COP of 3.16 are estimated at 17°F. These performance estimates are slightly optimistic since the model for configuration RDHPOV neglects the reversing value.

The delivered heating air temperature of high efficiency heat pumps available today is often uncomfortably low. In contrast, the Westinghouse/DOE heat pump provides a relatively high delivered air

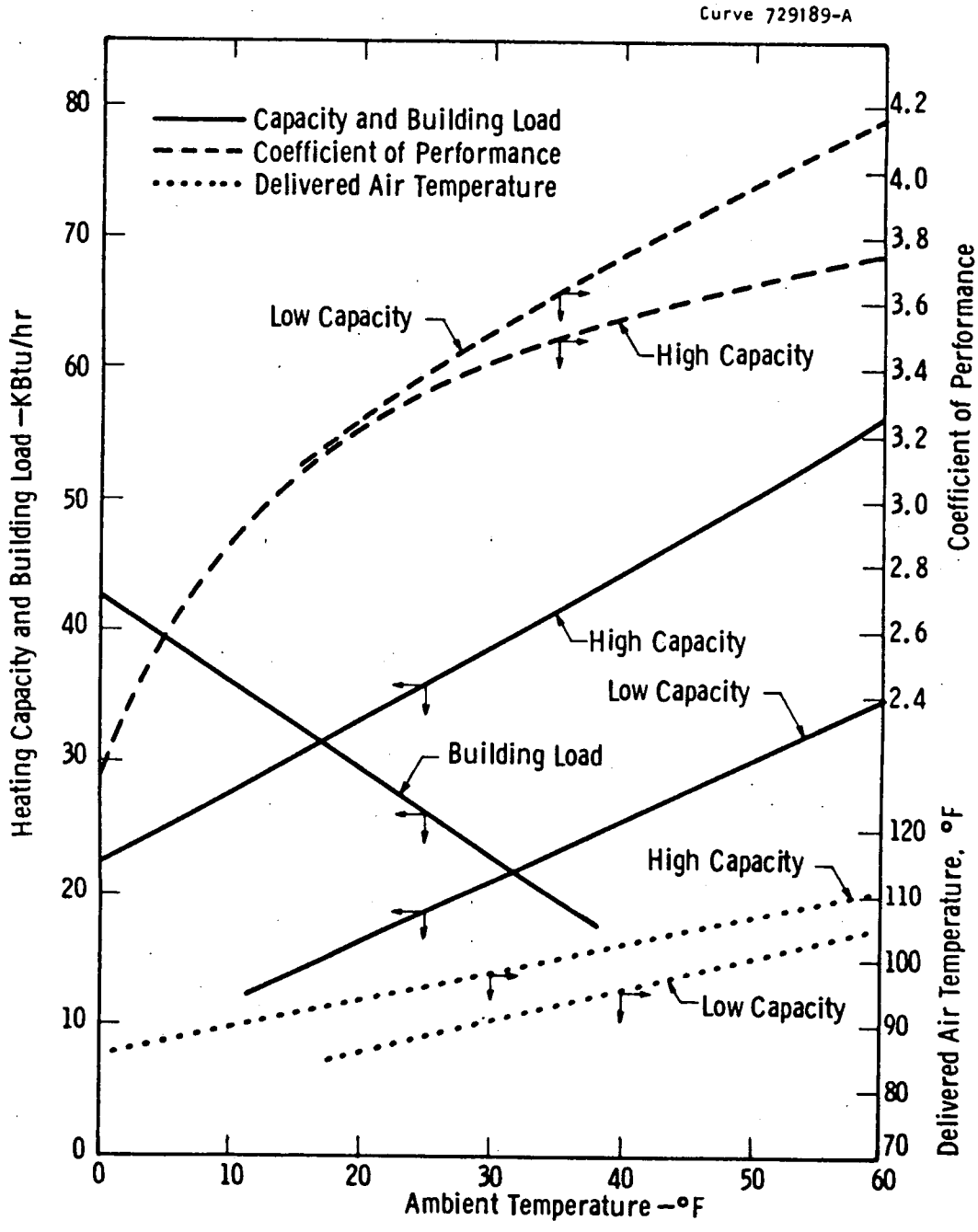

Figure 2.2-1 - Heating performance of the dual-stroke heat pump: Configuration RDHPOV

temperature with a low indoor air flow for a heat pump of this capacity, and this should provide better comfort for the occupants of the building. Specifically, at 47°F the delivered air temperature of the Westinghouse/DOE heat pump is 99°F in the low capacity mode and 105°F in the high capacity mode. At 17°F the delivered air temperature in the high capacity mode is over 90°F.

In order to produce the MOD I compressor, we had to adapt the dual-stroke mechanism to an existing compressor. In the long-stroke mode, the clearance volume fraction is higher than normal for compressors of this class. Our MOD II compressor has reduced clearance volume (see Section 3.1), and as a result we expect the performance of a system using the MOD II to be better at low ambient temperatures.

The estimated cooling performance is shown in Figure 2.2-2. At 95°F the high capacity mode gives an EER of 9.5 Btu/W-h and a capacity of 48,200 Btu/h. The low capacity mode at 95°F gives an EER of 10.7 Btu/W-h. At 82°F, the low capacity EER is 12.3 and capacity is 32,000 Btu/h. High-efficiency air conditioners and heat pumps in the cooling mode generally provide poor humidity control due to high evaporator temperatures. In this system the evaporator temperature is maintained at a level which provides a comfortable sensible to total capacity ratio of 0.7 at 95°F in the low capacity mode, decreasing slightly to 0.67 at 82°F.

2.3 Estimated Seasonal Performance Comparisons

The predicted annual energy consumption for a high-efficiency single-speed heat pump in a 1600 ft^2 house with level 2 insulation[3] in Minneapolis is shown graphically in Figure 2.3-1. The heat pump has

---

3. H. S. Kirschbaum, S. E. Veyo, "An Investigation of Methods to Improve Heat Pump Performance and Reliability in a Northern Climate," EM 319 (Research Project 544-1) Electric Power Research Institute, Palo Alto, CA, January, 1977.

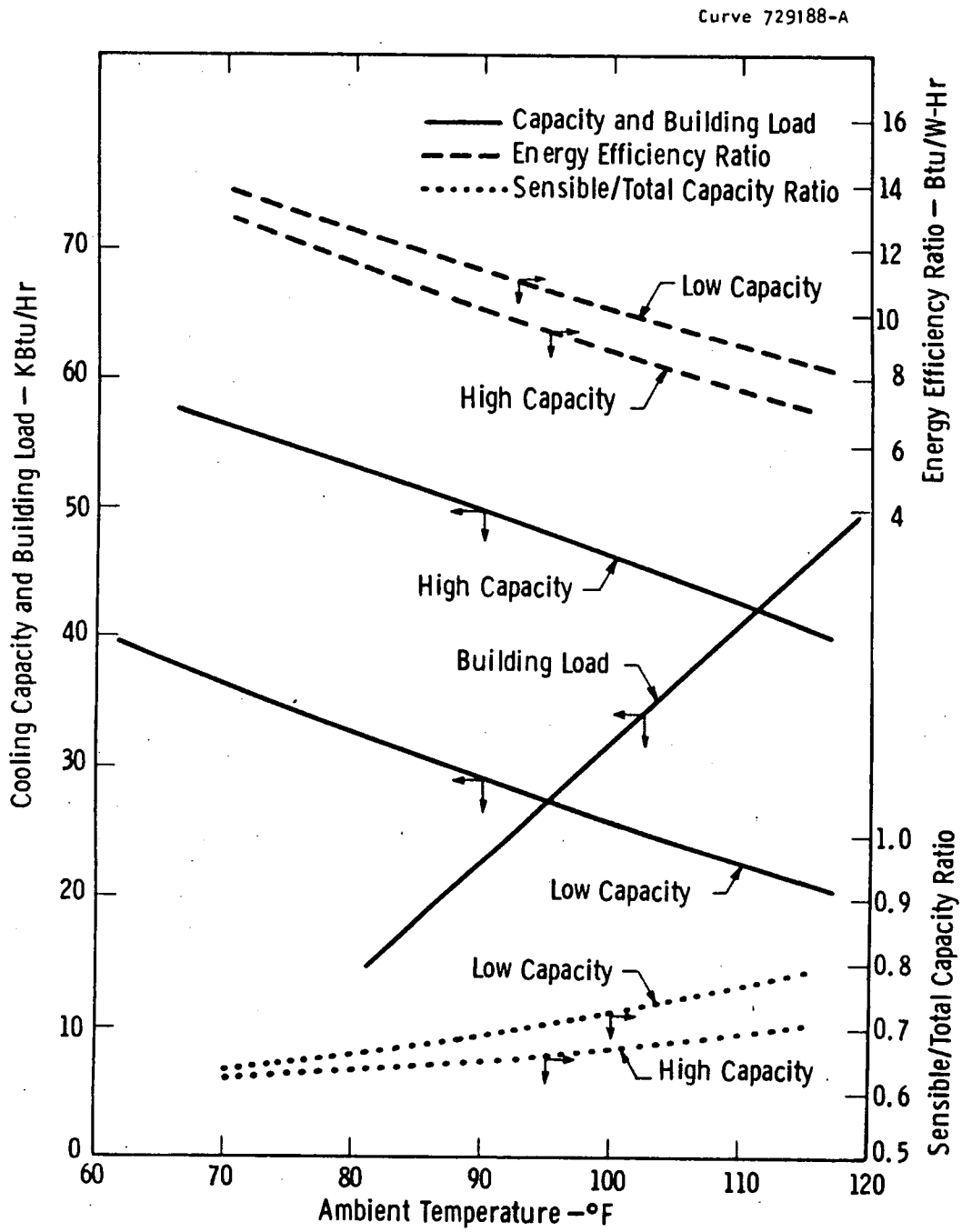

Figure 2.2-2 - Cooling performance of the dual-stroke heat pump: Configuration RDHPOV

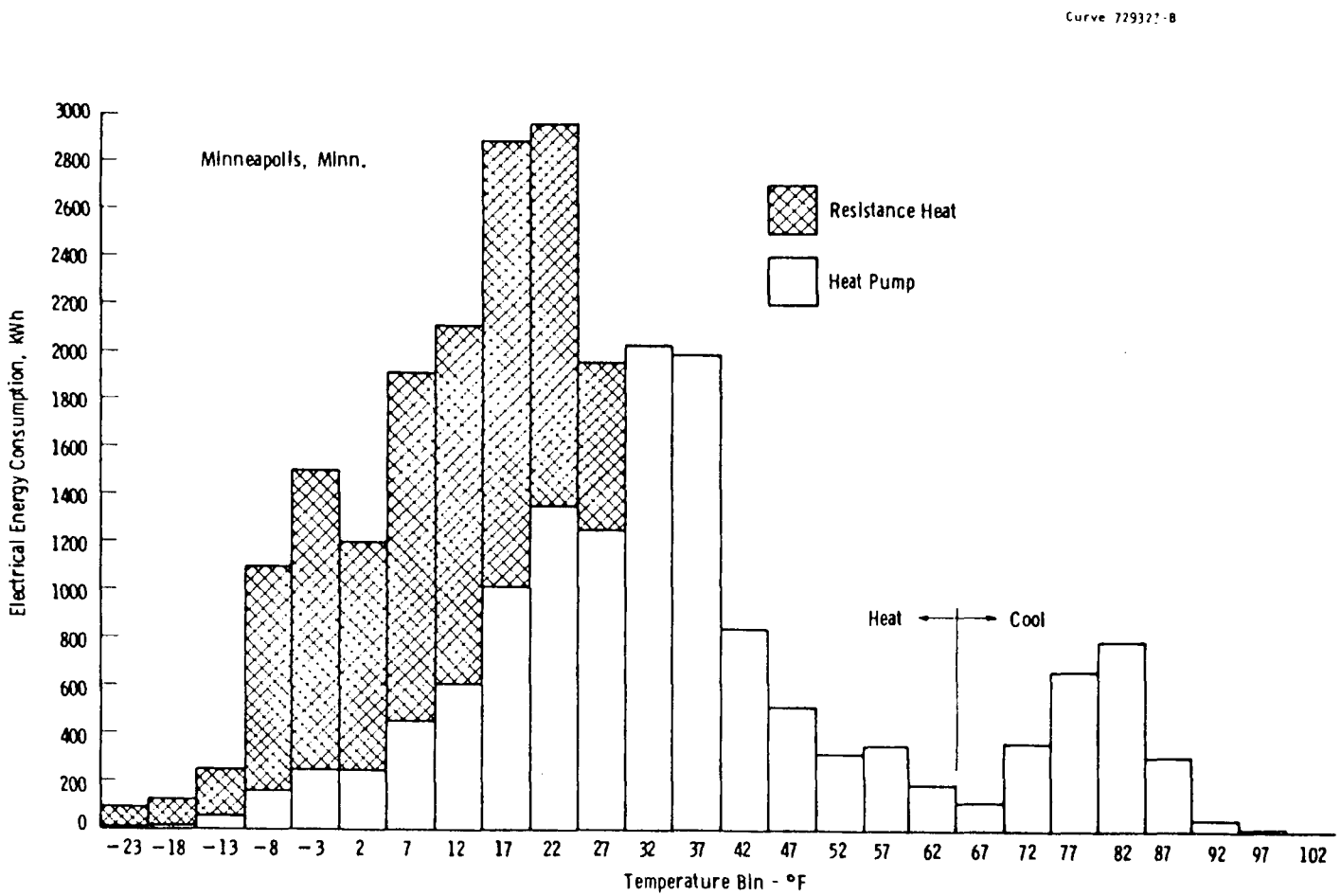

Figure 2.3-1 - Annual electrical energy consumption for a high-efficiency single-capacity heat pump

been sized according to conventional practice, giving a heating balance of 32°F. The sizing has been shown to be approximately optimum. At temperatures below the balance point, resistance heat is assumed to be added in 5 kW stages as required to carry the building load.

An analysis of the energy consumption for a presently available high-efficiency two-speed heat pump is shown in Figure 2.3-2 as applied to the same 1600 ft^2 house in Minneappolis. This unit is approximately the same size as the Westinghouse/DOE heat pump. See Figures 2.3-4 and -5 for a direct comparision between the estimated performance of the Westinghouse/DOE heat pump and published data for the two-speed unit.

A similar analysis for the energy consumption of the Westinghouse/DOE dual-stroke system is shown in Figure 2.3-3. The predicted total annual energy consumption for the dual-stroke heat pump system is 17,300 kWh, more than 30 percent less than the single capacity system and more than 20 percent less than the two-speed system. About 88 percent of the energy is used for heating. A major portion of the reduction in energy consumption is the result of a reduction in resistance heat from 11,000 kWh in the single-capacity system to 4,000 kWh for the dual-stroke system.

The Westinghouse/DOE heat pump configuration RDHPOV has been optimized to provide minimum annual cost per unit of heating and cooling beneficially delivered to the building. This optimization assumes a fixed electricity cost of 4.97¢/kWh and a 15-year service life in DOE region V. The optimum lower heating balance point for this system is 17°F. Resistance heat is assumed to be added in 5 kW increments. A second stage of resistance heat is required at 3°F and a third stage at -10°F. Clearly, in many locations two 5 kW stages of resistance heat will be sufficient with the dual-stroke heat pump, while three stages would be required with a single-capacity heat pump.

A seasonal performance comparison between the Westinghouse/DOE heat pump and both high-efficiency single-speed and two-speed heat pumps in different DOE climate regions is presented in Table 2.3-1.

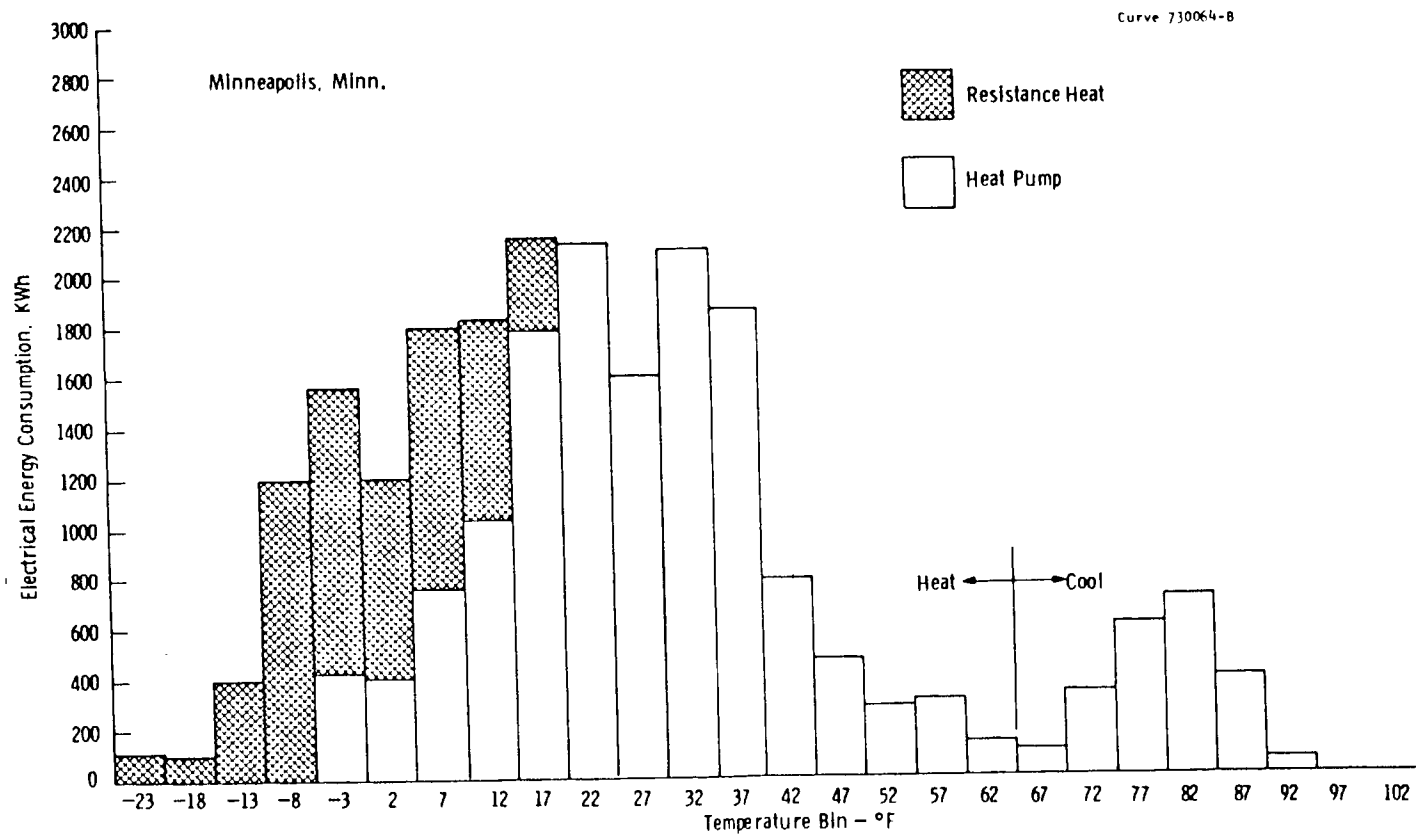

Figure 2.3-2 - Annual electrical energy consumption for a high-efficiency two-speed heat pump

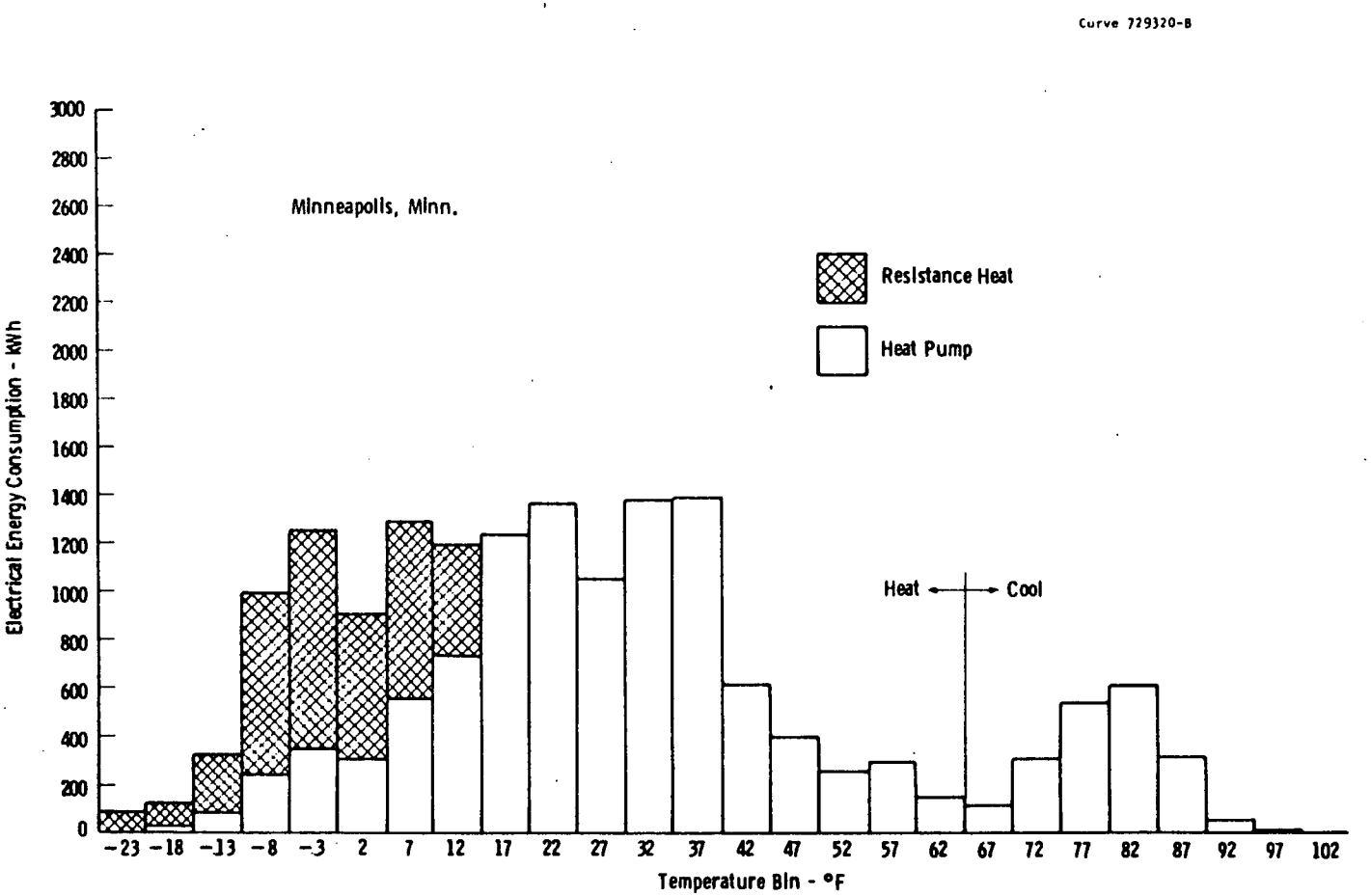

Figure 2.3-3 - Annual electrical energy consumption: dual-stroke heat pump (configuration RDHPOV)

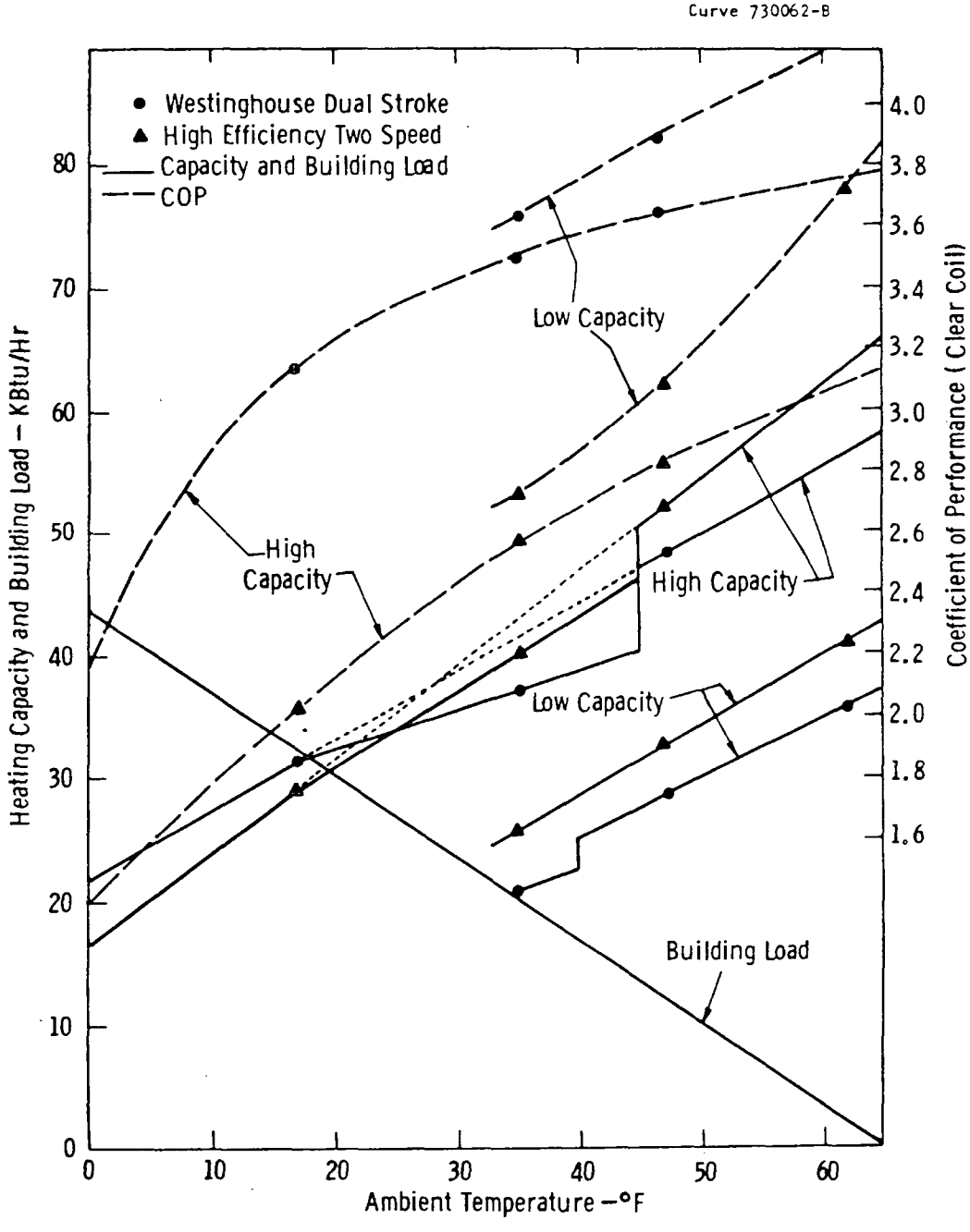

Figure 2.3-4 - Comparison of heat pump performance--heating

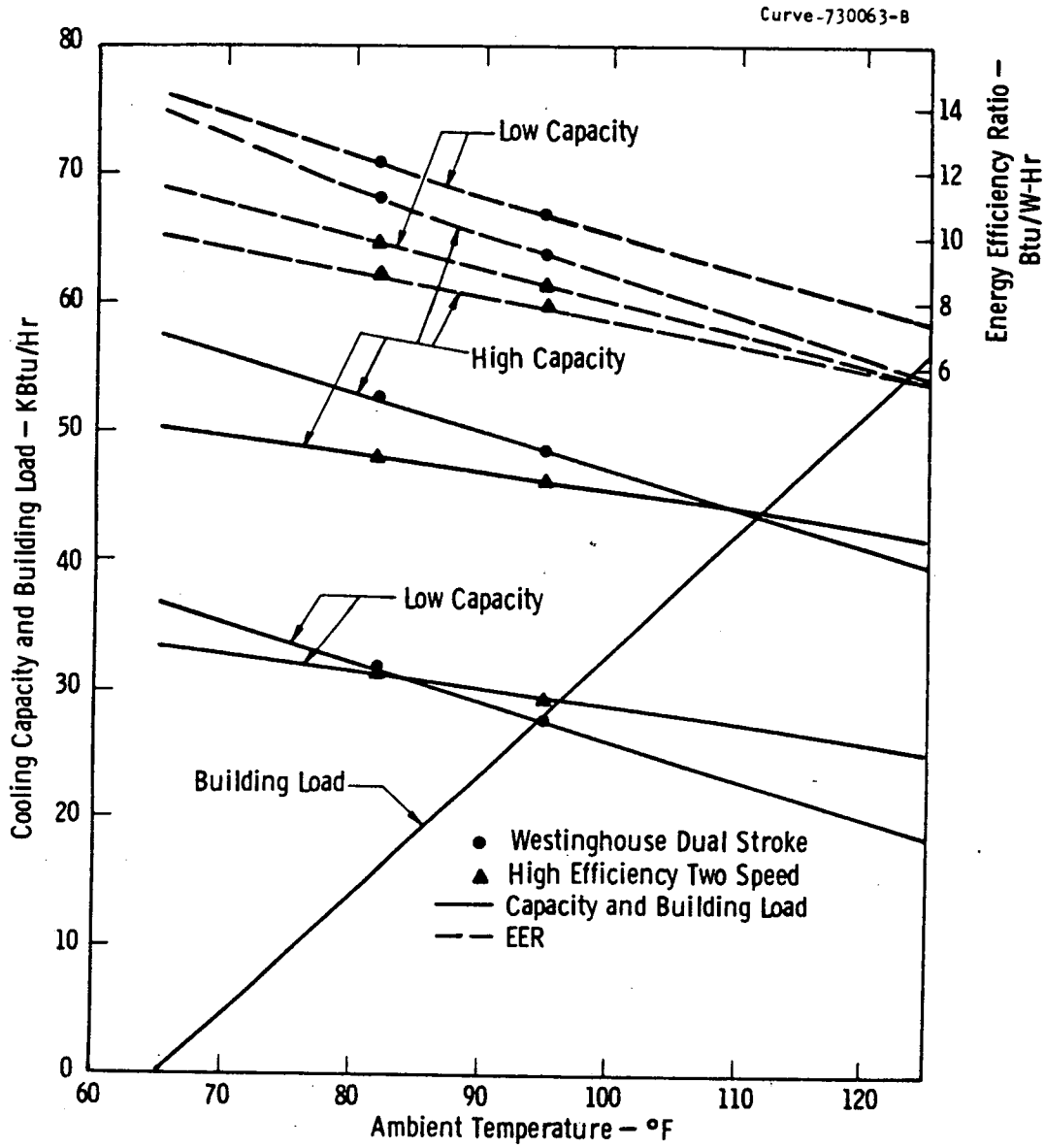

Figure 2.3-5 - Comparison of heat pump performance--cooling

The estimated performance of the Westinghouse/DOE heat pump is better than that required in the performance specifications.[2]

Note that the appropriateness of the heat pump size to the house load will influence the expected seasonal performance. The sizing used to generate Table 2.3-1 is appropriate for a northern climate as typified by Minneapolis or Pittsburgh. For other climatic regions the more appropriate match would use the three specific heat pumps considered in larger houses than the nominal 1600 ft^2 dwelling considered here. A discussion of optimum sizing is not germain to this report on system and component development.

2.4 Conclusions

1) The Westinghouse/DOE advanced electric heat pump meets or exceeds its performance specifications.

2) Relative to state of the art components, the incremental cost to the heat pump purchaser of the advanced design components used in the Westinghouse/DOE heat pump is amortized in less than 4 years by energy savings, using a simple pay-back methodology.

---

2. op. cit.

Table 2.3-1
Comparison of Seasonal Performance[1]
(1600 ft^2 Level 2 House)[2]

Climate Region (DOE)		II[3]	III[4]	IV[5]	V[6]
Heating Load (MMBtu)		31.56	68.77	109.78	128.60
Cooling (MMBtu)		83.92	39.87	16.61	20.87
W Dual Stroke Heat Pump	Installed Cost[7]	1.49	1.49	1.49	1.52
	Ownership Cost[9]	0.77	0.74	0.84	1.02
	$/MMBtu	7.98	8.17	7.96	8.18
	HSPF	10.69	9.92	9.57	8.41
	SEER	9.99	10.57	10.29	10.53
High Efficiency Single Speed Heat Pump[10] (2.5 Ton)	Installed Cost[8]	0.97	0.97	1.00	1.03
	Ownership Cost[9]	0.76	0.79	1.00	1.28
	$/MMBtu	8.18	8.75	9.47	10.26
	HSPF	8.43	7.10	6.35	5.50
	SEER	8.04	8.40	8.41	8.45
High Efficiency Two Speed Heat Pump[11]	Installed Cost[8]	1.50	1.50	1.53	1.56
	Ownership Cost[9]	0.87	0.86	1.02	1.27
	$/MMBtu	9.06	9.50	9.69	10.13
	HSPF	8.67	7.69	7.17	6.26
	SEER	8.22	8.65	8.54	8.67
High Efficiency Single Speed Heat Pump[12] (4 Ton)	Installed Cost[8]	1.22	1.22	1.25	1.28
	Ownership Cost	0.91	0.87	1.02	1.27
	$/MMBtu	9.38	9.56	9.66	10.16
	HSPF	7.75	7.10	6.72	5.95
	SEER	7.08	7.50	7.54	7.56

NOTE:

1. W modified DOE Procedure (Fed. Register 12-27-79)
2. EM319, EPRI
3. Phoenix, AZ
4. Nashville, TN
5. Pittsburgh, PA (Cleveland weather)
6. Minneapolis, MN (Madison weather)
7. Estimated
8. Estimated via market study
9. Energy (@ 4.97¢/kWh) + Amortized Installed Cost (15 year life and 3% true interest) + Maintenance (2.5% of installed cost per year)
10. Manufacturer A - single speed, 2.5 ton
11. Manufacturer B - two speed, 4 ton
12. Manufacturer A - single speed, 4 ton

3. COMPONENT DEVELOPMENT

3.1 Compressor Design and Development

The key to a commercially viable, high annual performance, advanced electric heat pump, is a high efficiency compressor with low cost capacity modulation means. The performance advantage due to capacity modulation depends upon the range over which compressor capacity can be modulated, i.e., the ratio of maximum to minimum capacity at a fixed set of conditions, and upon the number of capacity steps available in that range. Although continuous modulation appears to be most advantageous in terms of performance, capacity modulation by means of two steps can yield performance nearly as good, provided that the capacity ratio is judiciously chosen. The known means to provide stepwise variable compressor capacity include two-speed drive motors, cylinder suction cut-off, and parallel compressors. To complement these, Westinghouse has developed a dual-stroke compressor and a geared, two-speed compressor drive system. Any of these discretely variable-capacity compressor concepts costs considerably less than the continuously-variable frequency electric-drive system for achieving continuous-compressor capacity modulation.

Among the compressor concepts with stepwise-modulatable capacity, only the dual-stroke scheme and the geared speed-change scheme can provide a flexible capacity ratio at low cost. The two-speed drive motor concept not only is more costly, but inflexible--the capacity ratio is fixed. Parallel compressors provide flexibility, but at high cost. Cylinder suction cut-off on say a multi-cylinder machine with different bore sizes can provide design flexibility at low cost, but once bore size is fixed then so is capacity ratio. The following sections detail the design and performance aspects of both the dual-

stroke and the geared speed-change compressors. The dual-stroke compressor is the clear choice and will be used in the preprototype advanced heat pump.

3.1.1 Dual Stroke Compressor Design

Introduction

Westinghouse has reduced to practice a unique, low cost means to achieve compressor capacity modulation via stroke change. The concept is disclosed in U.S. Patents 4,236,874 and 4,248,053. The concept employs a circular eccentrically bored cam between crankpin and connecting rod. The action of the cam is such that it is driven against one of two rotational stops attached to the crankpin, depending upon the direction of rotation of the crankshaft.

In one cam position, the connecting rod reciprocates at its maximum stroke, displacing the piston to its minimum clearance volume position at top dead center. At the other cam position, corresponding to crankshaft rotation in the opposite sense, the connecting rod reciprocates with a much shorter stroke and thus with a much greater clearance volume at top dead center position. In the shorter stroke position, compressor flow rate (i.e., capacity) is decreased by both the reduction of piston displacement and the reduction of compressor volumetric efficiency because of the increased clearance volume. As a consequence, compressor flow rate is reduced more at high pressure ratios than at low pressure ratios. However, since the low capacity mode of the machine is generally required only during low pressure ratio conditions on the system (i.e., cooling mode and heating mode above 30°F ambient), it is possible to select low stroke cam eccentricities that provide the optimum capacity reduction without appreciably affecting system performance.

The ratio of minimum to maximum compressor capacity is determined by the cam eccentricity. The magnitude of the minimum stroke

is bounded between zero and the maximum stroke; its precise value is a subject for a system optimization.

In addition to the dual-stroke mechanism, our preprototype compressor embodies complementary efficiency-improving design features. These include:

a) means for keeping drive motor heat, friction and windage losses and discharge gas heat out of the compressor suction gas and available elsewhere as useful heat,

b) means for maximizing drive motor efficiency over the complete range of operating conditions,

c) means for increasing the volumetric efficiency of the compressor,

d) improved suction and discharge valving.

Technical Discussion

Figure 3.1-1 illustrates the function of the cam in its two operating positions. Three different methods of cam construction were evaluated and the selected configuration is shown in Figure 3.1-2. The design is horizontally split to allow the use of standard journal sizes on the upper crankshaft bearings. Due to the split arrangement, the cam can be installed without passing over the journals. The design includes the key pocket in the upper section to provide end stop positions for the loading key. Figure 3.1-3 illustrates the installation of the cam on a standard Westinghouse CD048 compressor crankshaft.

The preprototype hardware is fabricated from machined, heat treated and ground 4140 tool steel. It is anticipated that this component would be manufactured in quantity from pressed powder, sintered and ground tool steel. This process has been investigated and recommended by Westinghouse manufacturing personnel.

The geometry of the cam, crankpin and other compressor details is as follows:

Dwg. 7758A32

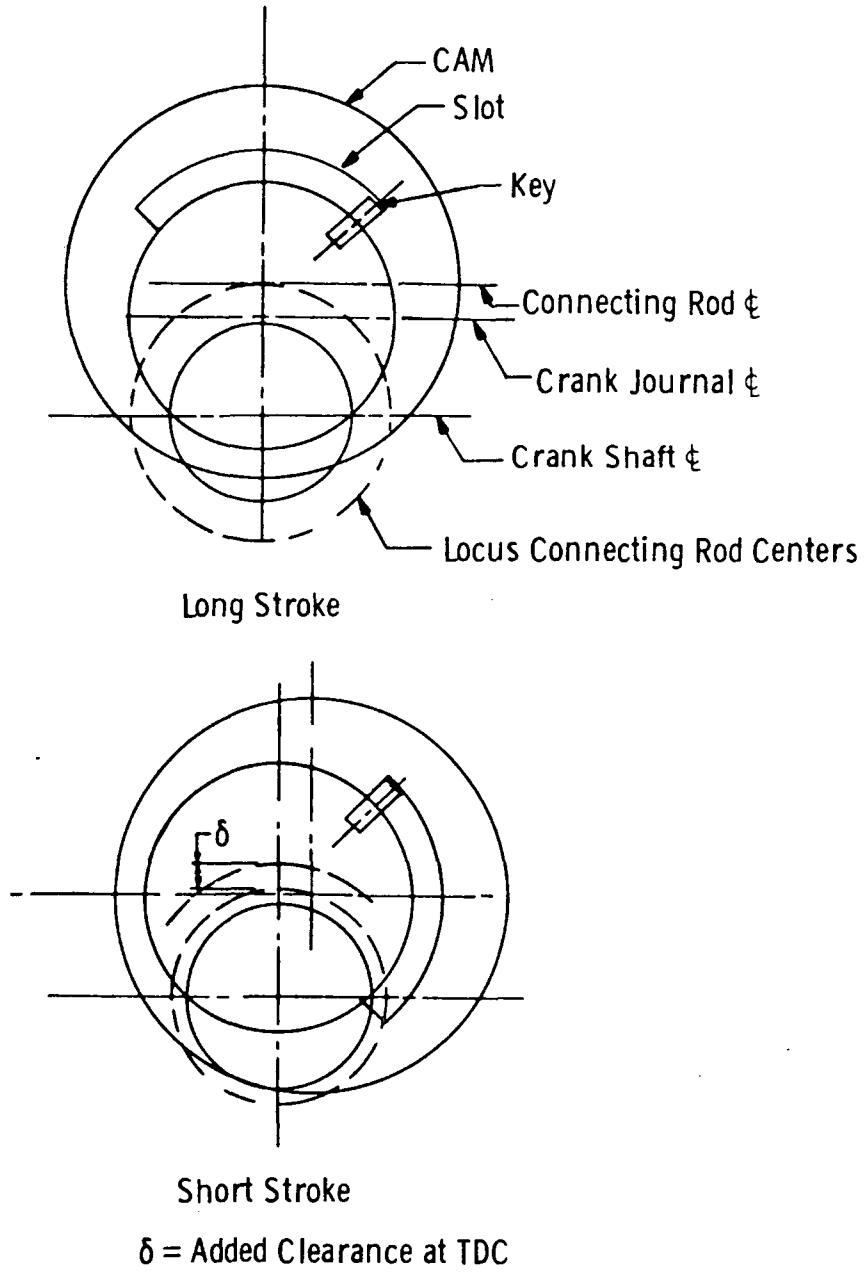

Figure 3.1-1 - Dual-stroke cam configuration

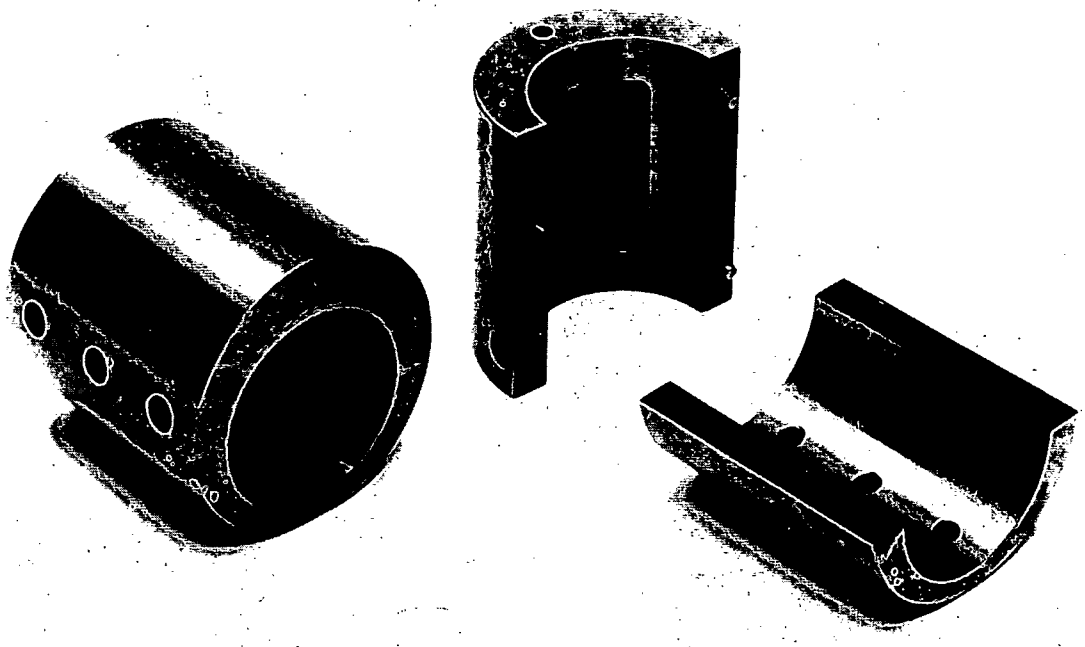

Figure 3.1-2 - Horizontally split cam configuration

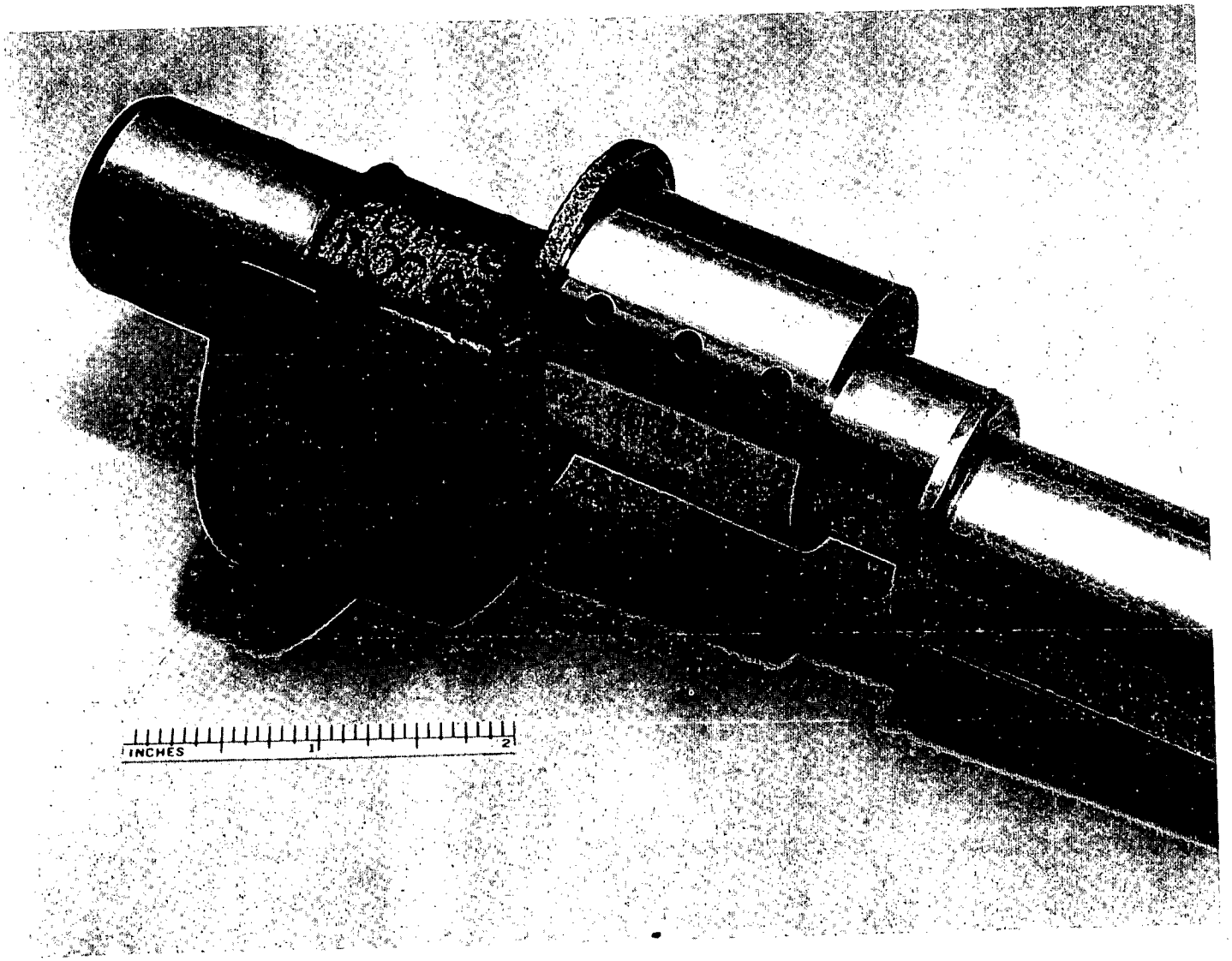

Figure 3.1-3 - Dual-stroke cam installed on three-cylinder crankshaft

Crankpin throw = 0.25 in

Crankpin Outside Diameter = $1.000^{+.0003}$

Cam Inside Diameter = $1.0006^{+.0003}$

Cam Outside Diameter = $1.4375^{-.0003}$

Cam Eccentricity = 0.100 in

Cam Rotation on Crankpin = 90°

Maximum Connecting Rod Throw = 0.25 + 0.100 = 0.35 in

Maximum Stroke = 0.70 in

Minimum Connecting Rod Throw = $\sqrt{0.25^2 \times 0.100^2}$ = 0.269 in

Minimum Stroke = 0.538 in

Clearance Volume @ Max Stroke = 3.5%

Clearance Volume @ Min Stroke = 20.3%

Piston Diameter = 1.750 in

Connecting Rod Center Distance = 2.160 in

In order to incorporate the cam arrangement into a standard CD048 compressor, modifications to crankshaft, crankcase and connecting rods were necessary:

a) A new crankshaft was machined with a crankpin eccentricity of 0.25 in, a crankpin journal diameter of 1.00 in, a main lubrication passage with an eccentricity of 0.281 in, and two upper bearing journals of 1.00 in diameter. In addition, a key slot was machined in both the rotor bore and the motor shaft to facilitate easy removal of the motor rotor. The crankshaft was chrome plated with ARMALOY ^{R} plating.

b) New connecting rods with larger center bores were obtained and larger crankpin bores were machined from castings.

c) An improved reversible single-phase drive motor was used with the leads for both main and auxiliary windings taken outside of the hermetic cam for connection through a switching relay.

These modifications reduced the displacement of the CD048 compressor by approximately 12 percent.

It is well known that the use of suction gas to cool a hermetic compressor and its drive motor degrades its potential throughput and efficiency significantly. We have investigated several alternative means for compressor cooling and have reduced to practice a concept which employs the external cooling of circulated oil.

The preprototype oil-cooled dual-stroke compressor is shown in section view in Figure 3.1-4. Figure 3.1-5 illustrates the final hardware embodiment. Functionally, the design delivers cool oil directly to the drive motor and provides the suction gas a direct inlet to the cylinder. The discharge gas from each cylinder is delivered to a common manifold which then carries the gas to the external system. A reversible oil pump is provided at the bottom crankshaft end to pump and circulate the cooling oil from the sump to an external air-cooled heat exchanger where it is cooled and returned to the compressor via an inlet line directly above the motor rotor. Oil flows over and through the windings of the motor, capturing heat in an efficient manner. The flow rate of the oil is approximately 1.5 gal/min against a 2-3 psi head.

The suction gas is introduced to the oil separator/suction line through a vented opening at the top of the separator. The gas is prevented from mixing with and gaining heat from the internal gas environment as is normally done in the suction gas-cooled machine. Suction gas is thus drawn directly into the crankcase cylinder suction cavity. Minimal heat transfer occurs in this area, and the resultant suction gas to the cylinder is significantly reduced in superheat relative to conventional compressors. Substantially all of the drive motor heat loss is rejected to the cooling oil and in turn rejected to the external heat exchanger and its environment.

The preprototype compressor incorporates an improved suction and discharge valve and valve plate system that produces a low clearance volume in the high stroke mode while providing improved valve flappers of increased open area and rapid response. The natural frequency of the system is greater than 525 cycles per second to ensure that valve

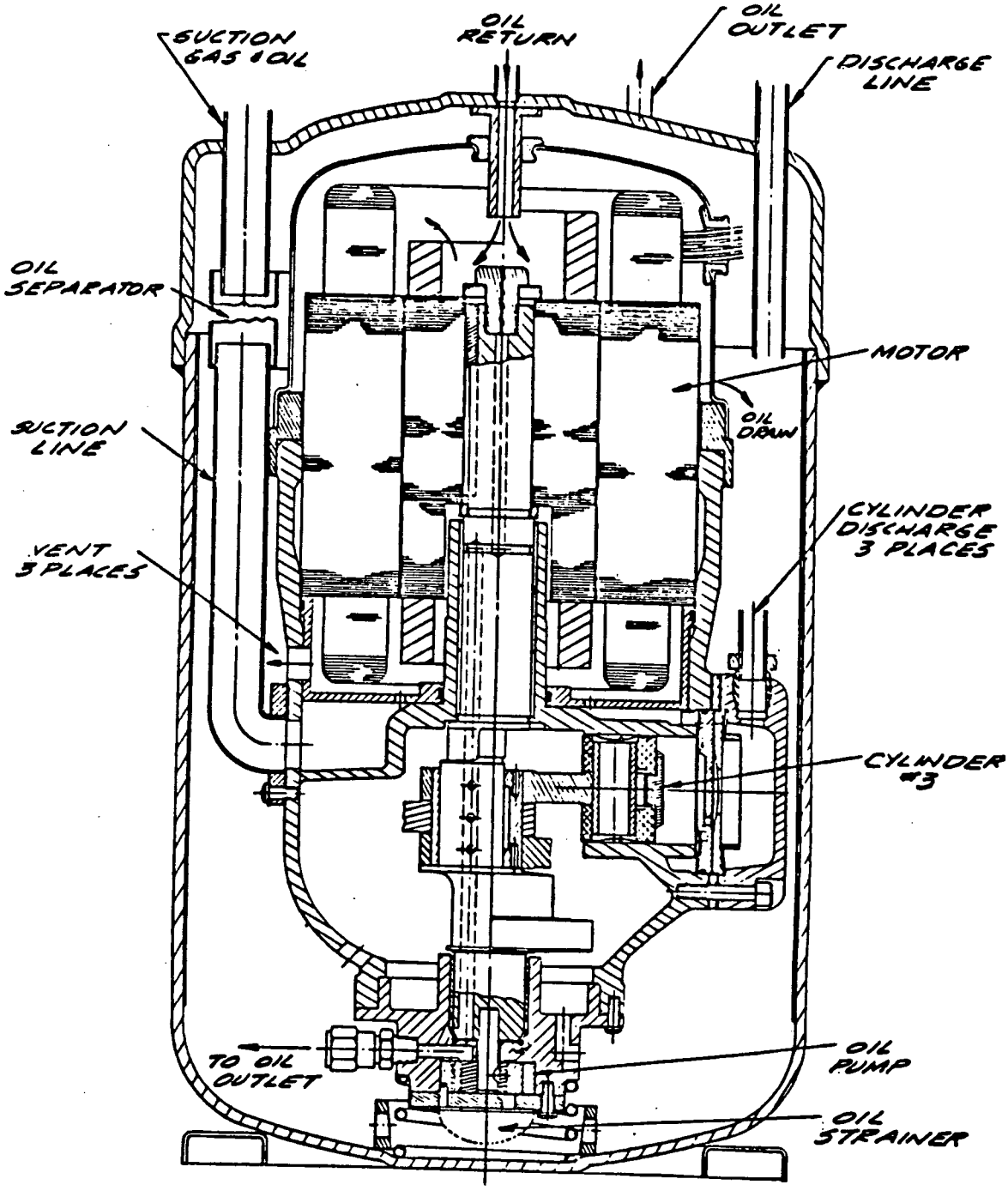

Figure 3.1-4 - Cross section of oil cooled compressor with direct suction

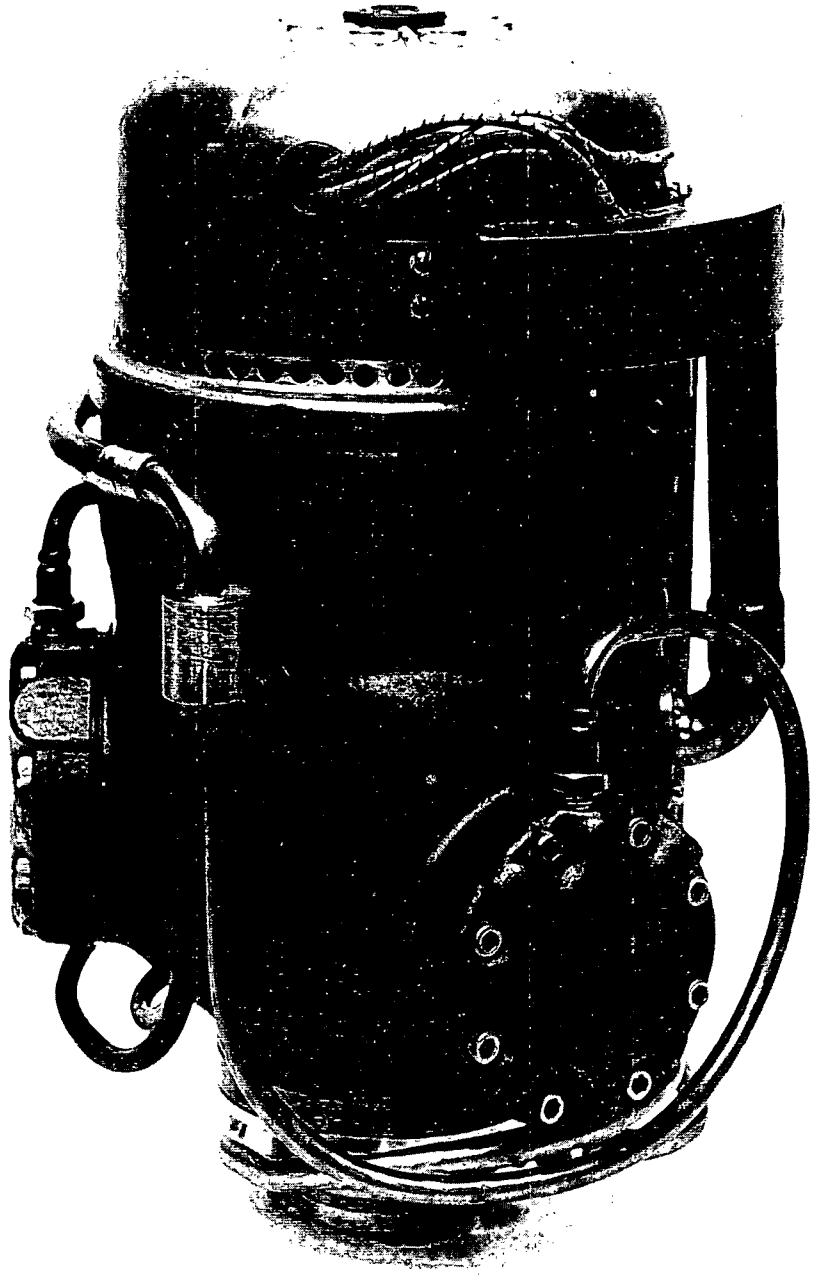

Figure 3.1-5 - Oil cooled compressor

closure is obtained in approximately 10 degrees of crankshaft rotation. Further, the natural frequency does not correspond to any harmonic of the drive frequency.

Figure 3.1-6 depicts the open center suction valve on the cylinder. This valve arrangement was designed to operate with a "crowned" piston; therefore, the center support was eliminated. This valve opens into a "disked" configuration rather than a "butterfly" shape, and the cylinder cutout supporting the minimum flex tab was modified to a 20° angle to allow the disk deflection. The stop cutouts in the cylinder wall were not modified. The valves are .012 in thick. Figure 3.1-7 illustrates the valve system, including crowned piston, valve plate and open center suction valve. This valve plate was specifically designed to be used with a crowned piston and the disked deflection open center suction valve. The calculated clearance volume of this system is 3.5 percent.

As part of the valve system, Figure 3.1-8 shows the cantilevered discharge flapper valve with end restraint. The valve plate is shown in a bottom view of the orientation previously illustrated in Figure 3.1-7. The flapper is rigidly supported at one end but is allowed to move under the stop at the opposite end. The stop is a double curved arch with equal radii for each curve. The curvature limits the maximum stress in the valve as well as the lift.

The basic geometry and dimensions of the improved valve system with reduced clearance volume are given below.

a) Discharge Valve

Port area	0.441 in^2
Flapper thickness	0.010 in
Lift max. curvature	0.100 in
Lift curvature radii	3.0 in
Port outside diameter	1.087 in
Port inside diameter	0.787 in

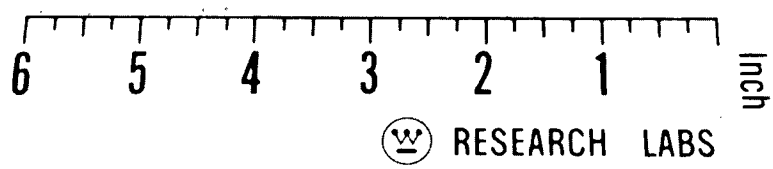

Figure 3.1-6 - Open center suction valve (two-cylinder crankcase)

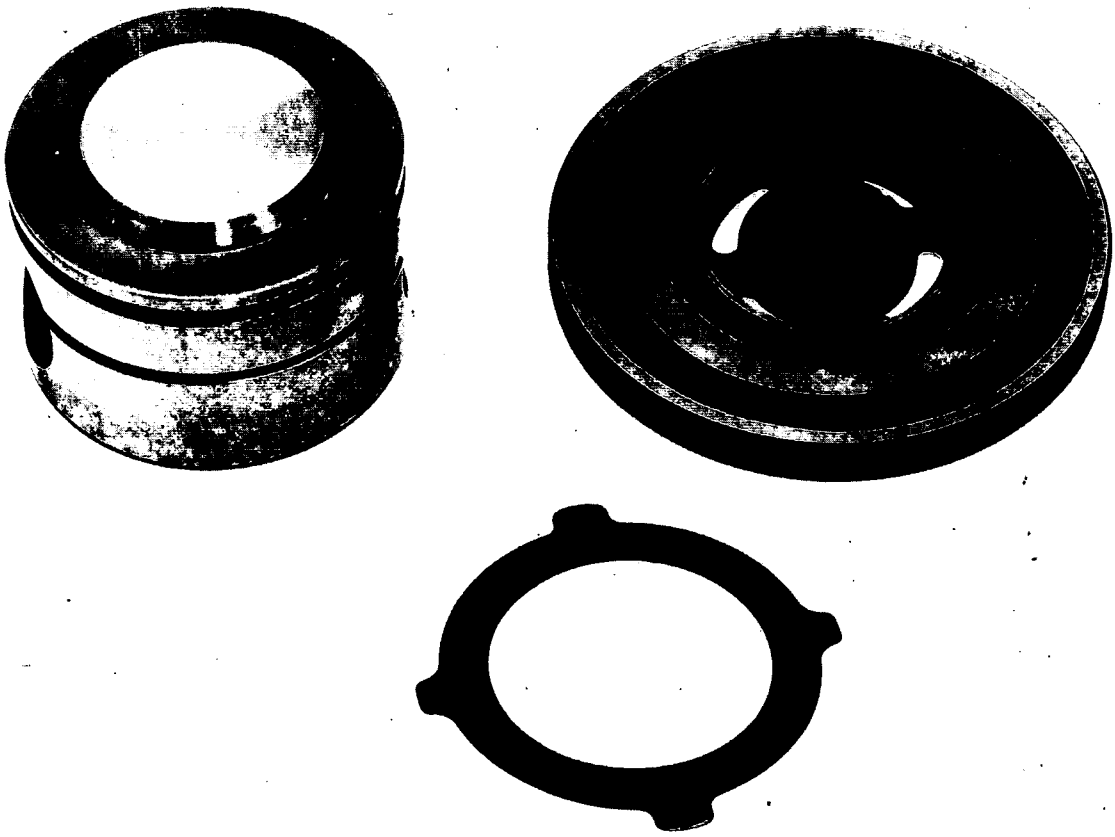

Figure 3.1-7 - Suction valve with valve plate and crowned piston

Figure 3.1-8 - Discharge valve with cantilevered flapper and end restraint

b) Suction Valve

Port area	0.653 in^2
Flapper thickness	0.012 in
Lift stops	0.065 in
Port outside diameter	1.563 in
Port inside diameter	1.269 in

3.1.2 Compressor Motor

Introduction

The compressor motor used in the prototype heat pump has been designed to match the requirements of the dual-stroke compressor. Although suboptimization of the motor design was not a part of this program, the motor as designed provides significant cost-benefit improvement over the original motor intended for this compressor. In addition, although it is 1/2 in longer in the stack than the original motor, the height of the resulting hermetic shell can be accommodated in the physical layout of the unit.

Technical Discussion

The dual-stroke compressor as used in the prototype heat pump has the characteristic that on short stroke it unloads the motor. The short-stroke operation corresponds to a low capacity mode of heat pump operation, a mode that will occur perhaps as much as 75 to 80 percent of the heat pump operating hours. In the low capacity mode, a typical value of required shaft horsepower for the compressor would be 1-3/4 hp. If the original single-phase motor (as designed) were required to supply this horsepower, its efficiency would be 75.8 percent as compared with its efficiency at its nominal 4 hp rating of 85.8 percent. The 4 hp load would be a typical load in the high capacity mode of operation. Curve No. 3 of Figure 3.1-9 is the efficiency versus shaft horsepower curve for what will be designated as the "original" motor. A method that uses a reconnection of the installed windings plus a change in

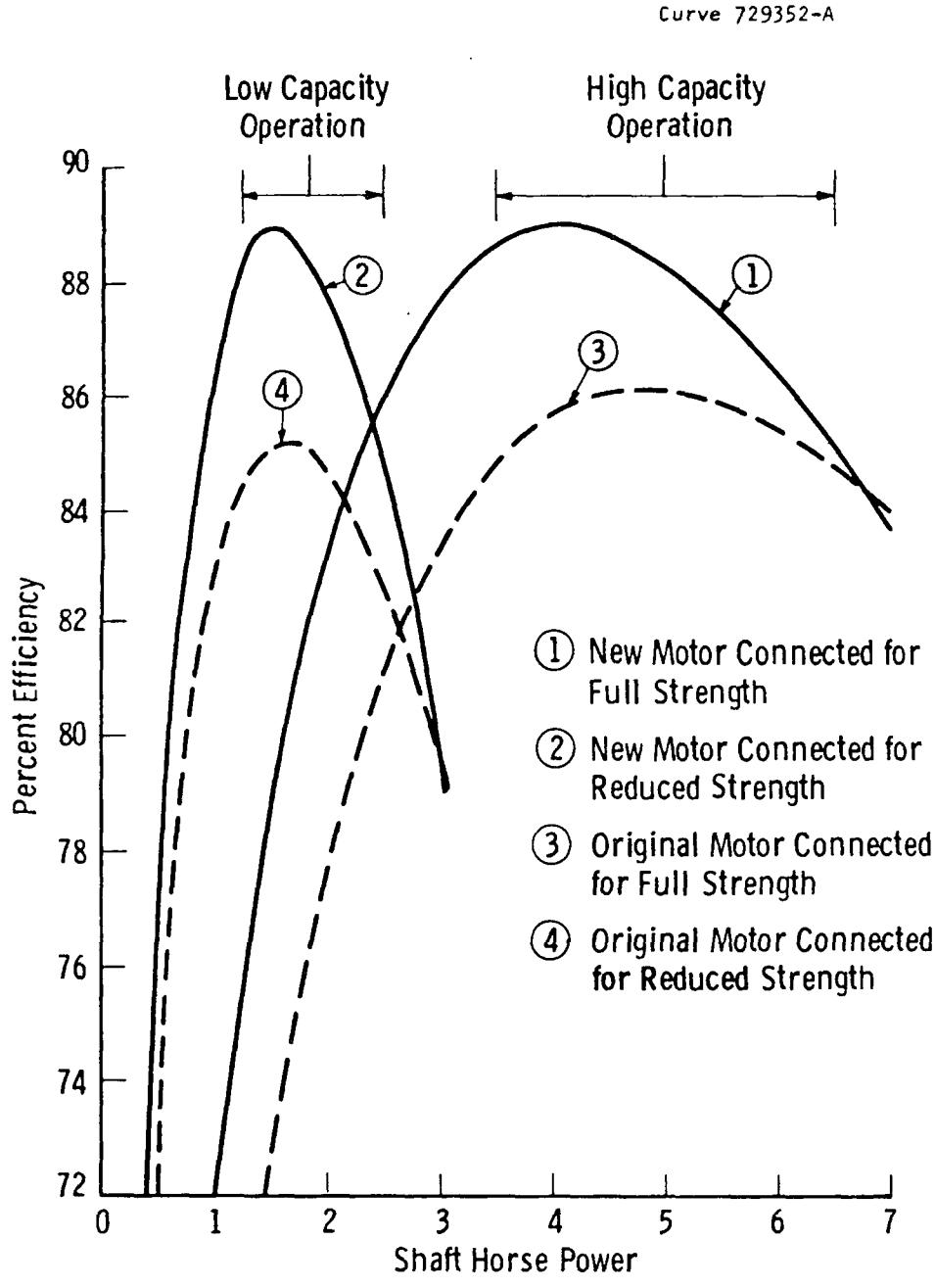

Figure 3.1-9 - Single-phase compressor motor efficiency versus shaft horsepower (25°C winding temperature)

connected capacitance was devised to improve low capacity motor operation. To evaluate this approach, it was possible to modify the internal coil connections of the original motor to implement this method.

Curve No. 4 of Figure 3.1-9 shows the efficiency versus shaft horsepower curve for this reconnected motor. As can be seen, the motor's efficiency in the range of interest for low capacity operation is considerably improved over that of the original motor. This is true even though the windings of the original motor are not properly proportioned to take full advantage of this approach. The calorimeter performance using the modified "original" motor at an evaporating temperature of 30°F showed a heating COP improvement of 15.8 percent over that obtained with the unmodified "original" motor.

One additional feature of the approach used was that the motor naturally changes direction of rotation when switched from high capacity mode to low capacity mode. A change of rotational direction is required to actuate the stroke-changing cam system. Thus, this approach eliminates the necessity for any special reversing contactors, as would be required if the original motor were to be used per se. On the other hand, contactors are required to switch the winding configuration to obtain the reduced strength properties at low capacity. To a first approximation, the contactor incremental cost between implementing the dual-strength motor approach and retaining the "original" motor with reversing contactors should be a standoff.

The laboratory implementation of the dual-strength motor using the modified original motor required two capacitors (15 μfd and 25 μfd). The 15 μfd capacitor was used in the low strength configuration and the total of 40 μfd was used in the full strength configuration; the original motor was designed to use 40 μfd. Using pricing information available from both GE and Cornell- Dubilier for metallized film capacitors, it appears that the cost penalty for acquiring two capacitors is $0.78 to $0.96 for an OEM purchaser.

Before selecting a final design for the motor, three designs in addition to the modified original design were considered. Over the course of the contract, the motor vendor has supplied motor costs which reflect changes in copper, steel and aluminum costs. To make valid cost comparisons, the motor costs for the designs under consideration were scaled to the average of the material costs for all of the motors being considered.

The motors considered are listed in Table 3.1-1 along with the required complement of capacitors. Table 3.1-2 shows OEM motor costs, capacitor costs and total OEM cost of each motor/capacitor combination.

Table 3.1-1

Motors Considered

Motor No.	Punching (in)	Stack Length (in)	Windings	Capacitors (μfd)	Comment
1	6 Round	4.25	Unbalanced	15 and 25	Original modified
2	6 Round	4.25	Balanced	15 and 25	
3	6 Round	4.75	Balanced	10 and 25	
4	7 Hexagonal	4.75	Balanced	20 and 30	

No attempt is made here to show the costs of switching equipment. However, within the complement of four motors being considered that employ the reduced strength principle of operation, there should be no difference in switching costs.

The No. 4 design was investigated because it had significantly larger slots and would permit more effective winding usage. However, its efficiency was only marginally better than that of motor No. 3. That this was so is probably attributable to the fact that it had considerably more steel and as a consequence more "iron" losses than did motor No. 3.

Table 3.1-2

Motor/Capacitor Costs

Motor Number	Motor Cost	Capacitor Cost*	Total Cost
1	$48.85	$ 9.07	$57.92
2	51.89	9.07	60.96
3	55.56	8.27	63.83
4	65.31	10.96	76.27

---

*Based on Cornell-Dubilier metallized-foil capacitors in quantities of 5000

Cost benefit analyses were made for motors 2 and 3 relative to motor No. 1, and motor No. 3 was selected for incorporation into the preprototype heat pump. The efficiency of motor 3 is shown in Figure 3.1-9 as a function of delivered horsepower.

The cost-benefit analysis for a comparison of motors 1 and 3 is shown in Table 3.1-3. This analysis is based upon typical horsepower requirements of 1.75 and 4.0 for low and high capacity, respectively, 4500 and 1500 hours of operation in low and high capacity, respectively, and all energy cost at $0.05 per kWh.

The incremental cost of motor/capacitor combination No. 3 over No. 1 was multiplied by 2.5 to reflect the impact of this cost increment at the market level. The payback period of 7-1/2 months is very impressive and probably reflects the fact that previously used motors were designed with first-cost considerations being paramount. This motor design is not optimized for this requirement, so future improvements in cost-benefit should be achievable.

Motor Design

The motor as finally designed employs the 6-in round punching which contains the large slot option of the motor vendor, with a stack

Table 3.1-3

Cost-Benefit Analysis

	Motor No. 1	Motor No. 3
Efficiency at 1.75 hp	0.851	0.885
Efficiency at 4.00 hp	0.857	0.888
Power at 1.75 hp	1538.5 watts	1475.1 watts
Power at 4.00 hp	3481.9 watts	3360.4 watts
Energy at 1.75 hp (4500 hours)	6923.3 kWh	6638.1 kWh
Energy at 4.00 hp (1500 hours)	5222.9 kWh	5040.5 kWh
Total Energy	12,146.2 kWh	11,678.6 kWh
Total Energy Cost	$607.30	$583.90
Total Motor/Capacitor Cost	$57.92	$63.83

Incremental Savings	$23.40/year
Incremental Cost	$5.91 OEM ≅ $14.78 @ retail
Payback Period	0.63 yr (7-1/2 Months)

length of 4.75 inches. The main and auxiliary windings are designed for approximate equality of winding weight in each winding and are designed so that the main winding has two parallel paths (each portion of the main winding being made available for either parallel or series connection). The turns ratio (auxiliary turns/main turns, paralleled) is 1.627. The rotor is of a standard design used for this motor frame size.

System Design

The principle involved in two-strength operation provides that the roles of the main and auxiliary windings are reversed when going from full-strength operation to reduced-strength operation. Also, the two paths available in the main winding are in parallel during the high-strength operation and are in series in the low-strength operation.

When so connected, the turns ratio (considering that the old main winding now performs the role of a new auxiliary winding with twice its original turns) becomes 1.229. For best performance in the high-strength mode, the required capacitance is 35 μfd and in the low-strength mode it is 10 μfd.

Figure 3.1-10 is a schematic showing how the motor switching functions would be implemented in going from high to low capacity and vice-versa. The normally closed contacts S3 and S4 would correspond to low-strength operation. As can be seen, with these contacts closed and all others open, the main windings are in series and connected to the 230 volt line through the 10 μfd capacitor. The auxiliary winding is directly connected to the 230 volt line. In this configuration the auxiliary winding is serving the role of a main winding and the main winding is serving the role of an auxiliary winding.

When control information requires the high-strength mode, S1, S2 and S5 are closed, and S3 and S4 opened. In this configuration, the main windings are connected in parallel and directly to the 230 volt line, whereas the auxiliary winding is connected to the 230 volt line through the 10 μfd and 25 μfd capacitors in parallel. Switching under load is not contemplated, contacts S1 through S5 being used for set-up purposes only.

In the laboratory where the modified original motor was being operated in the low-strength configuration, the motor had difficulty in starting the compressor. For this reason, a hard-start capacitor (not shown in Figure 3.1-10) has been incorporated in the complete control schematic diagram of Figure 3.4-4.

Summary

The compressor drive motor is a dual-strength, high efficiency, single-phase reversible induction motor with a nominal rating of 4 hp.

It should be noted that the 4 hp motor rating is used primarily as a convenient designator since the motor is capable of supplying 8 hp

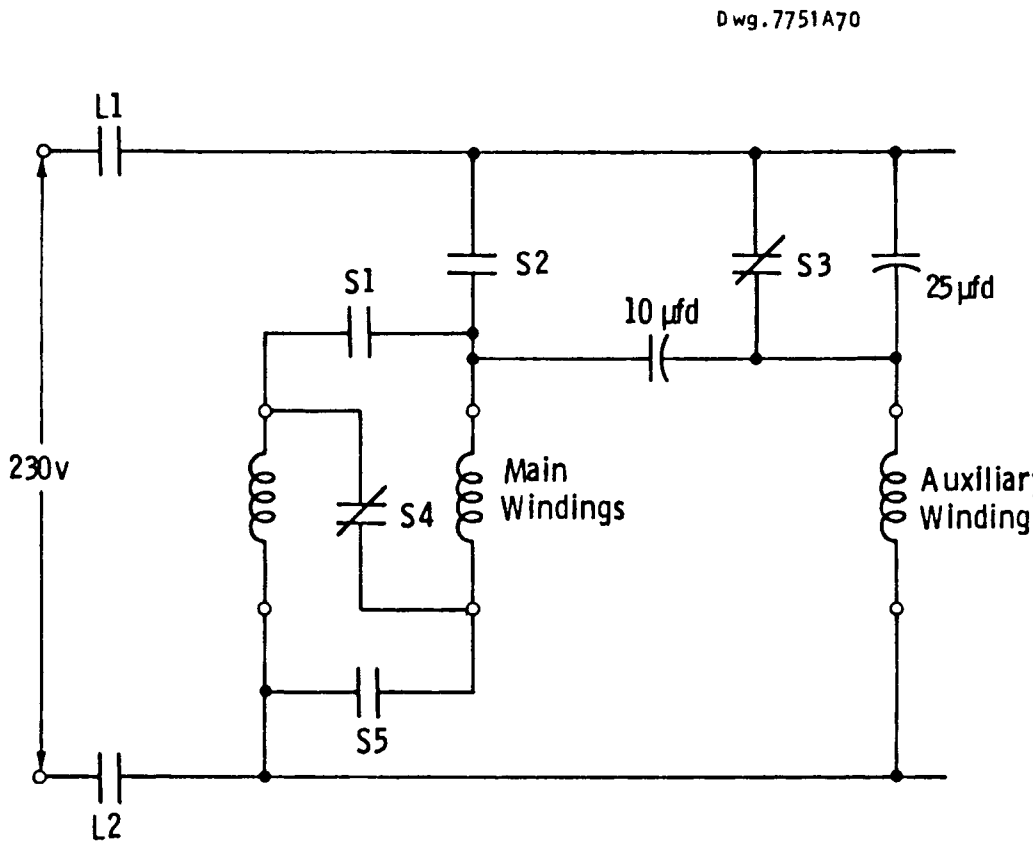

Figure 3.1-10 - Two-strength motor circuit

continuously in extreme air conditioning service. The dual-strength feature is achieved by a novel winding design and switching arrangement that reverses the respective roles of the main and auxiliary windings during low-stroke operation and reconnects the available capacitors. This arrangement significantly improves compressor efficiency at the low power levels experienced during low-stroke operation. Configured in the preprototype model, the motor efficiency exceeds 88 percent in both high-capacity and low-capacity operation at the respective design points.

3.1.3 Dual-Stroke Compressor Performance

Compressor performance characteristics were obtained on two complementary test facilities. For preliminary testing, a conventional compressor calorimeter manufactured by Starco, Inc., Dayton, Ohio (Model 50,000 Btu/H) was used. This system is illustrated in Figure 3.1-11. Key performance points were measured to permit qualification of the compressor over a range of suction pressure and discharge pressures. At all points, suction superheat was maintained at 20°F and subcooling at 15°F. Upon qualification, the compressor was installed in an automatically controlled calorimeter as depicted in Figure 3.1-12. The full performance map was developed over a range of -20°F to 50°F saturation suction temperature and 100°F to 130°F standard discharge temperature. Oil cooling of the compressor motor was achieved through a water-to-Freon heat exchanger, with oil return temperature maintained at 130°F. This arrangement simulated the estimated system performance of the air to Freon heat exchanger in the delivery air stream.

The performance of the preprototype compressor is shown in Figure 3.1-13. It should be noted that while compressor performance in both capacity modes is given for a wide range of saturation condensor and suction temperatures, actual operation of the compressor will be limited to an optimum range for each capacity based on system considerations. For example, operation at low stroke in heating mode will not be permitted below a suction temperature of less than approximately 30°F.

Figure 3.1-11 - Calorimeter and test table--front view

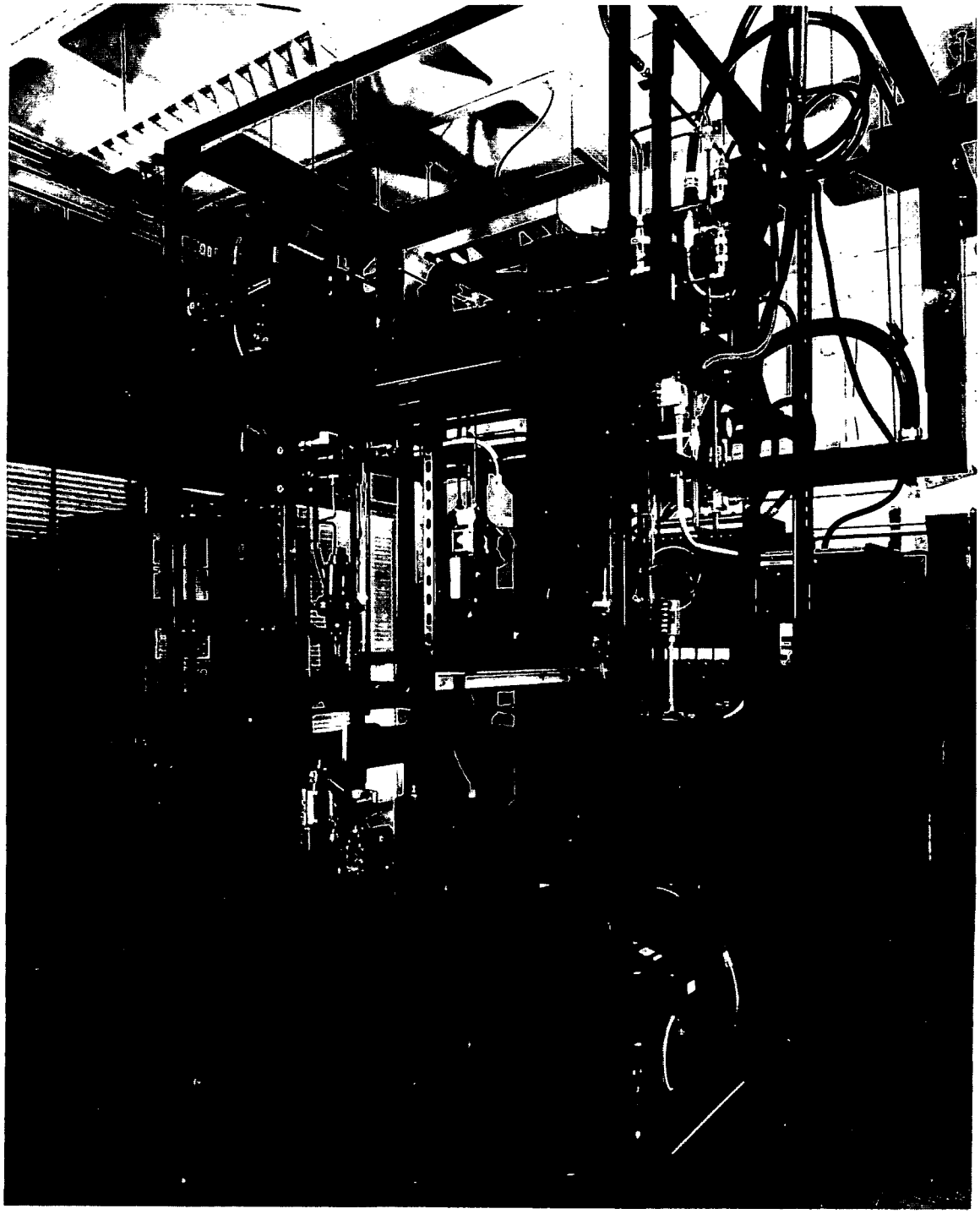

Figure 3.1-12 - Compressor calorimeter

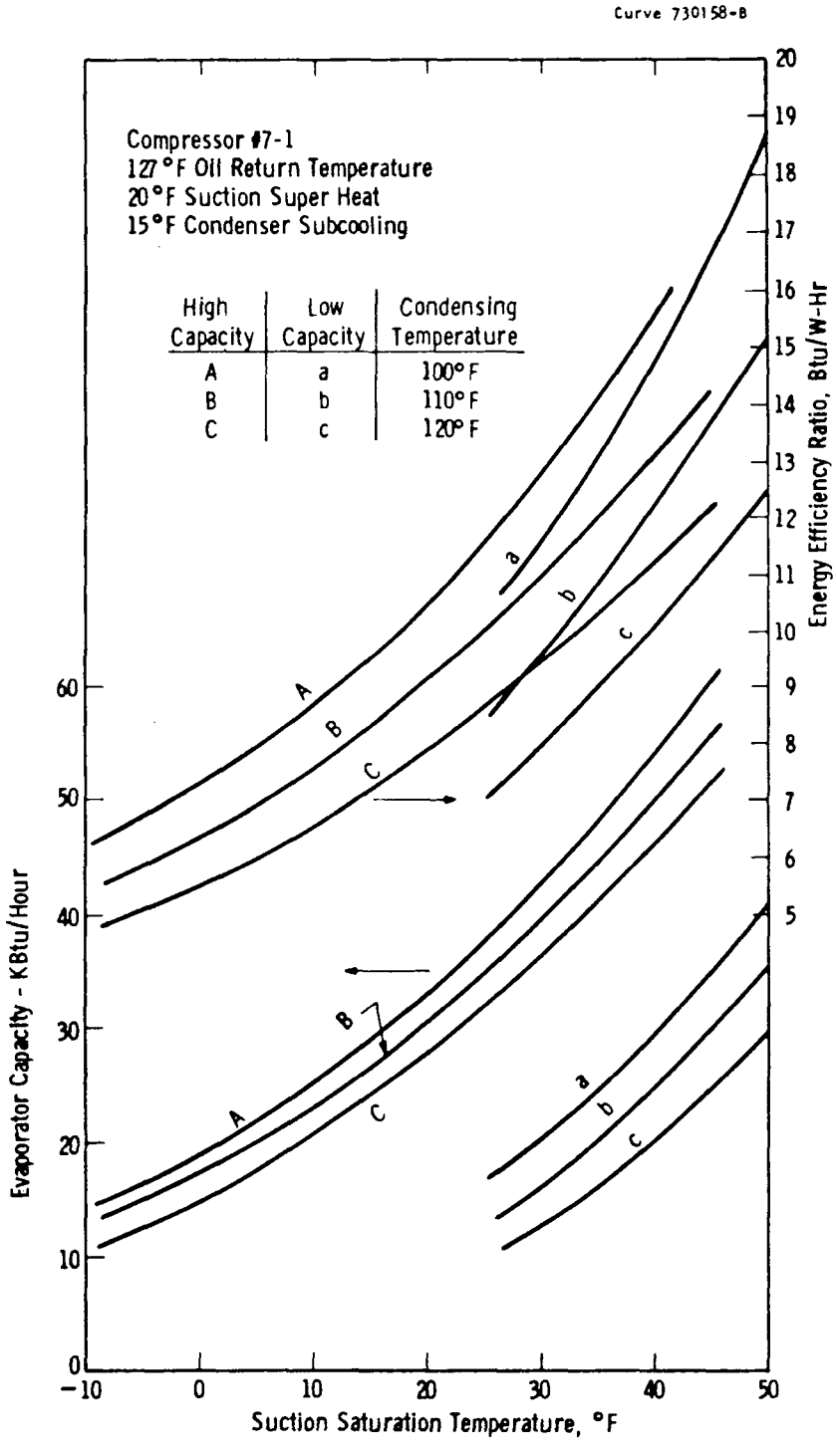

Figure 3.1-13 - Performance of prototype dual-stroke compressor (Mod II)

Similarly, high capacity operation in heating mode will not occur above 30°F suction temperature and during cooling mode when suction temperature decreases below 45°F.

3.1.4 Geared Two-Speed Compressor

Introduction

The geared two-speed method of capacity modulation was identified for development under this program as an alternate to the dual-stroke design. This development effort proceeded in parallel with the dual-stroke development until sufficient evidence was available to make an engineering and economic selection of the most cost effective design. The development of the geared two-speed compressor progressed to the point that thermodynamic performance was measured but durability was not demonstrated. Because of time and financial constraints, the development of geared speed-change design was terminated upon selection of the dual-stroke design as the preferred technology.

Technical Discussion

The geared two-speed compressor consists of five functional assemblies. They are: (a) a modified section of the crankcase from a standard Westinghouse CD048 compressor plus standard pistons, connecting rods, bearings and that portion of the crankshaft in contact with these parts; (b) a positive displacement oil pump which is substituted for the integral low head centrifugal pump; (c) a reversible motor; (d) a separate motor housing with support bearings; and (e) a transmission between the reversible motor and the compressor.

The function of the transmission in the geared speed-change compressor is to drive the compressor crankshaft at two different speeds, depending on the direction of rotation of the drive motor. In concept, this is accomplished by driving the crankshaft through overrunning clutches that idle one speed gear while the other speed gear is active.

External spur gears were used throughout the transmission. For space conservation, the input and output shafts of the transmission were on the same nominal centerline. Two alternate ways of driving the crankshaft in the high-speed mode were evaluated.

The first model transmission that was built and tested utilized five external spur gears and consisted of (a) a motor drive shaft gear; (b) two idler gears; (c) a high-speed output gear with an overrunning clutch in the hub; and (d) a three-to-one step-down gear with an overrunning clutch in the hub as the low-speed output.

Both gears drove the cantilevered crankshaft stub through the clutches in their hubs. In this design the compressor crankshaft, which rotates at the same speed and in the same direction as the motor, was not directly coupled to the motor shaft through the clutch. Instead, the motor shaft gear drove the first idler gear, which in turn drove the crankshaft through the high-speed output gear and clutch. This design is shown in Figure 3.1-14.

The second transmission was a variation on the previous model. This design, shown in Figure 3.1-15, employed a direct-drive coupling between the motor drive shaft and the crankshaft instead of driving through the first idler gear as in the previous design. The goal of this design approach was to reduce gear box losses in the high-capacity mode by eliminating loaded gear meshes. The arrangement also contained one less gear than the first model.

Torrington drawn cup clutch bearings were selected for use in this transmission because of their compact size in the radial dimension. They were the only available clutches that enabled the transmission to fit within the radial dimension of the compressor crankcase. The maximum size that would be utilized in this transmission was also limited by the diameter of the crankshaft bearings since the clutch drive output shaft was a part of the crankshaft and had to fit through the bearings.

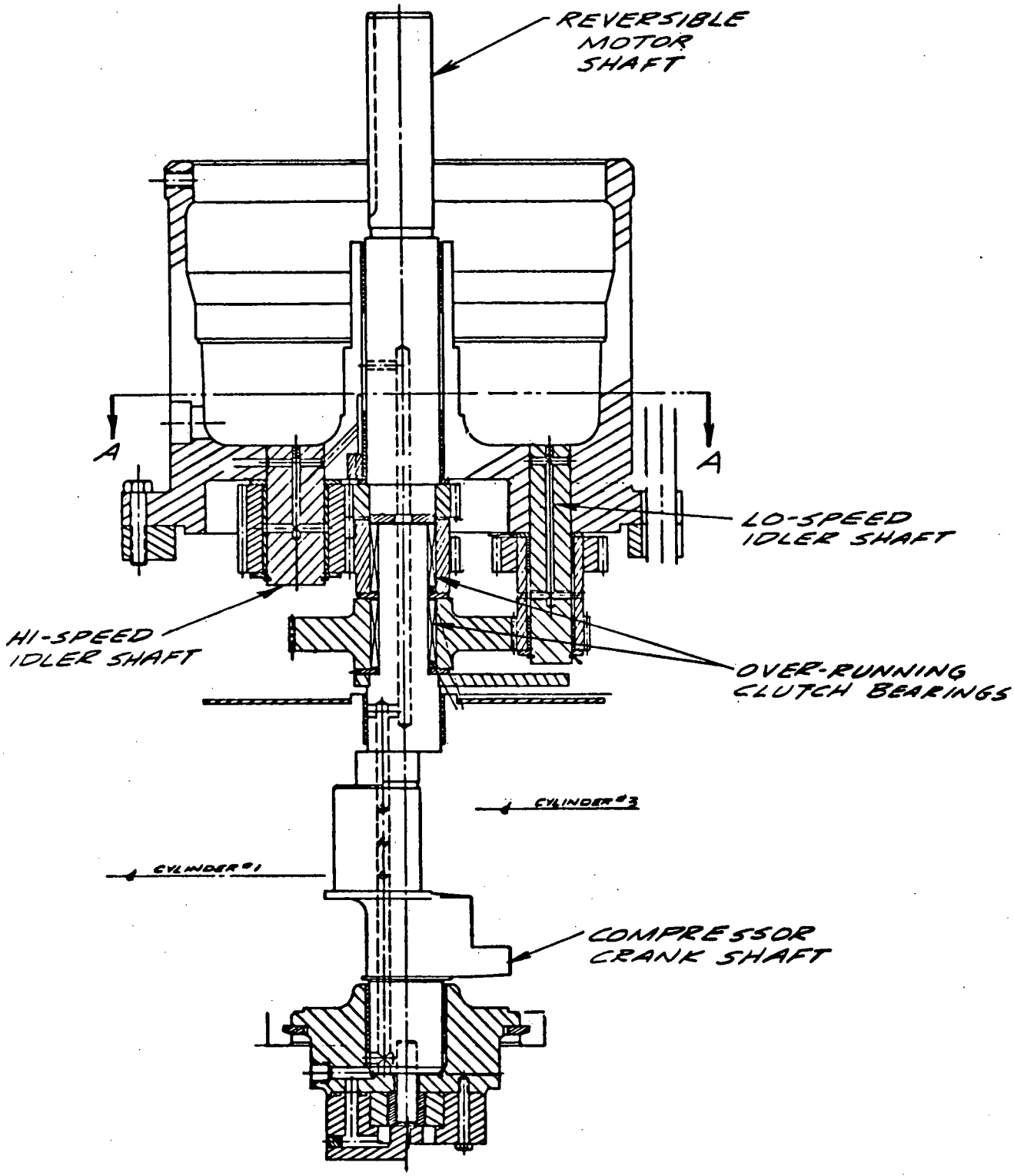

Figure 3.1-14 - Double fixed shaft idler

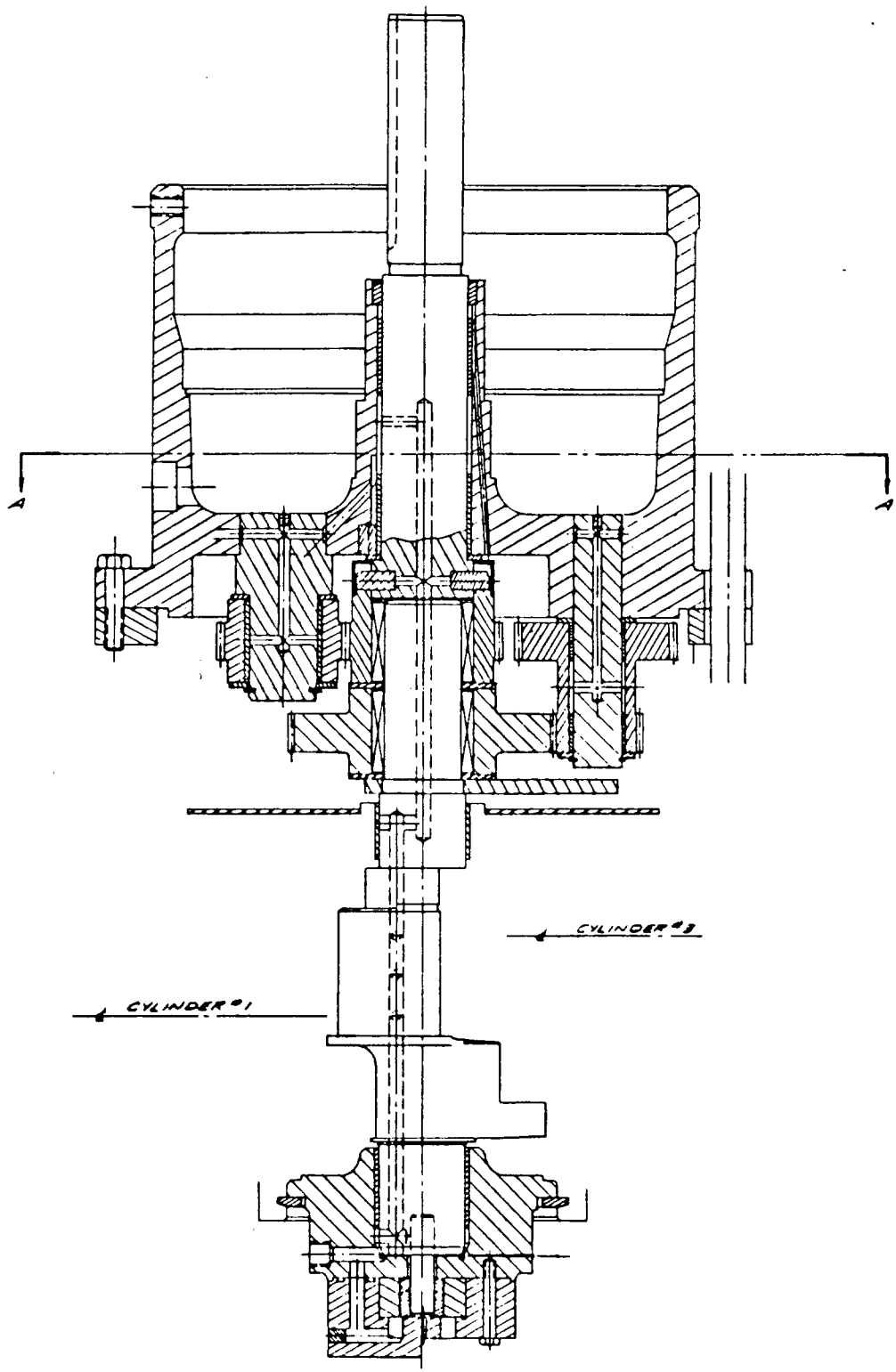

Figure 3.1-15 - Double idler--direct drive

Each transmission contained two clutch bearings of the same size. The first model transmission built and tested contained 3/4 in ID clutch bearings. The second transmission contained two 1 in ID clutch bearings.

Preliminary Testing

Each model compressor was first bench tested open to the atmosphere to provide a mechanical check, and to insure that the oil pump was functioning and that little or no oil was being pumped in the refrigerant circuit. The units were also operated in both motor directions at this time.

Each unit was then operated in a refrigerant test loop for short periods of time in both high- and low-capacity modes. This was to provide a load on the transmission. Frequent inspections were made for early signs of wear.

After short duration testing was deemed satisfactory, longer runs of up to several hours were made. If the units passed this period of testing, they were then operated on the calorimeter to obtain their performance.

Compressor Performance

The first geared two-speed compressor tested used the idler gear high-speed drive path. This was expected to load the high speed clutch/bearing in the most favorable way. The compressor performance curves for this configuration are shown in Figure 3.1-16. As expected, the curves indicate slightly lower capacity and slightly higher power than for the standard CD048 compressor. An estimate of the losses in the gear box was made by scaling up the compressor to match the capacity of the standard machine and then comparing the resulting power requirement. When this comparison was made, the initial tests indicated that the losses were higher than expected. These estimates of the gear box

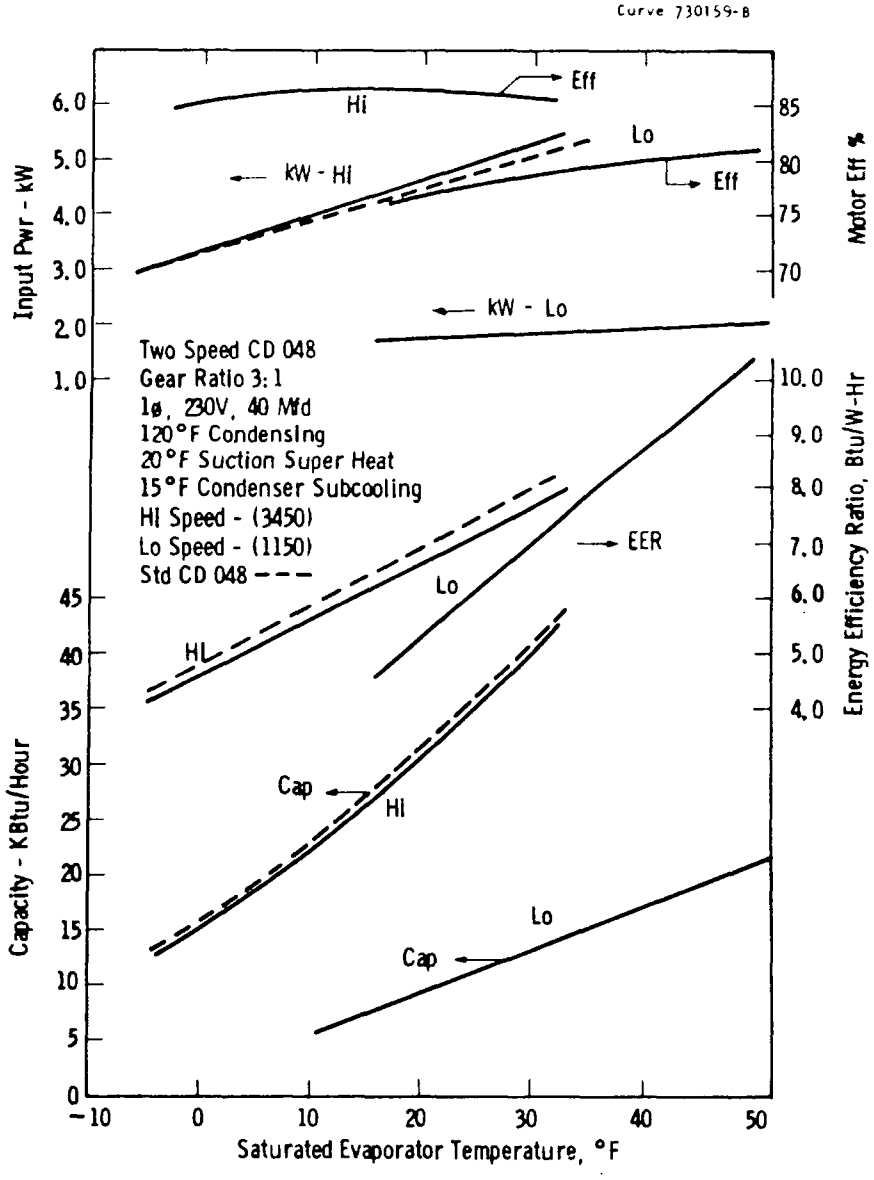

Figure 3.1-16 - Geared two-speed compressor performance (idler gear high-speed path)

losses from measurements are presented in Figures 3.1-17 and 3.1-18 for the high-speed and low-speed operations, respectively.

The second model configuration employed the direct-drive high-speed coupling that was driven by the motor shaft through a gimbal arrangement. The performance of this model is shown in Figure 3.1-19. This configuration showed a slight improvement over the previous drive, although the improvement was not as great as expected.

The operational life of these compressors was extremely short: less than 400 hours. The high-speed clutch bearing failed in both models. The smaller (3/4 in ID) clutch bearing was completely destroyed in 400 hours and the 1 in ID clutch bearing showed definite signs of failure after only 100 hours. Analysis of the failed clutches indicated that they failed due to torque overloads.

Since the 1 in clutch was the largest torque-rated clutch that would fit within the space limitation of the equipment, the development effort was discontinued at this point. A major redesign of the compressor housing would have to be undertaken to provide space for a larger diameter clutch that would be capable of withstanding the torque loads imposed by this compressor.

3.1.5 Evaluation

The performance of the prototype dual-stroke compressor in its high-capacity mode is compared with several competing high-efficiency compressors in Figure 3.1-20 at a saturated condensing temperature of 120°F. Clearly, the oil-cooled-dual-stroke compressor has higher capacity at low evaporating temperature and has significantly higher efficiency across the saturated evaporator temperature range.

Table 3.1-4 presents an estimate of the cost adders associated with each new or modified component in the dual-stroke compressor.

This incremental cost as seen by the manufacturer will be reflected in the marketplace as a cost premium of at least $110 for the compression system alone.

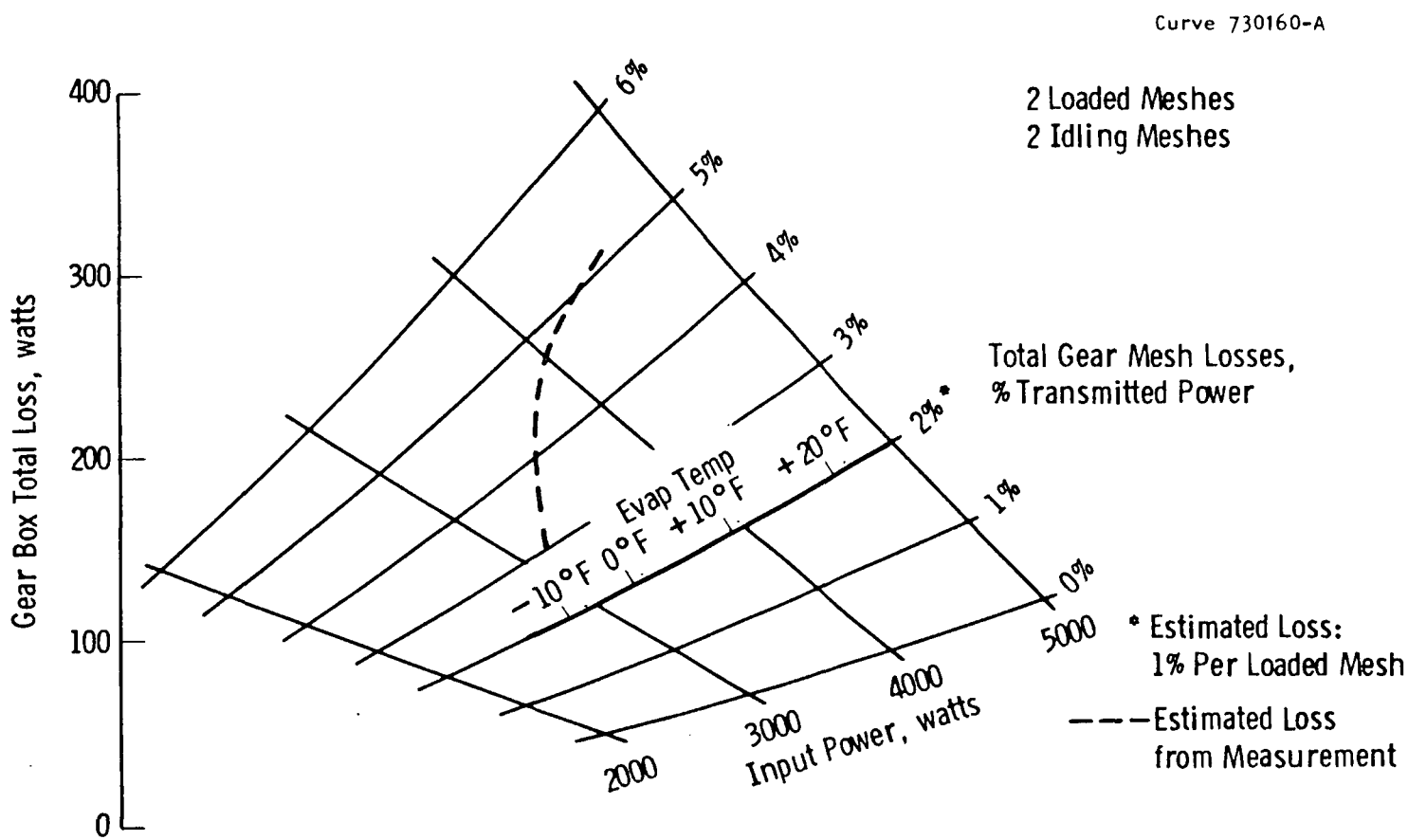

Figure 3.1-17 - Estimated gear box losses--high speed

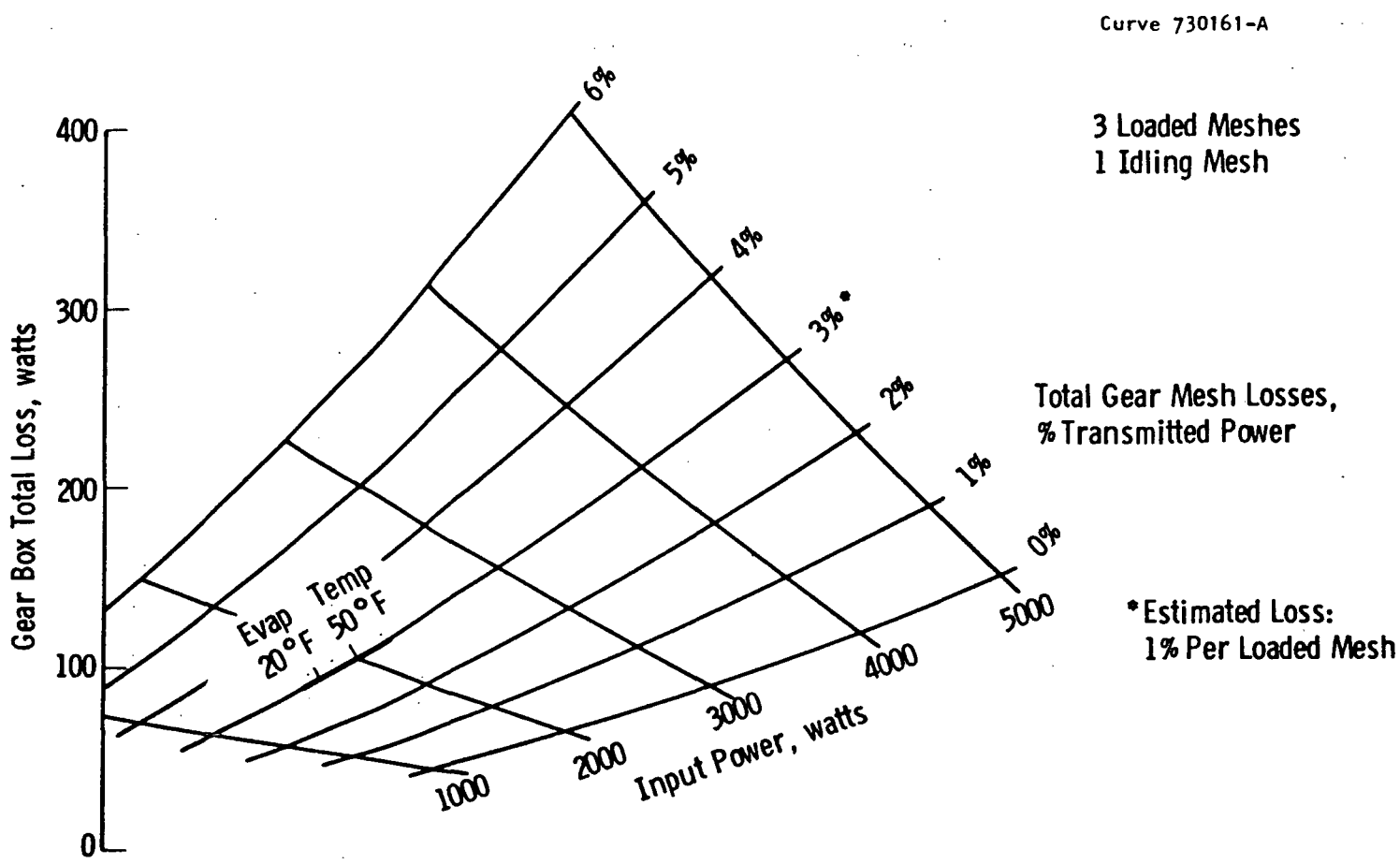

Figure 3.1-18 - Estimated gear box losses--low speed

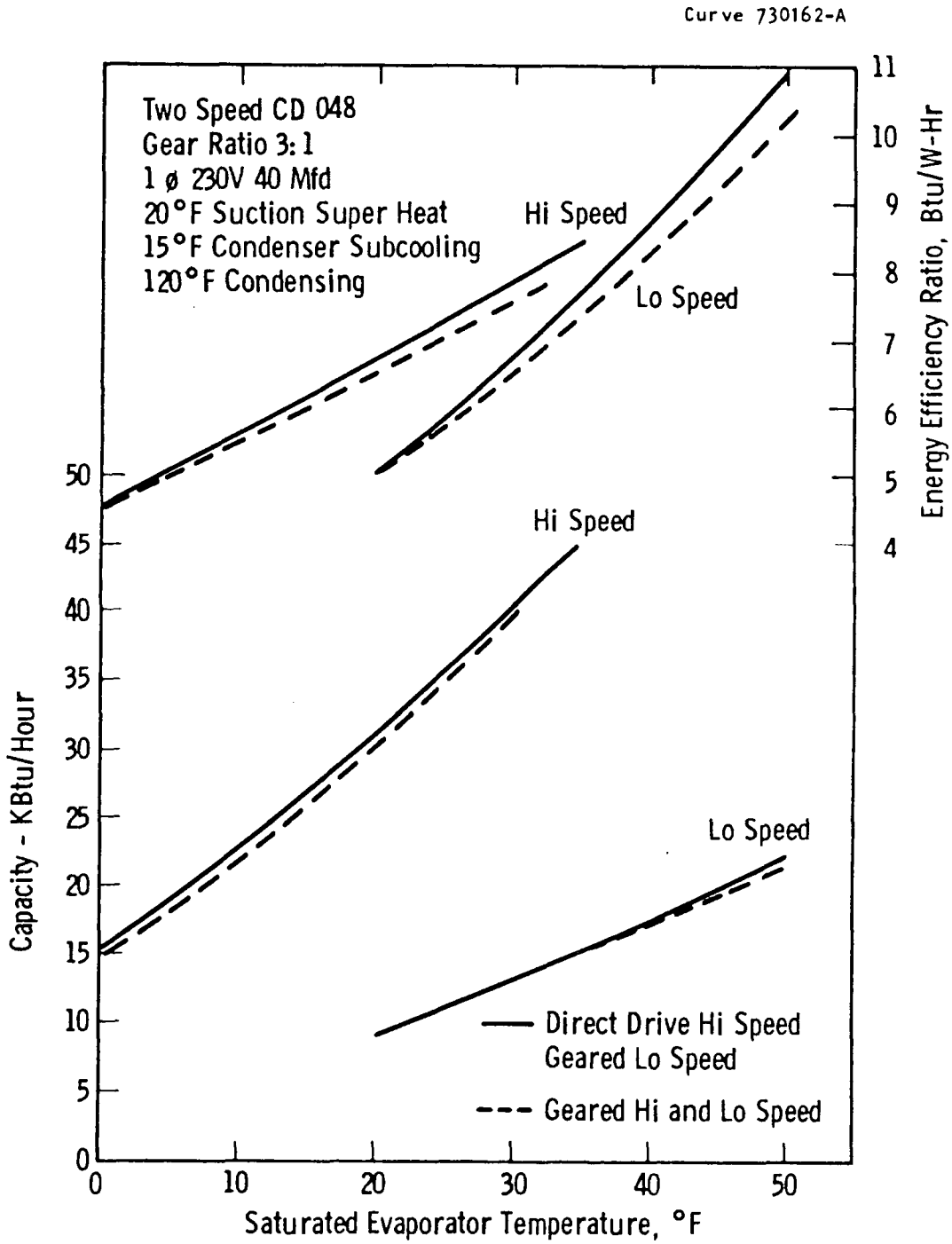

Figure 3.1-19 - Geared two-speed compressor performance (comparison of direct versus geared high-speed path)

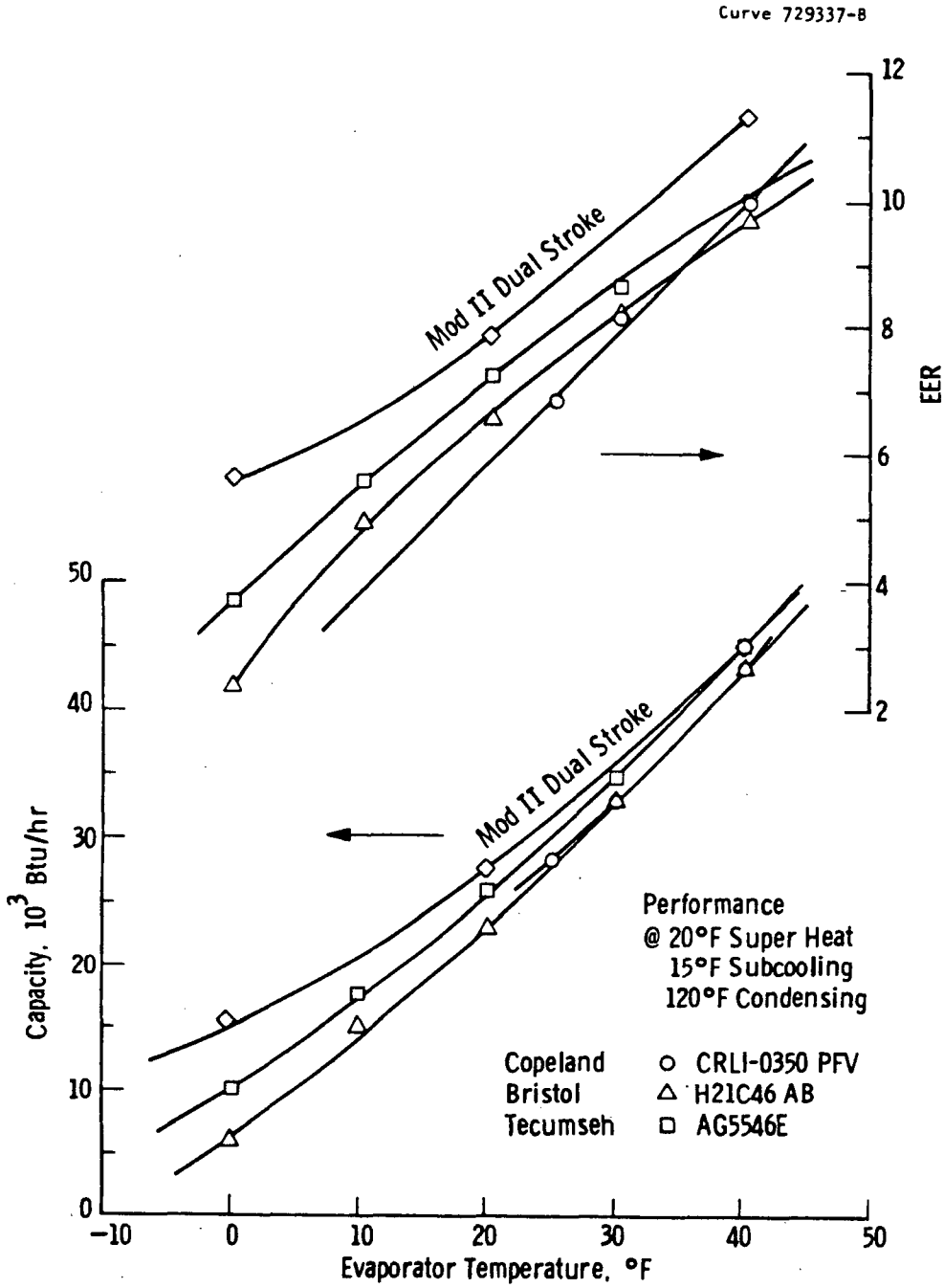

Figure 3.1-20 - Comparison of Mod II dual-stroke compressor versus competitors

Table 3.1-4

Analysis of Incremental Costs for the Dual-Stroke Compressor

(Production volume of 100,000 units per year)

Crankcase modifications	$0.80	
Crankshaft modifications	0.25	
Cam (labor and material)	4.00	
Lower shell modifications	1.19	
Upper shell modifications	0.83	
High-efficiency motor	6.71	
Capacitor change		$(0.80)
Reversing contactor	16.70	
Miscellaneous hardware	1.09	
Suction gas-cooled-compressor		30.77
Oil cooler	5.15	
Reversible oil pump	4.00	
Oil pump housing	3.10	
Suction piping	0.69	
Discharge piping modifications	0.16	
Oil cooling adder		13.10
Oil-cooled dual-stroke compressor		$43.87

Similarly, the estimated costs of the added components for the geared speed change compressor are given in Table 3.1-5.

Table 3.1-5

Analysis of Incremental Costs for the Geared Two-Speed Compressor

(Production volume of 100,000 units per year)

Gear set	$18.00	
Two clutch bearings	8.00	
Two idler shafts	2.00	
Motor housing	5.00	
Crankcase Divider	0.30	
Motor shaft	1.50	
Crankcase stub	0.75	
Oil pump (non-reversible)	2.50	
Oil pump housing	3.10	
Crankcase modifications	0.55	
Suction piping	0.75	
Lower shell modification	2.00	
Reversing contactor	16.70	
Miscelleneous hardware	1.25	
High-efficiency motor	6.71	
Capacitor change		$(0.80)
Suction gas cooled		68.31
Oil cooler	5.15	
Oil cooled		$73.46

The geared speed-change compressor costs 70 percent more than the dual-stroke machine and, quite clearly, the dual-stroke machine is preferred over the gear speed-change machine.

3.1.6 Supporting Computer Analyses

Introduction

To support the parallel analytical system development effort, the performance characteristics of as yet unbuilt or untested compressors was needed. In addition, as potentially advantageous

compressor design changes were hypothesized, the analytical model was used to determine if the impact of those changes upon compressor performance made a hardware development effort worthwhile. The necessary performance maps were generated using a Westinghouse proprietary computer code for the simulation of reciprocating compressors. A brief summary of the analytical effort follows.

Summary

The alternative heat pump compressors that were studied analytically are shown in Table 3.1-6. Detailed results are too voluminous for inclusion in this report.

3.2 Heat Exchanger Design and Development

The refrigerant circuitry for a conventional heat pump outdoor coil is a compromise between the requirements for evaporator service and condenser service. The selection of the number of parallel circuits in both operating modes is a trade-off between the desire for high refrigerant velocities in the tubes to improve the tube side heat transfer coefficient and the desire to minimize refrigerant pressure drop to maintain the maximum temperature difference between the refrigerant and the air. Minimizing refrigerant pressure drop is particularly important in heat pump outdoor coils at low ambient temperature since the derivative of saturation temperature with respect to pressure increases as the saturation temperature declines.

The natural circulation driven boiling thermosiphon heat exchange coil is attractive for this service since a large number of parallel circuits can be used to minimize refrigerant pressure drop without significantly penalizing the tube-side heat transfer coefficient.

In condenser service a large number of parallel paths is felt to be undesirable at exit because the low liquid velocities will limit the tube-side heat transfer coefficient, and as a result adequate subcooling

Table 3.1-6
Alternative Heat Pump Compressor Configurations

No	Configuration Description	No. Cyl.	Motor[1]	Stroke[2]	Clearance Volume	Discharge Valve[3]	Suction Valve[3]	Cooling[4]	Suction Ports	Nominal rpm	Computer Run	Hardware Test
1	Standard CD048	3	0	0	.05	0	0	0	0	3450	+	+
2	"	3	0	0	.05	0	0	+	0	3450	+	0
3	Two Stroke-Long Crank	3	0	+	.06	0	0	0	0	3450	+	+
4	Two Stroke-Short Crank #1	3	0	+	.229	0	0	0	0	3450	+	+
5	Two Stroke-Long Crank	3	+	+	.02	+	+	+	0	3450	+	0
6	Two Stroke-Short Crank #1	3	+	+	.175	+	+	+	0	3450	+	0
7	" #2	3	+	+	.087	+	+	+	0	3450	+	0
8	" #3	3	+	+	.291	+	+	+	0	3450	+	0
9	#4	3	+	+	Optimum	+	+	+	0	3450	+	0
10	" -Long Crank	3	+	+	.02	+	+	+	+	3450	+	?
11	Standard CD030	2	0	0	.054	0	0	0	0	3450	+	+
12	"	2	0	0	.054	0	0	+	0	3450	+	+
13	"	2	0	0	.022	+	+	0	0	3450	+	+
14	Standard CD048-Gearbox #1	3	0	0	.05	0	0	0	0	3450	+	+
15	" #1	3	0	0	.05	0	0	0	0	1128	+	+
16	" #1	3	+	0	.02	+	+	+	0	3450	+	0
17	" #1	3	+	0	.02	+	+	+	0	1128	+	0
18	" #2	3	+	0	.02	+	+	+	0	1725	+	0
19	" #3	3	+	0	.02	+	+	+	0	?	+	0
20	" #4	3	+	0	.02	+	+	+	0	Optimum	+	0/+
21	Standard CD048-Motor #1	3	0	0	.02	+	+	+	0	3450	+	0
22	" #1	3	0	0	.02	+	+	+	0	1725	+	0
23	" #2	3	0	0	.02	+	+	+	0	3450	+?	0
24	" #2	3	0	0	.02	+	+	+	0	1125	+?	0
25	" #3	3	+	0	.02	+	+	+	0	3450	+?	0
26	" #3	3	+	0	.02	+	+	+	0	1725	+?	0
27	Two Stroke-Long Crank	3	++	+	.06	0	0	Oil	0	3450	0	+
28	Two Stroke-Short Crank-1	3	++	+	.229	0	0	Oil	0	3450	0	+
29	Two Stroke-Short Crank-2	3	++	+	.087	0	0	Oil	0	3450	0	0
30	Two Stroke-Short Crank-3	3	++	+	.291	0	0	Oil	0	3450	0	0
31	CD048 Super	3	+	0	.02	+	+	+	0	3450	+	0 Same as 5
32	CD048 Improved	3	+	0	.05	0	0	Oil	0	3450	+	
33	Gearbox #1	3	++	0	.05	0	0	Oil	0	3450	+	
34	"	3	++	0	.05	0	0	Oil	0	1128	+	
35	Gearbox #2	3	++	0	.05	0	0	Oil	0	1725	+	
36	Gearbox #3	3	++	0	.05	0	0	Oil	0	Optimum	+	
37	Gearbox #1	3	0	0	.05	0	0	0	0	3450		+ #14 As built
38	"	3	0	0	.05	0	0	0	0	1128		+ #15 As built
39	Two Stroke-Long Crank	3	0	+	.06	0	0	0	0	3450	0	+ #3 As built
40	Two Stroke-Short Crank-1	3	0	+	.229	0	0	0	0	3450	0	+ #4 As built
41	Two Stroke-Short Crank-4	3	++	+	Optimum	0	0	Oil	0	3450	0	0

NOTE 1 - Scaled Motor = +, Specified Motor = 0, Dual Peak Efficiency = ++.
NOTE 2 - Two Stroke = +, Single Stroke = 0.
NOTE 3 - New Model = +, Existing Model = 0.
NOTE 4 - Adiabatic Suction = +, Suction Gas Cooled Motor = 0, Cooled Motor = Oil.

will be difficult to obtain. Further, subcooling in a large number of parallel paths makes coupling of the condenser with the expansion device difficult because a requirement for more subcooling backs up liquid in the heat exchanger; but since the all-parallel tube layout results in a low-heat transfer coefficient to the liquid, more surface will be consumed for the same degree of subcooling in the gravity-driven all-parallel configuration than in the forced-flow conventional configuration.

This report documents an investigation of the forced air warmed gravity driven boiling thermosiphon evaporator in a heat pump system. Similarly, this same heat exchanger is investigated as a condenser for the heat pump when operating in the air conditioning mode.

Both theoretical and experimental results are presented and discussed.

3.2.1 Boiling Thermosiphon

Introduction

A thermosiphon relies on the fluid circulation caused by the static pressure head difference between the heated less-dense riser leg and the unheated (or cooled) more-dense downcomer leg. Figure 3.2-1 shows the elements of a boiling thermosiphon. The two-phase refrigerant with specified enthalpy enters the bottom manifold, mixes with the circulating liquid refrigerant, and evaporates inside the riser tubes by absorbing heat from the air passing over the finned outer tube surface.

The vaporized refrigerant goes out the top of the manifold. The nonvaporized liquid refrigerant flows downward through downcomers to the bottom manifold to complete the circulation. The circulation ratio for the heat exchanger is defined as the ratio of the total mass flow to that vaporized.

Without downcomers and the liquid recirculation, the system becomes a conventional forced flow evaporator. This report investigates

Dwg. 7755A52

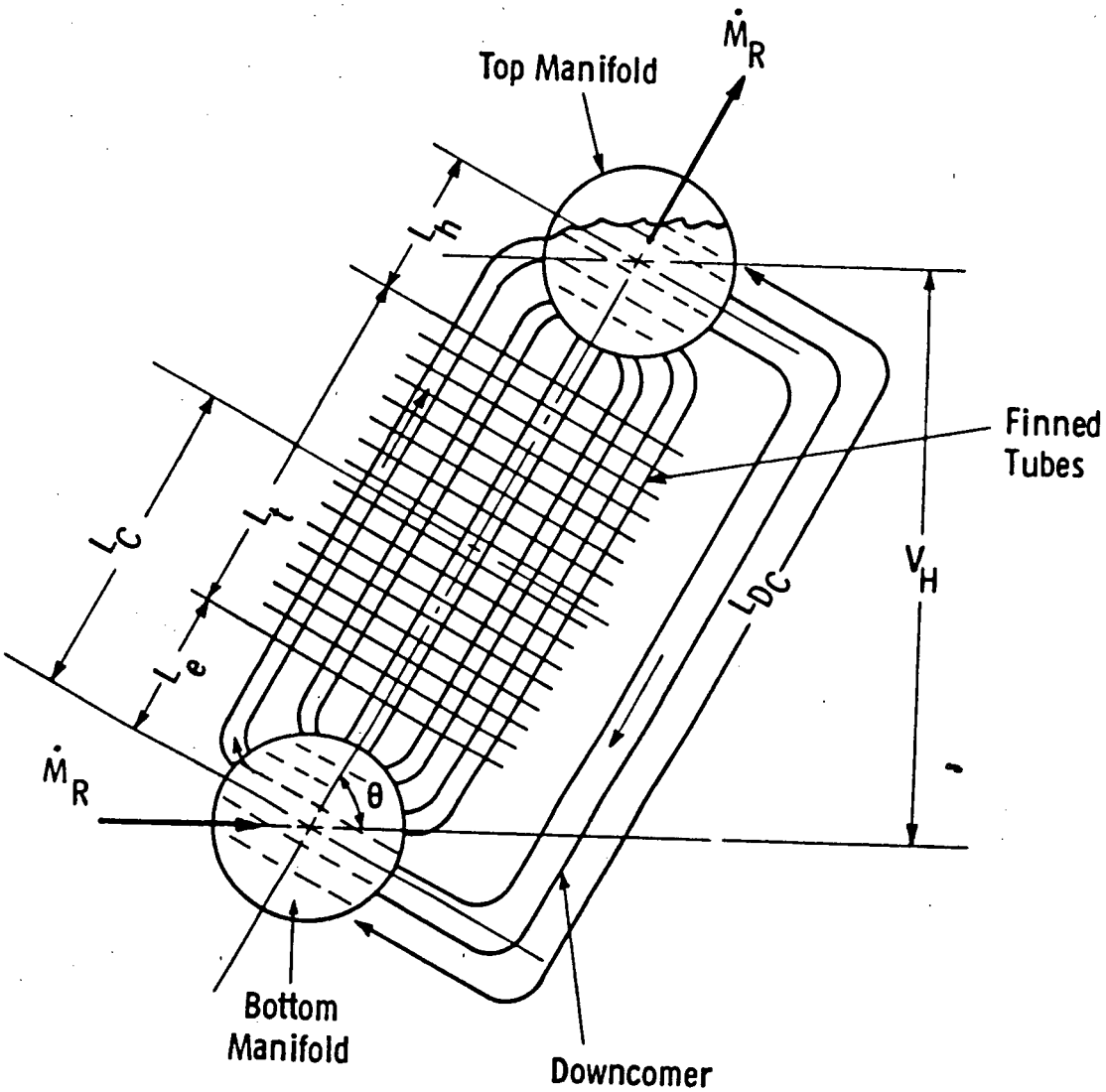

Figure 3.2-1 - Schematic diagram of boiling thermosiphon heat exchanger

the effect of the design parameters upon the performance of an inclined boiling thermosiphon evaporator. A computer program has been written in subroutine form for integration into the computer code representing the entire heat pump system.

Numerical Results and Discussion

Table 3.2-1 lists some characteristics for a boiling thermosiphon evaporator designed to fit into a proposed 2 x 3 x 4 ft box (the corresponding angle of the evaporator tube inclined from the horizontal position is about 53°). The data were based on the following dimensions:

Evaporator tube: D_o = 0.393 in D_i = 0.323 in
L_t = 4 ft L_c = 2.5 ft
$L_e = L_h$ = 0.5 ft
Downcomer: V_H = 4 ft L_{DC} = 5.25 ft
Fin thickness t_f = 0.00550 in
Number of fins N_f = 13 fins/in of tube length
Tube transverse pitch P_t = 1.00 in
Tube longitudinal pitch P_ℓ = 0.866 in
Number of tubes per row = 25 tubes/row
Flow conditions:
Refrigerant mass flow rate $\dot{M}_R$ = 540.65 lbm/h
Inlet enthalpy h_{in} = 20.01 Btu/lb
Standard air volume flow rate V_a = 3500 SCFM
Air inlet temperature T_{ai} = 47°F

The heat exchanger effectiveness (ε) is used to measure the effectiveness of the actual heat transfer relative to the maximum possible rate of heat exchange. It is defined as

$$\varepsilon = \frac{T_{ai} - T_{ae}}{T_{ai} - T_{sat}}$$

Table 3.2-1

Design Characteristics of a Thermosiphon Reboiler

Properties	Downcomer D_{DC} = 1.0", N_{DC} = 1 5 Rows 125 Tubes	4 Rows 100 Tubes	3 Rows 75 Tubes	Downcomer D_{DC} = 2.0" N_{DC} = 1 100 Tubes	Downcomer D_{DC} = 3.0" N_{DC} = 1 100 Tubes	Downcomer D_{DC} = 1.0" N_{DC} = 2 100 Tubes	Downcomer D_{DC} = 1.0" N_{DC} = 3 100 Tubes	Downcomer D_{DC} = 1.0" N_{DC} = 1, 100 Tubes 30% more friction drop
(1) Heat Transfer Capacity, Btu/hr	47201	47127	46991	47139	47146	47131	47134	47127
(2) Operating Pressure, psia	70.36	68.39	64.95	68.71	68.89	68.52	68.58	68.39
(3) Saturation Temperature, °F	30.60	29.05	26.25	29.30	29.45	29.15	29.20	29.05
(4) Refrigerant Inlet Quality, %	1.422	1.907	2.773	1.829	1.783	1.876	1.861	1.907
(5) Inlet Quality at the Entrance of Evaporator Tube, %	0.075	0.100	0.146	0.034	0.024	0.059	0.044	0.10
(6) Circulation Head, psia	1.181	1.204	1.247	0.746	0.600	0.971	0.847	1.205
(7) Circulation Ratio	19.35	19.46	19.58	54.05	76.947	32.66	43.00	19.41
(8) Exit Quality, %	5.243	5.240	5.253	1.885	1.323	3.121	2.370	5.252
(9) Evaporator Tube Mass Velocity, lb/hr-ft^2	1.450×10^5	1.813×10^5	2.412×10^5	5.041×10^5	7.181×10^5	3.045×10^5	4.009×10^5	1.809×10^5
(10) Downcomer Flow Velocity, ft/sec	6.192	6.182	6.141	4.450	2.834	5.306	4.695	6.167
(11) Refrigerant Tube Inlet Velocity, ft/sec	0.524	0.665	0.909	1.777	2.514	1.089	1.421	0.663
(12) Refrigerant Tube Outlet Velocity, ft/sec	2.109	2.692	3.727	3.796	4.529	3.113	3.444	2.690
(13) Head of Downcomers, psia	2.233	2.238	2.247	2.237	2.236	2.237	2.237	2.238
of Evaporator Tubes	0.785	0.771	0.744	1.168	1.293	0.974	1.081	0.770
of Extending Tube to Bottom Manifold	0.213	0.210	0.204	0.219	0.220	0.215	0.217	0.210
of Extending Tube to Top Manifold	0.054	0.053	0.051	0.104	0.124	0.077	0.092	0.053
(14) Pressure Drop of Downcomer, psia	1.139	1.139	1.129	0.504	0.195	0.846	0.667	1.134
of Evaporator Tube - Friction	0.014	0.021	0.037	0.086	0.147	0.042	0.061	0.027
- Acceleration	0.014	0.022	0.041	0.061	0.087	0.037	0.049	0.022
of Extending Tube to Bottom Manifold	0.003	0.004	0.007	0.026	0.050	0.010	0.017	0.004
of Extending Tube to Top Manifold	0.012	0.019	0.034	0.072	0.121	0.036	0.052	0.019
(15) Evaporator Exit Pressure, psia	69.26	67.29	63.83	66.97	66.85	67.13	67.01	67.287
(16) Air Exit Temperature, °F	34.513	34.533	34.569	34.529	34.528	34.531	34.531	34.533
(17) Evaporator Coil Air Pressure Drop, inch of water	0.210	0.168	0.126	0.168	0.168	0.168	0.168	0.168
(18) Heat Exchanger Effectiveness, ε	0.761	0.695	0.599	0.705	0.711	0.699	0.701	0.695

where T_{ae} is the exit air temperature and T_{sat} the refrigerant saturation temperature at inlet.

From Table 3.2-1 we can see the heat exchanger effectiveness increases with an increasing number of evaporator tubes, while the circulation head is decreased with an increasing number of evaporator tubes. With the same number of evaporator tubes and increasing the diameter of the downcomer, the heat exchanger effectiveness increases but the circulation head decreases. Similarly, with the same diameter downcomer and increasing the number of downcomers, the heat exchanger effectiveness increases but the circulation head decreases. Increasing the diameter of the downcomer, the circulation ratio increases. Further increasing the downcomer diameter, the circulation ratio tends to increase slowly and approach an asymptotic value as expected (see Figure 3.2-2).

Further study shows that the uncertainty in the frictional pressure drop in two-phase flow has little effect on the design performance as shown in the last column of Table 3.2-1. This is due to the fact that the frictional pressure drop is very small compared to the circulation head of the entire system. Any uncertainty in the pressure drop in the evaporator tubes has little effect on the performance of a boiling thermosiphon evaporator.

System Studies

The mathematical model for the natural circulation coil as an evaporator was incorporated into the system performance computer program.

A Westinghouse HP048 heat pump, a 4-ton single capacity system, contains in the outdoor unit approximately the same amount of heat exchanger surface as represented by 88 tubes, each finned for 48 inches at 13 fins/in.

When this two-row 88 tube boiling thermosiphon evaporator is considered as a direct substitute for the conventional outdoor coil, then the system capacity and the system COP are predicted to improve as

Curve 729833-A

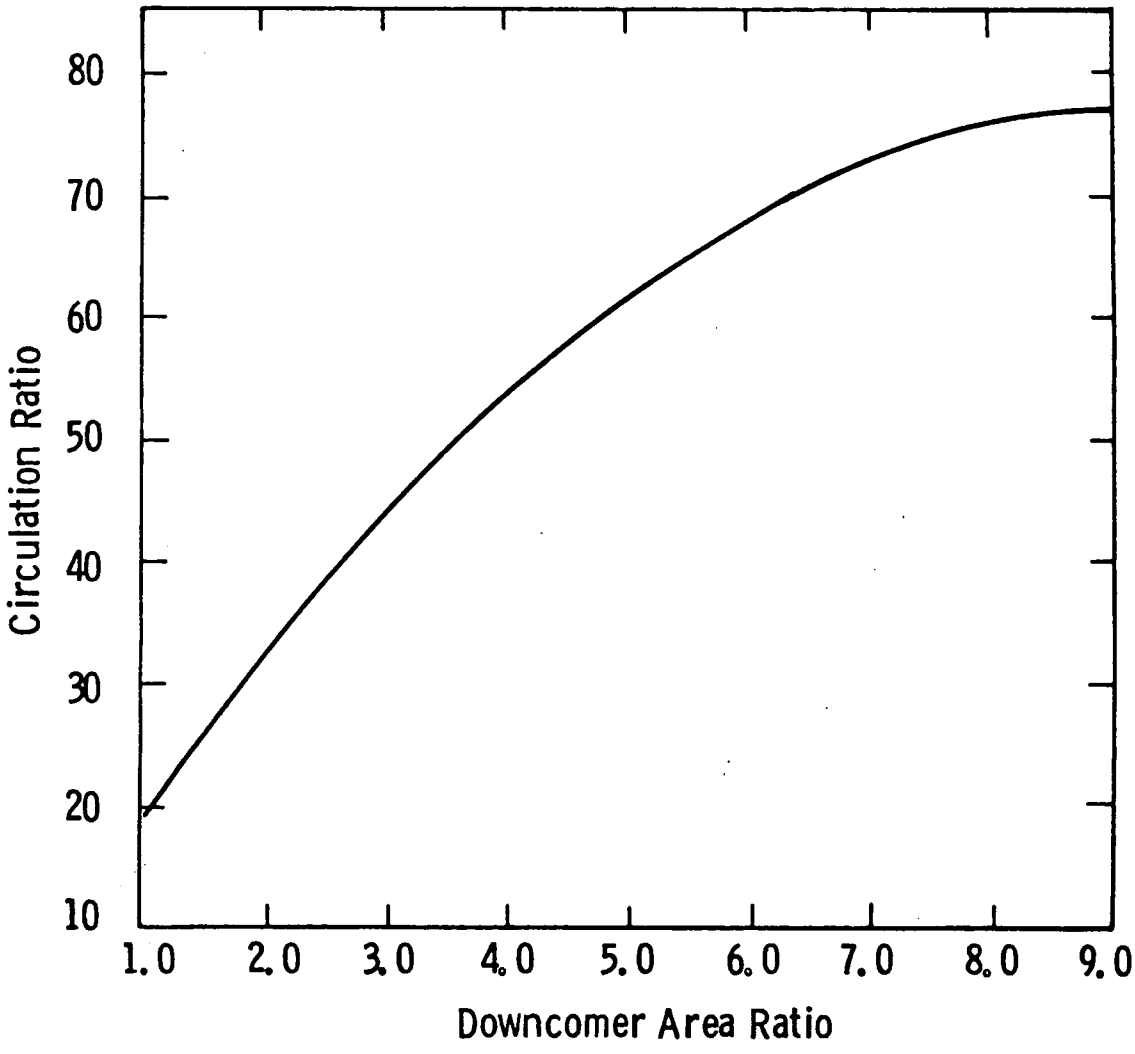

Figure 3.2-2 - Circulation ratio versus downcomer area ratio (based on 100 tubes with 1.0 in ID downcomer

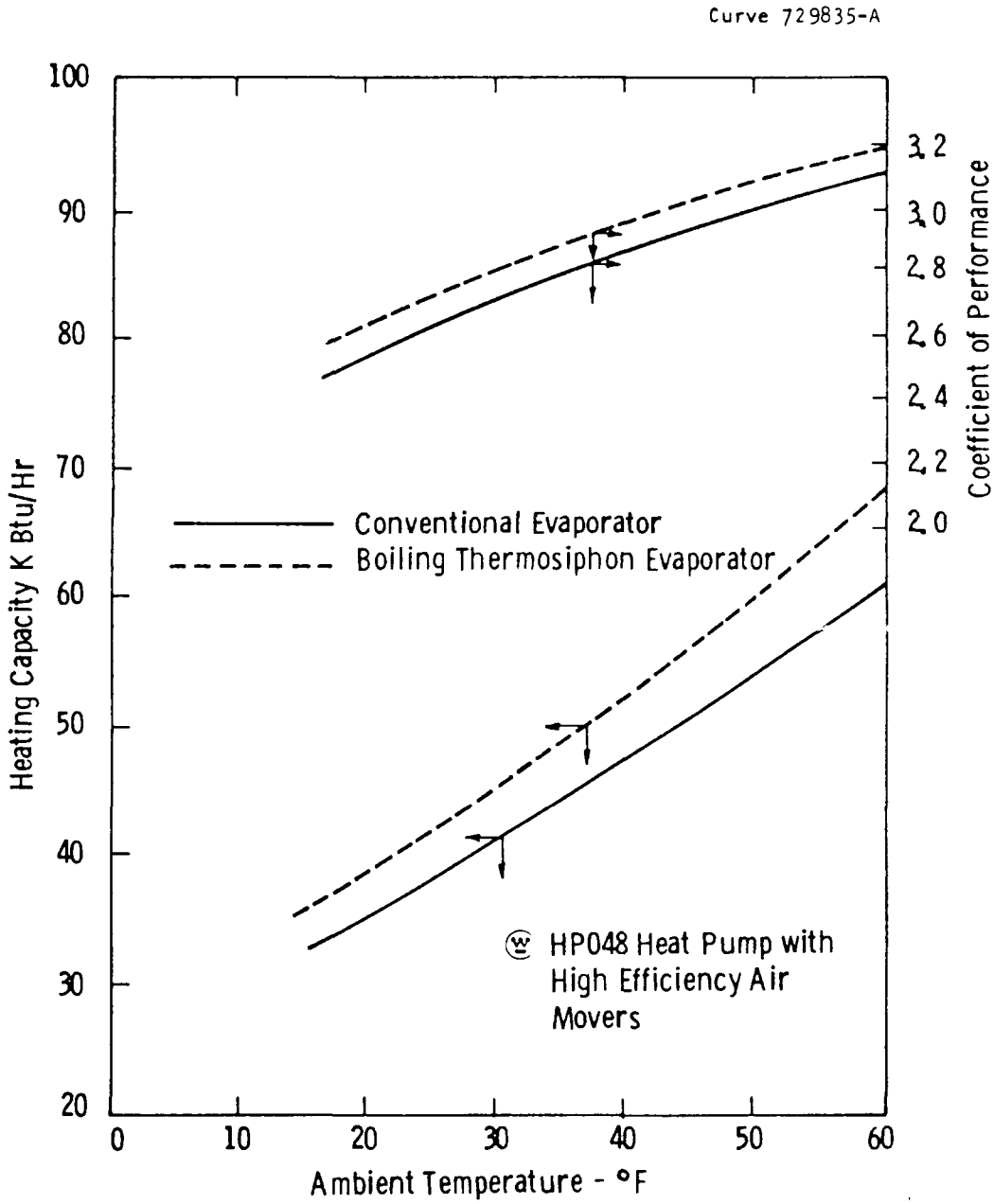

Figure 3.2-3 - Boiling thermosiphon evaporator impact on system heating performance (calculated)

shown in Figure 3.2-3. (Note that the example shown assumes higher efficiency air movers than the reference unit contains.)

The refrigerant pressure drop in the boiling thermosiphon evaporator is predicted to be about 2 psi compared to 8 - 18 psi for the conventional coil. The capacity is increased by 9 - 11 percent and the coefficient of performance by 3 - 4 percent. The condenser surface is unchanged and the condensing temperature must rise to condense the higher mass flow with the boiling thermosiphon evaporator.

A conventional system configured and optimized with the estimated characteristics of our advanced dual-stroke compressor (compressor configuration No. 5) was studied with a natural circulation outdoor coil of equivalent surface area substituted for this conventional outdoor coil. The estimated performance of the system in the high capacity heating mode of operation is shown in Figure 3.2-4. Predicted system heating capacity at 47°F for this system is 9.5 percent greater than that for the optimized system with a conventional evaporator, while system COP is improved by about 3 percent.

For an equivalent investment in heat exchanger surface, the boiling thermosiphon evaporator should conservatively improve COP by 0.10 or 3 percent based on a nominal COP of 3.0 at 47°F ambient air temperature while increasing capacity by 6 to 9 percent.

Experimental Results

An engineering prototype natural circulation coil has been fabricated and tested in the heat exchanger test facility at the Westinghouse R&D Center. The test coil, shown in Figure 3.2-5, used a conventional plate fin-tube surface with 3/8 in OD copper tubes and 1.0 in equilateral triangular pitch. Patterned aluminum fins with a thickness of 0.005 in and a 13 fin/in spacing were used. The four-row test coil has a finned length of 43.5 in (parallel to the tubes) and a finned width of 27 inches.

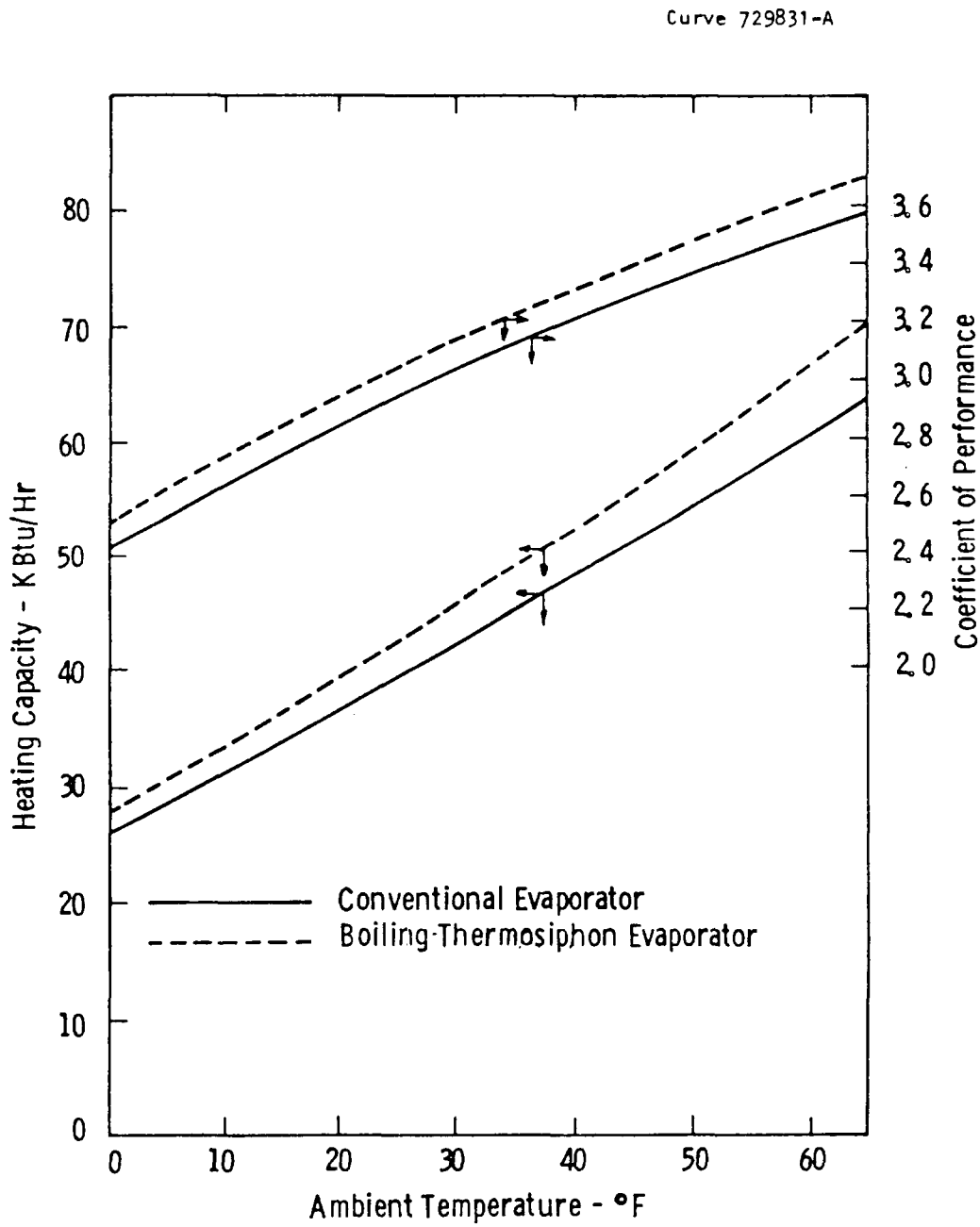

Figure 3.2-4 - Calculated effect of boiling thermosiphon evaporator upon heat pump heating performance (system optimized using dual-stroke compressor configuration No. 5)

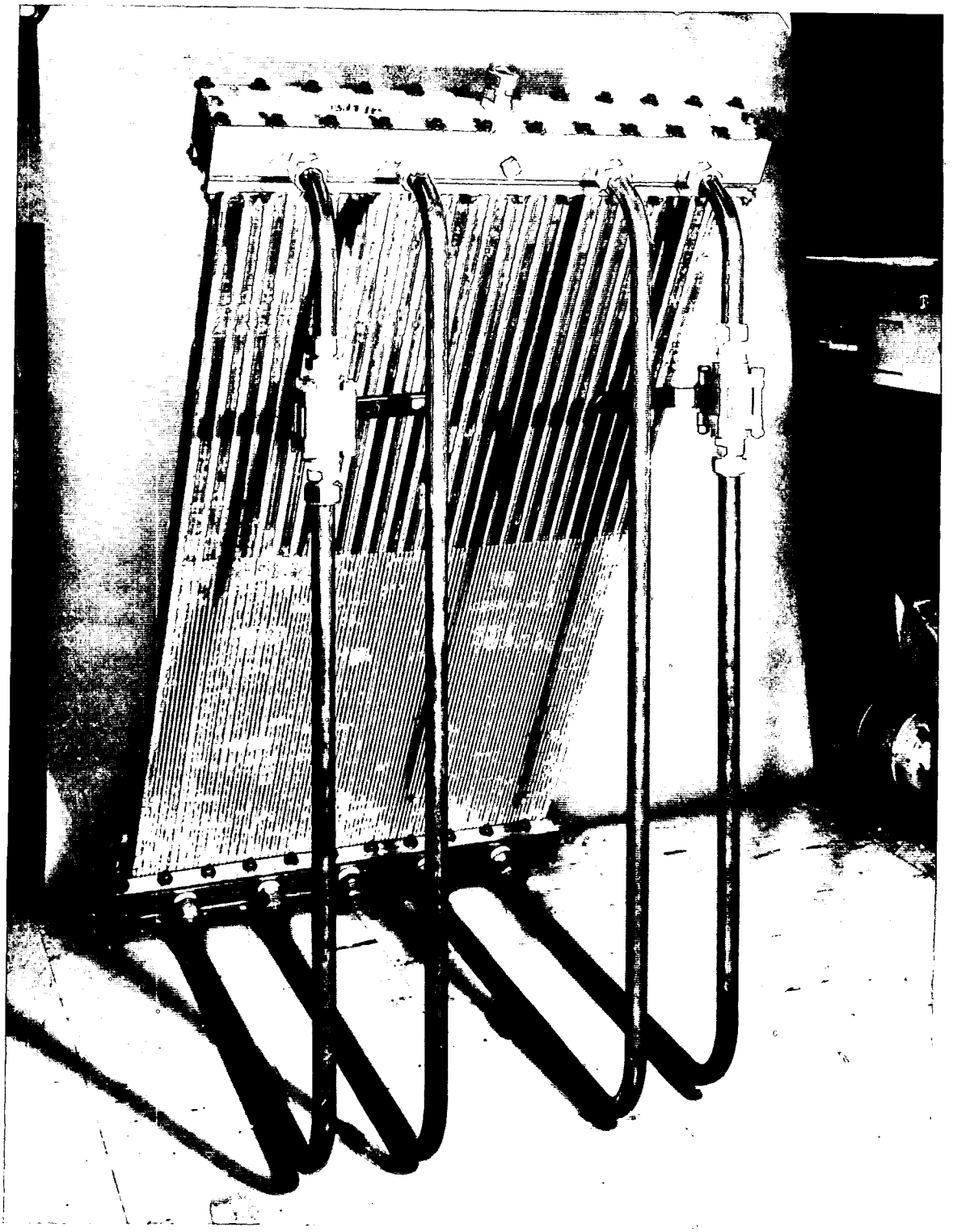

Figure 3.2-5 - Boiling thermosiphon heat exchanger

The basic 104 finned tube coil block was fabricated at Westinghouse Luxaire. The special headers and recirculation downcomers were added at the R&D Center.

Twelve type K thermocouples were attached to the tube outer surface in such a way as to yield the axial temperature profile. It is expected that the axial temperature profile will be fairly uniform when the coil functions in the evaporator mode, but when the coil is used as a condenser an estimate of the extent of the desuperheating, condensing and subcooling lengths should be evident from the profile. Additional thermocouples were inserted in the upper and lower headers.

Two of the four 7/8 in ID recirculation downcomers can be valved closed to test the sensitivity of evaporator performance to downcomer cross-sectional area. The coil is inclined at an angle of 60° from the horizontal and two of the 1.0 in diameter downcomers were used during the test series. At nominal air flows of 2000 to 3000 SCFM (245 to 358 ft/min standard face velocity) and inlet air temperatures of 17°F, 32°F, 47°F and 62°F, the refrigerant evaporating pressure was varied to obtain a map of coil performance. The measured capacity and the capacity predicted by the model at 3000 SCFM air flow are shown in Figure 3.2-6. The measured capacity and predicted capacity are substantially in agreement. The computer model predicts refrigerant pressure drops in the 2 to 4 psi range. The measured refrigerant pressure drop is less than 1 psi for all of the test points. Therefore, the actual system performance should meet or exceed the predicted system performance.

The boiling thermosiphon heat exchanger has been tested at the DOE frost accumulation conditions (35°F dry bulb, 30°F dew point). Both standard reverse cycle defrost and reverse cycle defrost with expansion device bypass have been exercised. The behavior of the refrigeration system during defrost is very similar to that of systems with conventional evaporators. The tested embodiment of the reboiler concept does not fully drain the defrost melt, since significant moisture holdup was observed at the termination of defrost.

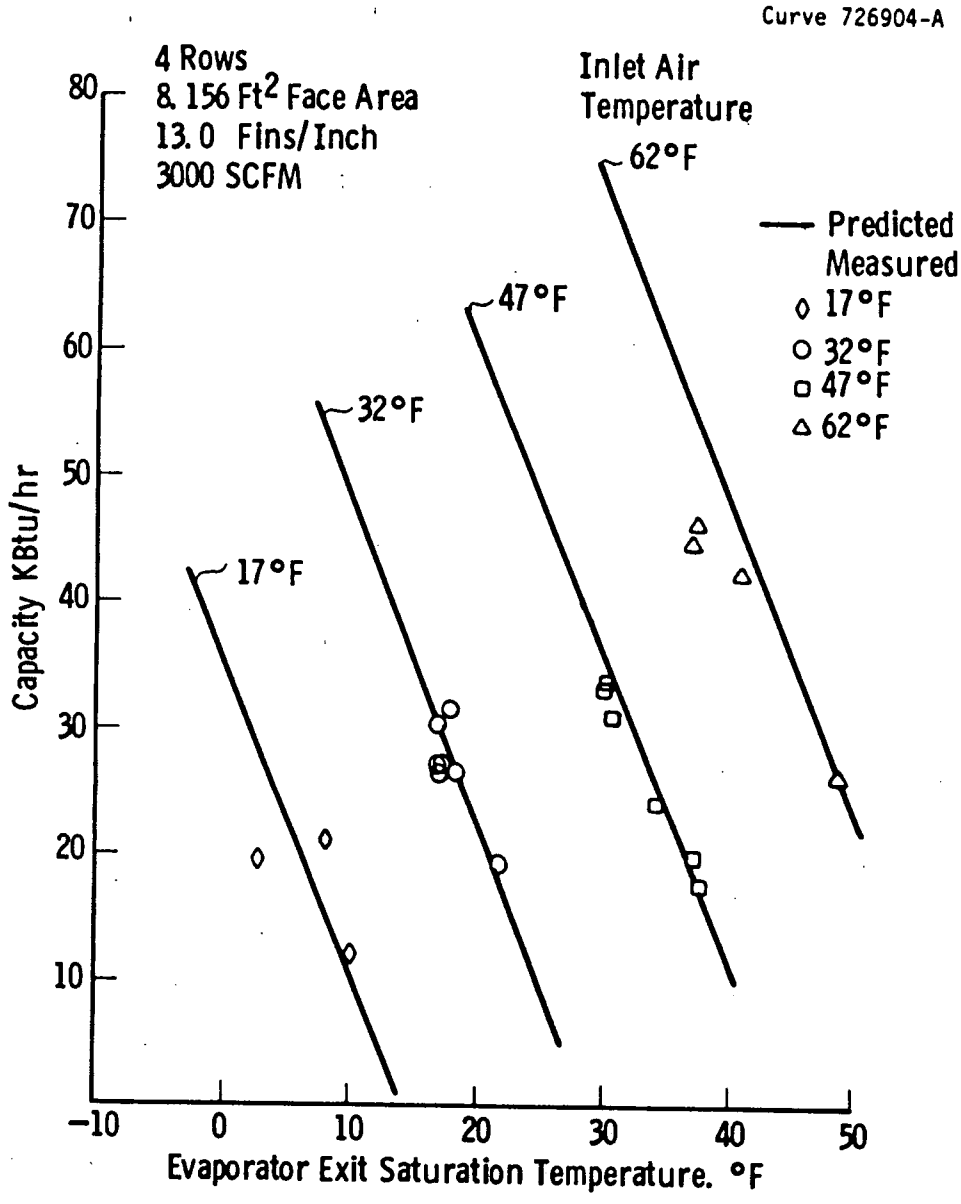

Figure 3.2-6 - Boiling thermosiphon evaporator performance

The major disadvantage of the natural circulation coil in the configuration tested proved to be the difficulty of removing moisture from the coil following a defrost.

The coil accumulates frost in an unusually uniform manner. Several different heat pumps with conventional coils have been observed under frosting conditions and, in all cases, the frost appeared to accumulate most rapidly in certain local areas of the coil. With the natural circulation coil, the appearance of the frost was completely uniform over the entire coil surface.

During defrost, the frost melted at the top of the coil first, uniformly across the width of the coil. It was anticipated that moisture would run down to the bottom edge of the coil and then flow down the coil surface to the bottom into the drain pan. In practice, moisture did not run down the coil face, but dripped off the fins, creating a "rainstorm" beneath the coil. When defrost was completed, significant amounts of moisture remained on the coil surface in droplet form. When the heat pump was returned to the heating mode, these droplets froze into solid ice.

Modifications to the coil face to improve drainage were considered, but time did not permit testing these concepts. The most promising concepts require considerable alteration of the coil configuration so that the fin edges are not horizontal. Other concepts, such as running vertical wires along the coil face appeared to have a low probability of practical success.

No cost effective means has been devised to improve the drainage of defrost melt for the tested coil. Note however that to obtain a thermosyphon driving head, there need be only a head difference of several feet between the center of heat addition (the centroid of the heat exchanger) and the center of heat rejection (the vapor exit). A nearly horizontal tube arrangement with nearly vertical fins should function perfectly well, provided that a vapor/liquid separation header is added a foot or two above the heat exchanger exit. This configuration has not been tested.

3.2.2 Gravity Driven Condenser

Introduction

The function of the condenser in a refrigeration system is to remove heat from the superheated vapor exiting the compressor to condense it into the liquid phase. Before bulk condensing occurs, the superheated vapor must be cooled to its saturated state. If the condenser tube is long enough, the saturated vapor not only condenses to the saturated liquid but also cools more to become subcooled liquid. The theoretical analysis of a condenser, therefore, is logically subdivided into three sections: desuperheating, condensing and subcooling.

Figure 3.2-7 is a schematic diagram of a multiple parallel finned tube refrigerant to air heat exchanger oriented so that the condensing refrigerant fluid flow in the tubes is gravity driven. Superheated vapor enters the top manifold and is assumed to distribute itself uniformly in all condenser tubes. Fan-driven cooling air will blow through the condenser and over the finned outer surface of the tubes to remove heat from the refrigerant flowing downward inside the tube. The condensed liquid then flows out from the bottom manifold.

A FORTRAN computer program written in a subroutine form was developed to quantitatively evaluate condenser performance.

Numerical Results and Discussion

The results of a limited parameter study showing the effect of the number of condenser tubes is presented in Table 3.2-2. The geometric data are the same as used in the study of the boiling thermosiphon evaporator (Table 3.2-1).

D_o = 0.393 in	D_i = 0.323 in
L_t = 4 ft	L_c = 2.5 ft
$L_e = L_h$ = 0.5 ft	V_H - 4 ft
P_t = 1.00 in	P_ℓ = 0.8661 in

Dwg. 7758A38

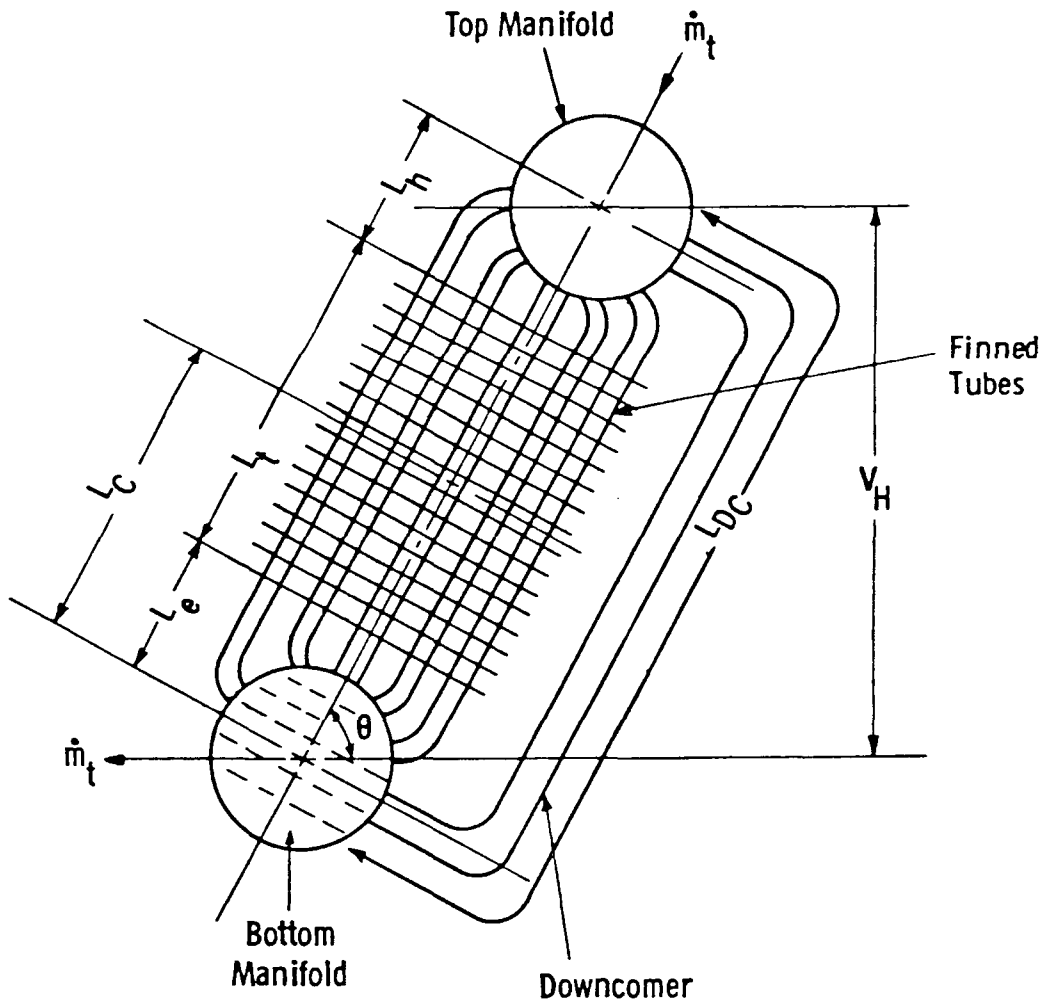

Figure 3.2-7 - Schematic diagram of a gravity-driven condenser

Table 3.2-2

Performance Characteristics of Condensers

	Properties	4 Ft Condenser Length (25 Tubes/Row) 125 Tubes	100 Tubes	75 Tubes
(1)	Inlet pressure, psia	279.80	279.80	283.20
(2)	Inlet temperature, °F	219.70	219.70	220.49
(3)	Condenser Saturation Temperature, °F	121.46	121.46	122.41
(4)	Entropy of Superheated Vapor, Btu/lb-°F	0.241	0.241	0.240
(5)	Error on Isentropic Condition, %	0	0	0.062
(6)	Air Face Velocity, ft/min	423.35	423.35	423.35
(7)	Heat Rejection in Desuperheating Section, B/hr	1.30×10^4	1.30×10^4	1.30×10^4
	Heat Rejection in Condensing Section, B/hr	3.97×10^4	3.97×10^4	3.95×10^4
	Heat Rejection in Subcooling Section, B/hr	0.209×10^4	0.139×10^4	0
(8)	Tube Length for Desuperheating, ft	0.532	0.647	0.805
	Tube Length for Condensing, ft	2.299	2.666	3.206
	Tube Length for Subcooling, ft	1.169	0.687	0
(9)	Average Air Exit Temperature, °F	109.47	109.29	108.88
	Air Exit Temperature in Desuperheating, °F	120.77	116.19	112.06
	Air Exit Temperature in Condensing, °F	113.26	110.75	108.04
	Air Exit Temperature in Subcooling, °F	96.89	97.13	∿
(10)	Pressure Drop in Desuperheating, psia	0.252×10^{-3}	0.407×10^{-3}	0.744×10^{-3}
	Pressure Drop in Condensing, psia	0.215	0.241	0.278
	Pressure Drop in Subcooling, psia	0.0625×10^{-3}	0.0612×10^{-3}	∿
	Total Pressure Drop in Condenser, psia	0.215	0.242	0.280
(11)	Condenser Exit Pressure, psia	279.59	279.56	282.92
(12)	Condenser Coil Air Pressure Drop, Inch Water	0.283	0.204	0.170
(13)	Degree of Subcooling, °F	10.74	7.08	0

t_f = 0.00550 in

N_f = 13 fins/in of tube length

Number of tubes per row = 25

Flow conditions:

Refrigerant 22 (or R22) mass flow rate $\dot{m}_t$ = 595.0 lbm/h
Standard air volume flow rate V_a = 3500 SCFM
Air inlet temperature T_{ai} = 95°F

The initial input data for inlet pressure and temperature are P_{in} - 279.80 psia, T_{in} = 219.70°F and for L_t, 4 ft of condenser length. The inlet pressure and temperature will be adjusted until all vapor condenses within the available tube length.

Table 3.2-2 shows that a minimum of 75 condenser tubes with 4 ft effective tube length will be required to condense the given refrigerant flow at the specified inlet pressure and temperature. The degree of subcooling increases as the number of tubes increases. The condenser with 100 condenser tubes, each with 4 ft of effective length, may be considered to be a reasonable design choice because this configuration yields approximately 7°F of subcooling and an air-side pressure drop confined to well below the required 0.23 in of water.

Figure 3.2-8 shows the length required for desuperheating and condensing as a function of tube inclination angle for the case of 100 condenser tubes arranged in four rows. Since the condensing coefficients are gravity-controlled for most cases in the illustrated examples, the heat transfer coefficients decrease with decreasing angles of inclination. The length required for condensation thus increases with decreasing inclination angle. The tube length required for condensation is not a strong function of the inclination angle for angles greater than 60° from the horizontal. It should be noted that the condensing heat transfer coefficient used here is based upon data for nearly vertical tubes. For any inclining angle smaller than 20°, one should use a correlation for horizontal tubes as indicated in the

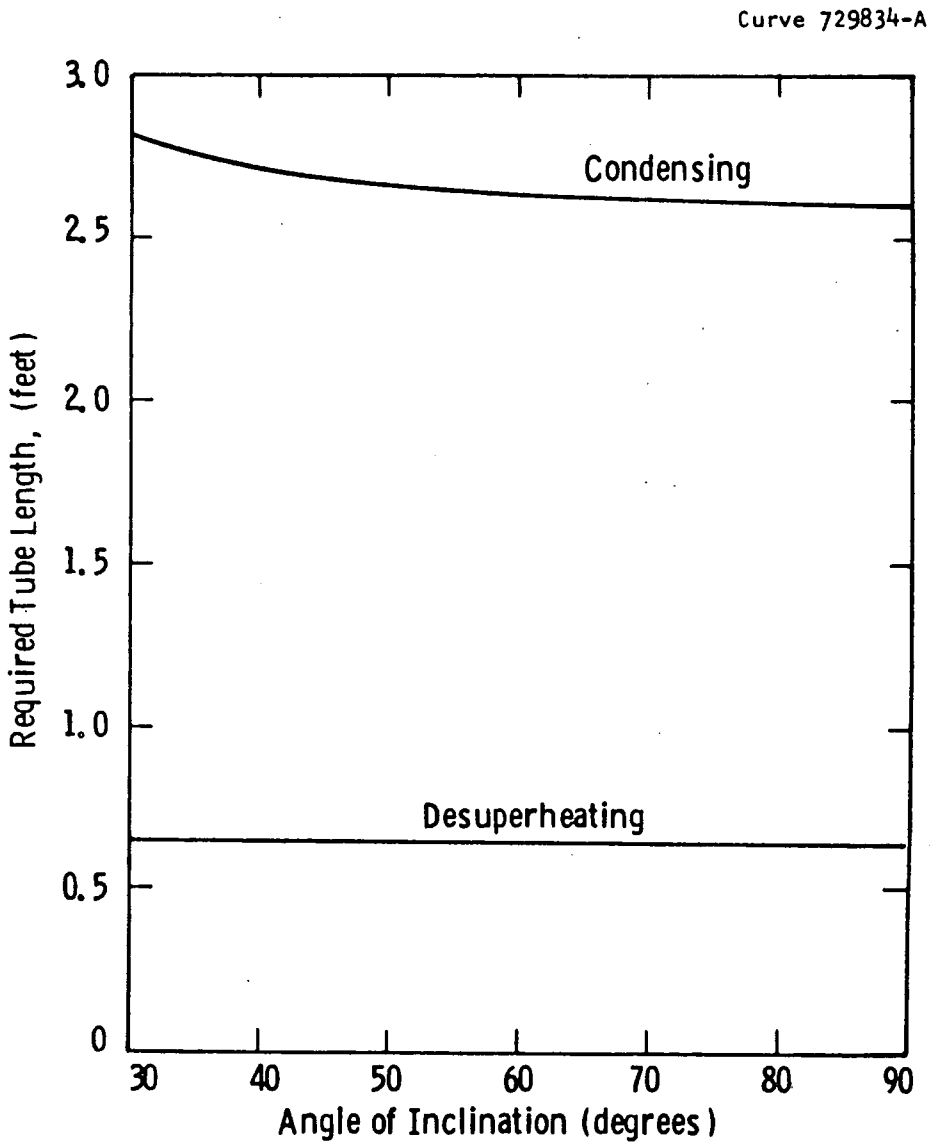

Figure 3.2-8 - Effect of inclination angle upon condenser tube utilization

HTRI Design Manual. In the present example, the tube inclining angle is 53°.

System Studies

The mathematical model for the natural circulation coil in condenser service was incorporated into the system performance computer program. A conventional system configured and optimized with the estimated characteristics of our advanced dual-stroke compressor (compressor configuration No. 5) was studied with a natural circulation outdoor coil of equivalent surface area substituted for this conventional outdoor coil. A subcooler using 14.67 feet of similarly finned tubing was included since the natural circulation coil was predicted to yield insufficient subcooling. The estimated performance of this system in the high capacity cooling mode of operation is shown in Figure 3.2-9. Predicted system cooling capacity is 3 to 5 percent less than for this unit with a conventional outdoor coil, while the predicted EER is 7 to 8 percent less.

Experimental Results

The prototype coil was tested as a condenser with nominal air flows of 2000 to 2800 SCFM and inlet air temperatures of $82^{o}F$ and $95^{o}F$. Due to the large variations in inlet superheat and exit subcooling, it is difficult to summarize the data in a single figure. However, some specific examples representative of the entire test series are shown in Table 3.2-3. In addition to the measured performance, the predicted performance for the natural circulation coil and a conventional coil with the same surface area are tabulated. The results indicate that the measured capacity and subcooling are significantly higher than the predicted values for a gravity driven coil. The measured capacity and subcooling are equivalent to a conventional coil with the same surface area. Therefore, the expected loss in capacity and EER in the cooling mode has not been observed, and the cooling performance of a system

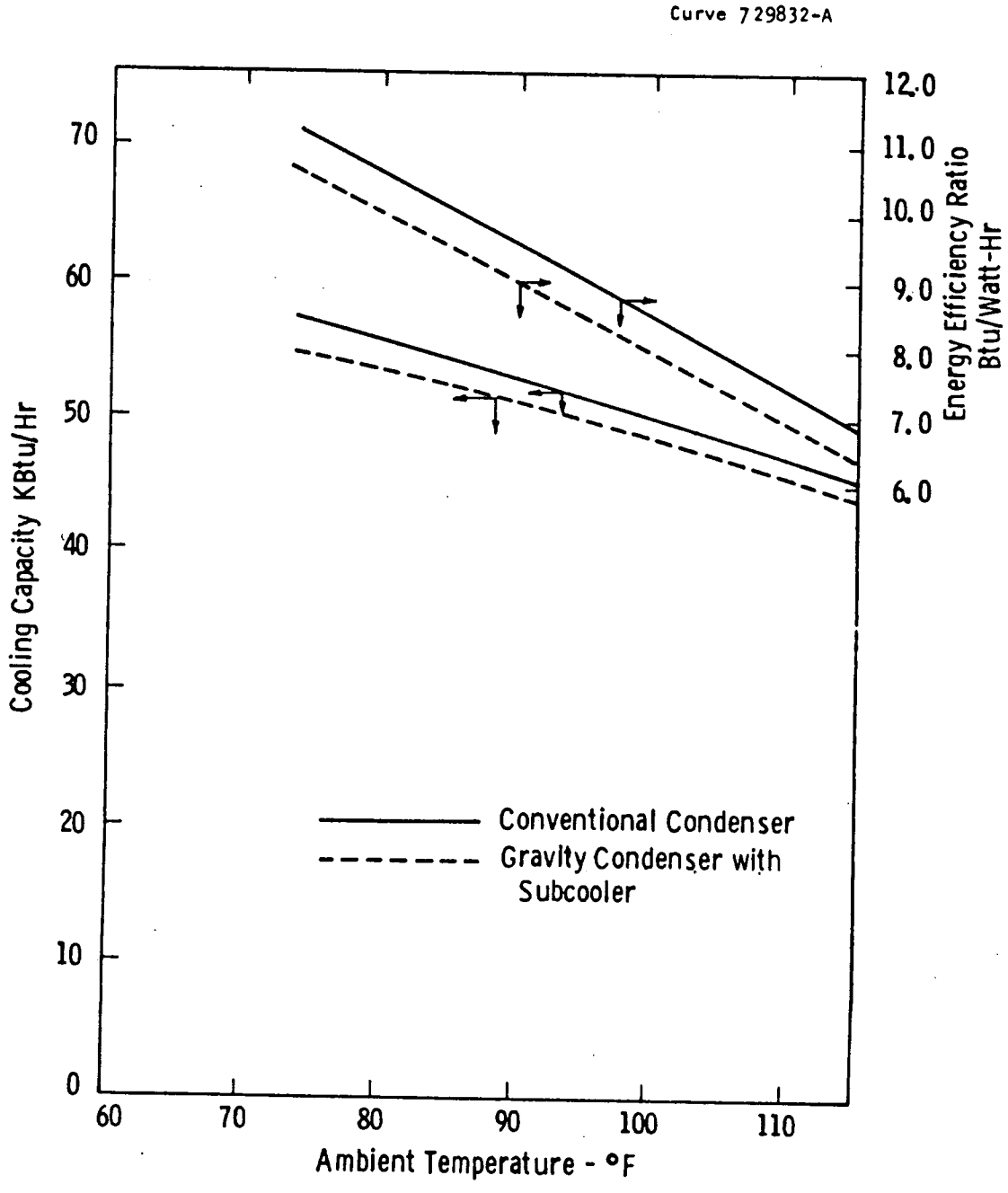

Figure 3.2-9 - Effect of gravity-driven condenser upon heat pump cooling performance (system optimized using dual-stroke compressor No. 5)

Table 3.2-3

Comparison of Measured and Predicted Performance
For a Natural Circulation Condenser

Test No.	Inlet Air Temp (°F)	Air Flow (SCFM)	Refrigerant Temp(°F)	Refrigerant Press. (psia)	Refrigerant Flow (lb/hr)	Exit Refrigerant Temp (°F)	Coil Capacity (Btu/hr)	
41	94.6	2657	208.1	270.7	427.5	95.4	40452	Measured
						94.6	40562	Predicted-Conventional
						109.6	38547	Predicted-Natural Circulation
45	81.9	2699	208.6	245.6	621.7	82.3	61535	Measured
						85.6	61247	Predicted-Conventional
						107.7	57073	Predicted-Natural Circulation
52	82.0	2495	224.8	257.5	628.9	83.9	64242	Measured
						84.9	63948	Predicted-Conventional
						109.9	59181	Predicted-Natural Circulation

using the gravity-driven coil should be equivalent to that of a conventional system.

3.2.3 Evaluation

The natural circulation driven boiling thermosiphon evaporator has demonstrated its thermodynamic advantage over conventional heat exchanger circuit designs in heat pump heating mode service. On a direct surface area replacement basis, the boiling thermosiphon evaporator yields a 3 percent improvement in coefficient of performance and an improvement in capacity of roughly 8 percent across the heat pump operating range for ambient temperature. The all-parallel tube circuit design yields uniform loading and hence a very uniform frost accumulation pattern. Oil return proved to be reliable in the tested configuration which used the Westinghouse Hi-Re-Li circuit.

The flaw in the tested design lies with its inability to shed enough of its large frost melt load to prevent rapid reicing. This flaw was to be expected since the tested design had fins which were inclined only 30° relative to horizontal. Insufficient resources were available to show the parametric evaluation of various angles of inclination. However, previous experience indicates that if the fins were inclined at 60° or more relative to the horizontal, then water drainage would be very good. A slab coil design with nearly vertical fins, and thus horizontal tubes with the face of the heat exchanger nearly parallel to the earth's surface, is quite feasible.

For natural circulation to occur, only a liquid/vapor separator vessel is required a foot or two above the heat exchanger refrigerant exit.

The tested heat exchanger performed much better as a condenser than expected, although the amount of liquid subcooling available is only marginally adequate for control purposes and a separate subcooling coil would be recommended. Note, however, that condensing in a horizontal or nearly horizontal orientation for the tubes was not evaluated.

The cost of the natural circulation heat exchanger is expected to be higher than that of the conventional coil with equivalent surface area because of the special headering required to yield all-parallel paths. It is necessary to note that conventional plate fin-on-tube air-to-refrigerant heat exchangers are manufactured using hairpin-shaped "U" tubes. Tube-to-tube connections are thus brazed at only one heat exchanger end sheet. These tube-to-tube connections are simple return bends or relatively simple tripods. The all-parallel tube natural-circulation-driven coil requires a log manifold type of header. The simplest would employ one entrance and one exit header per row. With so many headers at each end sheet, the arrangement is very crowded. The best headering arrangement would be one header at each end sheet. This header would require as many nipples as there were tube ends. The commercial practicality of this arrangement remains to be determined; however, a simple calculation can provide guidance. Assume that at the 3 ton size, the incremental installed cost of a high efficiency 4 ton unit is $600 more than a 3 ton unit. Thus, the incremental cost is $600/12,000 Btu/h = $50/1000 Btu/h. An 8 percent capacity improvement on 36,000 Btu/h is 2880 Btu/h, and hence this capacity improvement has a worth of $144 in installed cost. At the factory the incremental manufacturing cost must be of the order of $40 if the concept is to be commercially practical. Our analysis indicates that it should be practical.

3.2.4 Conclusions

1. The natural-circulation-driven boiling thermosiphon heat exchanger is a thermodynamically superior heat pump evaporator.
2. The heat exchanger tested is a satisfactory condenser, especially if coupled with a separate subcooler.
3. For an equivalent investment in heat exchanger surface, a heating COP improvement of roughly 3 percent is achievable.

4. For the equivalent investment in heat exchanger surface, a heating capacity improvement of roughly 8 percent can be expected.

5. An incremental capacity improvement of 8 percent has an economic worth that should be sufficient to more than cover the incremental cost of the higher headering and plumbing costs required in a heat pump equipped with a natural-circulation-driven outdoor heat exchanger.

6. Oil entrapment, an anticipated potential problem with the reboiler type of evaporator design, did not occur in the specimen tested based upon observation of oil level in the system compressor.

3.3 Air Mover Design and Development

In a typical state of the art heat pump, the outdoor air mover is a two to four bladed propellor fan turning at 6 pole (1020 rpm) or 8 pole (825 rpm) speed. The propellor blades are typically of large chord, more or less shovel-shaped, and attached to a simple spider driven by the motor. The propellor rotates in a running ring with a generous clearance of a quarter inch or more between fan tip and shroud.

The fan motor for residential units is typically a permanently split capacitor type of 1/6 to 1/3 horsepower rating, depending upon unit capacity, and is of a weatherproof design yielding about 55 percent efficiency.

The indoor-air mover is typically a squirrel cage (forwardly curved vane) blower, 9 to 10 inches in diameter and 8 to 12 inches wide, with double air entry. The blower wheel is mounted in a simple volute shroud. The motor is of the permanent split capacitor type and of open design with a rated capacity of 1/3 to 1/2 horsepower. Because of the good cooling available when such motors are mounted in the eye of the blower wheel, it is not uncommon for the delivered shaft horsepower to be 50 percent more than the motor nameplate rating with an operating efficiency of about 50 percent.

Total air moving electrical power will be of the order of one kilowatt for a 3 to 4 ton heat pump. Since, historically, half of the heat delivered by a heat pump system during the heating season is electrical resistance heat, there is little incentive to develop or employ high-efficiency air movers.

Industrial practice has known for many years the art of high-efficiency air-mover design. The industrial axial fan for low-pressure applications and the industrial backwardly inclined air-foil-bladed centrifugal blower for higher pressure applications look significantly different than their residential heat pump counterparts.

The big difference between the residential and industrial air movers, after accounting for scale or size differences, is the significantly higher cost required to achieve a factor of two improvement in air-moving efficiency. A significant portion of the higher cost is due to the need for smaller clearance dimensions in higher efficiency air movers.

Note that if air-mover efficiency is improved, then motor size is less. It is well known that because of geometric effects, the practically achievable efficiency of small fractional horsepower single-phase motors is only of the order of 60 to 70 percent, with motors as typically applied being 50 to 55 percent efficient. This contrasts markedly with the 90 percent efficient 3-phase motors used in integral horsepower industrial air movers. The adoption of 3-phase residential service in the U. S. is not likely. Furthermore, the widespread application of 3-phase variable frequency electronic drive systems to residential heat pumps is also unlikely because of high cost. Thus, the horizon for motor efficiency is about 65 percent.

The prospect of designing higher efficiency air movers for a residential size heat pump that would roughly halve the required air moving electrical power looks attractive. On a seasonal basis, a high-efficiency heat pump should displace significant resistance heat and also operate nearly continuously during both winter and summer. The

saving of one-half kW for say 6000 hours per year at 5 cents per kilowatt hour would represent a user savings of $150 per year. This economic benefit to the user represents a significant incentive to develop improved heat pump air movers, using even the more pessimistic views of user market acceptance of higher efficiency at higher price.

3.3.1 Outdoor Air Mover Development

Introduction

Selection of a fan for the outdoor unit of a heat pump involves several considerations, including air volume flow, air static pressure, sound levels, packaging, fan motor characteristics, and cost. The traditional method for characterizing the operating regime of fans is specific speed, a parameter relating rpm, the delivered volume flow rate, and the static pressure rise across the fan. Both dimensionless and dimensional forms of this parameter are in common use, but all use the same exponents to modulate the volume flow and pressure rise. A dimensional form used in fan vendor literature is:

$$N_s = \frac{\text{rpm}\ \sqrt{\text{CFM}}}{(\Delta P)^{3/4}}$$

where ΔP = static pressure in inches of water and N_s is the specific speed.

Two measures of air-mover efficiency are in use, total efficiency and static efficiency. Total efficiency is a ratio calculated as the total power imparted to the moving air stream divided by the shaft power absorbed by the air mover. The total power in the air stream, the air horsepower, consists of a static effect or change in potential energy due to the static pressure rise imparted by the air mover, plus a dynamic effect due to the kinetic energy change in the flowing air cross the air mover. The kinetic energy of the moving air stream is of no value to ventilating machinery, so the static efficiency is the more meaningful measure of air-mover efficiency. Static

efficiency is defined as the ratio calculated from the static pressure head imparted to the air stream by the air mover divided by the shaft power absorbed by the air mover.

In Figure 3.3-1, the fan static efficiency is related to dimensional specific speed for the three fan types most commonly used in residential HVAC equipment.

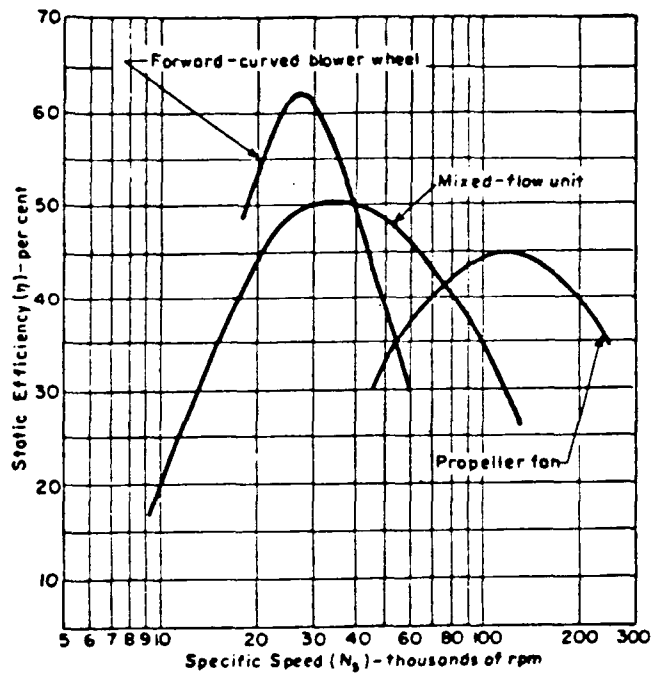

Figure 3.3-1 - Static efficiency versus specific speed (from Torrington Manufacturing Company, "Application of Mixed Flow Blower Units," reprinted from Air Conditioning Heating and Ventilating, April, 1958.)

The outdoor unit of a heat pump typically requires a high-air volume flow at a low static head; it is therefore a high specific speed application. For example, a Westinghouse model HP048 heat pump was designed for an air volume flow of 3300 SCFM with a static pressure of about 0.17 in of water. With a rotational speed of 825 rpm, the dimensional specific speed would be 179,000, near the peak efficiency range for a propeller fan as shown in Figure 3.3-1, and far beyond the

specific speed range where mixed-flow fans or forward curved blower wheels have peak efficiency. A propeller fan is clearly the best suited of these three types for this application, and most heat pump outdoor units do use propeller fans.

Space limitations generally result in a restricted fan inlet and short diffuser rings. Product cost pressure has substituted high air flow for heat exchanger surface and forced a trade-off of low air mover cost for good aerodynamic design. Consequently, outdoor air mover static efficiencies as applied are generally 20 to 35 percent rather than the 45 percent peak efficiency shown in Figure 3.3-1. With a 35 percent fan static efficiency and a 55 percent efficient fan motor, the air moving efficiency is only 19 percent. In the Westinghouse HP048 unit, the outdoor fan motor draws about 250 watts, less than 5 percent of the system power input at 47°F and about 8 percent at -20°F. Obviously, increasing the fan/motor efficiency will not dramatically increase the seasonal coefficient of performance, but the cost of the electricity used to drive the outdoor fan is not insignificant. A 250-watt motor operating for 6000 hours per year will have an annual energy cost of $75 at an electricity cost of 5¢/kWh. The potential saving of $30/yr is sufficient to warrant consideration of more expensive fans and fan motors.

The typical propeller fan used in HVAC systems is a four-blade design with blades stamped from aluminum sheet and riveted to a steel "spider" hub. The blades are commonly of constant thickness, camber, and incidence, and of high solidity, overlapping in many designs. The leading and trailing edges of the blades have sharp corners, resulting from the stamping process. The hub of the fan wheel is relatively open; air can recirculate through the hub in some applications. A typical propeller fan design is shown in Figure 3.3-2.

Alternate fan designs which will provide good static efficiency over a wide range of operating speeds are available. A multi-vane axial flow design is well suited for this application. A fan of this type has

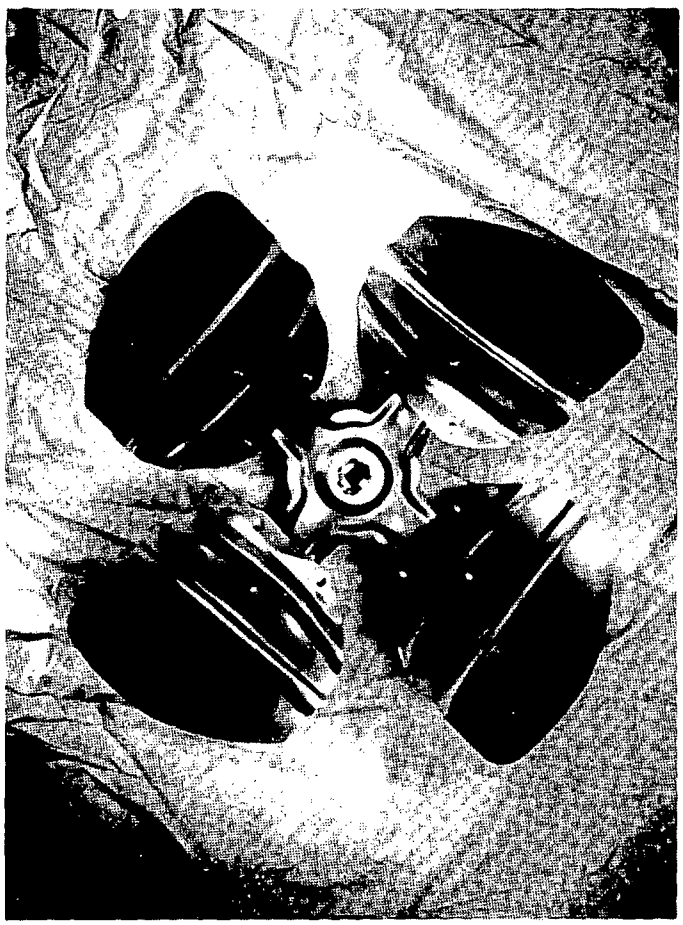

Figure 3.3-2 - Typical heat pump outdoor unit fan

five or more blades of relatively narrow chord and low solidity. A large solid hub is used to prevent recirculation.

Technical Analysis

The objective for outdoor-fan improvement was to raise fan static efficiency to the 60 percent range while employing a high-efficiency motor (65 percent efficiency) to drive the fan.

The requirements and specifications for the outdoor-fan assembly were formalized as follows: The fan should be a vertical shaft-type directly driven by the motor. It should draw air through the outdoor heat exchanger and deliver 2900 CFM against an upstream static pressure resistance of 0.2 inches of H_2O. The fan should operate stably at 80 percent of design flow (2320 CFM) and should achieve a static efficiency approaching 60 percent. Size is constrained to a 24 inches maximum outside diameter with a desired overall length of 12 inches or less. Noise (according to ARI Standard 270-75)[1] should not exceed a noise rating of 20, and 18 was desired.

The design procedure applied to the heat pump outdoor fan had three levels. First, since a quiet fan with good static efficiency was desired, the performance and size contraints were examined to produce a fan having minimal blade surface velocities. Second, since high-static efficiency was the primary design criterion, the fan parameters developed in the first level were examined in greater detail with systematic variation of the parameters, using an appropriate efficiency analysis procedure. Third, the best design candidates developed in the second level were examined in detail using the more rigorous computerized analyses of the programs AXDES and AXOFF (Westinghouse proprietary programs).

As used in the first level of analysis, an aerodynamic parameter was developed to relate subsonic axial fan noise to the fundamental flow

---

1. Sound Rating of Outdoor Unitary Equipment, ARI Standard 270-75, 1975.

behavior in the blade row of an axial fan. This variable is the peak blade surface velocity, V_p, which in an axial fan is dependent on local relative velocities and the induced blade surface velocity associated with the generation of the head, H.

An example of the use of peak velocity analysis is given in Figure 3.3-3. Calculated peak blade surface velocities are shown for direct-connected speeds of 1725, 1135, 840 and 665 rpm. Diameter was varied from 1 to 3 ft, and the noise prediction in db-W re 10^{-12} watts, associated with the diameters for which V_p is a minimum, are indicated in the figure. (Also shown are noise values at diameters associated with best static-efficiency performance.) This result indicates that the fan should be designed with the lowest acceptable motor speed and a reasonably large diameter, although the size constraint of $D \leq 2$ ft is acceptable in terms of minimum velocity.

The second level of analysis, estimation of static efficiency, is carried out in the range of sizes and speeds which are near the minima shown on the curves of Figure 3.3-3. Estimation is based on an approximate method developed to model the dominant loss modes of axial fans and includes the influence of swirl or vane row loss, blade profile loss, tip clearance loss, losses in a downstream diffuser and velocity pressure loss at the discharge of the fan. Static efficiency is defined as:

$$\eta_s = 1.576 \times 10^{-2} \, \Delta P_s \, Q/W_s$$

where ΔP_s = static pressure rise across fan (inches of water)

Q = volume flow rate (CFM)

W_s = fan shaft horsepower (hp)

η_s = static efficiency (%)

An example of the second sweep efficiency analysis is shown in Figure 3.3-4. Calculated efficiencies are shown for the four speeds and diameter ranges used in the peak velocity studies. The total pressure

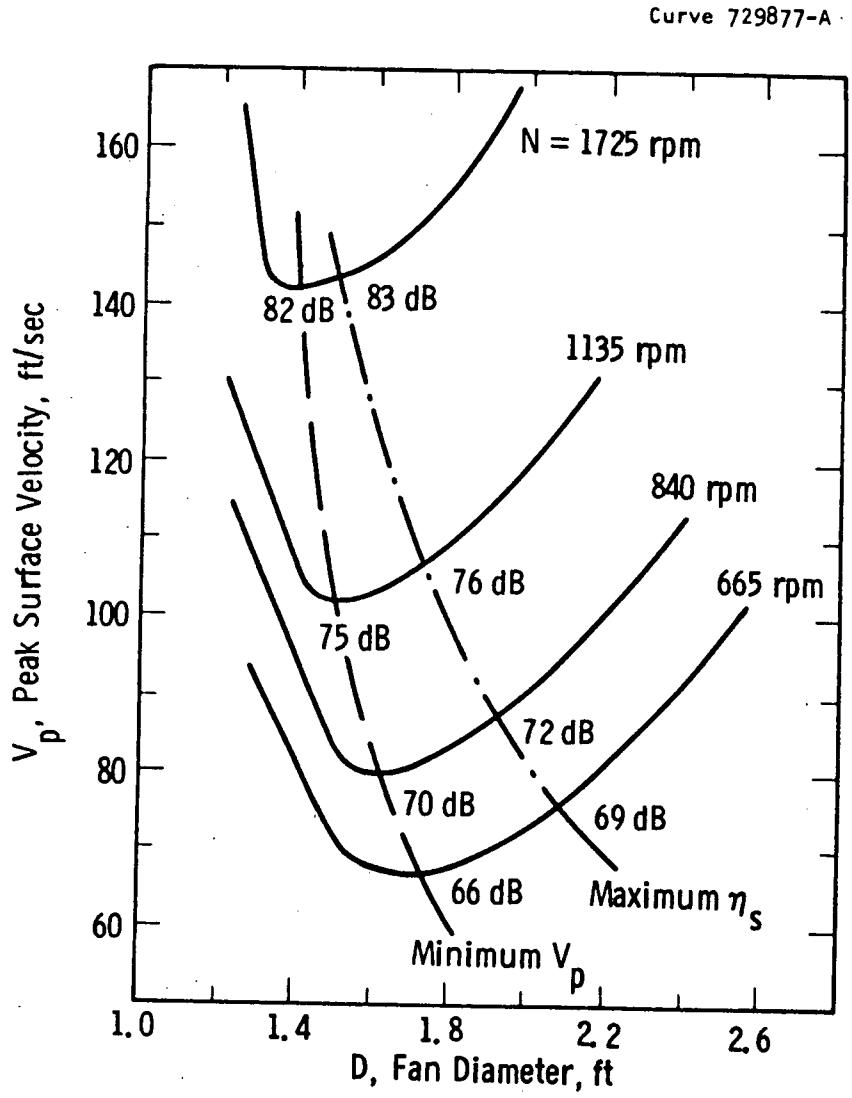

Figure 3.3-3 - Minimization of blade peak surface velocity (noise in dB-W re 10^{-12} watts)

lost in the vane row and diffuser was estimated by using a nominal vane loss and restricting diffuser length to 1 ft. Blade tip clearance was set at 1/8 inches. Static efficiency is calculated directly from total efficiency through use of the diffuser velocity pressure loss, based on the ratio of exit-to-inlet annulus area with maximum allowable recovery or expansion.

As seen in Figure 3.3-4, the peak static efficiencies at different speeds correspond to slightly larger diameters than those for minimum velocity. Noise predictions indicate that a modest increase is incurred by moving from the minimum velocity point to the point of best static efficiency. Since the lowest allowable motor speed is dictated by its eight-pole design, these results indicate that the best fan design for the application and constraints has a diameter of 2 ft running at about 840 rpm, and should produce a maximum static efficiency in the range of 55 percent. More thorough studies, including limitations on blade row diffusion and a more careful treatment of vane row and diffuser, set the hub diameter at 1 ft and indicated the need for high vane row solidity.

To give an independent check on sizing of the fan, the specific speed and diameter of the fan were calculated using the following definitions:

$$\Omega = N\hat{Q}^{1/2}/(gH)^{3/4}$$

$$\Delta = D\ (gH)^{1/4}/\hat{Q}^{1/2}$$

where Ω = specific speed, dimensionless

Δ = specific diameter, dimensionless

N = fan speed, radians per second (2π x rpm/60)

$\hat{Q}$ = volume flow rate, ft^3 per second (CFM/60)

D = fan diameter, ft

H = total head rise, ft

$$= \frac{\Delta P_s}{12}\left(\frac{\rho_W}{\rho_a}\right) + \frac{V_e^2 - V_\infty^2}{2\ g_c}$$

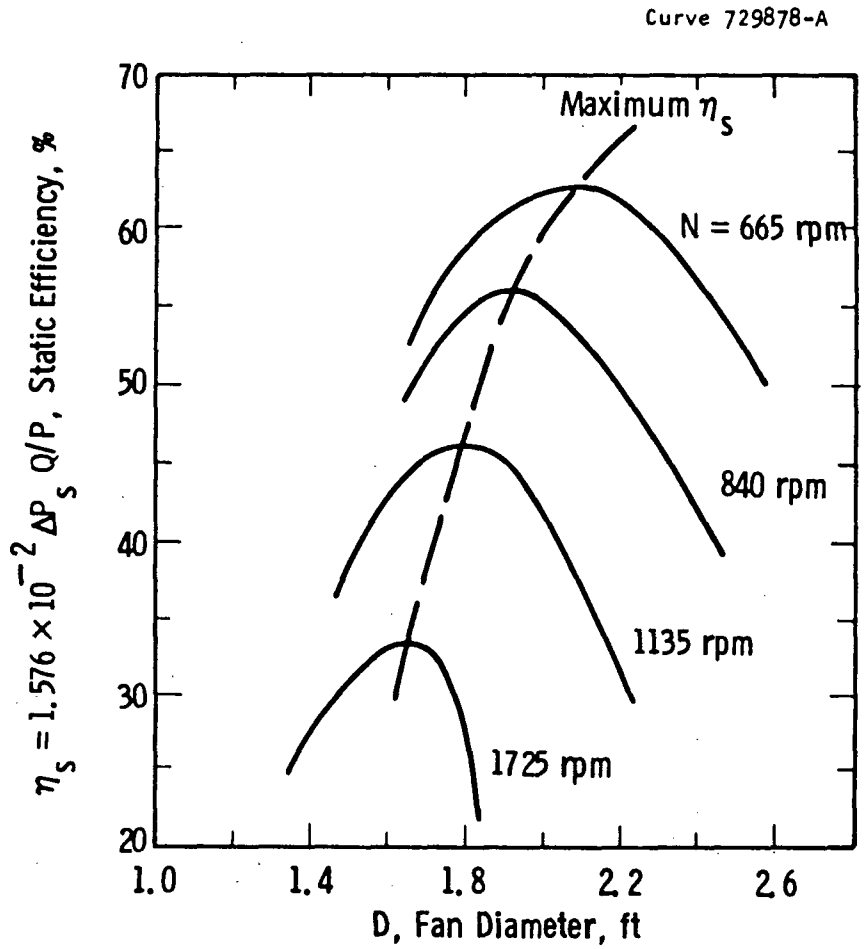

Figure 3.3-4 - Constrained optimization of static efficiency at direct-connected fan speeds

ΔP_s = static pressure rise, inches of water

ρ_W = density of water, 62.4 lbm/ft^3

ρ_a = density of air, 0.075 lbm/ft^3

g_c = gravitational constant, 32.2 ft/sec^2

V_∞ = far field entrance velocity, ~0 ft/sec

V_e = exit plane velocity, ft/sec

$= \hat{Q}/(\pi(D_e^2 - D_H^2)/4) \cong \hat{Q}/(\pi D_e^2/4)$

D_e = diffuser exit diameter, ft

D_H = hub diameter at exit, ft

The point representing our tentative design was then placed on the classical Cordier[2] diagram, Figure 3.3-5. The fan falls on the optimum line in the Ω, Δ plane with an indicated total efficiency of 76 percent. Total efficiency is defined as

$$\eta_T = 1.576 \times 10^{-12}\ Q\Delta\ P_T/W_s$$

where η_T = total efficiency, %

Q = air volume flow rate, CFM

W_s = shaft power, hp

ΔP_T = total pressure rise, inches of water

$= 12\ H\ (\rho_a/\rho_W)$

For the expected loss of 70 percent of annulus velocity pressure, the corresponding static efficiency is about 59 percent. The discrepancy between this estimate of static efficiency and the previous estimate of 55 percent is small and is largely attributable to the rather large tip gap used in the design study.

The sized fan parameters from the second level design sweep were then used to initiate more detailed design studies, incorporating the axial fan analysis program AXDES.

---

2. Csanady, D. C., Theory of Turbomachinery, The Macmillan Co., New York, 1964

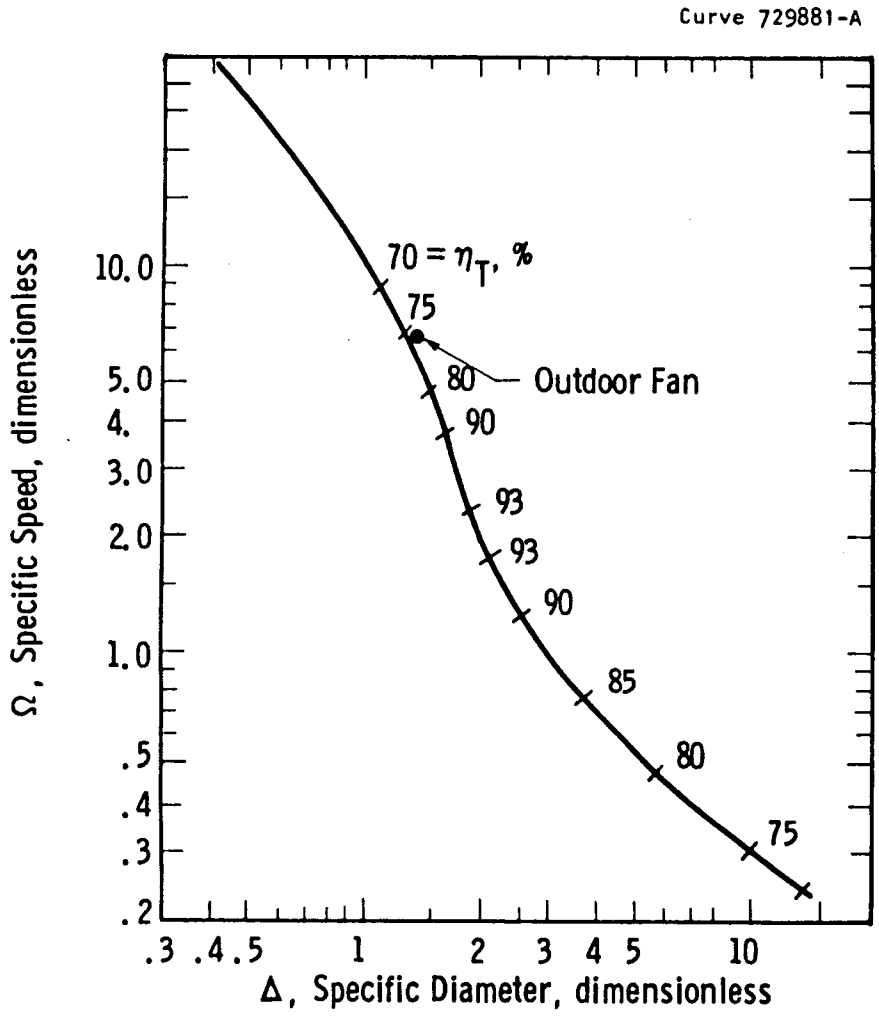

Figure 3.3-5 - Placement of the outdoor fan design on the Cordier diagram

AXDES is a design analysis computer program which provides a complete geometric description of an axial flow turbomachine, based on input requirements in terms of head rise, volume flow rate, rotational speed and diameter. The solution or design procedure is based on three basic elements: an inviscid, incompressible streamline solution; a semi-empirical cascade lift-prediction model; and an empirical loss and loading-limit calculation.

AXDES was supplied with the running speed, diameter, approximate hub diameter, and blade solidities, along with diffuser losses and the performance requirements. The design was investigated extensively with systematic variation of hub diameter and the blade and vane row solidities in order to optimize the static efficiency. Efficiency predictions based on AXDES results are 73.2 percent total efficiency and 57.9 percent static efficiency. These results are in substantial agreement with the earlier calculations.

Results

The test stand with instrumentation is shown schematically in Figure 3.3-6. Torque is measured on the strain-gage-instrumented reaction beam of the cradle-type dynamometer, and speed is read on a digital readout pulse counter operating from a 60-tooth gear. These data, along with a static load calibration and rotating tare readings, provide horsepower determination. Pressure drop across the nozzle plane measured on a calibrated electrical strain gage pressure transducer and static pressure measured at the fan discharge plane provide the flow-pressure rise performance data. All data handling and reduction, including scaling of performance to standard air density and reference fan speed, are done according to AMCA/ASHRAE standards.[3]

The breadboard axial fan was fabricated with an acrylic hub, acrylic blades and vanes, with a fiberglass inlet flare/running ring and

---

3. AMMA Standards, Bulletin Number 210-74.

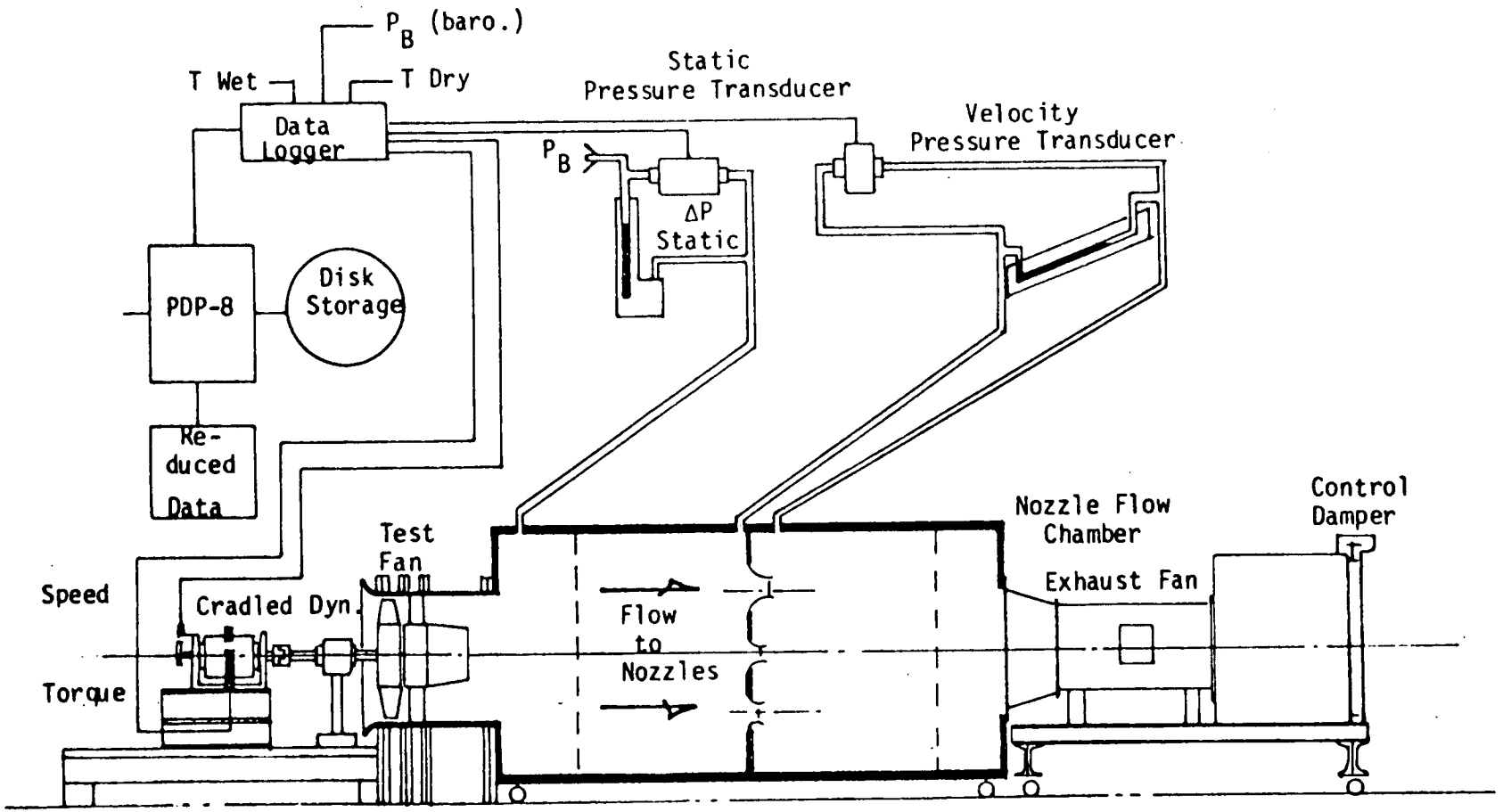

Figure 3.3-6 - Schematic arrangement of instrumentation and fan test stand

a sheet metal diffuser. The fan is shown in Figure 3.3-7. The blades consist of hot-formed 1/8 inch-thick sheet material mounted on steel tangs to provide adjustable pitch capability. The stator vanes were also hot-formed from 1/8 inch-thick sheet material and were glued into an annular section consisting of a 12 inch OD inner cylinder and a 24 inch ID ring, both 4 inches long and of acrylic. The diffuser section was formed with a 24 inch ID sheet metal cylinder and a conical sheet metal inner body mounted to the center section of the vane row. Both a 12 inch and a 6 inch diffuser were tested. The inlet flare and running ring as tested are shown in Figure 3.3-8. A photograph of the assembly, as prepared for a breadboard fan test, is shown in Figure 3.3-9. Final test results for the air mover with 6 inch diffuser are summarized in Figure 3.3-10. The configuration for this test included all components of the fan: inlet flare, blade row, vane row and 6 inch diffuser.

The performance curves for the outdoor fan (Figure 3.3-10) show that pressure rise and flow rate intersect the system resistance curve (based on 2900 cfm at 0.2 inch of water) slightly above the design target. Static efficiency for this operating condition is 52 percent with a shaft power requirement of 0.185 hp. The characteristic curve for the fan is very smooth with no regions of positive or unstable slope. At 80 percent of design flow (2320 CFM), the fan operates stably and smoothly. At flows of less then 80 percent of design, the fan continues to operate in a stable manner, with usable flow-pressure performance, although very significant increases in required power and generated noise accompany performance in this flow range. The mechanism for this unusually stable axial fan performance is the pattern of the blade stall occurrence. As flow is decreased below about 2300 CFM by throttling, the outer one-third of the blades enter into a stable stall-cell operating mode with strong flow reversal at the tips and forward flow just inboard. The pattern resembles a standing ring vortex, effectively blanking off the outer one-third of the blade row. On the inner two-thirds of the blade the flow patterns appear to be perfectly normal with clean, strong axial flow through the fan. This pattern of

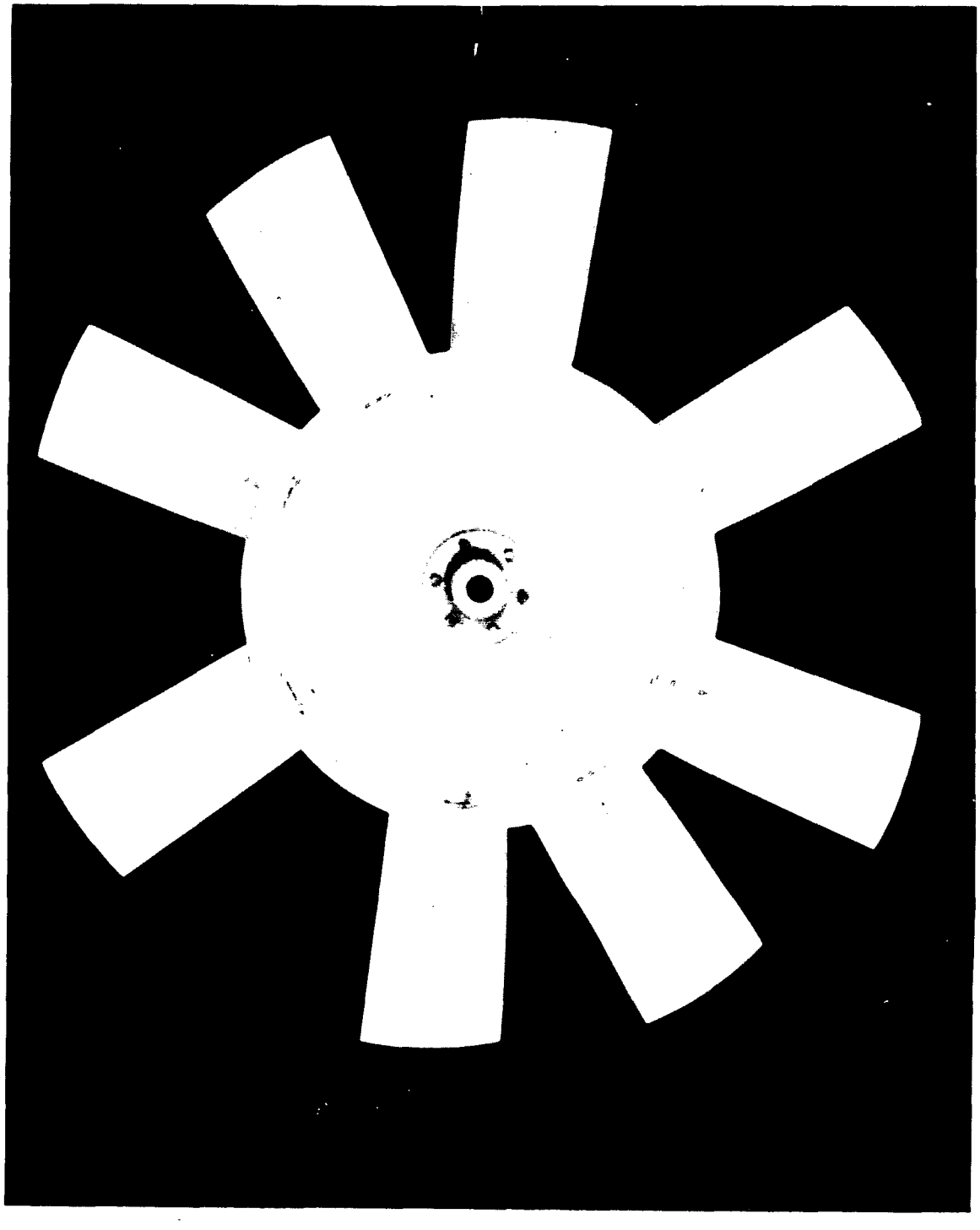

Figure 3.3-7 - Breadboard fan by Westinghouse

Dwg. 7758A34

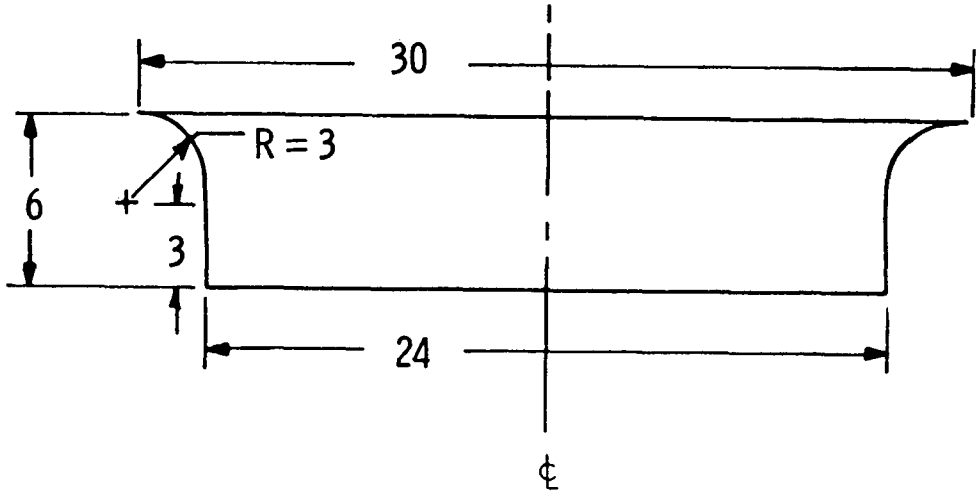

Figure 3.3-8 - Inlet flare and running ring, as tested (dimensions in inches)

partial through-flow persists at least down to 1000 CFM flow delivery at about 0.5 inches of water.

Because the fan was tested on a plenum chamber requiring an exhauster fan to overcome the pressure drop across the flow-measuring nozzles, it was not possible to perform meaningful noise measurements. However, approximate dBA meter readings with the fan detached from the flow box (running at free delivery) and subjective listening indicate that the fan is very quiet with no perceivable tonal content in the noise spectrum. It appears that there should be no difficulty in meeting and exceeding noise limitations stated in the design specifications.

To evaluate the benefit of the various components of the full fan assembly, tests were run using various combinations of components. At a fixed flow rate of 2900 CFM, removal of the vane row reduces static pressure by 18 percent and static efficiency by 7 points. Similarly, removal of the diffuser section reduces static pressure by 24 percent,

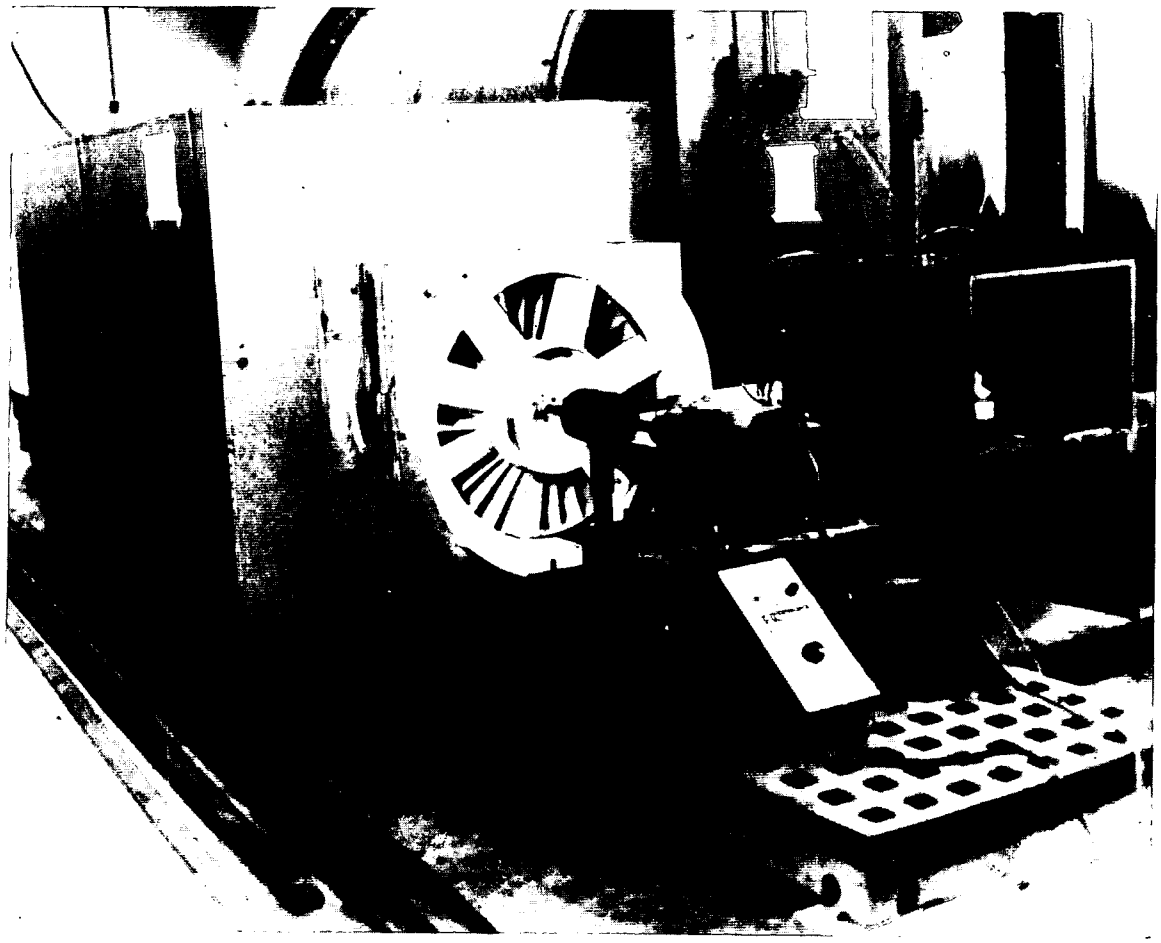

Figure 3.3-9 - Breadboard fan under test

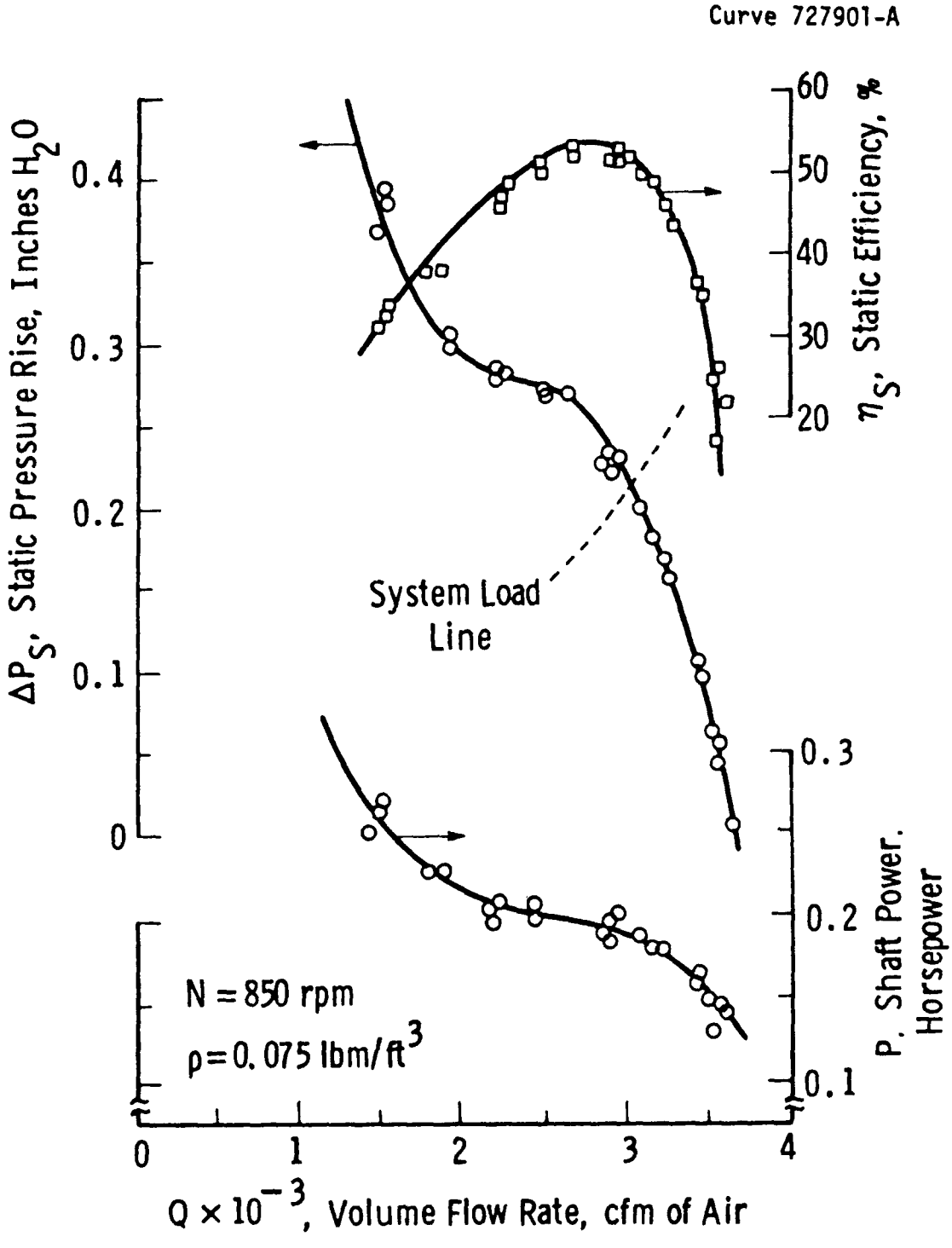

Figure 3.3-10 - Westinghouse outdoor fan performance (6 in diffuser)

and static efficiency by 6 points. Removal of both vane row and diffuser reduces static pressure 22 percent and static efficiency by 7 points. The apparent interaction between vane row and diffuser was substantiated in additional testing at other pitch angles, and it appears that either both elements or neither should be used in the fan. Removal of only the center body from the diffuser of the full fan assembly causes reductions of about 2 points in static efficiency and perhaps 5 percent in static pressure.

The results of testing combinations of components do not present a very clear picture and some contradictions appear. The difficulty may lie in variations in setup between reassembly for testing and in attempting to resolve differences in the orders of 0.01 horsepower and 0.01 inches of water in pressure rise.

About all that can be said with great confidence is that successive addition of the components downstream of the fan blade row is clearly beneficial, and that the full fan assembly offers a reduction in required power of about 15 percent when compared to the rotor-only configuration, but with the fan at reduced pressure. For the fan with rotor only to match the flow pressure performance of the full fan, the pitch angle must be increased and would require 0.250 horsepower. This is an increase of 35 percent, implying an increased wattage requirement (with a motor efficiency of 65 percent) of about 75 watts. That is, the downstream components of the fan are worth 75 watts.

Flow visualization, using yarn tufts and smoke, of the streamline behavior over the surfaces of the diffuser indicates that considerable separation occurs, particularly on the converging center body downstream of the vane row hub section. The test data indicate that none of the diffuser geometries provide really good velocity pressure recovery when compared to that expected from typical annular diffuser data. The problem may lie in the choice of inward diffusion (in order to keep within a diameter constraint) with consequent thickening of the boundary layers on the center body surface as

circumference of the cross section decreases. Use of a cylindrical center body with a conical expanding outer wall would alleviate this effect, although a final diameter of about 26 inches or more would be required in order to design for the same area ratios. If diffusion or velocity pressure recovery can be improved by 30 percent, static efficiency could be raised to perhaps 54 percent compared to the current 52 percent. It is not clear that two additional points in static efficiency can justify the negative impact of a larger diffuser upon both manufacturing cost and package size.

Limited tests were run at reduced speed to provide a measure of the sensitivity of the fan to reduction in efficiency with decreasing Reynolds number. Because of limitations of the test stand and exhauster, tests could not be carried out below about 700 rpm. However, testing between 700 and 850 rpm showed no measurable change in efficiency, indicating that the fan should provide a nearly constant or scalable performance over a reasonable range of fan speed. Reynolds number based on tip speed and tip blade chord for the fan operating at 850 rpm is 1.8×10^5. Studies by Pampreen[4] and Kittredge[5] indicate that dependence of losses on speed changes in this range of Reynolds number will be relatively weak. Scaling according to $(1-\eta_T)/(1-\eta'_T) = (Re'/Re)^n$ requires a value of n equal to about 0.15. [( )' relates to a changed condition relative to that tested.] With $\eta_T = 0.65$, a speed change from 850 rpm to 600 rpm would reduce total efficiency by 1 point. Operating at 300 rpm would reduce total efficiency by as much as 6 points, while power requirement would be reduced to less than 5 percent of the power required at 850 rpm. That is, over the range from 300 to 850 rpm, speed change effects should not result in a measurable increase in power requirement compared to that predicted by fan-law scaling.

---

4. Pampreen, R. C., "Small Turbomachinery Compressor and Fan Aerodynamics," ASME Paper No. 73-GT-6, 1973.

5. Kittridge, C. P., "Estimating the Efficiency of Prototype Pumps from Model Tests," ASME Paper No. 67-WA/FE-6, 1967.

To reduce the overall size of the air mover, it is recommended that the inlet flare be reduced in size as shown in Figure 3.3-11. No significant change in performance is expected.

Dwg. 7758A33

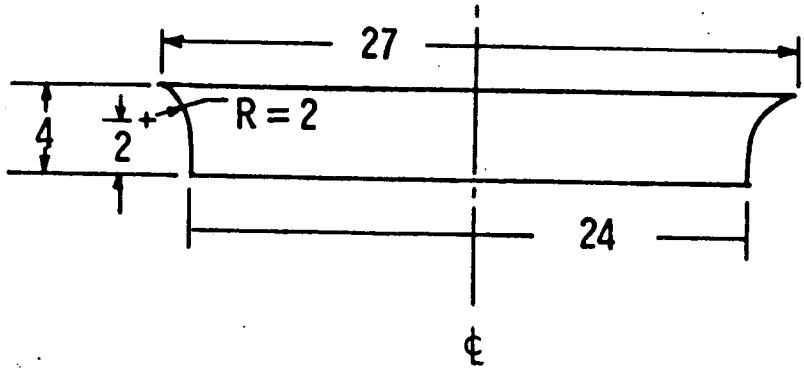

Figure 3.3-11 - Recommended reduced size inlet section (dimensions in inches)

Outside Vendor Effort

To ensure that a commercially practical fan design evolved, Westinghouse ordered from the Torin Corporation a prototype air mover built to the same specifications as those used by Westinghouse. A photograph of the Torin air mover is shown in Figure 3.3-12.

The fan and stator blades are molded in airfoil shape. The performance of the Torin fan is shown in Figure 3.3-13. Its flow pressure curve falls slightly below the initial design specification.

Note that both the Westinghouse and the Torin fan require about 0.18 shaft horsepower.

Figure 3.3-12 - Prototype outdoor air mover by Torin

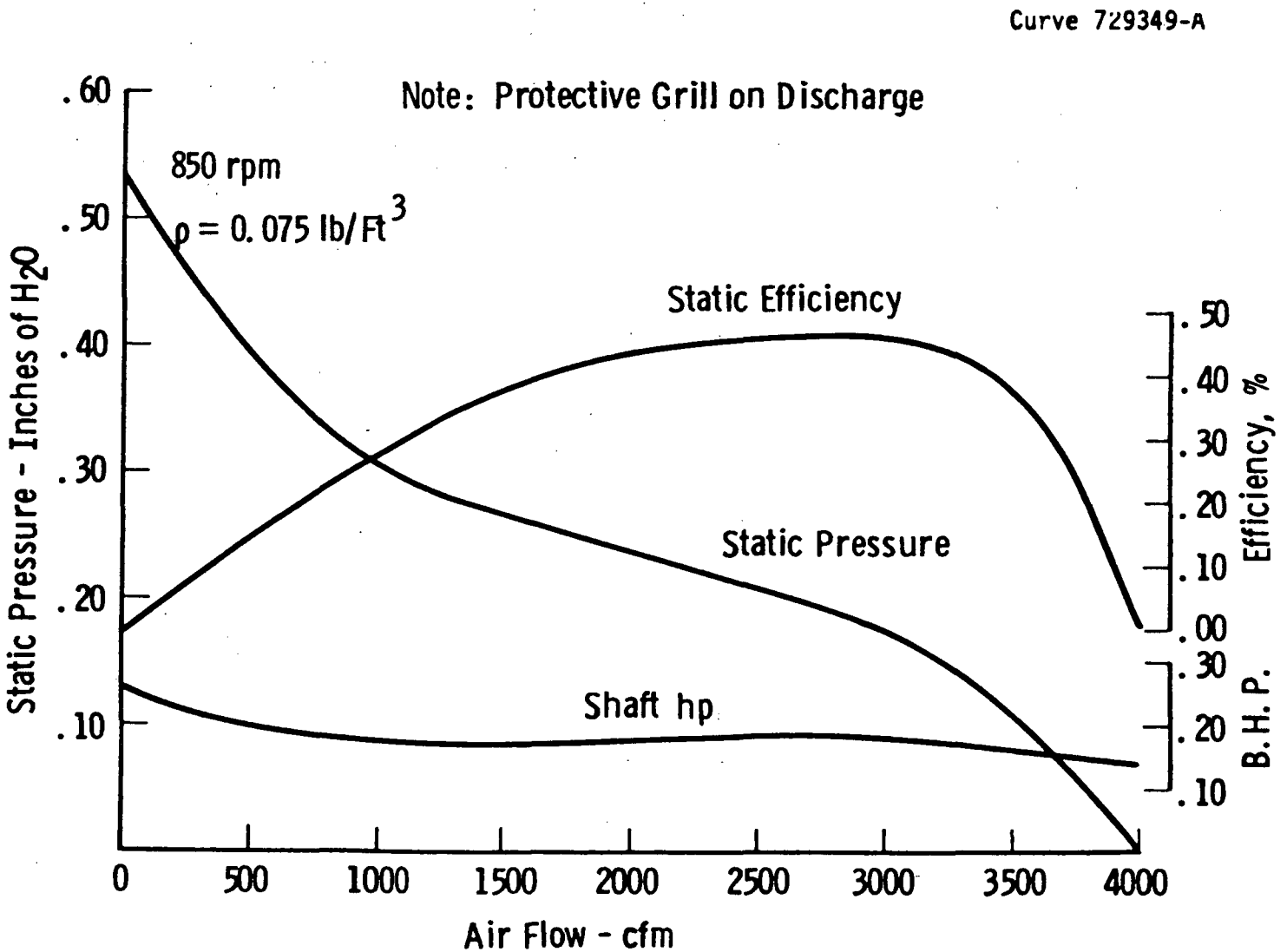

Fig. 3.3-13 - Performance of Torin outdoor air mover

Discussion

The preliminary outdoor air mover specification called for a direct-driven, vertical shaft fan drawing air through the outdoor heat exchanger with 2900 SCFM delivery against an upstream static pressure resistance of 0.20 inches of water. The fan should operate stably at 80 percent of design flow (2320 SCFM) and should strive for 60 percent static efficiency. The overall size of the air mover was to occupy a cylinder not larger in diameter than 24 inches (nominal exclusive of any mounting flange) and with an overall height of 12 inches.

The Torin air mover fits within a 24 inches diameter cylinder, 12 inches high. It has a static efficiency 14 percent less than our design goal and a flow delivery 6 percent less than our goal at design pressure rise.

The Westinghouse development process started with a 12 inch diffuser stack judged necessary to achieve the desired static efficiency. The diffuser was then shortened to approach the desired overall height, thereby reducing the achievable efficiency. The fan diameter was chosen as large as practical, 24 inches, so that the inlet flare extends beyond the specified 24 inch diameter constraint. With a diffuser shortened to 6 inches, the tested assembly still exceeds the height specification by 2 inches. This configuration, however, exceeds the design flow by 3 percent while missing the efficiency target by 8 percent. Redesigning the inlet section with a smaller radius inlet flare will reduce the air mover height to within the design goal without any appreciable reduction in efficiency.

The Westinghouse and the Torin fan, while markedly similar, are significantly different from current air mover practice in the HVAC industry. Both use a large number of blades (eight for Westinghouse, seven for Torin), a solid hub, a multi-vane stator row (31 vanes for Westinghouse, 11 vanes for Torin), a diffuser stack, and the same 8-pole drive motor. The efficiency of both fans is about twice that of current standard heat pump fans.

The Westinghouse fan is a little stronger (higher flow and pressure capability) than the specification called for, while the Torin fan is a little weaker. The performance of the Torin fan is, however, quite acceptable for the system design as it has evolved. The Westinghouse design should still provide acceptable performance at significantly lower cost, after the stator vane row is eliminated entirely, the exit diffuser stack enlarged in diameter to 26 inches at exit, and the assembly reduced to 12 inches in overall height.

Since the Westinghouse fan design uses cambered plate blades instead of airfoil sections, it can be fabricated inexpensively in sheet metal. The Torin fan is a molded plastic design.

The net result is that the Westinghouse fan design may be somewhat less expensive than the Torin design for the same performance but with larger size. The efficiency of the Westinghouse design could be improved by 3 to 5 percent with airfoil fan blading. The Torin design, if redesigned to permit larger diameter, could probably be simplified and still achieve the same efficiency and performance.

During the course of our system optimization process the design airflow was reduced from 2900 CFM to 2600 CFM at 0.2 inches of water pressure drop. With the required fan delivery so reduced, both air mover concepts are judged to be equally acceptable in terms of performance. Preliminary cost analyses, assuming large volume production with adequate tooling suggest that in simplified form (without stator vane row) both would cost about the same. We expect, therefore, that the outdoor air mover in prototypic form will require less than 0.185 horsepower to move 2600 CFM against 0.20 inches of water.

3.3.2 Indoor Air Mover

Introduction

The requirements for the blower in the indoor air handling unit differ considerably from those for the outdoor fan. The indoor air flow

is typically 50 percent of the outdoor air flow, and the static pressure requirement is much higher. The indoor unit blower must provide sufficient static pressure to overcome the duct air flow resistance (typically 0.3 to 0.6 inches of water), the air flow resistance of the electric resistance elements, air filter, and electronic air cleaner (0.2 to 0.3 inches of water), and the air flow resistance of the indoor coil (0.3 to 0.5 inches of water).

For a typical 3.5-ton heat pump, the design air flow for the indoor unit is 1575 SCFM with a static pressure drop of 0.85 inches of water. A conventional squirrel cage blower with a 11.2-inch OD double width, double-inlet wheel (DWDI) operating at 1070 rpm has an effective dimensional specific speed* of 34,000 near the peak efficiency for a forward curved blower wheel. Although Figure 3.3-1 indicates an achievable efficiency of 58 percent, the measured efficiency of this wheel is 34 percent at maximum, primarily because of the placement of the direct-drive motor in the eye of the blower wheel. So placed, the direct-drive motor saves space, improves reliability (by eliminating a belt drive), and reduces cost; air mover static efficiency, however, is significantly reduced. Furthermore, since the efficiency of the high-slip six-pole drive motor is typically between 50 and 60 percent, the total air moving efficiency is between 17 and 20 percent. The indoor air mover thus consumes between 800 and 900 watts of electrical power. The lower number taken for 6000 hours per year at 5¢ per kWh represents a cost to the consumer of $240 per year. A doubling in air mover efficiency would thus save the consumer $120 per year.

The preliminary specification for the indoor blower to be used in the 3.5 ton advanced electric heat pump is as follows:

---

*For a double-entry design, the effective specific speed is $1/\sqrt{2}$ times the nominal specific speed.

General - The indoor blower for the advanced heat pump is envisioned as a high efficiency single entry design (single width, single inlet-SWSI) with multiple backwardly curved airfoil blades directly driven by a high-efficiency motor mounted external to the blower wheel. In the design envisioned, air will be drawn through the return duct system, filter, the air-to-refrigerant exchanger, and discharged into a supply duct system.

Specific - The nominal airflow is 1575 SCFM with a flow resistance of 0.5 inches of water on the suction side and 0.35 inches of water on the discharge side. The blower must operate in a stable manner with a ± 50 percent variation in airflow resistance on the inlet side and a variation of flow resistance of 0 to 150 percent of the rated value on the discharge side. Target static efficiency is 65 percent with operation at four-pole motor speed. Four-pole speed is desirable in order to minimize blower wheel diameter and motor cost.

These specifications, simplified to establish a discrete design point, yield: Q (volume air flow) = 1575 SCFM; P_s (static pressure rise) = 0.85 inches of water at a standard air density; ρ_a = 0.075 lbm/ft^3. Four pole motor speed is taken as 1725 rpm.

The blower conventionally used for the indoor unit is the familiar squirrel-cage blower. A comparison of the pressure versus flow characteristics for the two types of blowers is illustrated by Figure 3.3-14. Both units have been scaled for size and speed to meet a common design point, and both employ a volute scroll. The continuous slope to the right of the peak-efficiency point for the backward curved airfoil blower indicates a broad stable operating range. The flat pressure-flow relationship for the forward curved blading indicates a less stable operating region in the vicinity of the peak efficiency point.

The efficiency and horsepower requirements for the two blowers are shown by Figure 3.3-15. Note that the efficiency of the backward curved airfoil blower mounted in a volute scroll is roughly twice the value of the forward curved blower similarly mounted at the specific

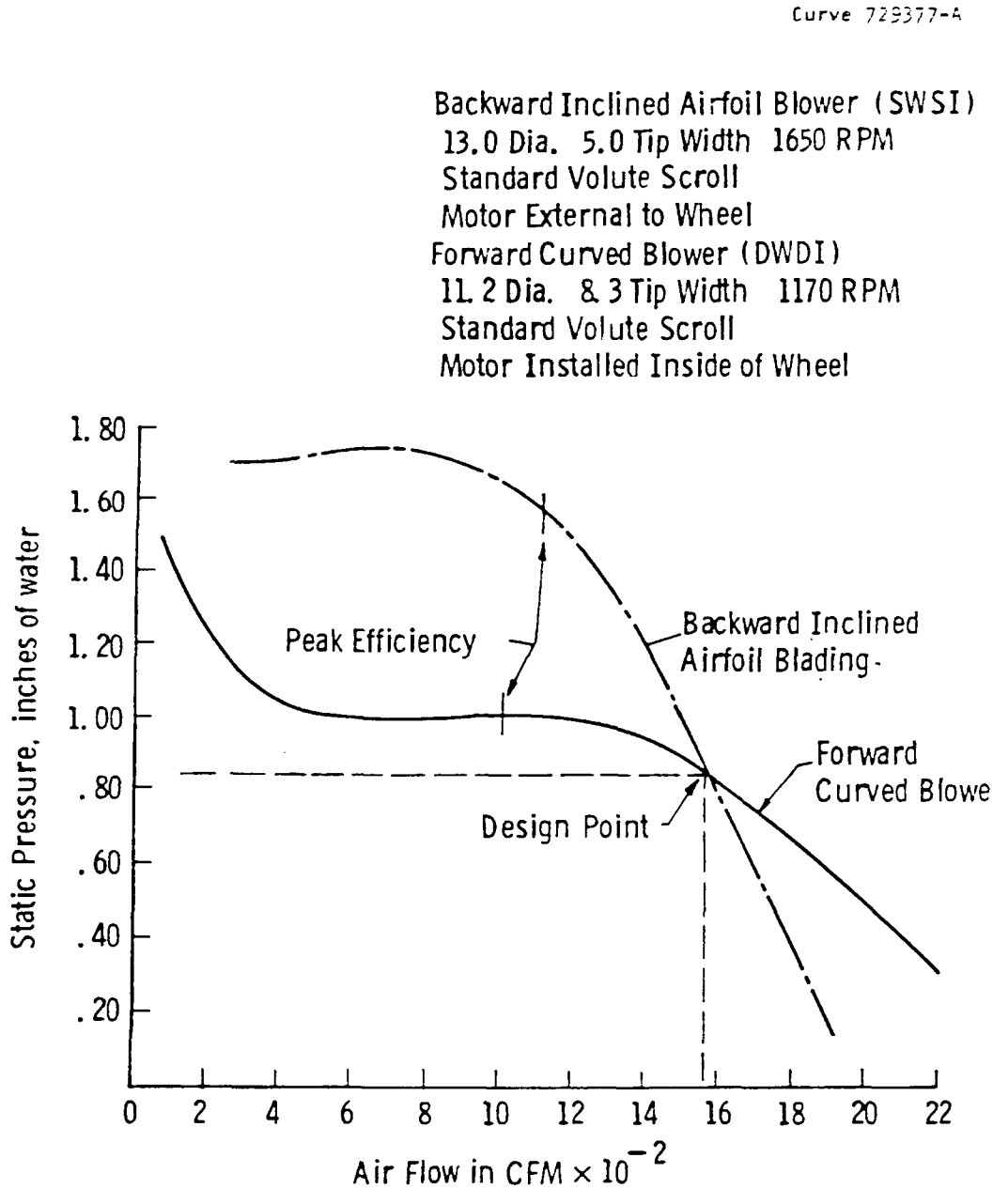

Figure 3.3-14 - Comparison of pressure versus flow characteristics for blowers (dimensions in inches)

Dwg. 729376-A

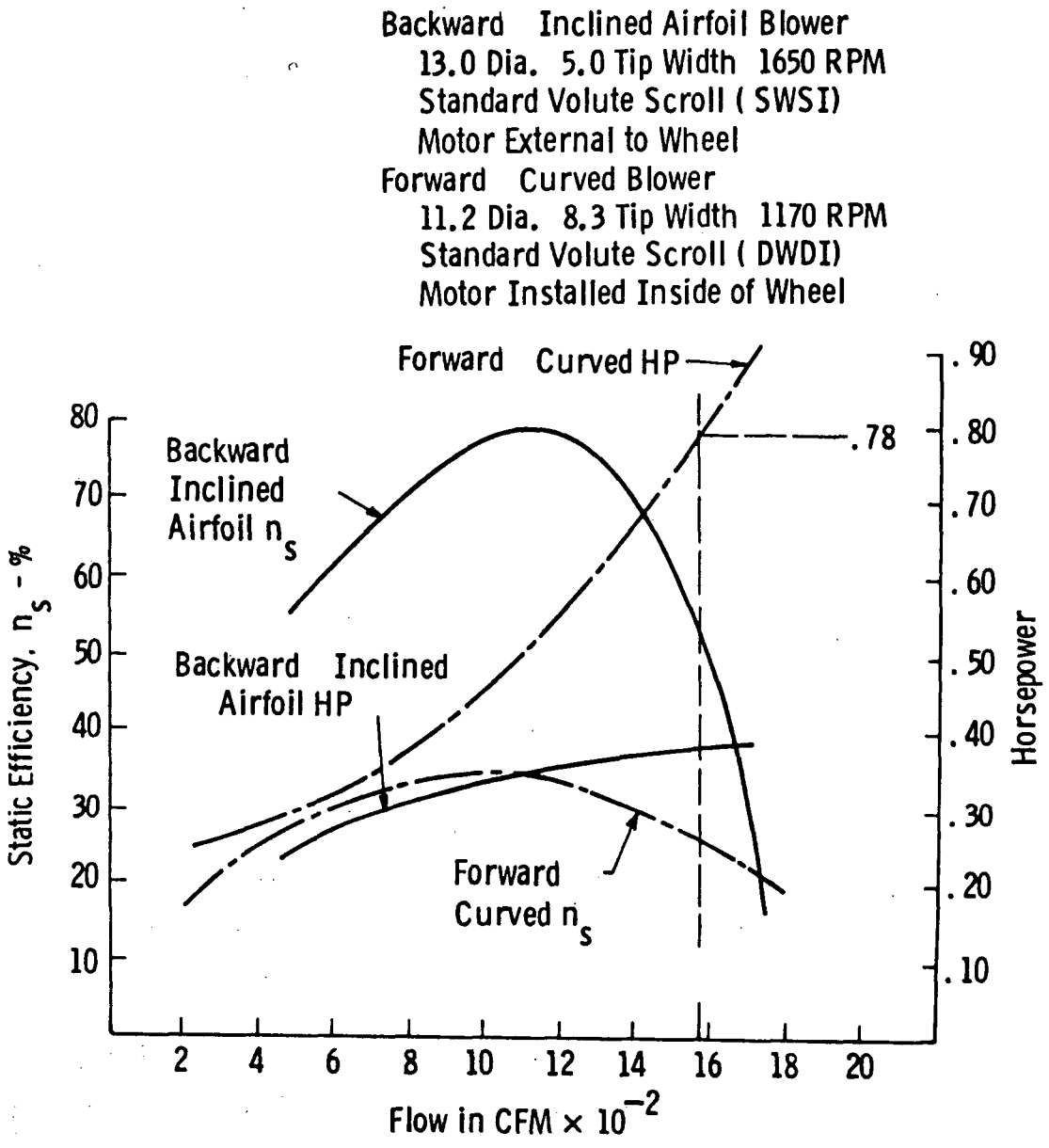

Figure 3.3-15 - Comparison of efficiency and power for blowers (dimensions in inches)

selection point. Preliminary calculations indicated that a 13 inch diameter backward curved airfoil blower wheel would be approximately correct for the specification. We had on hand an untested 13.5 in wheel from some previous work. It was deemed prudent to test this wheel for baseline data and scale a specific design if that proved necessary.

Preliminary Test Effort

For testing purposes the blower wheel was supported on an arbor and shrouded by a tubular duct. An inlet cone was mounted to the face of the duct and nested into the wheel. The rear flange of the duct was attached to a nozzle plenum chamber. This arrangement is illustrated schematically by Figure 3.3-16.

The air mover is driven by a 3/4 horsepower variable speed cradled dynamometer. The cradled dynamometer was calibrated by loading the torque arm with dead weights. Dynamic as well as static calibration is possible in this manner. The bearing drag and other losses were accounted for by removing the wheel from the shaft and reading out tare for various speeds. This method ignores the increased tare resulting from increased forces on the bearings due to the wheel weight. The bare shaft tare was used as a basis for this report despite indications that it may be somewhat conservative.

The static pressure difference across the nozzle plane (used to determine flow rate) is sensed by static-pressure taps in the wall of the plenum. The static pressure on the plenum side of the air mover/plenum interface is sensed in a similar manner. Piezometer ring arrangements are used to average the values on four sides of the plenum at each plane. Inlet air density is based on inlet static pressure, and ambient dry and wet bulb temperatures.

All pressures and torque signals are routed to electrical transducers. The transducers are excited by a stable 10 volt dc power supply. The transducer output signals are read by a data logging system

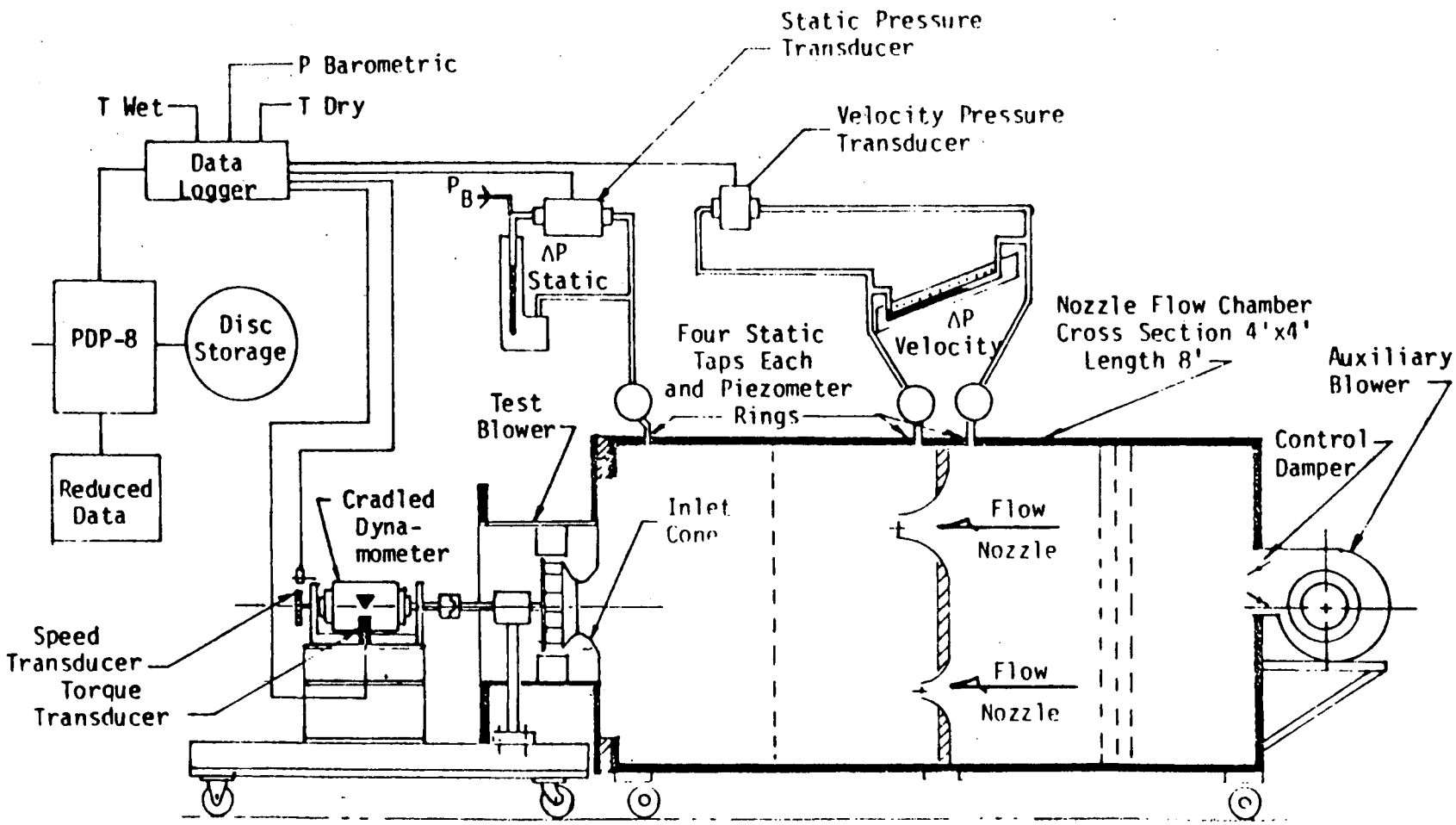

Figure 3.3-16 - Schematic arrangement of blower test equipment and instrumentation

embodying a digital voltmeter with 1-microvolt resolution. Speed and temperature are also read by the data logger.

All test data were transmitted by the data logger directly to an inhouse PDP-8 computer and stored on disk. The data were ultimately reduced by the PDP-8. The program used for data reduction has been used extensively on this type of test facility with demonstrated reliability.

The pressure transducers are recalibrated periodically against a micromanometer. Resolution of the transducer and micromanometer values are both of the order of 0.001 inches of water. The confidence level of the instrumentation is on the order of 0.01 inches of water. Twenty observations at 1-second intervals are taken to time-average cyclic values.

All test procedures and data reduction methods are in accordance with AMCA Standards, Bulletin 210-74.

The baseline blower is defined as follows:

Wheel diameter	13.5 inches
Tip width	5.25 inches
Blades	10 airfoil
Casing	23.25 in ID cylindrical
Inlet cone	30 degrees
Inlet vanes	none
Outlet vanes	4

The characteristic performance curve as developed by test at 1725 rpm is shown in Figure 3.3-17. A parabolic system curve is shown passing through the specified design point of 1575 CFM and 0.85 in of water static pressure rise. The baseline blower exceeds the required pressure rise and flow at 1725 rpm.*

---

*Initially, low motor slip operation at 1725 rpm was considered desirable to maximize motor efficiency. The need for multiple speed operation required a higher resistance motor rotor which yielded higher slip operation at approximately 1650 rpm.

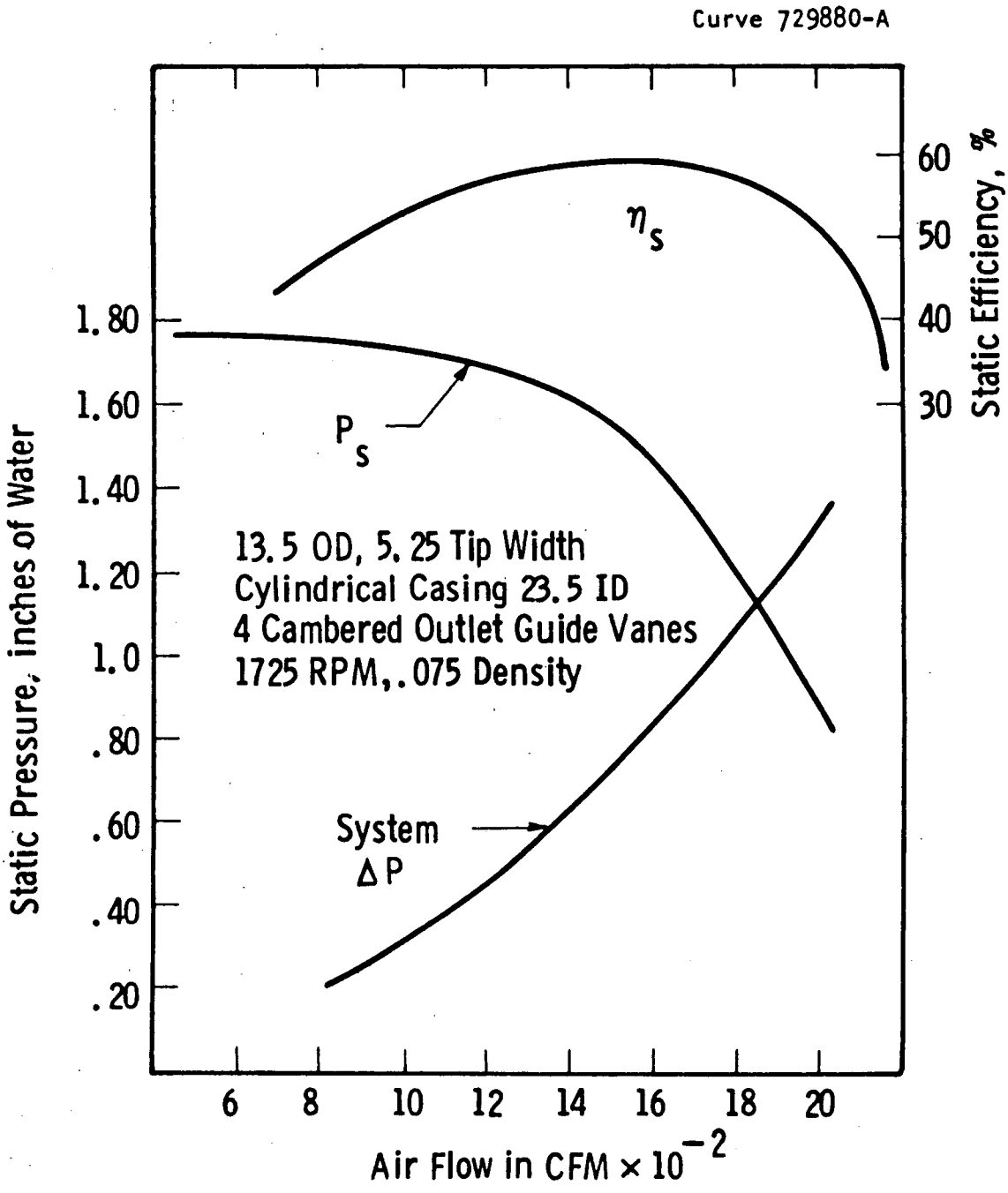

Figure 3.3-17 - Baseline airfoil blower characteristics (dimensions in inches)

A convenient method of presenting blower characteristics for analysis purposes is in a nondimensional format:

$$\psi = 234.55 \times 10^6 \frac{\Delta P}{D^2 N^2} \quad \text{pressure coefficient}$$

$$\phi = 700.3 \frac{Q}{D^3 N} \quad \text{flow coefficient}$$

$$\nu = \phi^{1/2} / \psi^{3/4}$$

or

$$\nu = 14 \times 10^{-6} \; N \times Q^{1/2} / \Delta P^{3/4} \quad \text{specific speed}$$

The coefficients reconcile the conventional units:

D = wheel diameter, inches

Q = volume flow rate, ft^3/min

ΔP = pressure rise, inches of water

N = wheel speed, rpm

Note that for the centrifugal blowers considered here, the static pressure rise at design point is from ten to fifty times greater than the change in dynamic pressure at air mover discharge. For this testing program, a good assumption therefore is $\Delta P \cong \Delta P_s$.

The ratio of casing-to-wheel diameter effect was investigated. The baseline wheel was maintained and the casing size reduced in increments. There is a marked reduction in performance for smaller casing diameters as shown in Figures 3.3-18 and 3.3-19.

The effect of outlet guide vanes on both performance and efficiency was also investigated and is shown in Figures 3.3-20 and 3.3-21. The improvement obtained with four cambered vanes is significant. Note the deleterious effect of straight radial vanes. Outlet guide vanes in conjunction with the variation of casing sizes was not investigated. There is a good probability that casing size could be reduced

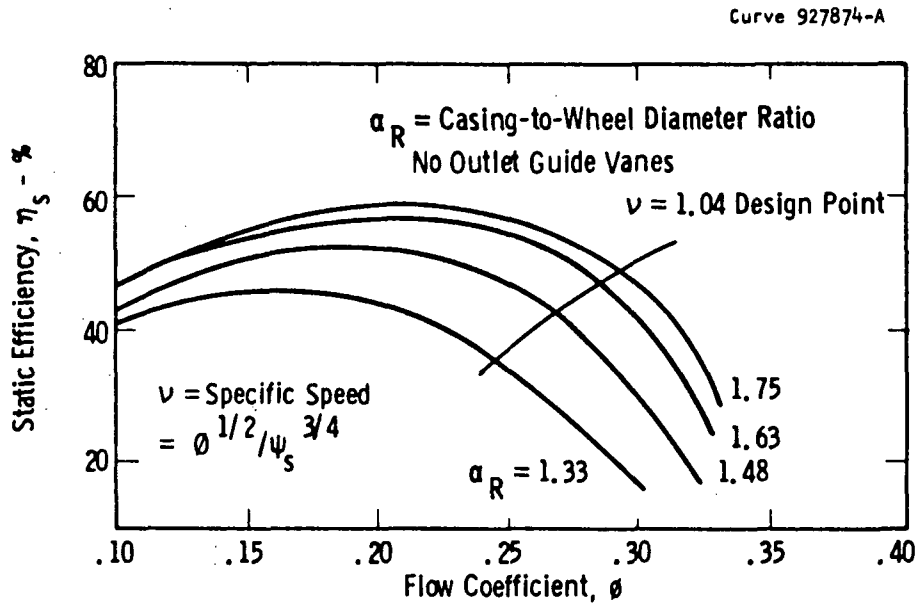

Figure 3.3-18 - Airfoil blower efficiency as a function of casing-to-wheel diameter ratio

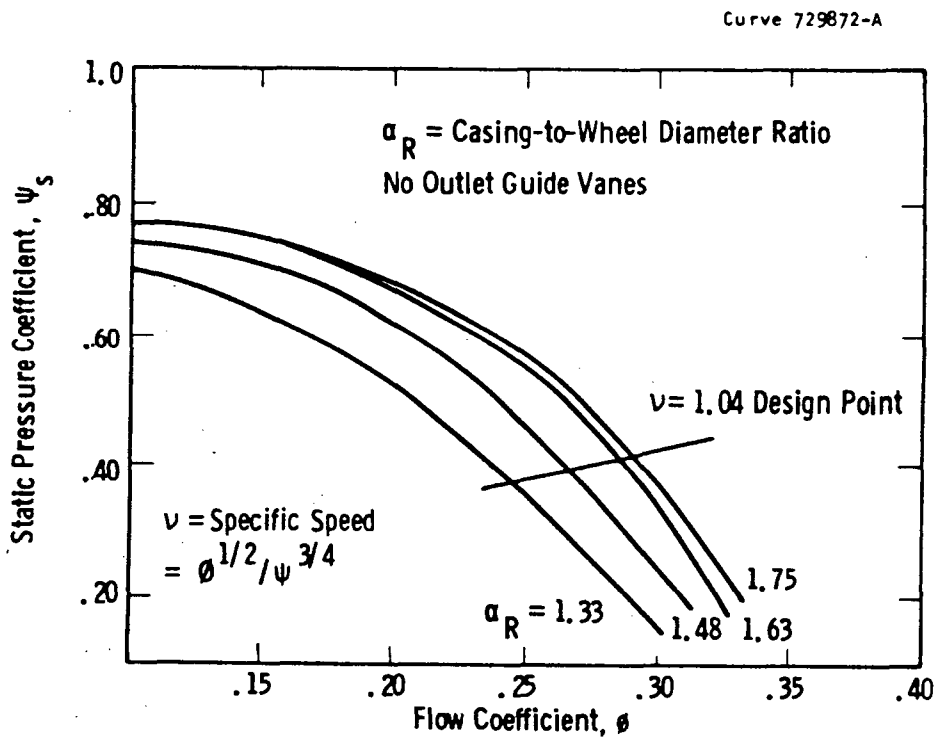

Figure 3.3-19 - Airfoil blower performance as a function of casing-to-wheel diameter ratio

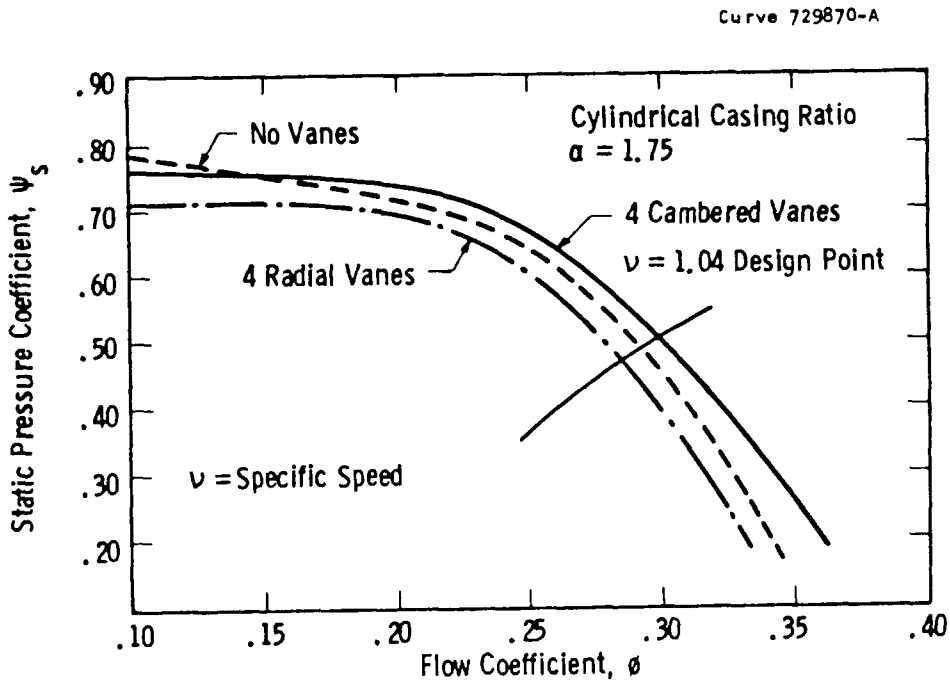

Figure 3.3-20 - Outlet guide vane effect on performance

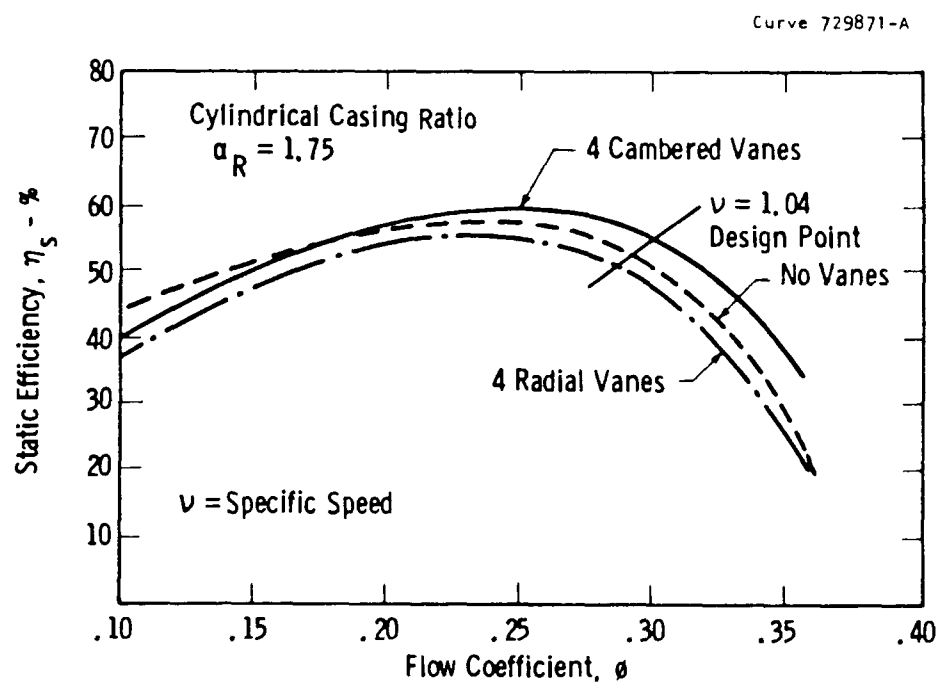

Figure 3.3-21 - Outlet guide vane effect on efficiency

without severe penalty by use of outlet guide vanes for swirl velocity recovery.

Preliminary Blower Design

While tests have been performed on a 13.5 inch tip diameter blower, final specifications for the 3.5-ton unit will be refined and a variation in both fan size and/or speed may be required. A prototype blower for four-pole motor drive may be resized on the basis of fan scaling laws as follows:

$$\Delta P_s \propto D^2 N^2 \rho_a$$

$$Q \propto D^3 N$$

$$W_s \propto D^5 N^3 \rho_a$$

where D = wheel diameter

N = rotational speed

ρ_a = air density

ΔP_s = static pressure rise

Q = volume flow rate

W_s = fan shaft power

The effect of Reynolds number on blower efficiency may be approximated by

$$\frac{\eta_m}{1 - \eta_m} \; \frac{1 - \eta_p}{\eta_p} = \frac{D_m}{D_p} \left(\frac{\eta_m}{\eta_p}\right)^{1/2}$$

where η = efficiency

m = model

p = prototype

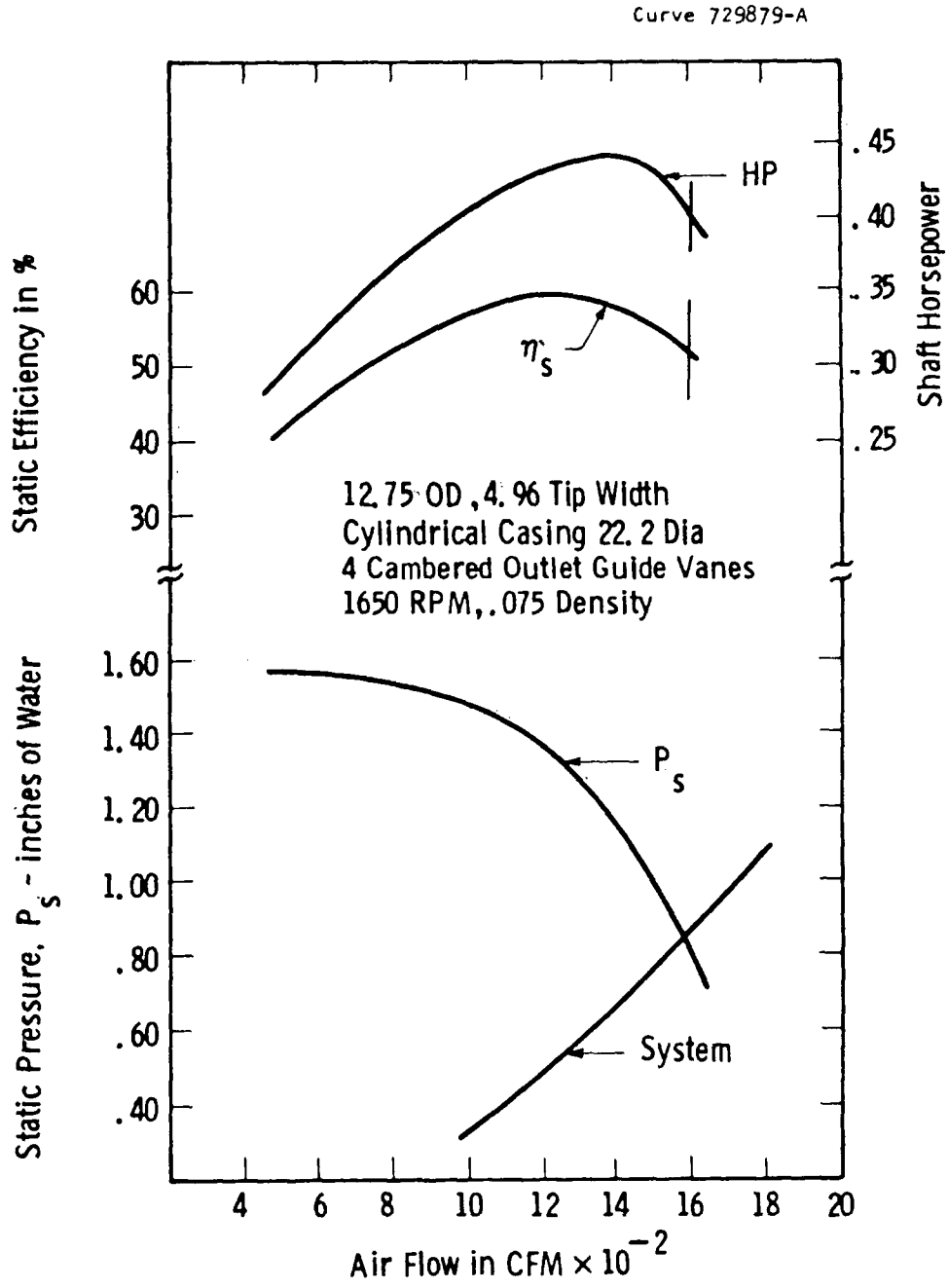

Figure 3.3-22 - Centrifugal blower scaled to performance specifications (dimensions in inches)

Using the test results described, the blower design can be downsized to meet the specified performance point from the scaling laws. The performance of a 12.75 inch tip diameter, 1650 rpm wheel geometrically similar to the 13.5 inch wheel is shown by Figure 3.3-22. The design goal can be met with 0.40 horsepower. Note that the baseline blower was tested at 1725 rpm because it was assumed that this was appropriate for high-efficiency operation at maximum flow. Multi-speed blower operation is viewed as necessary, however, and 1650 rpm is appropriate for a multi-speed four-pole blower motor.

Technical Analysis

Two configurations of the air mover are possible. The more conventional arrangement consists of a blower wheel in a volute scroll or housing as shown in Figure 3.3-23. The alternate arrangement consists of a centrifugal wheel mounted in a cylindrical casing as shown in Figure 3.3-24. The cylindrical arrangement may have the advantages of compactness, cost, and more uniform exit flow distribution. The voltage housing can have an efficiency advantage.

The design point for the advanced heat pump was initially specified as 1575 CFM at 0.85 in of water static pressure rise. The dimensionless specific speed at 1650 rpm is $\nu = 1.04$.

Performance data for a backward curved airfoil bladed blower wheel in a volute housing was available from previous work. These data are presented in dimensionless form along with data from our baseline blower mounted in a cylindrical casing in Figures 3.3-25 and 3.3-26.

Performance and efficiency of the 1650 rpm design in either mounting are nearly identical at the design flow coefficient, $\phi \cong .32$. It is necessary to select the blower with volute casing at a much lower specific speed in order to obtain a significant reduction in power or increase in efficiency.

A backward curved, airfoil bladed blower matched to a volute housing selected at the peak efficiency of 78 percent (find ϕ at peak

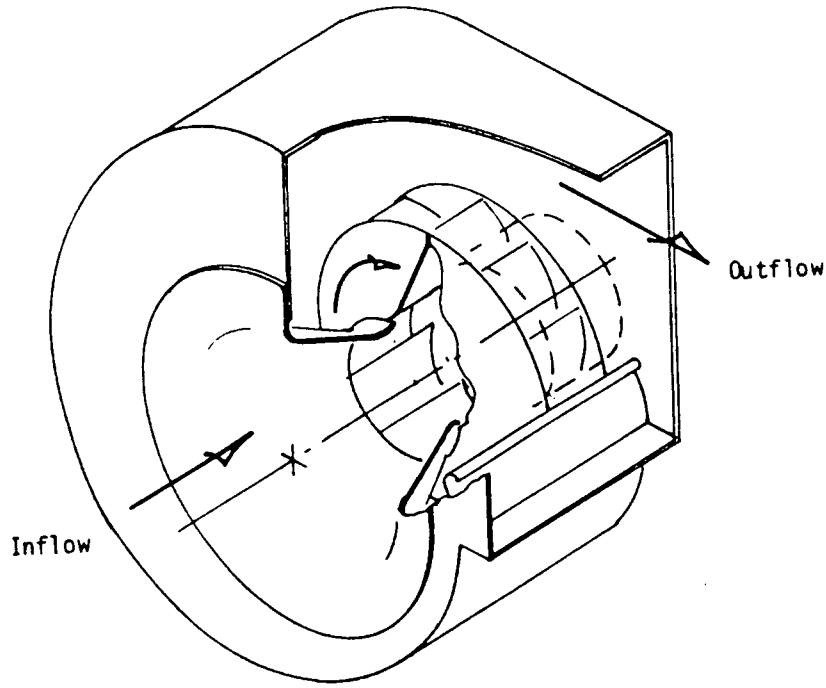

Figure 3.3-23 - Centrifugal blower in volute housing

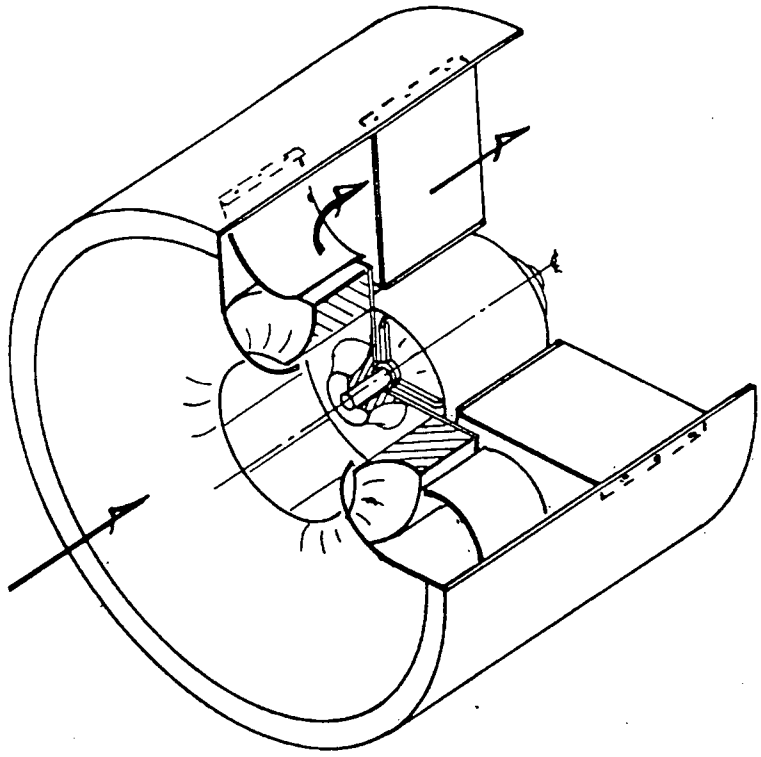

Figure 3.3-24 - Blower in an axisymmetric cylindrical casing

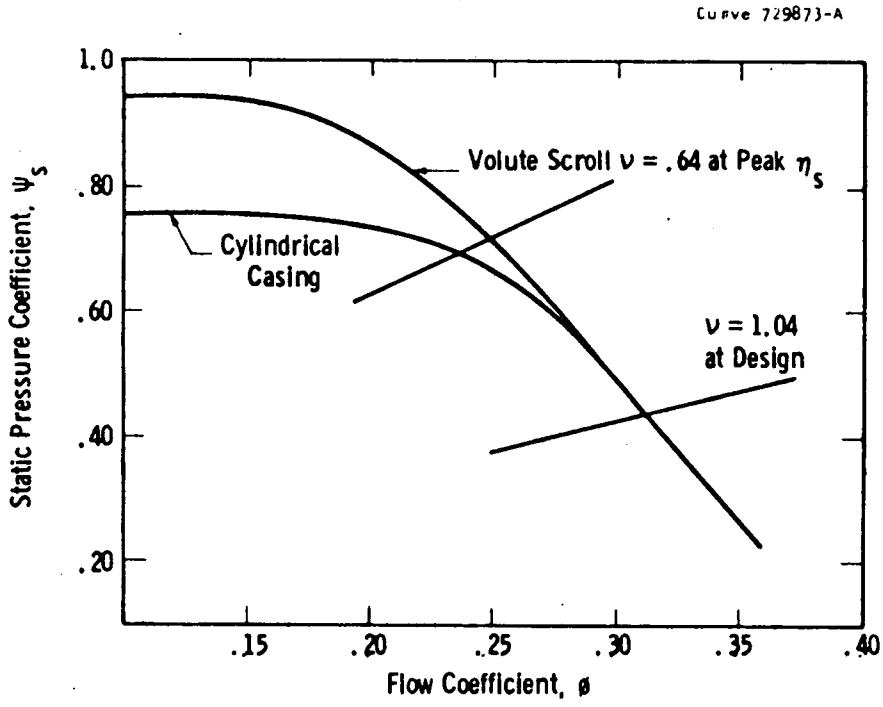

Figure 3.3-25 - Comparison of performance for an airfoil centrifugal blower in volute scroll and cylindrical casing

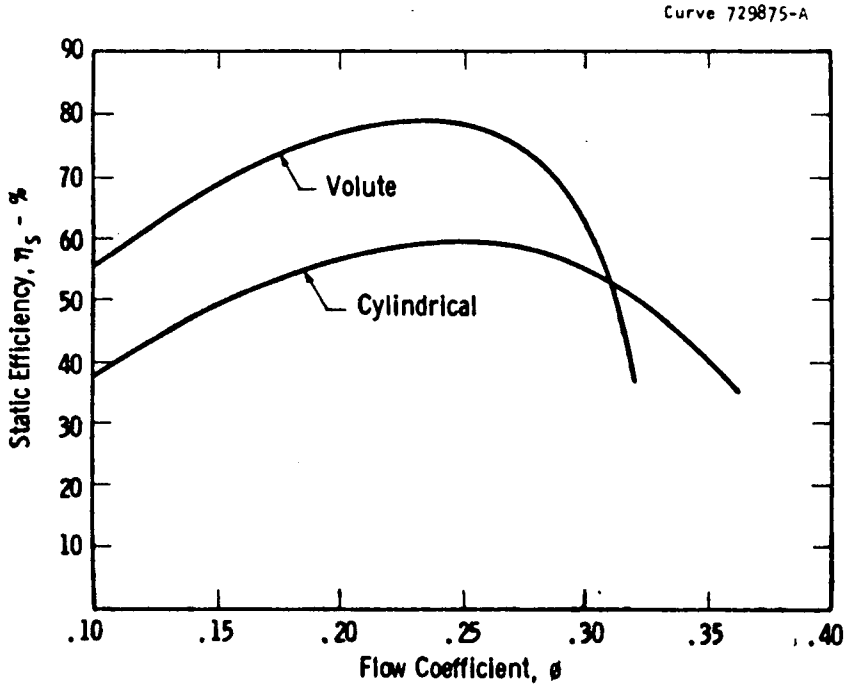

Figure 3.3-26 - Comparison of static efficiency for an airfoil centrifugal blower in a volute scroll and cylindrical casing

efficiency from Figure 3.3-26) and meeting the preliminary specifications (1575 SCFM at 0.85 inches of water) would have the following characteristics:

$$\nu \cong 0.64$$
$$\phi \cong 0.25$$
$$\psi \cong 0.75$$

where ψ is found from Figure 3.3-25 and $\nu = \phi^{1/2}/\psi^{3/4}$

$$N = \frac{\nu \Delta P^{3/4}}{14.0 \times 10^{-6} Q^{1/2}} = 1019 \text{ rpm}$$

and

$$D = \left(\frac{234.55 \times 10^6 \ \Delta P}{\psi \ N^2}\right)^{1/2} = 16.32$$

$$W_s = 0.27 \text{ hp}$$

Revised Blower Design

The indoor air flow rate was a parameter of optimization during the course of our heat pump system development effort. The optimum air flow rate depended, therefore, upon the design of the entire system. The preliminary specification called for 1575 CFM of air delivered with a static pressure rise of 0.85 inches of water. This was later revised to 1400 CFM at 0.85 inches of water static pressure rise, and the back plate and inlet cone for the blower wheel were ordered at 15.5 inches diameter. Based upon subsequent measurements taken with a mockup of the indoor unit, the pressure rise specification was increased to 0.95 inches of water. Modifications to the blower design to accommodate the final specification (1400 CFM at 0.95 inches of water) were therefore somewhat constrained. In order to achieve the higher pressure rise, the effective blower diameter was increased by projecting the blades outward beyond the diameter of the back plate and inlet cone by approximately 0.25 inches.

Two blower wheels were designed, built, and tested, the first using airfoil-shaped blades, the second using cambered-plate blades. The blower with airfoil blading was 5 to 8 percent more efficient.

The airfoil-bladed blower wheel is most effectively manufactured using a molded plastic design. Certification requirements dictated the use of an expensive plastic. In high-volume production the route is quite viable, and a significant efficiency gain is realizable. The tooling required to produce a prototype for this R&D effort was too expensive for the resources available, however.

Cambered plate blades are manufactured for a modest tooling investment and common metals can be used to limit cost. Additionally, a prototype model could be fabricated easily for evaluation. The performance penalty suffered upon adopting cambered-plate blades instead of airfoil-shaped blades is a modest 5 to 8 percentage points. As a result, the air movers produced for our preprototype advanced heat pump are constructed of aluminum and use cambered-plate blades.

A photograph of the Westinghouse preprototype blower appears in Figure 3.3-27. The measured performance of this 16 in diameter, 1070-rpm indoor air mover as produced for our preprototype is shown in Figure 3.3-28. Note that less than 1/3 shaft horsepower is required to deliver 1400 cfm into 0.95 inches of water. This blower uses cambered plate, backward curved blades, with the wheel mounted in a volute scroll, and delivers 63 percent static efficiency at its design point. Peak efficiency is 70 percent at lower flow and higher pressures, while at the original design flow (1575 CFM) a respectable 58 percent efficiency is achieved.

Discussion

Preliminary specifications for the indoor blower called for 1575 CFM into 0.85 inches of water. The use of backward curved blade blower technology was known to be necessary if a significant increase in operating efficiency relative to the conventionally applied squirrel

Figure 3.3-27 - Prototype blower wheel

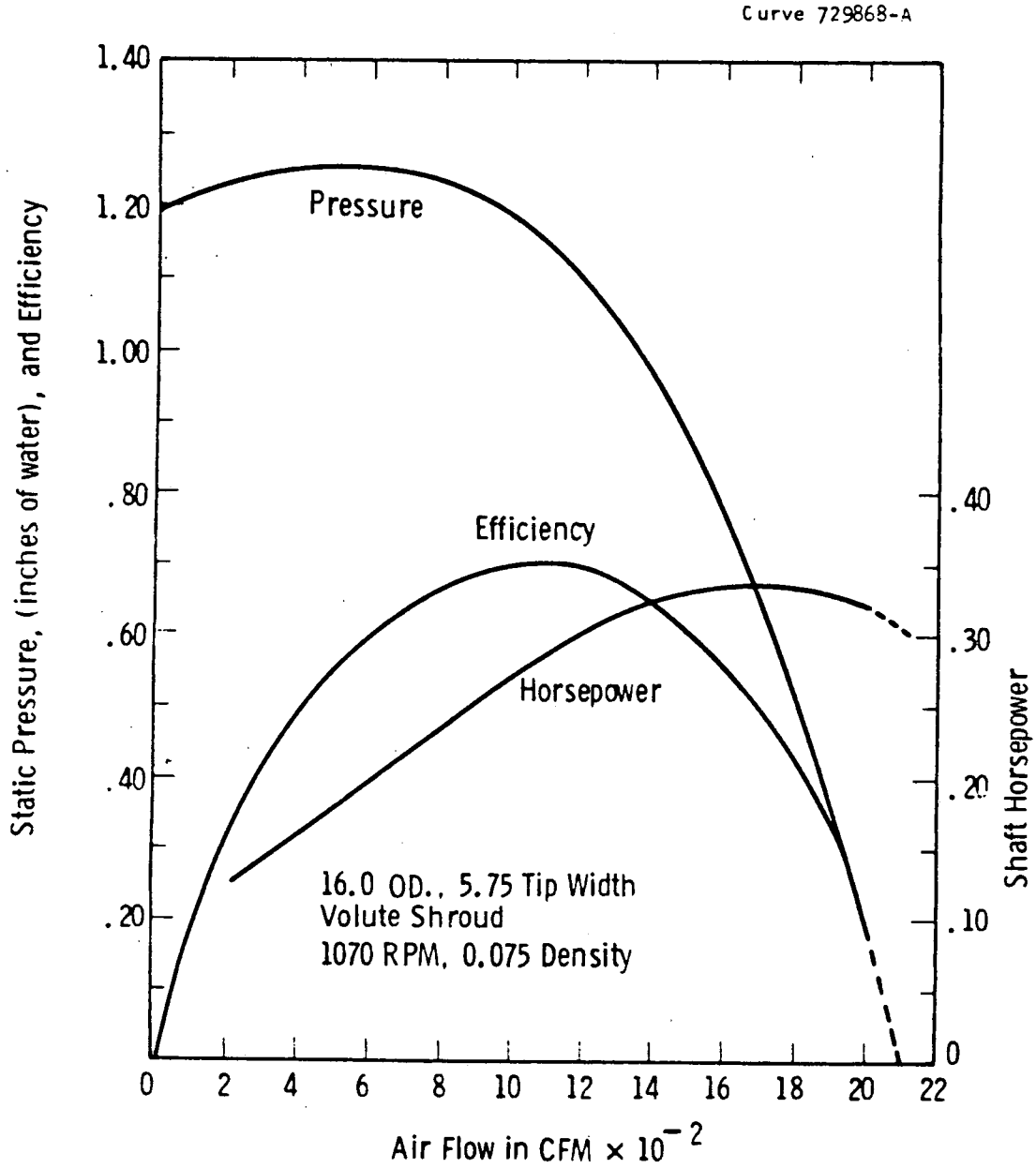

Figure 3.3-28 - Preprototype blower performance characteristics (dimensions in inches)

cage blower was to be achieved. Originally, a four-pole blower motor was considered because the motor would be less expensive, and the space occupied by the air mover less because the higher-speed blower wheel is smaller.

Preliminary testing of the breadboard blower wheel designed to operate at four-pole speed revealed a characteristic howling noise that some found objectionable. Since both lower noise and better blower efficiency were achievable at six-pole motor speed, our design effort was directed in this area.

Prior to the manufacture of our prototypical units, a system design change required a modification in the blower specifications from 1575 CFM at 0.85 inches of water static pressure rise to 1400 CFM at 0.95 inches of water pressure rise. Since the backplate and inlet cone for the blower wheel had been procured prior to receipt of the final specification, modification of the design to meet the final design point was constrained slightly. Given the opportunity to redesign the blower again, the blower side plates would be increased slightly in diameter, and an increase of approximately 3 to 4 percent in efficiency could be achieved over the unit as built.

Two blower wheels were designed, built and tested, the first using airfoil-shaped blades and the second using cambered-plate blades. The blower with airfoil blading was 5 to 8 percent more efficient. Since the use of cambered plate blading allowed us to meet our performance objective while promising lower ultimate cost, cambered plate blading was adopted for the prototype indoor air movers.

Our preprototype indoor air mover with cambered-plate blades has achieved its design goals by yielding an air moving, static efficiency of 63 percent, approximately twice that of current practice.

3.3.3 Blower Motor

Introduction

The blower motor design for the preprototype heat pump has evolved from a 0.4 hp, four-pole motor with "deep" speed reduction capabilities to a 0.3 hp, six-pole design with somewhat less speed reduction potential than in the case of the four-pole motor. The motor finally selected does not represent a precise optimum. This is partially due to the nonstationary targets for the design, necessitated by the overall system optimization study, and by the fact that the effort required to perform a complete suboptimization of the motor did not seem warranted since the contribution of the blower motor to overall system efficiency and system cost is small. Further, motor optimization was specifically excluded from the scope of our contract effort.

Constraints always confound any attempt at optimization, and in this case overall length of the blower motor was constrained by the available cabinet width and the size of the blower. Nevertheless, the end result of our motor design effort is a blower motor that is considerably more energy efficient than current state-of-the-art motors, and when measured against such a motor most certainly has a payback period of its cost premium of well under 4 years. It is judged to be close to optimum in design while meeting space constraints.

Final Design of the Motor

The 0.3 hp, six-pole blower motor design employs a 1.97 in stack with an approximate balance between the weight of copper in the main and auxiliary windings. The turns ratio (effective auxiliary turns to effective main turns) is 1.042. The capacitor required is 7.5 μfd. The rotor has a medium-resistance rotor which on a horsepower per unit basis is 0.113 per unit resistance. Our goal in the design was to effect the maximum feasible utilization of the slots within manufacturing capabilities, and to run close to balanced operation.

The analytically estimated torque speed curve for this motor is shown in Figure 3.3-29 along with the blower characteristics. The estimated efficiency at full load for this 0.3 hp, six-pole motor is 67.0 percent.

Speed Reduction

As described, the blower motor for the heat pump prototype is a six-pole permanent split capacitor, single-phase motor with a medium resistance rotor designed for deep speed reduction. In order to achieve the speed reduction called for by our system optimization studies, we devised a method which uses an autotransformer and a switchable capacitor network. The low-speed design objective was 72 percent of the operating high speed, or 777 rpm. The required voltage on the main winding to achieve this speed with a balanced motor is 106.5 volts, or 46.3 percent of 230 volts. The required auxiliary circuit voltage is 187.4 volts, with a total circuit capacitance in series with the auxiliary winding of 11.5 μfd. Figure 3.3-30 shows the "ideal" circuit arrangement, with the main winding connected to a 46.3 percent tap (as measured from the L2 end of the transformer) and the auxiliary winding connected to a capacitor divider network (9.37 μfd in series with 2.13 μfd). This capacitor network has a "Thevenin"* equivalent source consisting of a 187.4 volt source in series with 11.5 μfd. In actuality, the capacitors would have to be 9.5 μfd and 2.0 μfd, respectively, to be in accord with commercially available capacitors. The blower motor, when operated at full speed, requires a 7.5 μfd capacitor in series with the auxiliary winding. Thus, the required 9.5 μfd capacitance could be obtained by connecting a 2.0 μfd capacitor in parallel with the 7.5 μfd capacitor required for full speed operation. While this arrangement would give excellent operation at reduced speed, it would require switching capacitors in such a way as to cause a high

---

*Introduction to Circuit Analysis, J. D. Cowan and H. S. Kirschbaum, C. E. Merril Books, Inc., Columbus, OH, 1961,p 242ff.

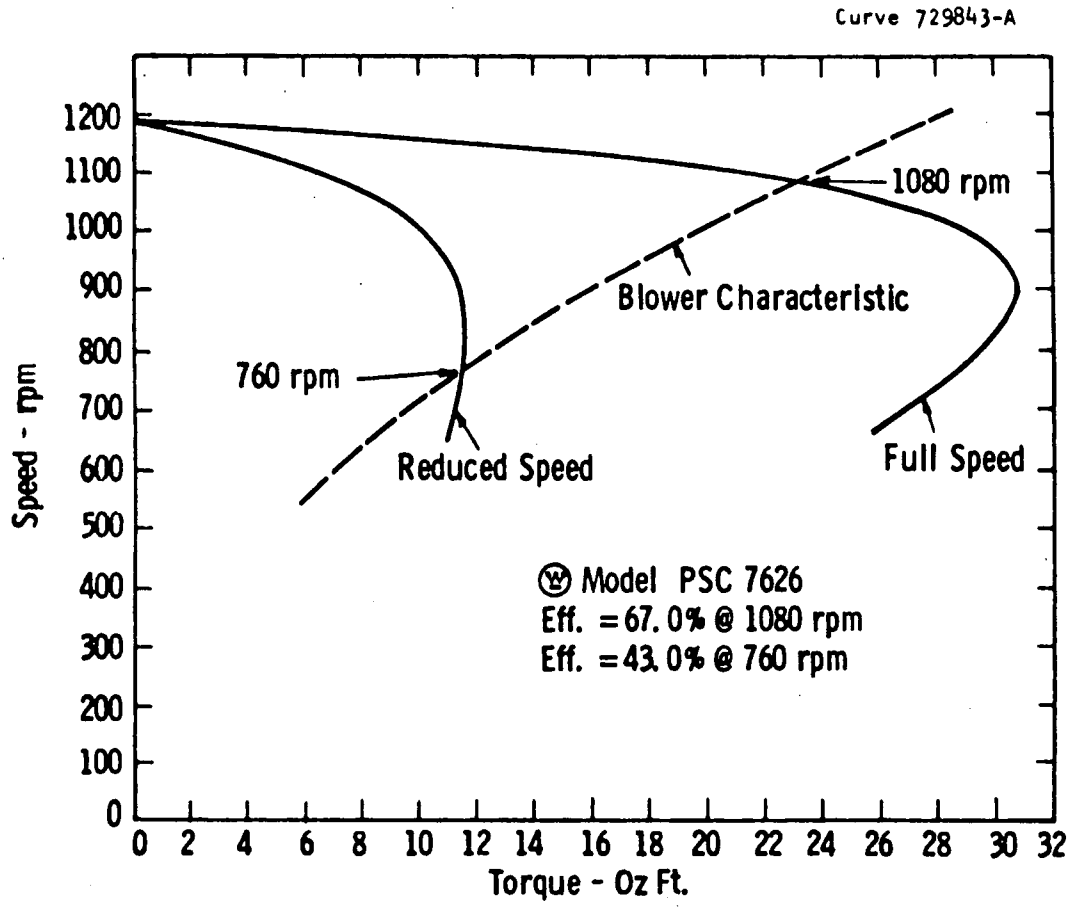

Figure 3.3-29 - Blower motor speed-torque characteristics (analytically estimated)

Dwg. 7751A31

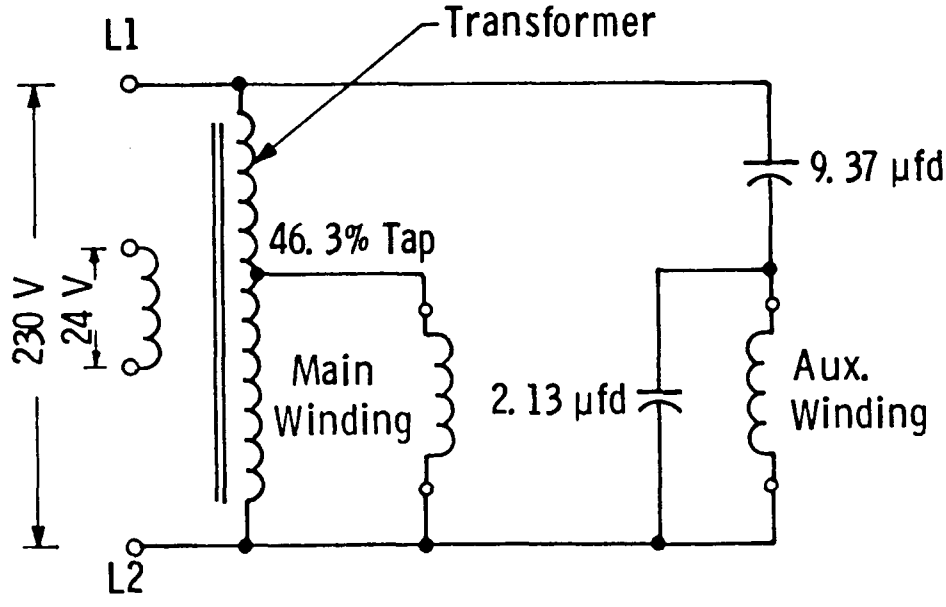

Figure 3.3-30 - Ideal circuit for low-speed motor operation

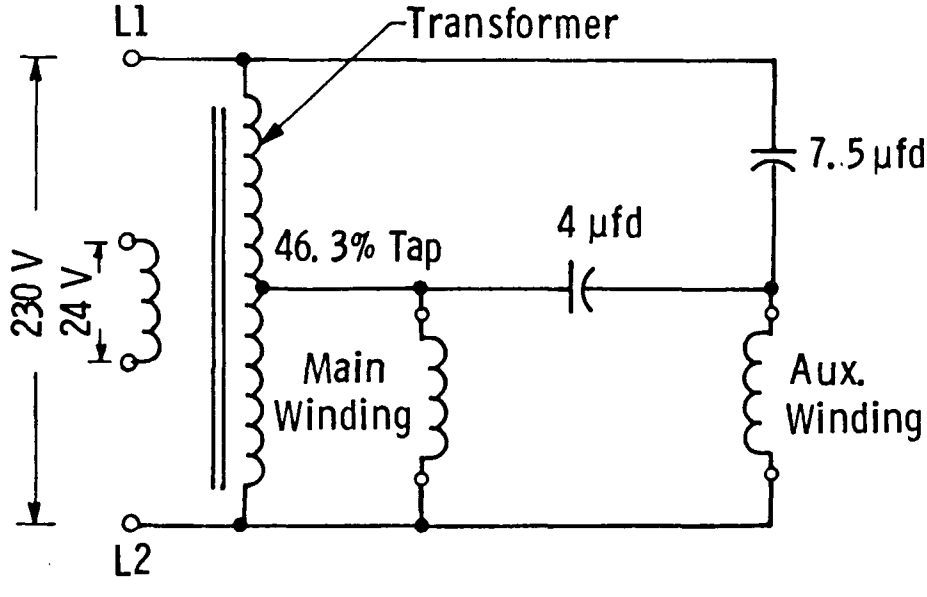

Figure 3.3-31 - Adopted blower motor low-speed circuit

probability of welding the relay contacts. The circuit of Figure 3.3-31 will give essentially the correct "Thevenin" equivalent source without the necessity of switching capacitor currents. The equivalent source voltage in this arrangement is very slightly lower than the required voltage, but the equivalent series source capacitance is 11.5 μfd as required. Figure 3.3-29 shows the analytically estimated speed-torque performance of the blower motor at both full speed and reduced speed. Low speed operation is predicted to be 760 rpm or 70.4 percent of full speed. The low speed motor efficiency is 43 percent.

The arrangement of Figure 3.3-31 is incorporated into the overall system electrical control circuits.

The OEM cost for this motor and its associated capacitors, excluding contactors and the autotransformer, is $14.56 less than the motor and capacitor used with a state of the art indoor air mover in an equivalent capacity (4 ton) heat pump.

3.3.4 Fan Motor

Introduction

The fan motor for the outdoor unit evolved toward a 0.2 hp, eight-pole design. The degree of concern with suboptimization of this motor was not the same as that given to the blower motor because of its lower power consumption. In fact, it was procured to a specification requiring 65 percent efficiency at rated power. The stack length required of this motor to meet the 65 percent efficiency requirement is 2.47 in. Consideration for deep speed reduction was given in this design in that a medium resistance rotor was selected. If the outdoor unit eventually is operated at only a single speed, a low resistance rotor may be substituted with an attendant efficiency of 67.5 percent.

Final Design of Motor

The outdoor fan motor is required to yield high reliability as well as high efficiency. The heat pump outdoor fan motor specifications are as follows: permanent split capacitor, eight-pole, totally enclosed, nonventilated, air-over, 230/208 volts, 60 Hz, single-phase, reversible direction by external reconnection, -20°F to +130°F environment, 50,000 hours expected life, ball bearing, double-sealed, synthetic grease (Mobil 28). Auxiliary winding insulation is Westinghouse Omega-Klad-EK; main winding insulation is Westinghouse Omega-Slip-HA; varnish is double-dip polyester. Lead-in is via potted insulation tubes and sealing grommet, leads 24 in long. Frame length is to be extra long (5.5 in maximum), end bell seal-silicone RTV, independent thermal protection, auxiliary and all leads out. Shaft is down, vertical mount. Design output is to be 0.20 hp at 825 rpm and 65 percent efficiency, with two-speed operation.

The 0.2 hp, eight-pole fan motor design employs a 2.47 in stack with an approximate balance between the weight of copper in the main and auxiliary windings. The turns ratio (effective auxiliary turns to effective main turns) is 1.318. A 4 μfd capacitor is required for this motor. The motor has a medium resistance rotor which on a horsepower per unit basis is 0.0654 per unit resistance. One feature of the design effort was an atempt to effect the maximum feasible utilization of the slots, within manufacturing capabilities, and to run at rated power close to balanced operation.

Figure 3.3-32 shows the experimentally determined speed versus torque characteristic for this motor with the medium resistance rotor in place. If a low resistance rotor were to be substituted, the efficiency at full load should improve to 67.5 percent.

Speed Reduction

In contrast with the blower motor, there is no firm requirement on low speed rpm other than it be less than 80 percent of the full speed rpm. Since the full-speed rpm is 825, the low-speed rpm should be less

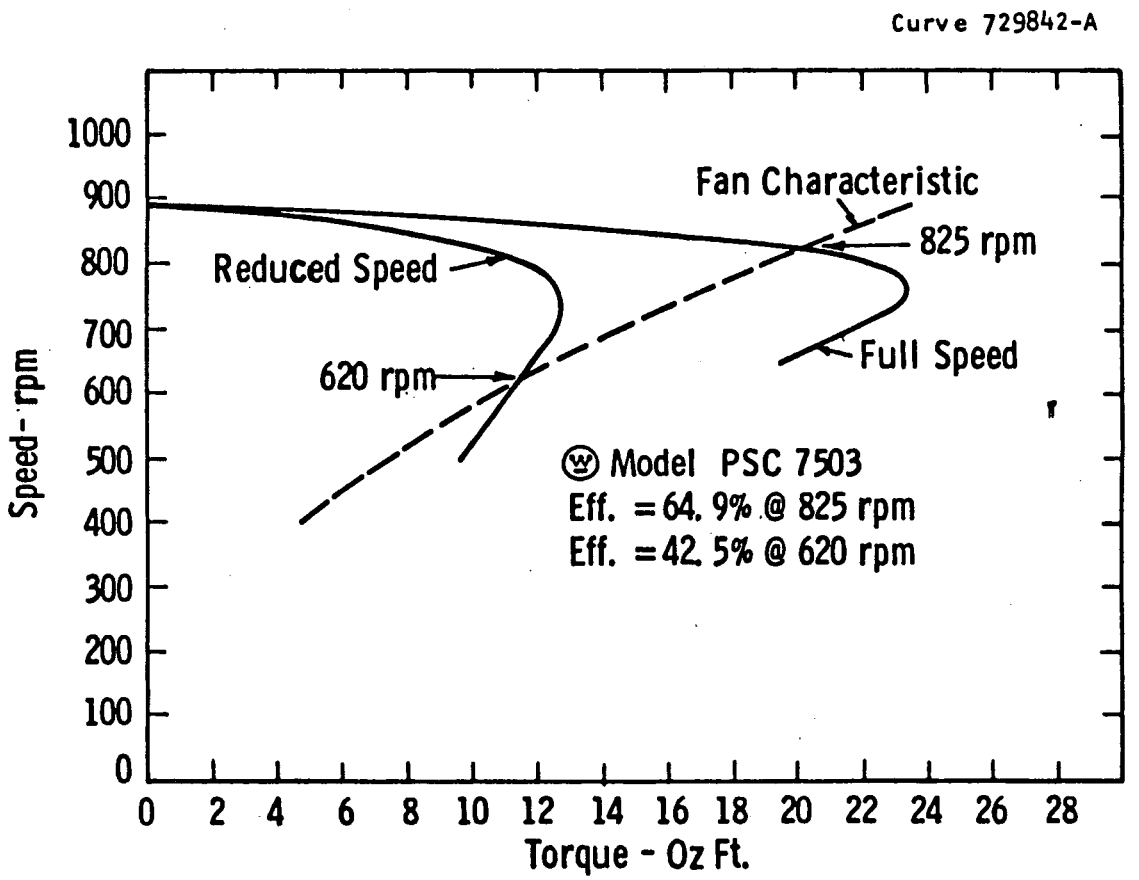

Figure 3.3-32 - Fan motor speed-torque characteristics

than 660. It is advantageous from the point of view of the auto-transformer design to connect the main winding of the fan motor across the 53.7 percent portion of the available line voltage as shown in Figure 3.3-33. (See also Figure 3.3-30.) It is then possible to compute the values of capacitance in the capacitor network applied to the auxiliary winding that will cause the motor to operate balanced at the intersection point between the motor speed torque curve and the fan torque/speed curve. The required ideal circuit to effect this operation is shown in Figure 3.3-33. The "Thevenin" equivalent source supplying the auxiliary winding is a 204.9 volt source in series with 6.69 μfd. In practice, a 1 μfd and a 6 μfd capacitor (consisting of a 2 μfd in parallel with a 4 μfd) would be used in place of the 0.73 μfd and 6.96 μfd capacitors, respectively.

The circuit of Figure 3.3-33 also presents problems with regard to the direct switching of capacitors and the resulting shortened relay contact life. The solution was to employ the same type of circuit as used for the blower motor (Figure 3.3-31), thus avoiding direct switching of capacitors. This is shown in Figure 3.3-34. For this circuit, the "Thevenin" equivalent voltage is 194.5 volts in series with 6 μfd of capacitance. The effect of lower auxiliary circuit voltage and lower than required capacitance is to cause the motor to operate considerably removed from balanced operation. However, because of the low power involved in the fan motor circuit and the low relative occurence of low speed operation, the circuit of Figure 3.3-34 was deemed acceptable. The speed torque curve for this mode of operation was calculated and is in agreement with the experimentally determined performance shown in Figure 3.3-32. The motor will operate in low speed at 620 rpm (75 percent of 825 rpm) at an efficiency of 42.5 percent.

The arrangement of Figure 3.3-34 is incorporated into the overall system electrical control circuits.

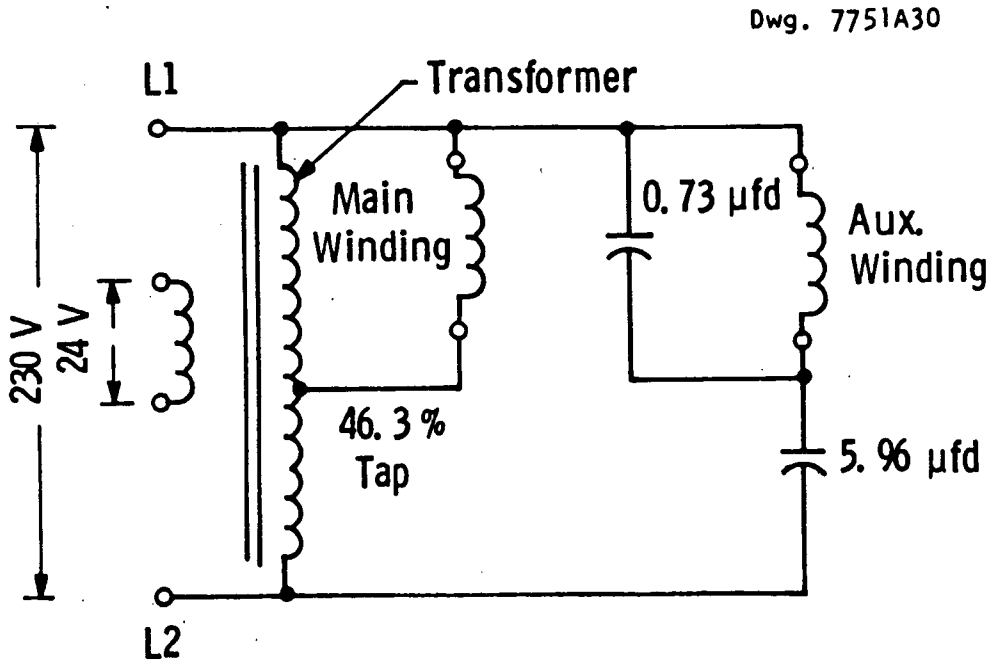

Figure 3.3-33 - Ideal circuit for low-speed fan operation

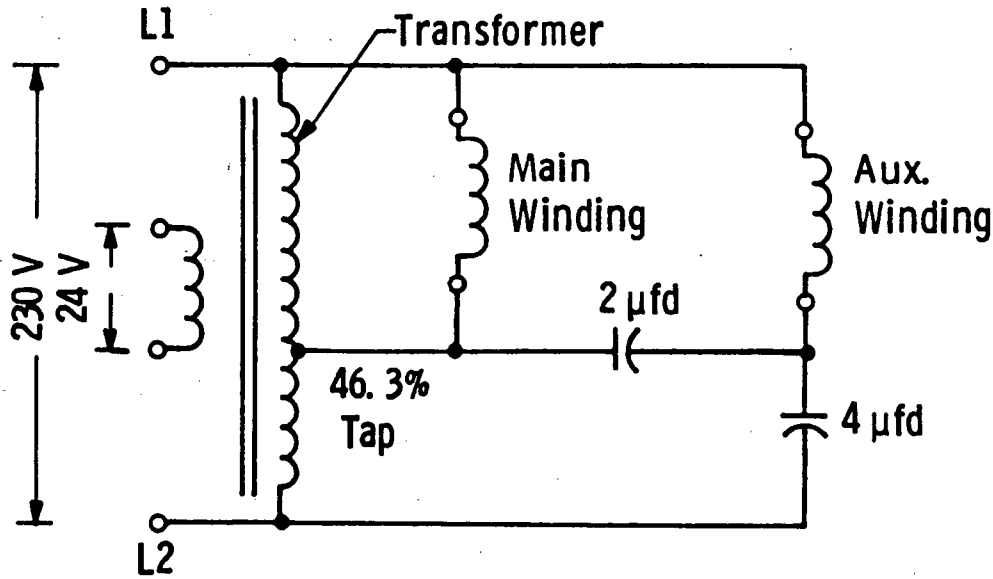

Figure 3.3-34 - Adopted fan motor low-speed circuit

3.3.5 Summary and Evaluation

The indoor blower for the advanced electric heat pump with 4 tons maximum cooling capacity is designed to deliver 1400 SCFM into a resistance of 0.95 inches of water static pressure. The static air horsepower is thus 0.209 or 156.27 watts. The air mover static efficiency is 63 percent and the motor efficiency is 67 percent at the full flow design point, thus yielding an overall indoor air mover efficiency of 42 percent, twice that of the air mover conventionally applied. At the full-flow design point, this air mover will consume about 370 watts. In the reduced flow mode, the air mover delivers 985 SCFM into the system and will consume 180 watts, approximately half of the full load power. Since the advanced system will operate most of the time in the low capacity mode, with reduced indoor air flow, the net energy savings to the consumer due to the higher efficiency indoor air mover should exceed $120 per year based upon 6000 hours of operation annually with the cost of electricity taken as 5¢/kWh.

The outdoor fan for the advanced electric heat pump will deliver 2600 SCFM into a flow resistance of 0.20 inches of water. The ideal static air horsepower is thus 0.0829 or 61.14 watts. As built, this fan will be at least 46 percent efficient and the motor 64.9 percent efficient at the design point thereby yielding an overall efficiency of 29.9 percent. Thus the outdoor air mover for the advanced heat pump will consume about 205 watts at full flow and half that at reduced flow.

Total air moving power is thus about 575 watts at full flow, about 55 percent of that consumed by state-of-the-art heat pumps. Without taking any credit for reduced flow operation, the advanced air movers will save 475 watts, which taken at 5¢/kWh and 6000 hours of operation annually, represents an annual savings of $142.50. Assuming that a customer level payback time of 4 years is acceptable, and assuming further that the ratio between manufacturing cost and acquisition price is about 1:2.5, then the acceptable added OEM cost increment for these air movers is $228. This should be possible.

3.4 Advanced Heat Pump Controller

3.4.1 Introduction

The microprocessor-based controller for the advanced electric heat pump manages a two-capacity heat pump system in response to wall thermostat signals, outdoor ambient temperature, and heat pump operating parameters. The overall system efficiency is optimized, within the constraints of safety and comfort, through control of compressor capacity, indoor air flow rate, auxiliary heat addition, and expansion device throughput.

The controller incorporates demand defrost of the outdoor coil. The demand defrost function is backed up by a timed defrost as a precaution against sensor failure.

The controller also monitors heat pump system operating parameters for anomaly detection. If an anomaly is detected, the controller will perform the necessary operations to prevent damage to heat pump components while minimizing discomfort of the building occupants.

Two controllers are being designed and built for use with the preprototype hardware. These controllers, although functionally the same as prototypical hardware, also contain features such as a telephone touch pad keyboard and an LED* alpha-numeric display that would not be incorporated in the prototype controller.

3.4.2 Technical Discussion

A block diagram of the preprototype controller is shown in Figure 3.4-1. The following is a description of the various blocks.

The preprototype controller is an 8085 microprocessor-based design. The controller consists of two printed circuit (PC) boards, a processor board, and a power/interface board. The processor board

---

*LED = light emitting diode

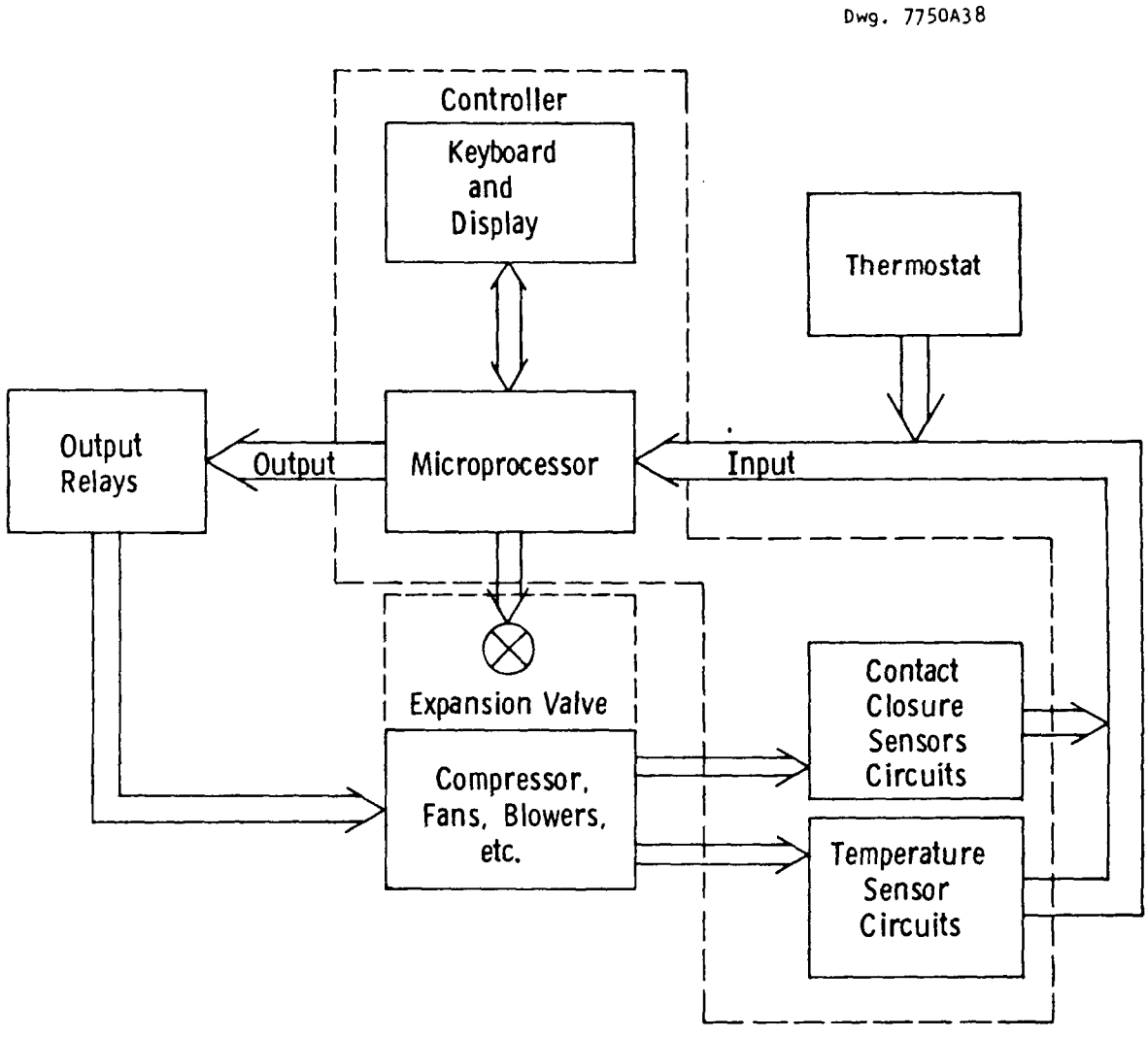

Figure 3.4-1 - System configuration

contains the microprocessor, memory, keyboard, display, analog to digital converter, and support circuitry. The power/interface board supplies the processor board with power and interfaces between the processor board and the input sensors, thermostat, expansion valve, and output relays.

The contact closure sensors and temperature sensor circuits convert the sensor output to an input that can be understood by the controller. These, along with the thermostat inputs, are used to determine which output relays to open and/or close.

The output relays interface the controller with the compressor, fan motor, blower motor, and auxiliary heat.

A photograph of the processor board is shown in Figure 3.4-2.

The keyboard and display are not typical of the prototype controller. The keyboard is a telephone touch pad keyboard, and the display consists of an alphanumeric LED display and discrete LED's. The prototype controller would have only the discrete LED's. The alphanumeric display is convenient for examining system inputs and for changing setpoints during the development and test phases of this effort. This capability, however, will not be required in prototype hardware.

Controller/Heat Pump Interface

Figure 3.4-3 shows the inputs to the controller. Ten of these are analog signals and eight are contact closure, or digital signals.

The analog signals are derived from thermistor temperature sensors. The ten temperatures monitored are: outdoor ambient temperature, inlet and outlet refrigerant temperature at the outdoor coil, crankcase temperature, compressor discharge temperature, return air temperature, refrigerant temperature as sensed at three locations in the indoor coil, and accumulator heat exchanger liquid line exit.

The digital inputs are signals indicating the state of the contact closure. An example is the discharge pressure cutoff switch.

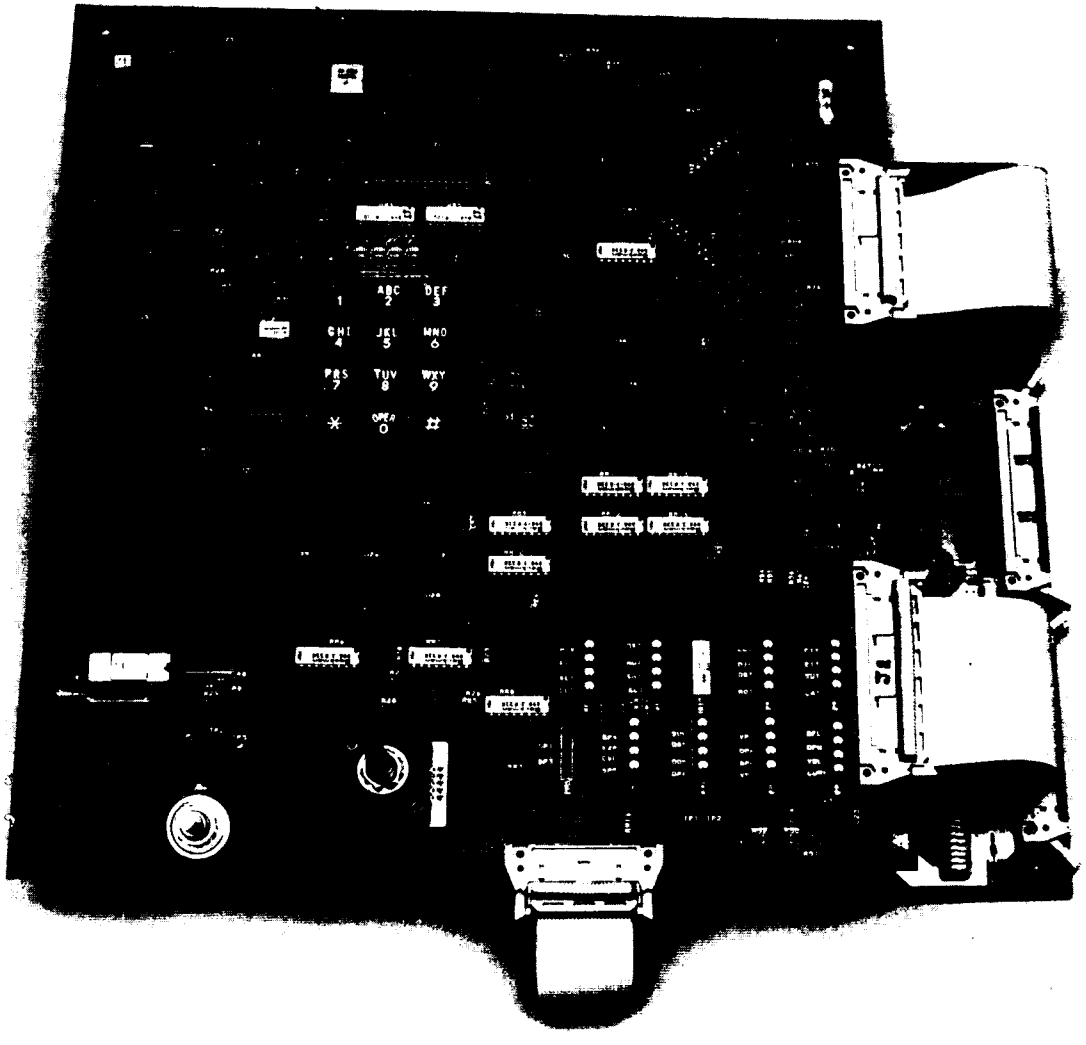

Figure 3.4-2 - Photograph of processor board

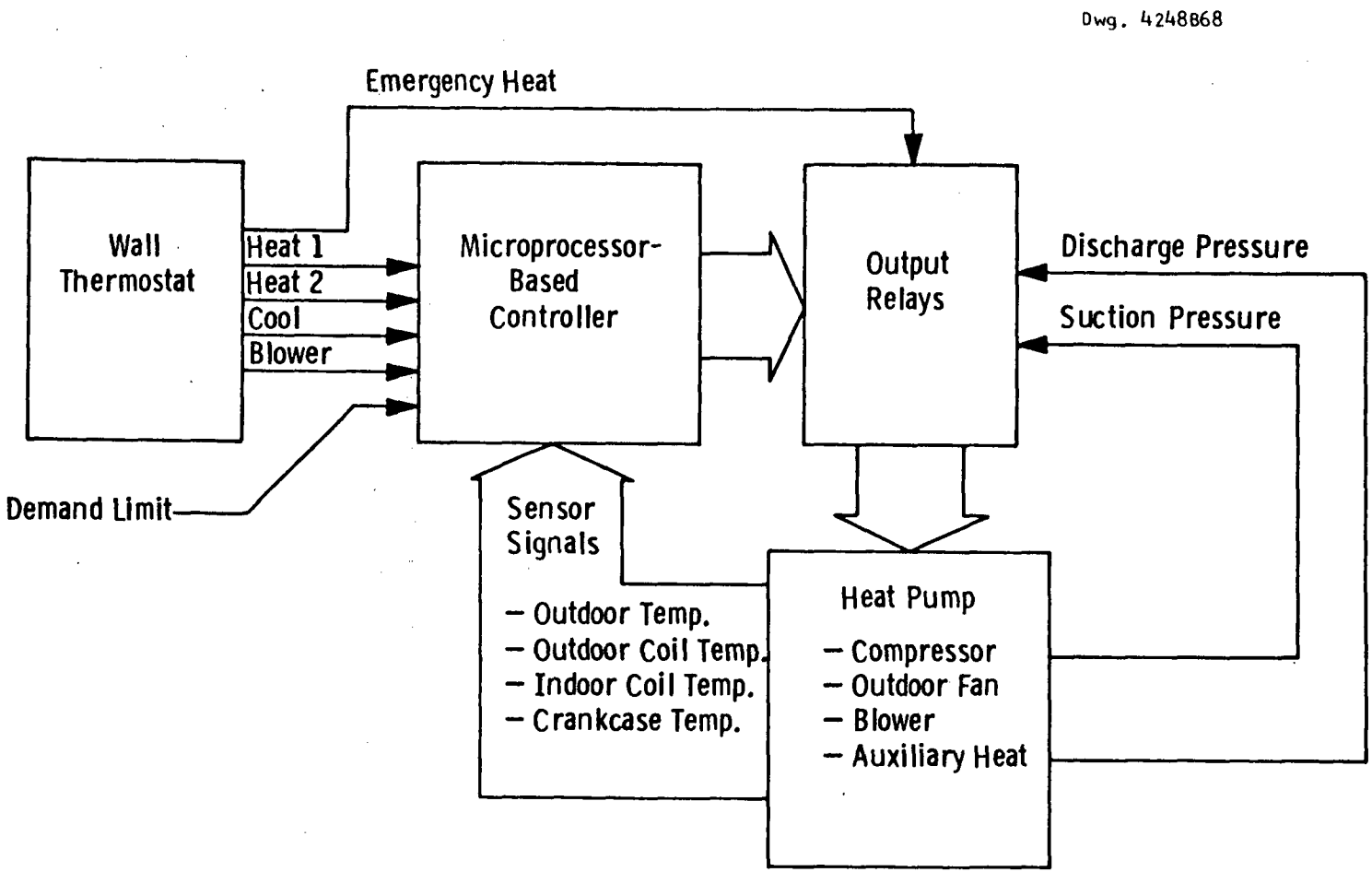

Figure 3.4-3 - Control system interface diagram

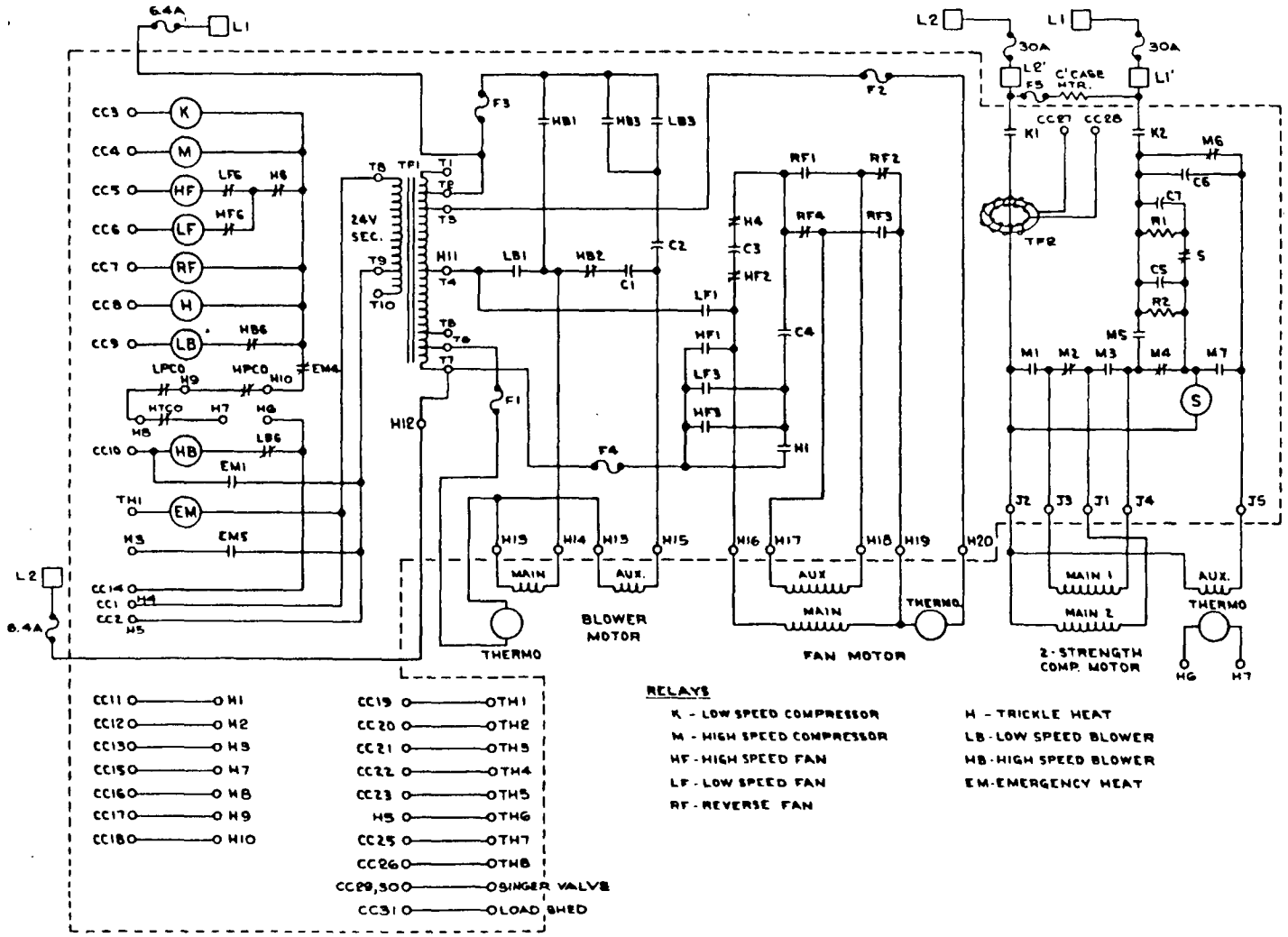

Figure 3.4-4 - Output relays

The state of this contact is sensed and fed into the controller. Other digital inputs are for excessively high discharge temperature, excessively low suction pressure, emergency heat, heat 1, heat 2, cool, continuous blower, and demand limit or load shedding.

The outputs of the controller are signals that open or close output relays, which then start or stop motors, the compressor, etc.

Figure 3.4-4 shows the output relay circuits. Lines marked "CCX" are signals from the microprocessor that drive the relay coils. Extensive use of interlocks, in the form of normally closed relay contacts, prevents potentially damaging combinations of closed relays.

System Mode Control

The system mode control performs the heating and cooling control of the conditioned space. This is accomplished through control of capacity, blower speed, and auxiliary heat if needed.

The controller uses the thermostat signals heat 1, heat 2, and cool, along with the outdoor ambient temperature to determine the desired state of the output relays. The determination is made by a matrix for heating and a matrix for cooling. These matricies are shown in Tables 3.4-1 and 3.4-2.

The state of the compressor, auxiliary heat, fan, and blower relays are determined by locating the outdoor ambient temperature, T, on the left-hand side of the table. This will isolate two rows. The thermostat inputs will determine which of the two rows to use. This row contains the needed information as to what state each relay should be in.

The thermostat "continuous fan" and "emergency fan" signals are different than the heating and cooling signals. The "continuous fan" signal determines if the blower should be run at all times or cycled on and off with the compressor.

The "emergency heat" is used as a backup to the heating mode of the heat pump. It is used to provide auxiliary heat independent of the

INFORMATION ON THIS PAGE SUBJECT TO
PATENT STATUS CLAUSE ON PAGE 1.

Table 3.4-1
Relay State Matrix for Heating Mode

Outdoor Temp., T	Thermostat Ht 1	Thermostat Ht 2 + Δ Time	Low Comp.	High Comp.	Aux Ht 1	Aux Ht 2	Aux Ht 3	Low Fan	Hi Fan	Low Blower	High Blower
T ≥ HHBP	1	0	1	0	0	0	0	0	1	1	0
	1	1	0	1	0	0	0	0	1	0	1
HHBP > T ≥ LHBF	1	0	0	1	0	0	0	0	1	0	1
	1	1	0	1	0	0	0	0	1	0	1
LHBP > T ≥ H1BP	1	0	0	1	0	0	0	0	1	0	1
	1	1	0	1	1	0	0	0	1	0	1
H1BP > T ≥ H2BP	1	0	0	1	1	0	0	0	1	0	1
	1	1	0	1	0	1	0	0	1	0	1
H2BP > T ≥ H3BP	1	0	0	1	0	1	0	0	1	0	1
	1	1	0	1	0	0	1	0	1	0	1
H3BP > T ≥ H4BP	1	0	0	1	0	0	1	0	1	0	1
	1	1	0	1	1	0	1	0	1	0	1
T < H4BP	1	1	0	1	1	0	1	0	1	0	1
	1	1	0	1	1	0	1	0	1	0	1

LHBP - Low Heat Balance Point
HHBP - High Heat Balance Point
H1BP - Aux. Ht. 1 Balance Point
H2BP - Aux. Ht. 2 Balance Point
H3BP - Aux. Ht. 3 Balance Point
H4BP - Aux. Ht. 4 Balance Point

INFORMATION ON THIS PAGE SUBJECT TO
PATENT STATUS CLAUSE ON PAGE i.

Table 3.4-2

Relay State Matrix for Cooling Mode

Outdoor Ambient	Thermostat		Low Comp.	High Comp.	Low Fan	Hi Fan	Low Blower	High Blower
	C1	C1 + ΔTime						
Below	1	0	1	0	1	0	0	1
LCSP	1	1	0	1	0	1	0	1
LCSP ≤ T ≤	1	0	1	0	0	1	0	1
HCSP	1	1	0	1	0	1	0	1
T > HCSP	1	0	0	1	0	1	0	1
	1	1	0	1	0	1	0	1

LCSP = LCBP - ΔT1 = Low Cool Balance Point - ΔT1

HCSP = HCBP - ΔT2 = High Cool Balance Point - ΔT2

ΔT_1, ΔT_2 = Temperature Offsets

controller. This switch will disable the compressor and the fan. The blower is locked into high speed. Emergency heat is also enabled if the microprocessor board fails. This also guarantees house heating even if the heat pump fails.

Defrost

Defrosting of the outdoor coil is initiated in one of two ways. The primary method is defrost on demand. The secondary method depends upon cumulative compressor running time. A defrost cycle lasts until either a set of temperature conditions is met or a defrost timer runs out.

The defrost initiation demand signal is the temperature difference between the refrigerant leaving the outdoor coil and the outdoor ambient. When this difference exceeds a limit, which is itself a function at the outdoor ambient temperature, a defrost cycle is started. A defrost cycle may also be started by the cumulative compressor running-time timer. This timer is set at zero at the end of every defrost cycle and is actuated only while the compressor is running. If the timer exceeds a limit, which is also a function of outdoor ambient temperature, a defrost cycle is initiated.

Defrost is terminated when one of two conditions is met. First, a defrost cycle is terminated if both the temperature and the rate of temperature rise of the refrigerant leaving the outdoor coil are above preset setpoints. Second, defrost is terminated regardless of temperature conditions by a defrost elapsed time timer, which limits any defrost cycle to a specified elapsed time interval.

The overall efficiency of the heat pump is increased by making both defrost initiation and termination a demand process. The heat pump should spend a minimal amount of time in the defrosting state, since a defrost cycle is only started when it is needed and is halted as soon as it has finished defrosting the coil.

Expansion Device Control

The use of an electric expansion valve coupled to a microprocessor control system offers several important advantages over conventional flow control devices such as capillary tubes:

- o Optimum subcooling or superheat over the entire operating range
- o Minimum flow restriction during defrost
- o Potentially high reliability
- o Bidirectional flow

The conventional subcool control valve as used by Westinghouse in the Hi-Re-Li system maintains nearly constant subcooling in the condenser over the entire operating range. Based upon previous work, the optimum condenser subcooling in the heating mode for a system using a dual compressor is shown in Figure 3.4-5. The optimum subcooling (the subcooling which maximizes COP above the balance point and maximizes capacity below the balance point) is a strong function of ambient temperature, and in the high capacity mode is significantly different from that in the low capacity mode.

The refrigerant flow control system or expansion device that we have adopted uses the Westinghouse Hi-Re-Li condenser subcooling control scheme for heating and evaporator superheat control during cooling.

During defrost, conventional flow control devices severely restrict refrigerant flow, increasing the time required for defrost unless a bypass flow path is provided. An electric expansion valve can be opened fully during defrost, reducing the defrost time and improving cyclic efficiency, provided its response time is adequate, thereby eliminating the need for a bypass.

The controller controls the amount of evaporator superheat in the cooling mode and the amount of condenser subcooling during the heating mode through manipulation of the expansion valve. The temperature difference between the refrigerant exiting the coil and a measure of saturation temperature is compared to setpoint. This

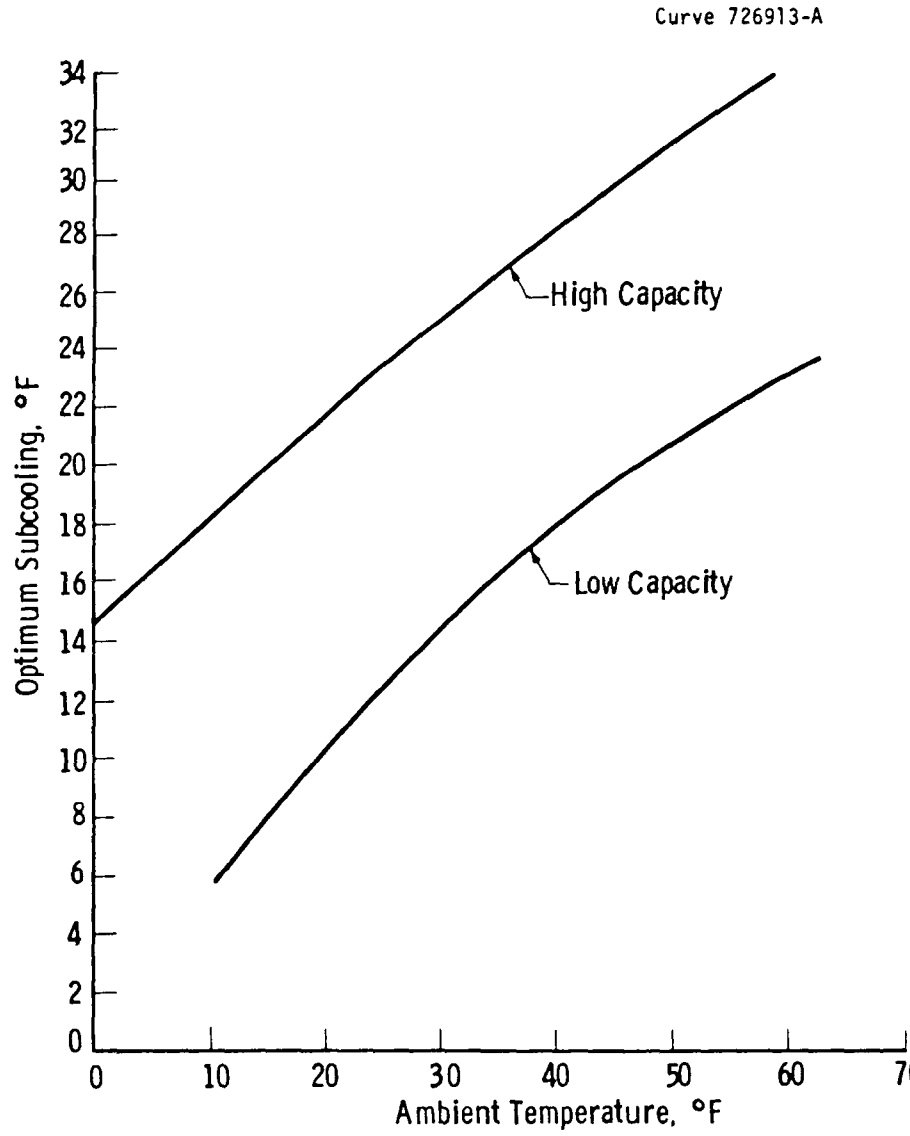

Figure 3.4-5 - Optimum subcooling versus ambient temperature for a dual-compressor heat pump in the heating mode

setpoint can be a function of the outdoor ambient temperature. This comparison yields an error signal which is fed back to the expansion valve through a transfer function. This closed-loop feedback is used to maximize either efficiency or capacity, as determined by the heat pump operating mode and ambient conditions.

Further, upon initiation of defrost, the expansion device is driven fully open to decrease defrost time.

Fault Monitoring

One of the important functions of the controller is that of monitoring the heat pump system for conditions that would cause damage. Fault determination can be reduced to the problem of sensing the thermodynamic and fluid-mechanical observables in the operating heat pump system, comparing them to their normal values which are functions of the ambient temperature and the space temperature, comparing the identity and sign of the departures to a truth table, then displaying the class or identity of the fault indicated by an "All True" match.

The practical observables are these:

1. Refrigerant volume flow
2. High side pressure and temperature (compressor discharge)
3. Suction pressure and temperature (compressor inlet)
4. Evaporator outlet pressure and temperature
5. Condenser outlet liquid pressure and temperature
6. Compressor power and current
7. Indoor and outdoor air flows and temperatures
8. Supply and return air temperatures
9. Ambient air temperature (redundant to 7)

A normal value for the observable must be available as a non-linear function of the ambient temperature, the space temperature, and additionally, in cooling mode, the space humidity.

Table 3.4-3 displays the relationship between some direct system faults and the observable symptoms while Table 3.4-4 gives notes concerning these faults. Further elucidation is provided in the literature.*

Clearly the generation or calculation of normal values for the nine observables listed plus the measurement of their actual values is a formidable and expensive undertaking. The first level of compromise or simplification involves an examination and evaluation of this list of practical observables to reduce the number of observables to the absolute minimum.

Pressure measurement is expensive in terms of system and transducer cost. It requires a reliable, hermetic penetration of the system plus a pressure transducer. Refrigerant flow measurement requires a pressure drop such as through an orifice, plus a ΔP measurement or a velocity or momentum transducer, plus in most cases one or more reliable hermetic penetrations. Temperature via the thermistor or the like semiconductor device is cheaper and does not necessarily require a penetration. Pressures may be inferred from a saturated temperature measurement, but this requires application of the temperature transducer to a region in which the two phases are surely present with sufficient vapor throughflow to insure low noncondensible partial pressure. In fact, given a true measure of saturation temperature, pressure measurement may not be necessary for any of the symptom comparisons needed for fault identification and perhaps should be avoided.

The next compromise level is that of reducing the demand upon mechanization of fault identification and transferring more burden to

---

*Mueller, Dale A., Bonne, Ulrich, "Heat Pump Control Solutions Using Advanced Microelectronic Technology," ASHRAE Transactions, 1980, V 86, Part 2.

Table 3.4-3

Fault vs. Symptom

DIRECT SYSTEM FAULT	Refrig. Flow	Comp. Power	Comp. Current	Suction Pressure	Suction Temp.	Suction Sup.Heat	Disch. Pressure	Disch. Temp.	Cond. Subcool	Accum. Level	Heating Supply Air Temp.	Auxil. Heat	Power Factor	Coil Air ΔP
Compressor														
Defective Valve	L to O	L	L	H	N	N	L	H	L to O	N	L	H	L	N
Lubrication Defective	N	H	H	N	N	N	N	H	N	N	N	N	N	N
Mechanical Failure	O	O&H	O&H	L	N	O	L	L	O	N	L	H	L	N
Capacitor Short	N	N	H	N	N	N	N	N	N	N	N	N	L	N
Capacitor Open	N	N	N?	N	N	N	N	N	N	N	N	N	L	N
Condenser														
Zero Air Flow (Fan Fault)	N	H	H	N	N	N	H	H	L	H	?	?	N	O
Low Air Flow	N	H	H	N	N	N	H	H	L	N	H	N	N	H
Dirty Coil or Filter														
Evaporator														
Zero Air Flow (Fan Fault)	L	L	L	L	N	N	L	N	H	H	L	H	L	O
Low Air Flow (Dirty or Frosted Coil)	L	L	L	L	N	N	L	N	H	H	L	H	L	H
Ref. Flow Control														
Capillary														
Restricted	L	L	L	L	H	H	H	N	H	L	L	H	N	N
Low System Charge	L	L	L	L	H	H	L	N	L to O	L to O	L	H	L	N
TX Valve														
Low Bulb Charge	L	L	L	L	H	H	H	N	H	L	L	H	N	N
Low System Charge	L	L	L	L	H	H	L	N	L to O	L to O	L	H	L	N
SC Valve														
Low Bulb Charge	N	L	L	N	H	N to H	L	L	L to O	N	L	H	N	N
Low System Charge	L	L	L	L	H	H	L	N	L to O	L to O	L	H	L	N
Four-Way Valve														
Bypassing	N	L	L	N	H	N to H	L	H	L to O	N	L	H	N	N
Heating-Stuck in Cooling	H	H	H	H	N	N	L	L	H	L	L	H	N	N
Cooling-Stuck in Heating	N	N	N	N	N	N	N	H	N	N	H	O	N	N

Key: L = low, H = high, N = normal, O = zero

Table 3.4-4

Fault vs. Notes

DIRECT SYSTEM FAULT	NOTES/BACKGROUND
Compressor	
Defective Valve	If flow present, discharge temperature peaks. Motor overloads and stops may recur. Discharge valves most vulnerable.
Lubrication Defective	Situation may develop to overload, damage, stops, lock-up due to bearing, ring and piston-cylinder destruction.
Mechanical Failure	Significant mechanical failure locks compressor - overload opens line. Motor current peaks on restart attempts, then zeroes.
Capacitor Short	Motor starts as resistance-split phase; runs as badly balanced quarter-phase.
Capacitor Open	Compressor will not start. Once-stopped same as "Mechanical Failure".
Condenser	
Zero Air Flow (Fan Fault)	Excess pressure protection will operate, followed by motor over temperature. Long off, short on cycling of compressor.
Low Air Flow	Extreme approaches Zero Air Flow list.
Dirty Coil or Filter	
Evaporator	
Zero Air Flow (Fan Fault)	Fan faults usally electrical failure and/or bearing failure. Cycling as below is probable.
Low Air Flow (Dirty or Frosted Coil)	At extreme may produce long off-short on cycling of motor protection.
Ref. Flow Control	
Capillary	
Restricted	Commonly deposits from solution, manufacturing dirt, mechanical damage.
Low System Charge	Leaks, mechanical joints (field) or "Schrader" valve caps.
TX Valve	
Low Bulb Charge	Symptoms depend in magnitude on size of valve bypass. Valve closes.
Low System Charge	Same as "Capillary."
SC Valve	
Low Bulb Charge	Valve open
Low System Charge	Valve closed
Four-Way Valve	
Bypassing	Symptoms very quantitative-minimum small capacity loss.
Heating-Stuck in Cooling	House symptoms not obvious due to Auxiliary Heat.
Cooling-Stuck in Heating	No defrost made; develops zero condenser air flow symptoms on return to heating, short cycles in defrost due to stopped outdoor fan. System symptoms in cooling made unimportant due to obvious reversed capacity.

the service-person. This amounts to requiring of the fault system only that it identify areas of fault, leaving to the service person identification of the specific nature of the fault. Table 3.4-5 illustrates this approach. It is capable of using only three observable (of five) departures from "normal" to identify one out of five significant fault areas. The service person (perhaps the owner) completes the diagnosis; he sees for example that low air flow = dirty filter.

Our breadboard controller monitors the system for the following faults:

Sensor out of range
Compressor failure to start
Loss of airflow, both indoor and outdoor
Loss of refrigerant charge
Reversing valve failure
Excessive crankcase temperature
High discharge pressure
Low suction pressure
High discharge temperature.

These faults are detected either directly, such as with a sensor out of range, or indirectly, such as with a loss of charge which is detected by a rise in compressor discharge temperature above a limit coupled with low suction pressure.

The controller reacts to a fault by shutting down the system, except for auxiliary heat and indoor blower, and displaying a fault code. This code indicates what caused the controller to halt operation. The heat pump must be manually reset.

The controller monitors itself by the use of a deadman circuit. If this circuit detects that the microprocessor or support circuitry has

Table 3.4-5

Simplified Heat Pump Diagnostics

Fault Classes Intermediate Causes	Suction Pressure	Discharge Pressure	Suction Sup. Heat	Liquid Subcool	Aux. Heat	Compressor Discharge Temperature	Component Attention
Low Condenser Air Flow	N	H	H	L	H	H	Fouled Coil, Filter, Fan Fault
Low Evaporator Air Flow	L	L	N	N	H	L	Same as above
Over-Restricted Liquid	L	H	H	H	H	H	Internal fouling, capillary damage lost TXV charge
Under-Restricted Liquid	N	L	N	L	H	L	Lost SCV charge, stuck 4-way valve
Refrigerant Undercharge	L	L	H	L	H	H	Leaks, field joints, Schrader valves

Key

H: High
L: Low
N: Normal

failed, it disables the controller, compressor, fans, etc. It also enables the auxiliary heat and blower to provide heat, if it is needed.

All motors are self-protected through internal thermal limit switches.

3.4.3 Summary

A control system has been developed to operate in conjunction with the advanced electric heat pump hardware. The two main products of this effort are: 1) development of design specifications for the control system hardware, and 2) construction and demonstration of two developmental or breadboard control systems. The resulting microprocessor-based control system manages the two-capacity heat pump system in response to wall thermostat signals, outdoor ambient temperature, and heat pump operating parameters. Heat pump capacity and auxiliary heat are controlled to yield greatest system efficiency within restrictions on comfort and safety.

Design specifications for the control system include not only specification of control functions to meet the load conditions, but also specifications for sensors (temperature and pressure) and interlock functions to guarantee safe system operation, detection and identification of anomalies and faults in the heat pump system, and design of the output relay system. The control functions include control of heating and cooling modes of operation, compressor capacity, outdoor fan, multispeed indoor blower, four stages of auxiliary heat, subcool and superheat control, and defrost initiation and termination. The interlock functions include software (microprocessor program) and output relay interlocks to prevent damage to the compressor and blower motors. Detection of faults and anomalies includes high and low refrigerant pressure faults, reversing valve failure, loss of refrigerant, loss of indoor or outdoor air flow, and several others. Nuisance trips due to short duration transient conditions are minimized by incorporating in the software permissable time intervals for which nominal parameter

values can be exceeded with ultimate protection provided by "not to exceed" parameter values. The formulation of these design specifications was in response to analysis of system performance requirements and operating data gathered in tests of the breadboard heat pump system.

The construction and testing of breadboard control circuiting was performed using sets of readily available microprocessor-based controller hardware modified to meet the requirements of this program. This hardware has many capabilities and features (e.g., local display of parameters and the ability to readily change setpoints) which will not be required on production control circuiting. However, these capabilities were useful in developing the final control specifications. Another development tool that was used to develop and test control functions was a Hewlett-Packard HP9825A programmable calculator. Testing and verification of the control software was performed on operating heat pump hardware using this calculator, and also with a test box simulating control and feedback signals to the controller.

At completion of the advanced heat pump program, two microprocessor control systems in a breadboard format will have been constructed.

3.5 Heat Pump Package Design and Development

The design for the heat pump package defines the configuration or shape of the constitutive, packaged elements, the number of individually packaged elements, and the arrangement of parts within each packaged element.

The package design for light commercial applications will continue to be the roof-top-mountable unitary or single-package system. Since our market study indicates that this segment of the market is and will continue to be small and will not lead the drive for higher efficiency, light commercial units were excluded from our detailed design and development effort.

We have considered in great detail alternative package designs for residential heat pump systems. The unitary or single-package heat pump will continue to be an insignificant factor in the residential heat pump market for a variety of reasons. The split-system residential heat pump, wherein the indoor and outdoor elements are separately housed and joined only by refrigerant and electrical lines, will continue to be dominant in the residential sector and is therefore the focus of our effort.

In previous work done for the Electric Power Research Institute[1], Westinghouse advocated the placement of the refrigerant compressor indoors, and therefore not contained within the heat pump outdoor unit. The Carrier Corporation, now a division of United Technologies Corporation, has introduced such a unit with the compressor housed within its own box and thus mountable with great flexibility within the dwelling's interior. Upon reexamining the merits and risks associated with indoor compressor placement, Westinghouse still asserts that indoor compressor placement is to be preferred. All of the package designs that we have considered therefore require that the compressor not be part of the outdoor unit. We do, however, find merit in designs that can accommodate the compressor either indoors or outdoors.

We require that the outdoor air mover be of a high-efficiency design as described in Section 3.3.1. High-efficiency axial-flow air movers require a rounded inlet flare, a close fitting running ring, and a diffuser stack. It is assumed that this air mover will be a sub-assembly that is mated with the outdoor package at assembly. It is

---

1. H. S. Kirschbaum and S. E. Veyo, "An Investigation of Methods to Improve Heat Pump Performance and Reliability in a Northern Climate," EM319 (Research Project 544-1), Electric Power Research Institute, Palo Alto, CA, January 1977.

further assumed that the air-mover subassembly be placed to ensure adequate air flow without flow reversal or pathway blockage.

We require that the path for defrost melt be unobstructed by coil mounting or support hardware in order to prevent coil and unit damage through ice buildup.

We require that the indoor air mover also be of high-efficiency design as described in Section 3.3.2. The size of the indoor blower assembly is approximately twice that of the conventionally used squirrel cage blower.

We require that the control system be microprocessor-based and that all relays, contactors, circuit boards, transformers, and capacitors be mounted as part of the heat pump indoor unit.

We require that the electrical hookup be at a single point, i.e., power is supplied to the system at just one place.

A description of our selected package, our rating procedure, and details of the alternatives that we considered follows.

3.5.1 Outdoor Unit Package Design and Development

Introduction

The main components which make up the outdoor unit are a heat exchange coil with associated headers and fittings, a high-efficiency fan package, and a sheet metal structure. There is no requirement to incorporate a compressor since this item is to be installed with the indoor unit. The objective of this effort was to achieve the optimum arrangement or packaging of fan and heat exchanger surface within a sheet metal housing that was aesthetically pleasing and viable from a cost viewpoint. The optimum arrangement is defined here as that arrangement which best satisfies the combined requirements of performance, manufacturability, maintainability, and marketability.

The Selected Advanced Heat Pump Outdoor Unit Design

The unit illustrated by Figure 3.5-1 had the highest figure of merit among the 27 designs conceived and evaluated. The heat exchanger coil is formed from four slabs, each tilted at 22 degrees to the vertical and arranged to form a "W." Mechanical details of the slab sections are listed in Table 3.5-1. Air is drawn into the two center slabs of the "W" through the gap formed between the base of the unit and the ground on all four sides. The height of this gap is controlled by the support legs which are adjustable to give a minimum of 7 inches and a maximum of 24 inches ground clearance. Additional air to the outside slabs of the "W" is drawn through a screened or louvered panel wich makes up the lower half of the unit side panel. Notice that the coil slabs are well protected from fin damage in shipment and during service.

The facility to raise the unit up to 2 feet off the ground without the use of a separate support frame is judged to be a valuable and unique feature. Great benefit is accrued in locations where heavy snowfalls are experienced. This feature is achieved by providing four long legs which are free to slide in channels formed by the bent sheet metal of the unit end plates. Locking is by a screw through the end plate. Additional benefits of this feature are that the unit can easily accommodate very uneven terrain, and the legs can be retracted completely for compactness when shipping.

From the coil the air is drawn upward through the fan package to discharge vertically. The fan subassembly is a basically rounded entrance, circular duct flared at its exit, into which a high-efficiency propellor fan, fan motor, and stator vane row are inserted and supported. The air exhaust end is covered with a wire-form grille. Two fan subassembly designs can be accommodated, one by Westinghouse, the other by Torin. Both are nominally 12 inches high and 24 inches in diameter. Mounting is achieved by dropping the fan subassembly, which has an externally protruding flange at its discharge plane, into a suitable hole in the top of the outdoor unit housing.

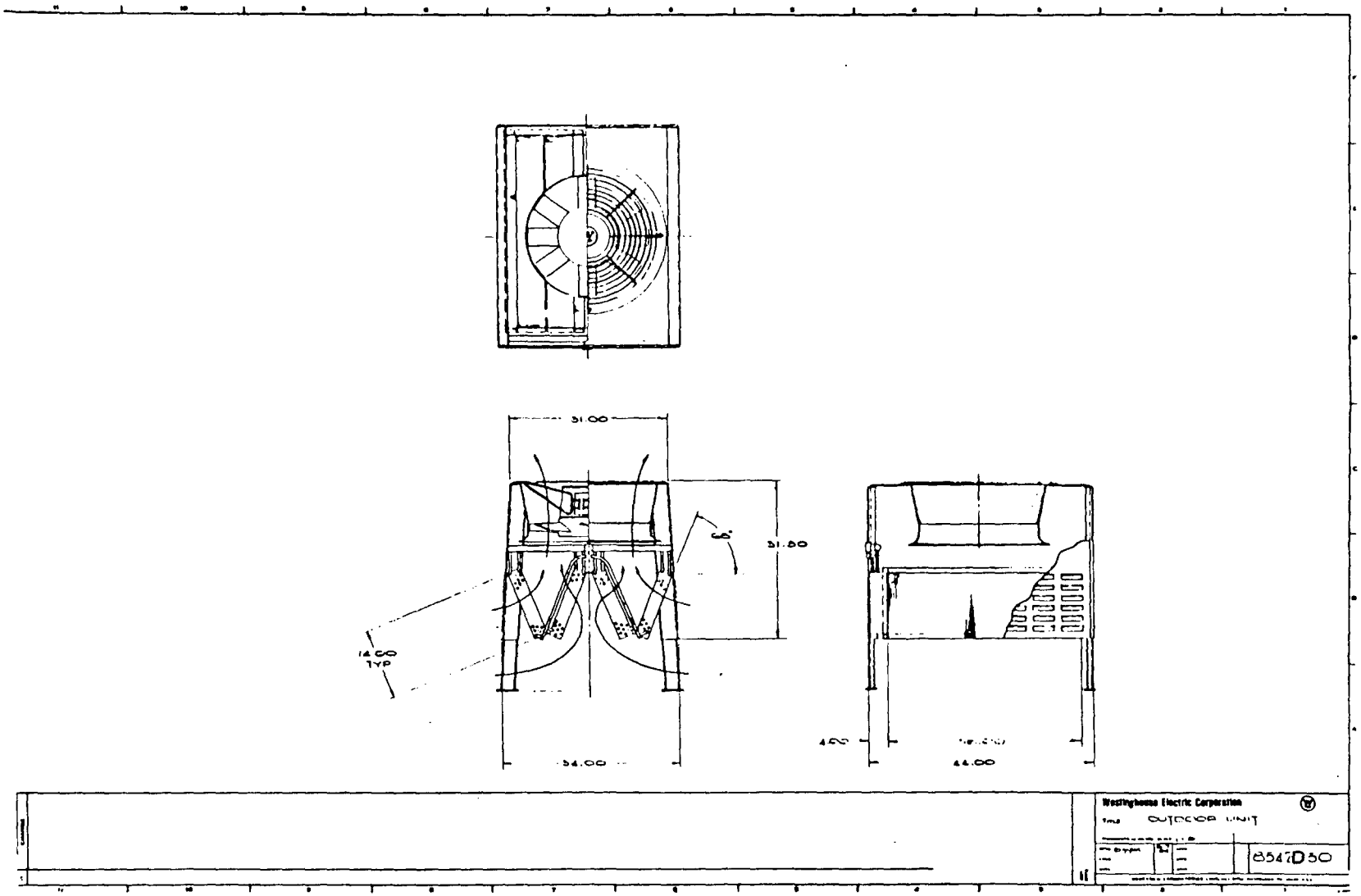

Figure 3.5-1 - The preferred outdoor package design "A"

Table 3.5-1

Details of Slab Coils for Outdoor Unit

Tube material	Copper
Tube diameter/wall thickness	0.375/0.017 inch
Tube length between end plates	38 inches
Number of tubes	42
Number of tube rows	3
Transverse/longitudinal pitch	1 /0.867 inch
Coil height	14 inches
Fin material	Aluminum
Fins per inch/thickness	13 /0.0045 inch
Ripples per pitch/ripple height	2 /0.046 inch
Number of such slabs to make coil	4

The housing for the outdoor unit consists of two trapezoidal-shaped end plates, and an upside down trapezoidal "U" shaped wrapper, all of galvanized sheet metal plus two grille panels, plated for corrosion resistance. Four channel-shaped galvanized sheet metal legs fit into long sockets formed as an integral part of the end sheets. The legs are fully inserted for shipping and can be extended as much as 24 inches at installation.

During manufacture, the "W" shaped coil is prepared as a leak-tested subassembly, and subsequently attached to the housing end plates with sheet metal screws. The legs are prestowed in their sockets. The wrapper is then snapped into place and attached with screws to the end plates. The two grille panels are then attached. The prechecked air mover subassembly is then dropped into place and secured and terminals wired. Final inspection is the last operation before insertion into the shipping carton.

All services, refrigerant lines and electrical service are accessed at one end plate.

The overall unit dimensions with legs extended 7-1/2 inches is 39 inches high, 34 inches wide at the base, and 44 inches long.

An isometric sketch of the preprototype outdoor section is shown in Figure 3.5-2, while Figures 3.5-3 and -4 present photographs of the assembled preprototype unit.

Analysis

The first step toward a satisfactory package design was the identification of important features upon which a design might be judged. These features could be grouped into four major categories: performance, manufacturing cost, marketability, and maintainability and handling. In all, twenty-four features were identified and are listed below. Under the performance category, we considered the following features:

Airside ΔP	Low airside ΔP reduces fan horsepower. This consideration favored coil designs with fewest tube rows and highest face area. For an equal number of rows, a slab coil where the fin is continuous was preferred over a bent coil formed from a number of single row coils and thus having a discontinuous surface.
Refrigerant ΔP	Low refrigerant pressure drop reduces power required to circulate the refrigerant and, for given indoor and outdoor temperature, increases Carnot COP. Thermosiphon coils were preferred since they use a large number of parallel flow paths.
Even Coil Loading	This was desirable for the most effective use of the coil. A fairly uniform distance between fan and coil over the entire coil surface was aimed for.
Susceptibility to Icing	Low susceptibility preserves performance during freezing rain conditions. A unit where the coil surface is protected from rainfall was preferred.

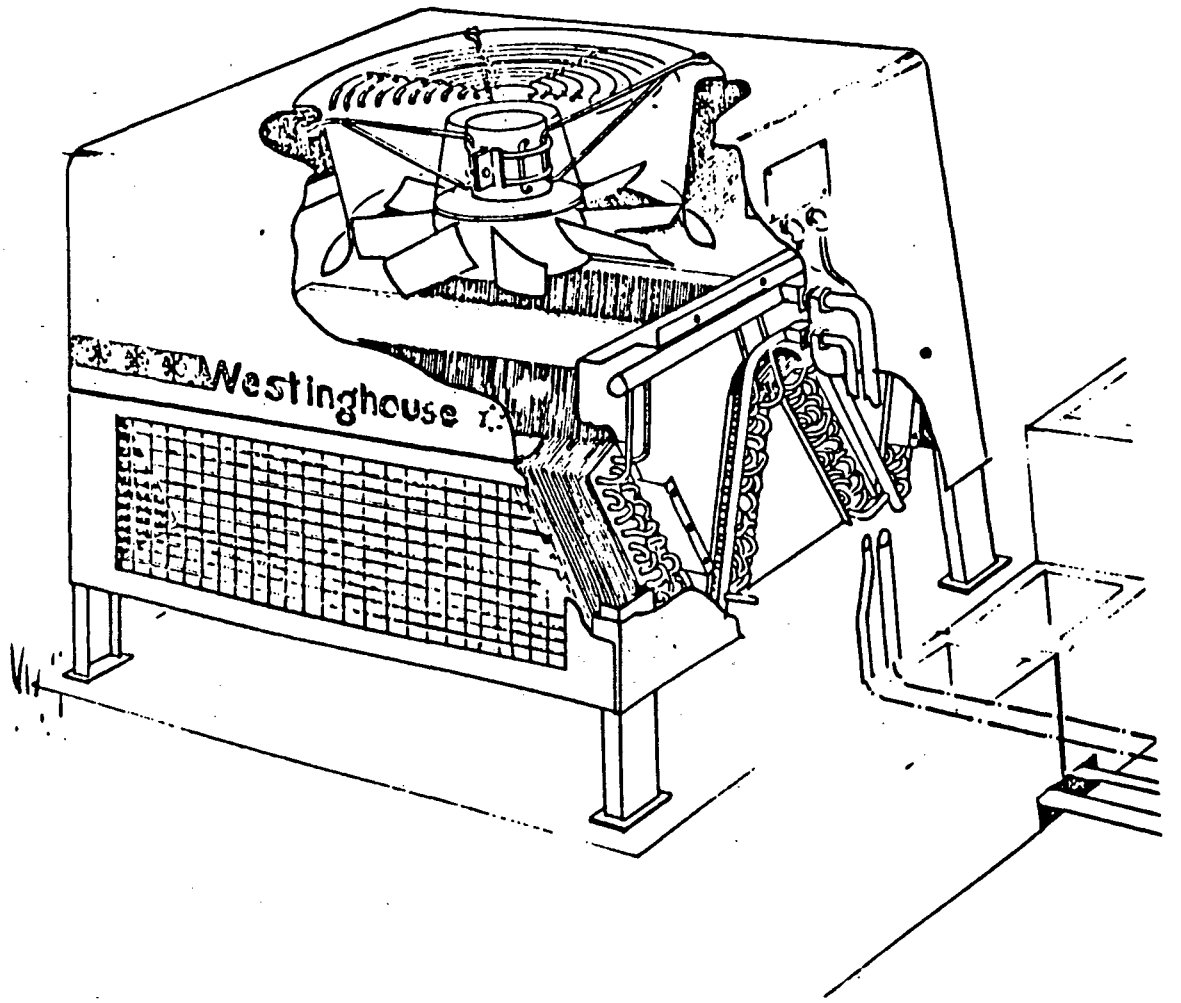

Figure 3.5-2 - Isometric sketch of preferred outdoor unit

INFORMATION ON THIS PAGE SUBJECT TO
PATENT STATUS CLAUSE ON PAGE i.

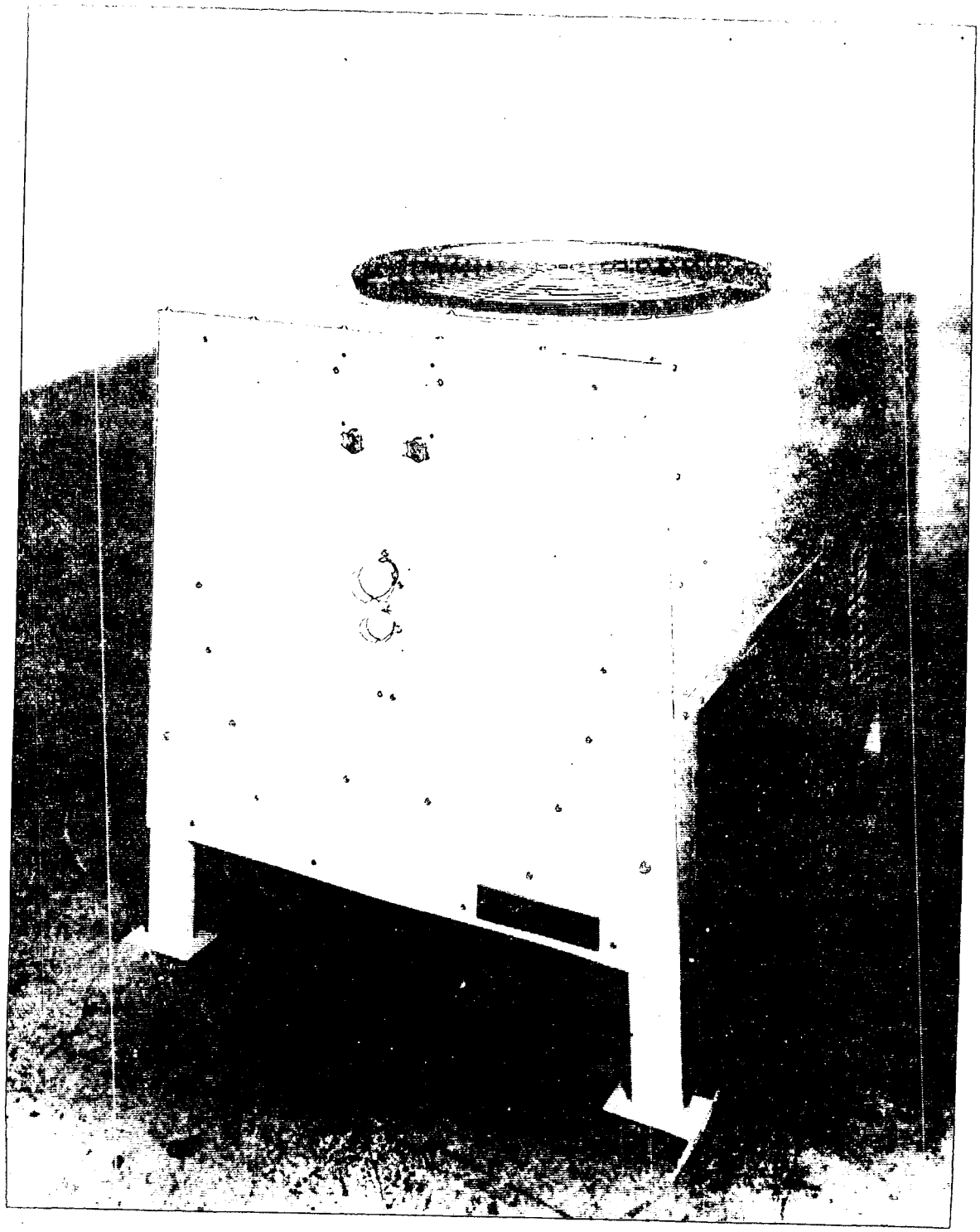

Figure 3.5-3 - End view photograph of outdoor unit in low mount position

INFORMATION ON THIS PAGE SUBJECT
TO PATENT STATUS CLAUSE ON PAGE i.

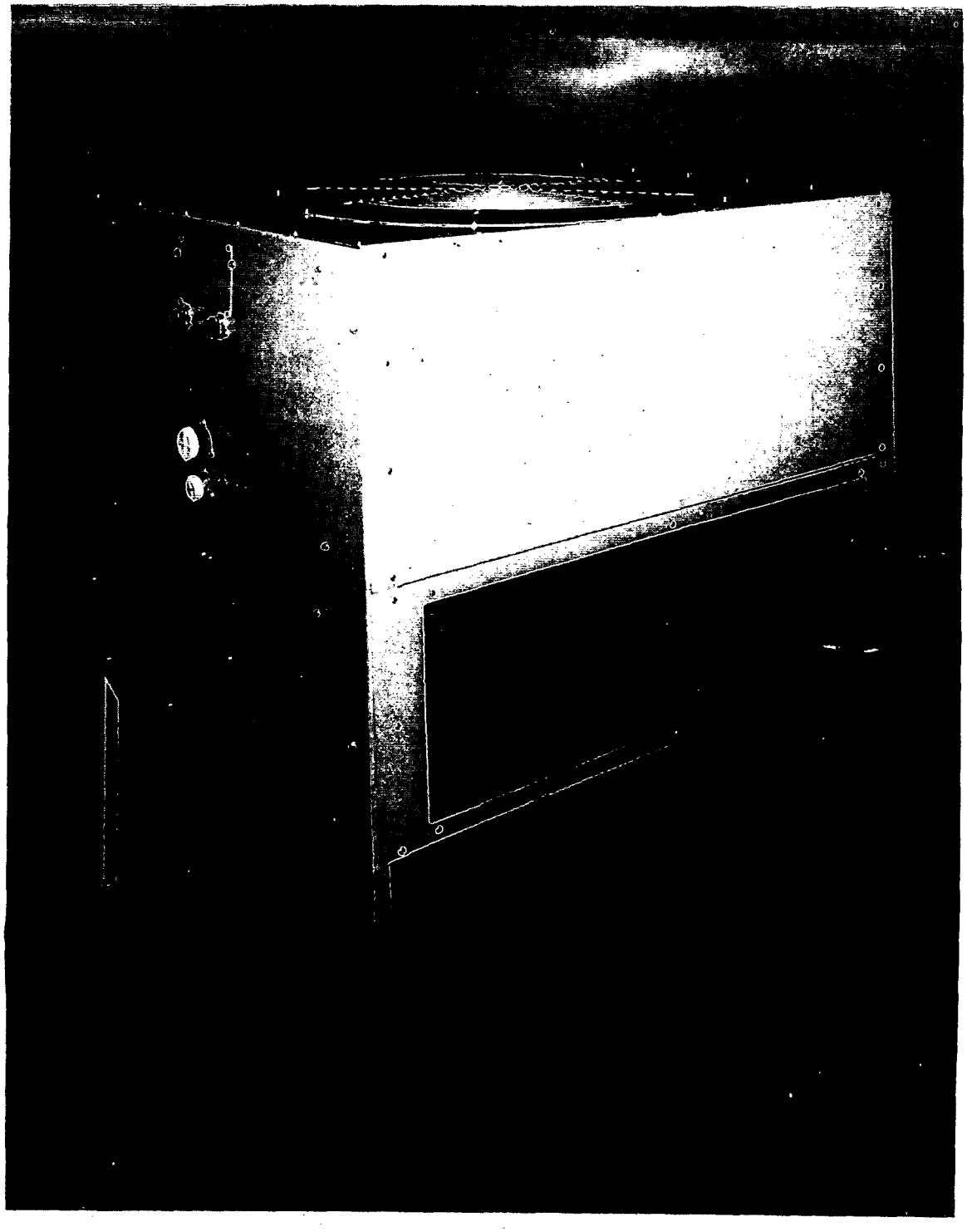

Figure 3.5-4 - Side view photograph of outdoor unit in high mount position

Susceptibility to Snow Blockage	Low susceptibility preserves performance during heavy or drifting snow conditions. Lifting the coil away from the ground, discharging air through the coil, and guarding the coil with sheetmetal were effective means of improving performance here.
Susceptibility to Debris Accumulation	Low susceptibility would preserve performance in the Fall when heavy leaf accumulation occurs. Means of avoiding blockage were the same as those for avoiding snow blockage.
Susceptibility to Air Recirculation	Low recirculation is required to maintain good thermo-dynamic performance. This was achievable by placing the air ingestion areas as far as possible from the air discharge area and by forcing the air to turn through the maximum possible angle before being reingested. Since heating performance was stressed, designs where the discharge was below the intake were favored.
Drainage of Defrost Melt	Excellent drainage was required so that the melt does not refreeze on the coil upon termination of defrost. Refreezing would lead to coil damage, possibly even failure. A requirement was for the plane of the fins to be vertical. The fin density of 13 per inch, common to all designs evaluated, was considered satisfactory. Designs with short coil height were preferable.
Noise	Low noise level is required from an owner comfort viewpoint. Given identical fan package designs, units where the fan is mounted in the horizontal plane performed better than those with the fan mounted in the vertical plane. Enclosing the fan within the sheet metal was seen as an advantage and,

	where the common top mounting of the fan was employed, tall units were better than short units.
Flexibility of Placement	The major consideration here is the ability of the design to function well in the event that the unit is placed against a wall. Designs where the air is discharged or ingested on all four sides were at a disadvantage.
Compatibility with Outdoor Compressor Placement	Although there was no intent to house the compressor within the outdoor unit, the ability of a design to accept a compressor is seen as an advantage. This stemmed from the notion that where the product line included cooling-only units, the outdoor unit would accept the compressor for those units.
Compatibility with a Unitary Design Concept	Although the outdoor package of this study is an isolated module for a split-system heat pump, the ability of the design to be united with the indoor unit is seen as an advantage. Designs where the air is drawn in or discharged on all sides could not be readily adapted.

Under the manufacturing category, we considered the following features:

Coil Fabrication Cost	Experience indicated that a unit utilizing a single slab coil would involve the least coil cost, and one utilizing a multiplicity of smaller slab coils would be only marginally more expensive. Coils of bent form, utilizing a number of single-row coils, are more expensive.
Tube Header Fabrication Cost	It is clear that a unit utilizing a single forced convection coil would involve the least cost. Whether the coil is slab or bent is not a factor. Cost was expected to increase with the

	number of coil elements and would be boosted significantly in the case of thermosiphon designs.
Sheet metal Cost	A simple shape requiring a minimum number of special forming tools is clearly advantageous.
Fan Package Cost	Although all of the designs considered in this study utilize the same fan package, this feature is included so the differently weighted score for overall features between one design and another can be seen in proper perspective relative to the absolute scores.

Under the marketability category, the following features were considered:

Package Height	A height between 30 and 40 inches is considered ideal. Units in this height range have achieved excellent market acceptance. Significantly lower units might suffer abuse by being sat or stood upon and objects might more readily fall or be thrust into the fan package. Much taller units would have aggravated shipping problems and would be subject to location limitations and possible mounting instability.
Package Width and Depth	For both of these dimensions a value not exceeding 30 inches is considered ideal. A value above 60 inches is unacceptable, and the degree of acceptance is taken to be in proportion to where the actual value falls between 30 and 60 inches.
Aesthetics	A pleasing appearance is expected to be an important selling pont. Such considerations as psychologically pleasant aspect ratio (about $\sqrt{2}$ to 1) and the absence of large unbroken surfaces were factors here.

Uniqueness	Uniqueness of appearance and concept is judged to be an asset, inasmuch as it endows a special identity and sets the design apart from its competition.

Under the maintainability and handling category, the following features were considered:

Access to Fan and Motor	As the only item containing moving parts and having electrical connections, the fan package should be easily accessible. Very tall units and units where the fan is concealed by sheet metal suffer in comparison to units of modest height where the fan package is exposed.
Protection from Fin Damage	Severely distressed fins could cause enough blockage to air flow so that performance would suffer. Designs where the fins are protected by sheetmetal would suffer less damage during handling and in service and thus score over designs where the coil is exposed.
Weight	The criterion here is the degree of ease with which one man can maneuver the unit into place above the location surface. It was required that two men should be capable of unloading the unit from a truck without the aid of lifting devices.

Clearly, the features varied in importance; therefore, a measure of weighting was assigned to each.

The second step in the packing study was weighting design features for degree of importance. First, an overall weight was assigned to each of the major categories under which the twenty-four design features were grouped, namely performance, manufacturing cost, marketability, and maintainability and handling.

Performance was seen to be first in importance. A poor level of performance would be rejected by an increasingly sophisticated buying public. Manufacturing cost was seen to be second in importance. The price at which a unit of given performance would secure a good fraction of the market would be largely dictated by what alternatives existed within the marketplace. Against this limitation, a competitive manufacturing cost was required to bring an adequate return to the manufacturer.

Marketability was placed third in importance. It was arguable that good performance and competitive pricing are the most marketable features, but these were given separate coverage here. Under this heading were those other features that would assist in achieving penetration. Maintainability and handling was placed fourth in importance. This placing was due largely to the relatively low level of mechanical complexity of the outdoor unit. The overall weight given to the four categories was as follows: Performance - 40, Manufacturing Cost - 35, Marketability - 20, and Maintainability and Handling - 15. The relative size of the weighting number reflects the degree of importance placed upon each category. The absolute size of the numbers was selected so that each could be divided between the features which make up the categories. In this way, a prioritization of the features within each category was possible. For example, within the performance category, drainage of defrost melt was considered more important than compatibility with a unitary design concept. The former feature was thus allocated 5 points of the 40 points within the performance category, while the latter was allocated only 2 points.

Each of the twenty-seven designs produced for this study was given a score from 0 to 10 on each of the twenty-four design features listed and weighted for relative importance in Table 3.5-2. For each design, the sum of the products of design feature weight and design score was taken for all design features to yield an overall figure of merit for the design. A rational basis for ranking the designs was thus obtained. The highest ranking design was selected for the prototype built. It attained a score of 894 out of a possible 1100 points.

Table 3.5-2

Prioritization of Design Features by Weight Assignment

Category	Design Feature	Weight
Performance (40 points)	Airside ΔP	4
	Refrigerant ΔP	3
	Even Coil Loading	3
	Susceptibility to Icing	3
	Susceptibility to Snow Blockage	2
	Susceptibility to Debris Accumulation	3
	Susceptibility to Air Recirculation	5
	Drainage of Defrost Melt	5
	Noise	5
	Flexibility of Placement	2
	Compatibility with Outdoor Compressor	3
	Compatibility with Unitary Design Concept	2
Manufacturing Cost (35 points)	Coil Fabrication Cost	10
	Tube Header Fabrication Cost	10
	Sheet Metal Fabrication Cost	5
	Fan Package Fabrication Cost	10
Marketability (20 points)	Package Height	5
	Package Width	3
	Package Depth	3
	Aesthetics	5
	Uniqueness	4
Maintainability and Handling (15 points)	Access to Fan and Motor	6
	Protection from Fin Damge	5
	Weight of Unit	4
	Total	110

Table 3.5-3 constitutes the complete rating table for all twenty-seven designs.

Description of the Design Alternatives

Based on preliminary information derived from the heat pump optimization program, the product of the number of tube rows and total coil face area was required to be 40 row ft^2. The same tube and fin materials and geometry were used for all coils.

All of the designs were capable of incorporating the same high-efficiency fan package.

There was no requirement to house the compressor within the package, although where a compressor could be located within the package the rating system awarded a small credit on the grounds that tooling could also be used on cooling-only units.

With regard to refrigerant flow, the design fell into two basic categories. The conventional forced convection mode was used on twenty-one of the twenty-seven designs. The remaining six designs utilized a coil design which functioned as a boiling thermosiphon during the heating mode. The thermosiphon yielded low refrigerant pressure drop at the expense of costly tube header fabrication. Eleven of the designs used slab coils with one, two, or four slab sections and with three, four, or five tube rows. The remaining sixteen designs utilized coils which required some sort of bend. Bending varied from a single short-radius 90 degree bend to form an "L" shape through two short-radius 90 degree bends to form a "U" shape, and a long radius 180 degree bend to form a "C" shape to a long radius 270 degree bend to form a horse-collar shape. Bent coils were of two and three rows.

Only three of the designs used the fan package mounted in the vertical plane, while twenty-four designs had the fan in the horizontal plane. Seven examples ingested air through the fan and discharged through the coil, and twenty examples ingested air through the coil and discharged through the fan. Discharge air was downward in four cases, horizontal in seven cases, and vertically upward in sixteen cases.

Table 3.5-3

Outdoor Unit Rating Chart

DWG. 5598C51

n	Catagory	Weight I (1 to 10)	2D50	0D20	4C26	4C24	1D60	4C30	4C31	4C56	4C54	4C42	0D18	0D16	0D08	0D07	9D60	9D82	9D87	0D48	0D63	0D64	1D46	0D66	1D40	1D45	1D58	1D27	1D69
			Design Dwg. Number																										
			Score j (0 to 10)																										
	Performance (total weight 40)																												
1	Airside ΔP	4	8	7	8	10	10	10	8	8	6	7	4	3	4	4	7	7	8	7	7	7	8	6	8	10	8	8	8
2	Refrigerant ΔP	3	6	6	6	6	6	6	6	6	6	6	6	6	6	8	10	10	10	6	6	6	6	10	6	6	6	10	6
3	Even Coil Loading	3	7	6	7	7	7	8	8	7	7	7	10	10	8	8	6	6	6	6	6	6	7	8	8	8	7	7	7
4	Susceptibility to Icing	3	8	5	6	6	6	6	6	6	7	5	6	8	8	8	7	7	8	6	6	6	6	8	6	6	7	6	8
5	Susceptibility to Snow Blocking	2	10	7	6	7	7	7	6	7	10	4	6	5	8	8	8	8	8	6	10	6	6	6	6	7	6	6	9
6	Susceptibility to Debris Accumulation	3	8	7	6	6	6	6	6	7	7	5	6	7	7	5	6	6	6	7	7	6	6	7	6	6	7	6	8
7	Susceptibility to Air Recirculation	5	7	7	7	7	7	7	7	6	6	6	8	7	7	7	7	7	8	6	5	7	7	8	7	7	7	7	7
8	Drainage of Defrost Melt	5	9	7	7	6	6	6	7	7	7	7	8	6	6	6	5	5	5	8	8	8	8	8	7	6	8	7	9
9	Noise	5	8	4	8	8	8	8	8	10	10	7	8	10	10	10	4	4	10	8	8	8	8	8	8	8	8	8	8
10	Flexibility of Placement	2	9	10	6	6	6	6	6	6	6	6	7	7	7	8	10	10	8	10	10	10	10	7	10	10	8	10	8
11	Compatibility with Outdoor Compressor Placement	3	0	8	6	6	6	6	6	6	6	0	0	0	0	0	0	0	0	0	0	0	6	5	10	10	0	10	0
12	Compatibility with Unitary Design	2	10	10	0	0	0	0	0	0	0	0	5	5	5	5	8	8	5	10	10	10	10	10	5	5	10	10	10
	Manufacturing Cost (total weight 35)																												
13	Coil Fabrication Cost	10	9	9	6	7	7	5	4	6	6	6	9	9	9	9	9	7	9	8	8	8	8	9	8	9	9	8	9
14	Header Fabrication Cost	10	7	7	8	8	8	8	8	8	8	8	9	9	9	3	3	4	3	9	9	9	9	5	9	9	7	5	5
15	Sheet Metal Fabrication Cost	5	9	9	9	8	8	8	9	7	7	8	7	7	7	7	7	7	6	9	9	9	9	7	9	8	8	7	8
16	Fan Package Fabrication Cost	10	8	8	8	8	8	8	8	8	8	8	8	8	8	8	8	8	8	8	8	8	8	8	8	8	8	8	8
	Marketability (total weight 20)																												
17	Package Height	5	10	9	8	7	8	4	7	10	10	9	6	6	6	6	6	6	5	10	10	10	10	6	8	7	10	8	10
18	Package Width	3	8	6	8	8	8	8	8	7	7	7	8	8	8	8	8	7	8	6	6	6	6	8	8	7	8	6	8
19	Package Depth	3	7	8	8	8	8	8	8	7	7	7	8	8	8	8	7	9	6	8	8	8	8	7	8	7	7	8	7
20	Aesthetics	5	9	7	8	5	6	5	7	9	9	7	6	6	6	6	5	6	4	7	7	7	7	9	9	7	8	6	7
21	Uniquness	4	9	7	6	6	6	6	6	10	10	9	7	7	7	9	9	9	9	7	7	7	7	9	7	7	8	9	9
	Maintainability and Handling (total weight 15)																												
22	Access to Fan & Motor	6	9	10	9	8	9	8	9	7	8	9	8	7	6	6	10	10	7	7	7	9	9	8	9	8	9	8	9
23	Protection from Fin Damage	5	10	7	6	6	6	6	6	6	6	6	10	10	10	10	8	7	8	7	7	7	7	8	7	7	8	7	10
24	Weight of Unit	4	8	8	8	6	7	6	8	7	7	9	6	6	5	5	5	5	4	8	8	8	8	7	8	8	8	7	8
	$\sum_{1}^{n} i \times j$		894	830	792	768	788	736	765	801	808	754	809	801	795	745	738	731	730	822	827	838	863	828	869	852	849	790	855
	Ranking		1 A	8	17	20	19	25	21	14	13	22	12	14	16	23	24	26	27	11	10	7	3 C	9	2 B	5 E	6	18	4 D

A wide variety of sheet metal shapes were used. In eight of the designs the sheet metal enclosed the coil, and in nineteen designs the coil surface was exposed except for a grille.

The preferred package design was described previously.

The second highest ranking design, Design "B" in Figure 3.5-5, utilized a single three-row coil bent to form a horse-collar shape. The coil was 24 inches high by 80 inches long and passed the refrigerant in the forced convection mode. Air was drawn through the coil in a radial horizontal direction over the 300 degree wrap of the coil. The fan packaging was mounted in the horizontal plane above the coil and discharged the air upward. The fins hang freely over an 8 inch high support plinth to facilitate effective drainage of the defrost melt. Overall dimensions were 36 inches wide by 36 inches deep by 42 inches high. The design could have accommodated a compressor.

The third through fifth highest ranking designs are shown in Figures 3.5-6, -7, and -8.

Conclusions

The essential features of an outdoor unit of a residential heat pump were identified and weighted in proportion to their importance. Twenty-seven designs were scrutinized and given a score on each of the twenty-four design features. An overall score was obtained for each design by summing the products of score and feature weighting over all features.

A unique design of relatively simple construction emerged as the first-ranking design. The second-ranking design was similar in several ways to some units presently available.

The initial few designs conceived were strongly influenced by current practice except for the inclusion of a high-efficiency fan package. As these designs were ranked by the rating method, their strengths and weaknesses were exposed. This interaction influenced the course of the design process very beneficially.

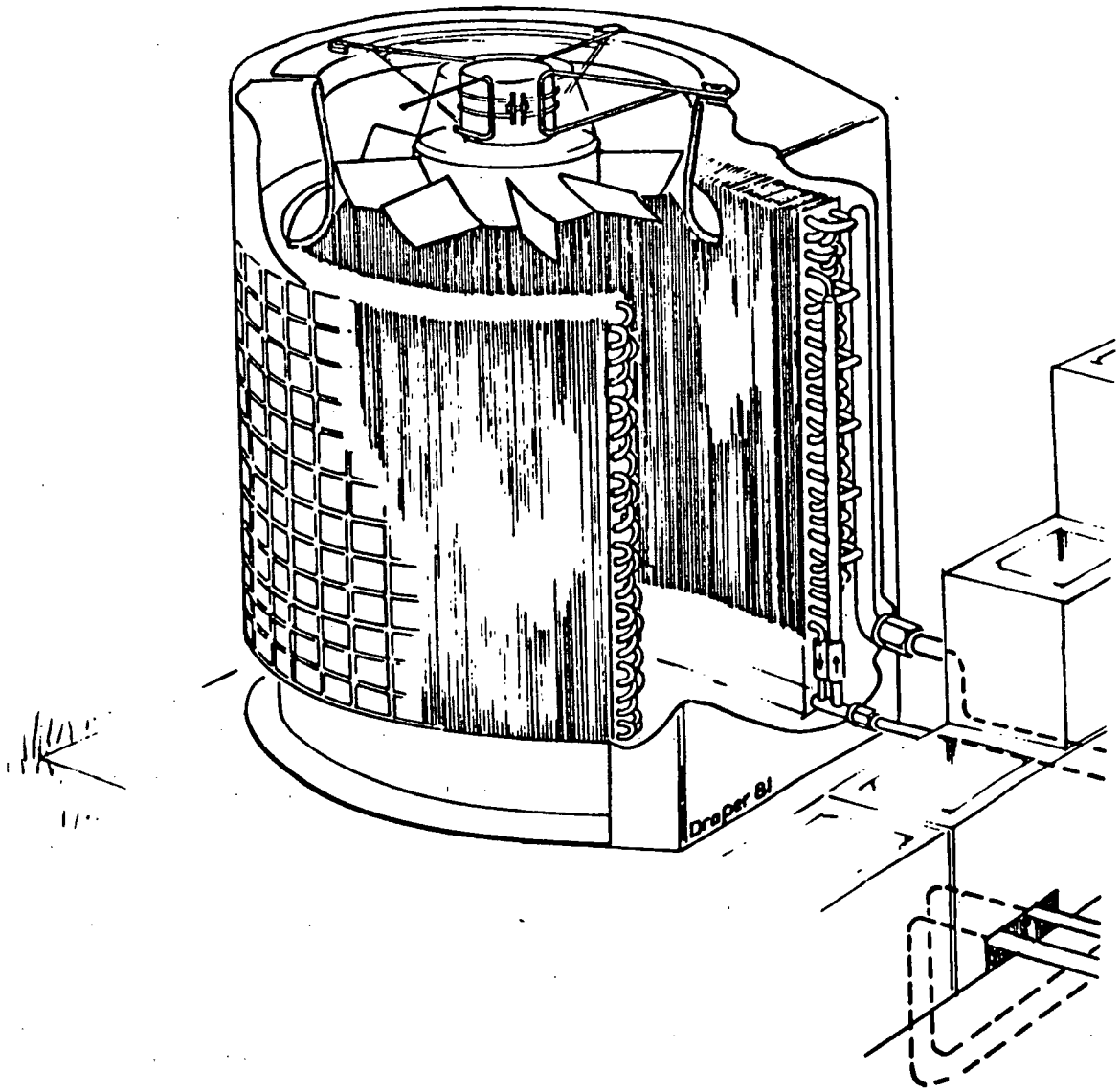

Figure 3.5-5 - Outdoor package design "B"

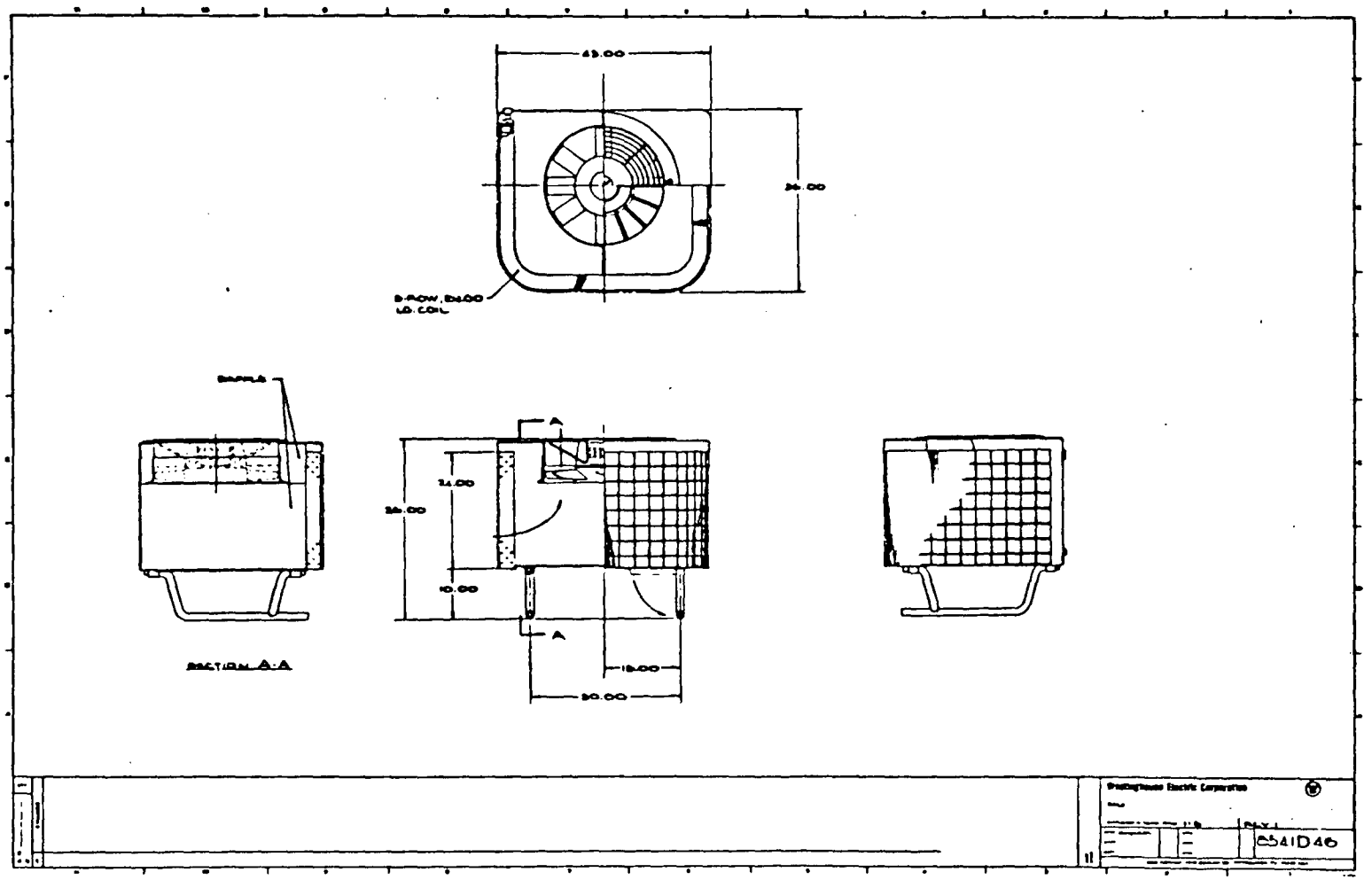

Figure 3.5-6- Outdoor Package Design "C"

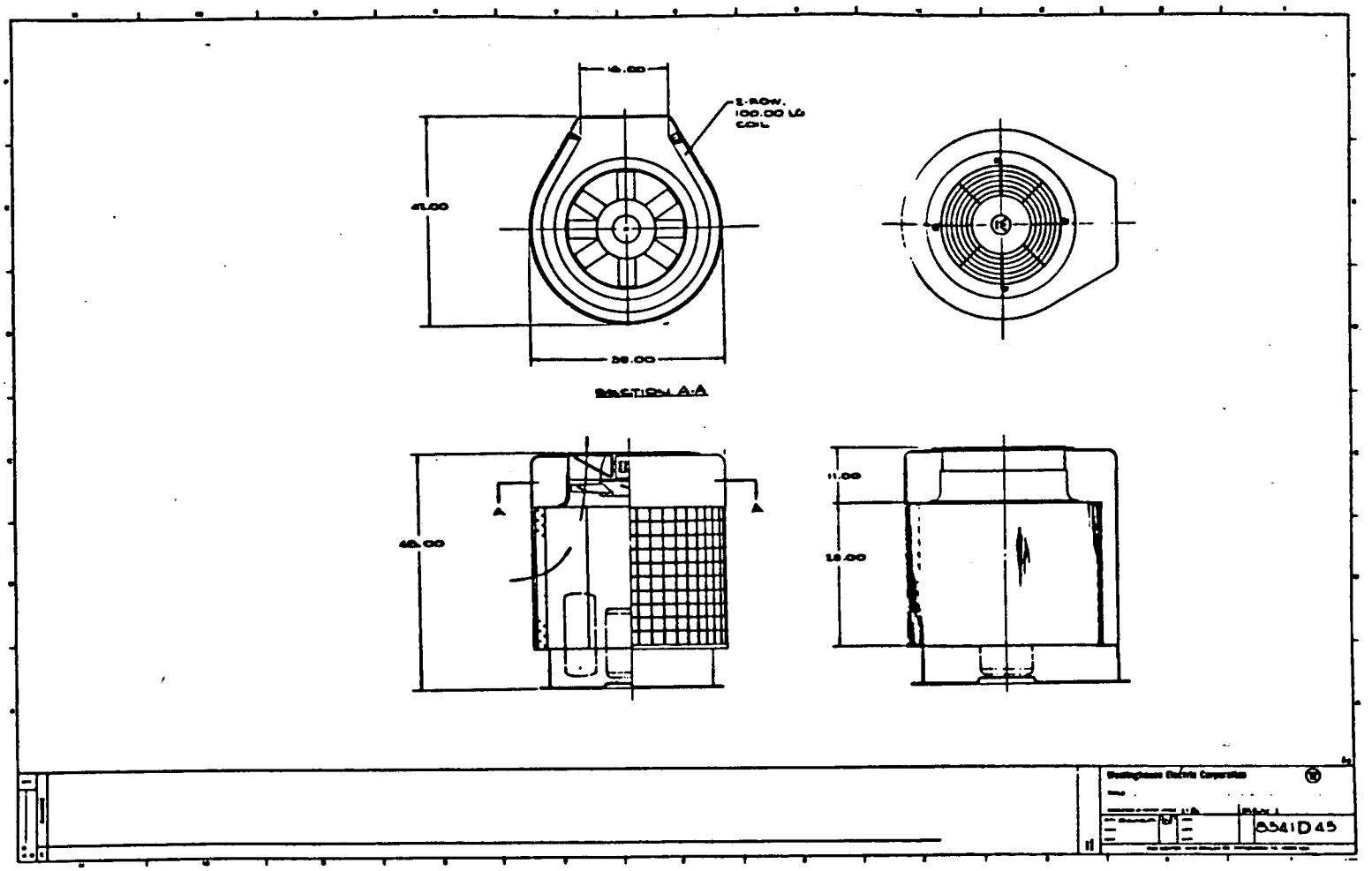

Figure 3.5-7 -Outdoor Package Design "D"

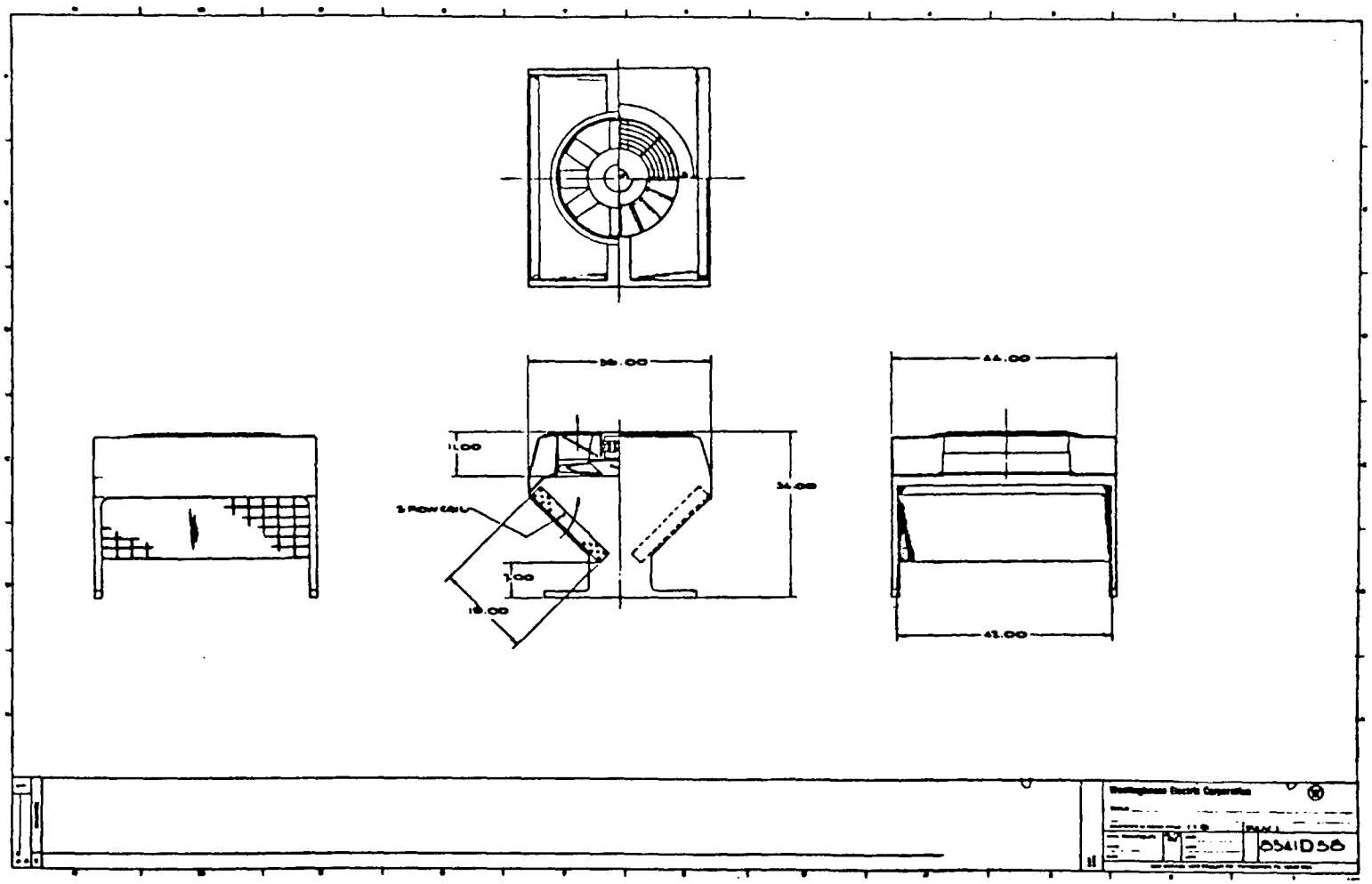

Figure 3.5-8 - Outdoor Package Design "E"

3.5.2 Indoor Unit Package Design and Development

Introduction

The heat pump indoor package encompasses the housing of the indoor air mover and heat exchanger, compressor, suction line accumulator, expansion device, reversing valve, supplementary resistance heat, the microprocessor-based control system, plus all transformers, relays, contactors, and capacitors. The air mover is a dual-speed high-efficiency design, and as such occupies considerably more space than the squirrel-cage blower which it replaces. In the evolution of the indoor package design, great emphasis was placed upon installation flexibility.

Description of the Selected Indoor Package

The adopted indoor package design is modular in three units. The first module contains the heat exchanger coil, compressor, and associated refrigerant plumbing. The second module contains the air mover and all electrical control elements. The third module contains the supplementary electrical resistance heaters. An artist's sketch of this indoor package in the preferred module arrangement is shown in Figure 3.5-9, while an assembly drawing is shown in Figure 3.5-10 with some critical dimensions.

The first module, the refrigeration machine module, contains the compressor, oil cooler, suction line accumulator, suction line filter/dryer, the four-way reversing valve, the bidirectional expansion device, the heat exchanger coil, and the coil partitioning solenoid valve in a sheet metal housing 22.5 inches wide by 36.0 inches deep by 28 inches high. Units less than 3.5 tons in capacity could have the depth dimension reduced to 28 inches.

The compressor and accumulator are enclosed in a laminated acoustic blanket and mounted to a galvanized subframe using vibration isolation mounts. The subframe, in turn, mounts to the module's structural base, using a second set of vibration isolation mounts. The

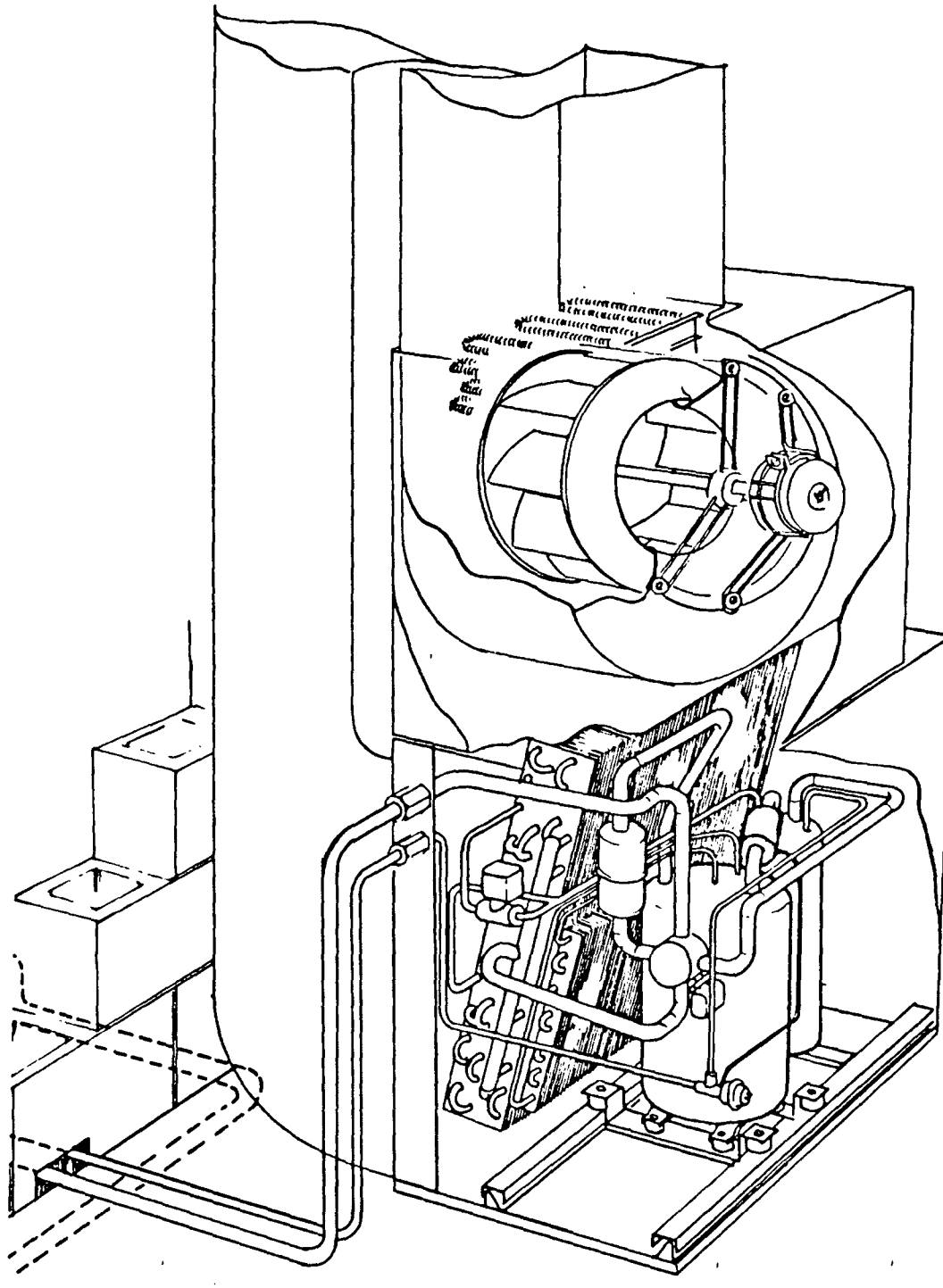

Figure 3.5-9 - Sketch of indoor package assembly

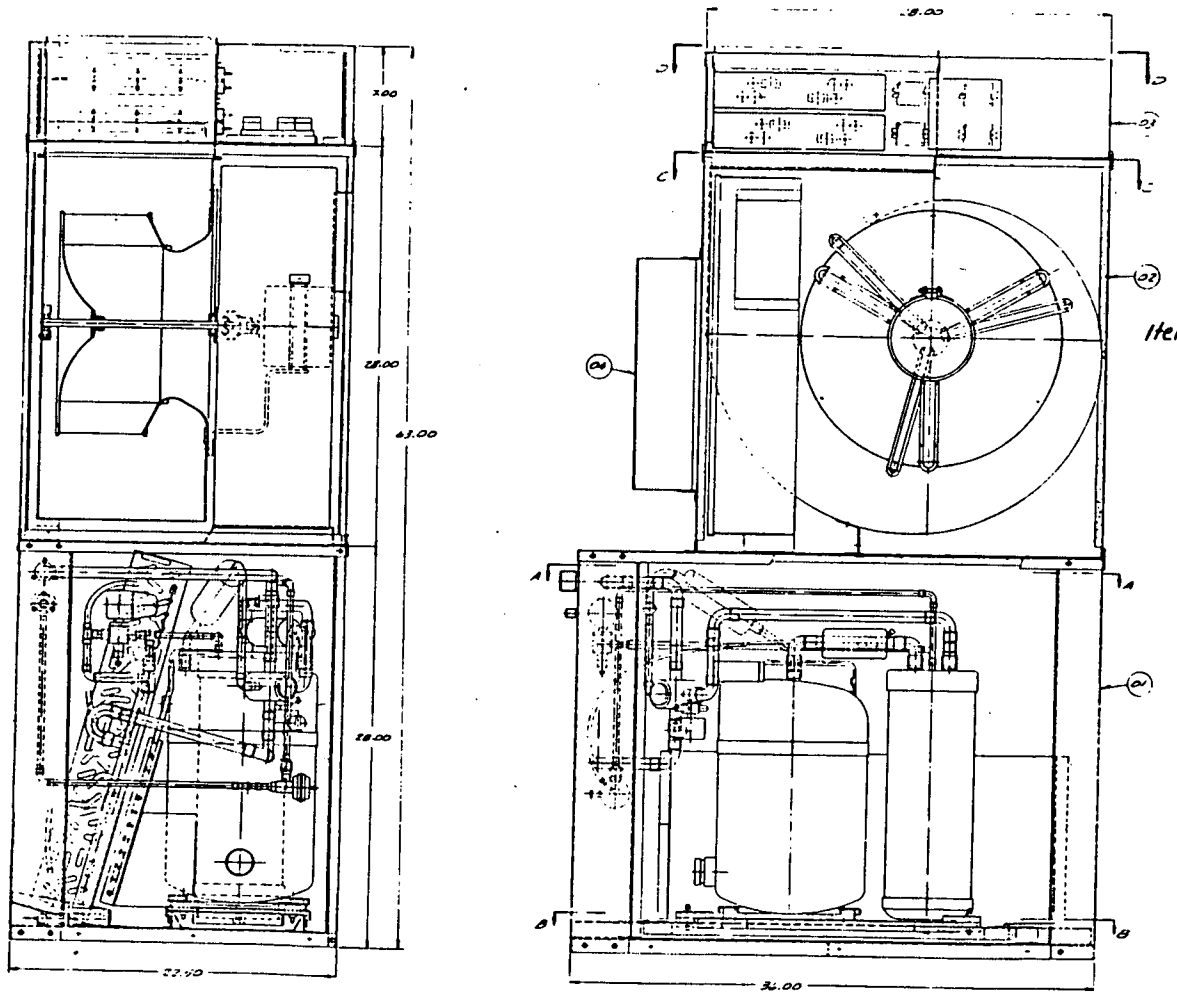

Layout of the Highest Ranked Design

Item ① Refrigerant Circuit Module.

② Air Mover Module.

③ Supplementary Electrical Heat Package.

④ Microprocessor Based Controller.

Dwg N° 5600C48

Figure 3.5-10 - Selected indoor package design assembly

interface between the subframe and the structural base is in the form of sliding rails.

In the event that the compressor needs to be removed, the end access panel is removed, four easily accessible refrigerant lines are parted, two clamps removed, and the subframe and its burden slide out of the unit for replacement or service. Upon reinstallation, refrigerant line reconnection is accomplished using the standard sleeving technique.

To accommodate less drastic service, the reversing valve, expansion device, coil partitioning solenoid valve, and heat exchanger return bends are easily accessible upon removal of the end access panel.

Although the preferred air flow direction is inward from the coil side through the heat exchanger over the compressor and out the top of this module, air inflow can be accommodated, flowing in the bottom or through the compressor side of this module, through the heat exchanger coil, and then upward out of the top of the module. The preferred air flow path yields slightly better performance.

Refrigerant line connections are via standard fittings located at the top coil side of the access panel end of the module.

The obvious advantage of this refrigeration machine package over the other concepts that house the compressor indoors is that there are only two refrigerant line connections to be made in the field at installation time. Further, any heat dissipated from the compressor and associated plumbing is available to provide comfort heat during heating mode operation. During cooling mode, with the preferred air flow path, there is a reheat effect that should provide for better dehumidification performance.

The second module, the air mover and controls module, measures 22.5 inches in width, 28 inches in height, and 28 inches in depth and contains the high-efficiency air mover subassembly. The air mover subassembly consists of a 16-inch diameter blower wheel with backward-curved blading mounted in a volute scroll with the blower wheel carried

on an integral bearing-supported shaft. This shaft is connected to the direct-drive high-efficiency motor by a flexible coupling. The motor is mounted to the scroll through a wire form spider. The transformer, capacitors, contactors, and relays are mounted in a large control box partitioned into high and low voltage sections. This box measures 7.5 inches in width, 6 inches in depth, and 25 inches in height and is aligned so that its access panel is directly above the access panel for the refrigeration machine module. The microprocessor boards are separately mounted in their own box and attached to the external surface of the module. To accommodate upflow air flow paths other than that preferred, the air mover subassembly is removed, the housing rotated 180° about a horizontal axis through the access end, and the air mover subassembly rotated 180° about a vertical axis and reinstalled in the module housing. The module is then restacked above the refrigeration machine module.

In order to horizontally align the modules, the air mover module is dropped alongside the refrigeration machine module, rotated 90° about a vertical axis and then 90° about a horizontal axis.

The motor and blower use permanently lubricated bearings. The air mover subassembly can be removed from the module housing for service after removing the relay control box.

The third module, the supplementary heat package, is produced as a right-hand assembly but is easily field modified to be a left-hand assembly. It is aligned so that the heating elements are over the air mover discharge. Power wiring is connected to terminals in the supplementary heat module. This location for the single-point wiring connection has the advantage that all heavy gauge wire is localized in this module.

Field wiring consists of interconnecting the refrigeration machine module, which is furnished with a wiring harness, to terminals in the control box of the air mover and controls module.

From the control box, power wiring is connected to the power terminals in the supplementary heat module. Similarly, a six-wire control cable and a five-wire power cable connect the control box to the outdoor unit.

In its preferred orientation, this indoor package is 22.5 inches wide so that it will fit in a standard closet; it is a maximum of 36 inches deep and 63 inches high, and is sufficiently short to accept air plenums at top and bottom and thus can be used with either side or bottom return air entry. Filters are external. The modules can also be arranged for horizontal mounting. The indoor package is acoustically insulated so that it is a quiet, flexible, highly efficient heat pump indoor section.

Analysis

Seven criteria were considered in evaluating alternative package designs: performance, manufacturing cost, market application, maintainability, construction ease, handleability, and aesthetics.

Performance aspects of the indoor package include noise potential, vibration potential, the air pressure drop through the package and the useful application of compressor heat. The unit must have acceptably low noise transmission through the ductwork (considering that the compressor is to be mounted indoors), and the lowest possible noise transmission is desirable. Note that since the air mover is more efficient, air moving noise should be lower, whereas the placement of the compressor in or near the air moving package adds a noise source not present in state-of-the-art units. The unit must have an acceptable low susceptibility to structural vibration, again considering that the indoor compressor might excite the package structure. Complete vibration isolation is desirable. The unit will have the compressor indoors; some arrangements will use the waste heat. The unit must have an internal air-side pressure drop compatible with the blower characteristics for all air entry and mounting options. The desirable nominal

value for air-side pressure drop is 0.5 inch of water external design, 0.3 inch of water internal, and 0.05 inch of water for the filter.

Unit manufacturing cost involves the complexity and cost of assembly components, controls, and electrical wiring, the cost of the basic cabinetry, the cost of heat exchanger coil fabrication, and the cost of executing the refrigerant plumbing. We are assuming that the minimum acceptable volume is 100,000 units annually with cabinetry and components shared across several capacity ranges. Single-point power wiring is assumed, with all low voltage control wiring localized in a single compartment. Coil fabrication cost is a function of its complexity: thus a single slab coil is better than an "A" coil, for example. The cost of refrigerant plumbing is a function of the package design in the sense that the more cramped and confined the plumbing, the more expensive; while conversely, a design with an independent compressor package also tends to be expensive because of the need for fittings as opposed to factory-brazed connections.

Market applicability refers to the degree to which the package can be applied to various installation techniques in a house. Generally, this involves the dimensions of the unit, its modularity, and the air flow options available. The unit must accommodate air entry through one of its sides, and it would be most desirable if it could accept air entry through either side, the back, or the bottom of the unit. In addition, study has indicated that the unit must not be higher than 63 inches to accommodate an air plenum both above and below within a standard 7-1/2 ft floor-to-ceiling distance. Similarly, the maximum acceptable width is 30 inches and the maximum acceptable depth is 36 inches. Desired unit height is 46 inches. Desired unit width is 22.5 inches or less to accommodate installation in a standard closet cavity after house framing is complete. Desired unit depth is 24 inches or less to permit mounting with front access in a standard closet cavity. Note that a unit with a separate compressor-only package must place the compressor somewhere. In the analysis, we assume that the compressor package size is charged against unit height.

Maintainability demands that all serviceable components be accessible. Quite obviously, the easier the access, the more desirable a package design is from the point of view of maintainability.

Construction and materials should be such that low cost thin gauge steel is sufficient, and forming should require a minimum tooling investment.

Handleability covers those aspects of the package design that impact upon the ease and cost of transportation and storage. For example, the shipping carton should be low in cost and not require an external skid. The carton dimensions should permit close packing in a standard truck trailer. The package and its carton must be able to withstand stacking five-high for warehouse storage.

Aesthetics refers generally to eye appeal. The unit must look well proportioned, have a pleasant color, and be easily wiped clean or, alternatively, should not easily show soil and smudge marks.

To quantitatively evaluate alternative indoor package designs, a unit decision-making methodology was used. (See Table 3.5-4.) For each package design, a score of from 0 to 10 was assigned to each subcategory within the seven major evaluation criteria. Each subcategory was assigned a relative importance weight of from 1 to 10. The figure of merit for each design then consists of this sum over all subcategories of the product of importance weight times category score. The ranking of alternative designs is according to the magnitude of this associated figure of merit.

Since the criteria used as well as the score assigned are to a large extent subjective, evaluation by another group of people could result in a different ranking for each alternative design. In the following discussion of these alternative indoor package designs, it must be borne in mind that the air mover of choice changed during the course of this study from a 13 inch diameter blower wheel in a cylindrical shroud to a 16 inch diameter blower wheel mounted in a

Table 3.5-4

Indoor Unit Rating Chart

Catagories and Design Features	Design Identification Dwg Number 5600 -	A C10	B C11	C C12	D C13	E C14	F C15	G C16
n	Weight i (1 to 10)	Score j (0 to 10)						
Performance (total weight 50)								
1 Blower Efficiency	10	6	6	7	7	9	9	9
2 Airside ΔP	7	7	8	7	8	9	8	7
3 Refrigerant Circuit ΔP	8	9	8	8	8	6	8	9
4 Even Coil Loading	5	8	7	8	8	9	7	8
5 Utilization of Compressor Heat	5	5	5	5	5	0	5	10
6 Drainage of Water Percipitant	3	6	8	8	8	8	8	6
7 Noise	10	5	5	7	7	10	9	8
8 Compatibility with Unitary Design	2	6	8	6	6	5	6	6
Manufacturing Cost (total weight 45)								
9 Coil Fabrication Cost	10	9	7	7	7	7	7	9
10 Circuit Fabrication Cost	7	8	7	8	7	5	7	8
11 Sheet Metal Fabrication Cost	8	9	9	7	7	8	9	7
12 Blower Assembly Cost	10	9	9	8	8	7	7	7
13 Ease of Final Assembly	8	7	9	7	9	9	9	8
14 Simplification of Cooling Only Unit	2	5	5	5	5	10	5	5
Marketability (total weight 40)								
15 Package Height	10	9	7	9	9	10	2	8
16 Package Width	9	5	5	5	5	10	10	10
17 Package Depth	5	9	9	8	8	8	8	6
18 Air-Flow Path Options	10	8	7	9	7	7	7	10
19 Aesthetics	2	8	7	7	7	7	6	8
20 Uniqueness	4	6	6	6	6	5	7	9
Maintainability and Handling (total weight 35)								
21 Access to Blower and Motor	8	6	6	6	6	9	9	8
22 Access to Refrigerant Valves	8	7	8	7	8	7	9	7
23 Access to Electrical Controls	10	9	6	8	7	9	9	9
24 Access to Major Machine Components	5	6	7	7	7	8	7	8
25 Weight of Largest Module	4	7	7	6	6	9	6	7
Items Common to All Designs (total weight 60)								
26 Combined Features Associated with Compressor	30	8	8	8	8	8	8	8
27 Combined Features Associated with Controls	20	9	9	9	9	9	9	9
28 Combined Features Associated with I^2R Htrs	10	7	7	7	7	7	7	7
	$\sum_{1}^{n} i \times j$	1742	1686	1718	1712	1829	1782	1877
	Rank	4	7	5	6	2	3	1

volute shroud because of the desire both to reduce noise and improve efficiency.

The unit listed in the rating chart as design "A" (Figure 3.5-11) uses a 13 inch diameter blower wheel in a cylindrical shroud. The overall dimensions are 25 inches wide by 25 inches deep by 62 inches high. The heat transfer surface is a four-row slab coil. The preferred air flow is upward through the unit, with entering air preferred from one side or through the bottom. The electrical resistance heat was located in the vertically exiting air stream.

This design has the advantage of a simple structure and hence low cost. Its disadvantages include a width greater than desired and a limited number of air flow entry options. The unit is made up of four modules and both vertical and horizontal alignment of the modules is possible.

Design "B" (shown in Figure 3.5-12) also uses the 13 inch diameter wheel and cylindrical shroud. The heat exchanger consists of two four-row slab coils in a "V" configuration. This design also houses the compressor and receiver in the base and has the auxiliary heat section at the top. Overall height is 63 inches, and air access is possible from any of the four sides and the bottom when the three modules are stacked. Horizontal alignment is also possible.

This design has the advantages of a simple structure and hence low cost, plus great flexibility in the air-entry position. Its width dimension limits it to basement-type locations rather than closet installations. The configuration was selected early in the program for our breadboard unit. A desire for a lower noise and higher efficiency air mover were the major reasons for its losing favor.

Design "C", Figure 3.5-13, is similar to design "A" in that it also incorporates a cylindrical blower shroud and a slab coil configuration; however, it uses a 16-inch diameter wheel and therefore requires increased width and depth, resulting in a 30 inch by 30 inch footprint. Its air entry directions include one side, one end, and the bottom when

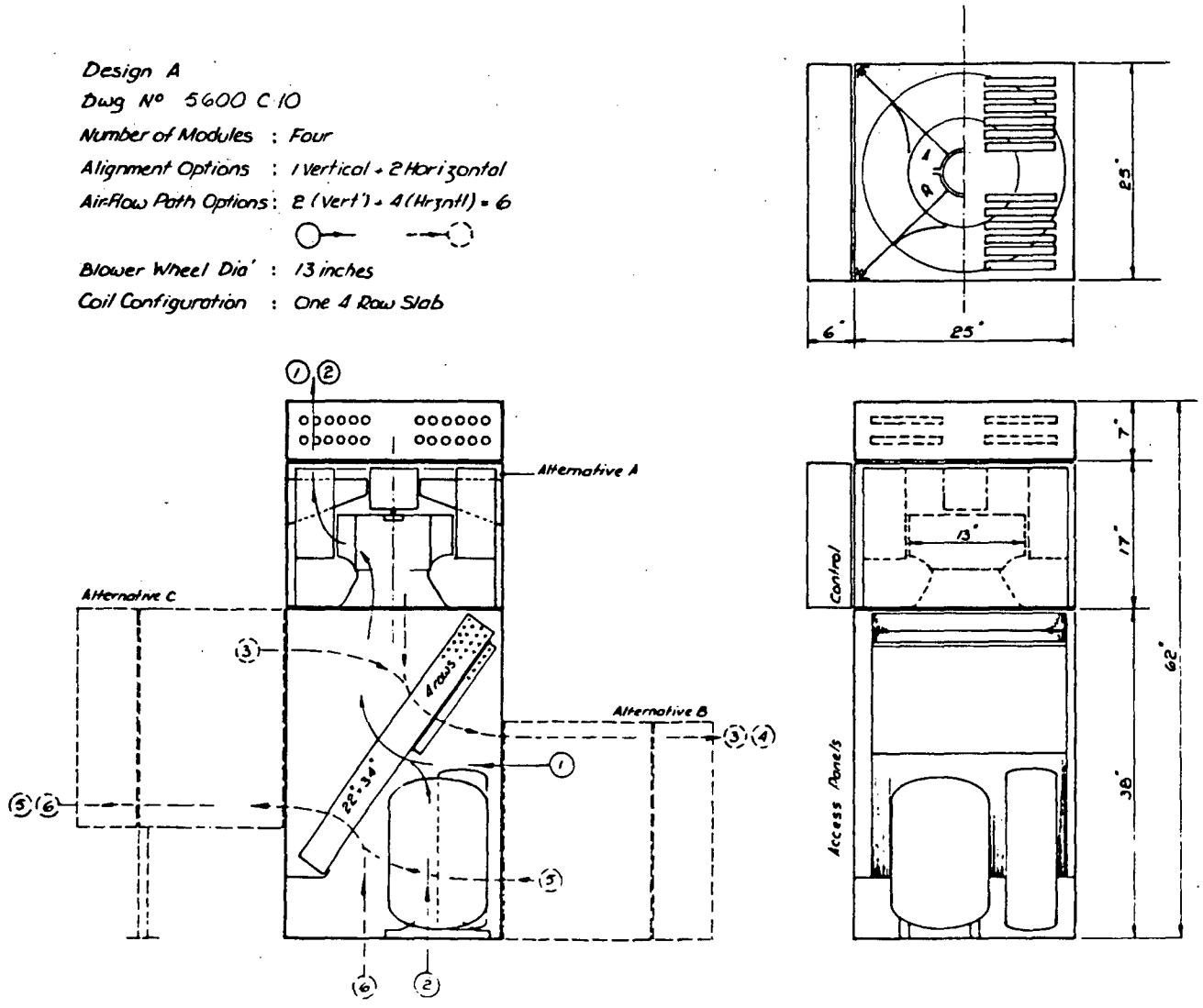

Figure 3.5-11 - Indoor package configuration "A"

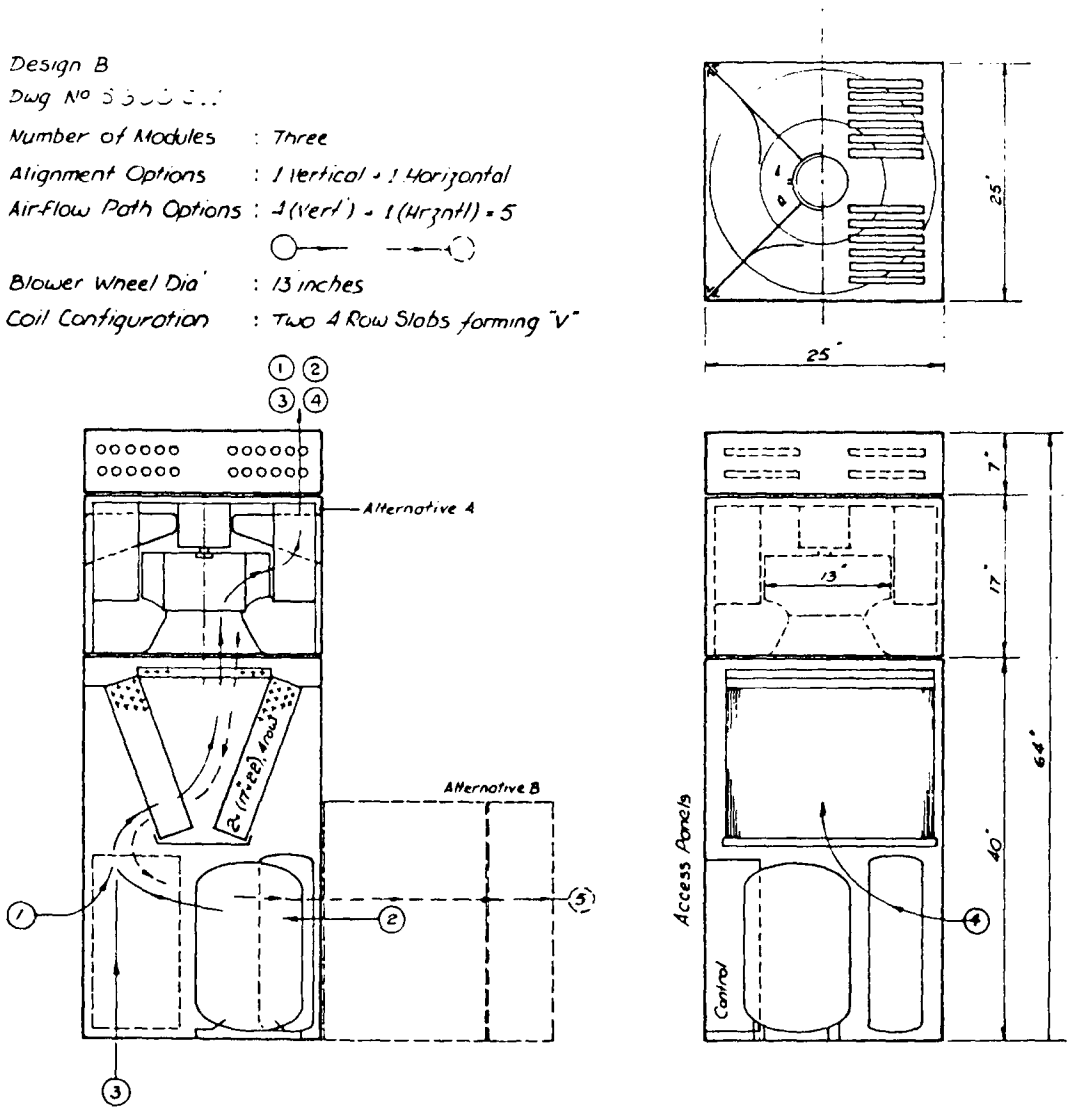

Figure 3.5-12 - Indoor package configuration "B"

5600 C11

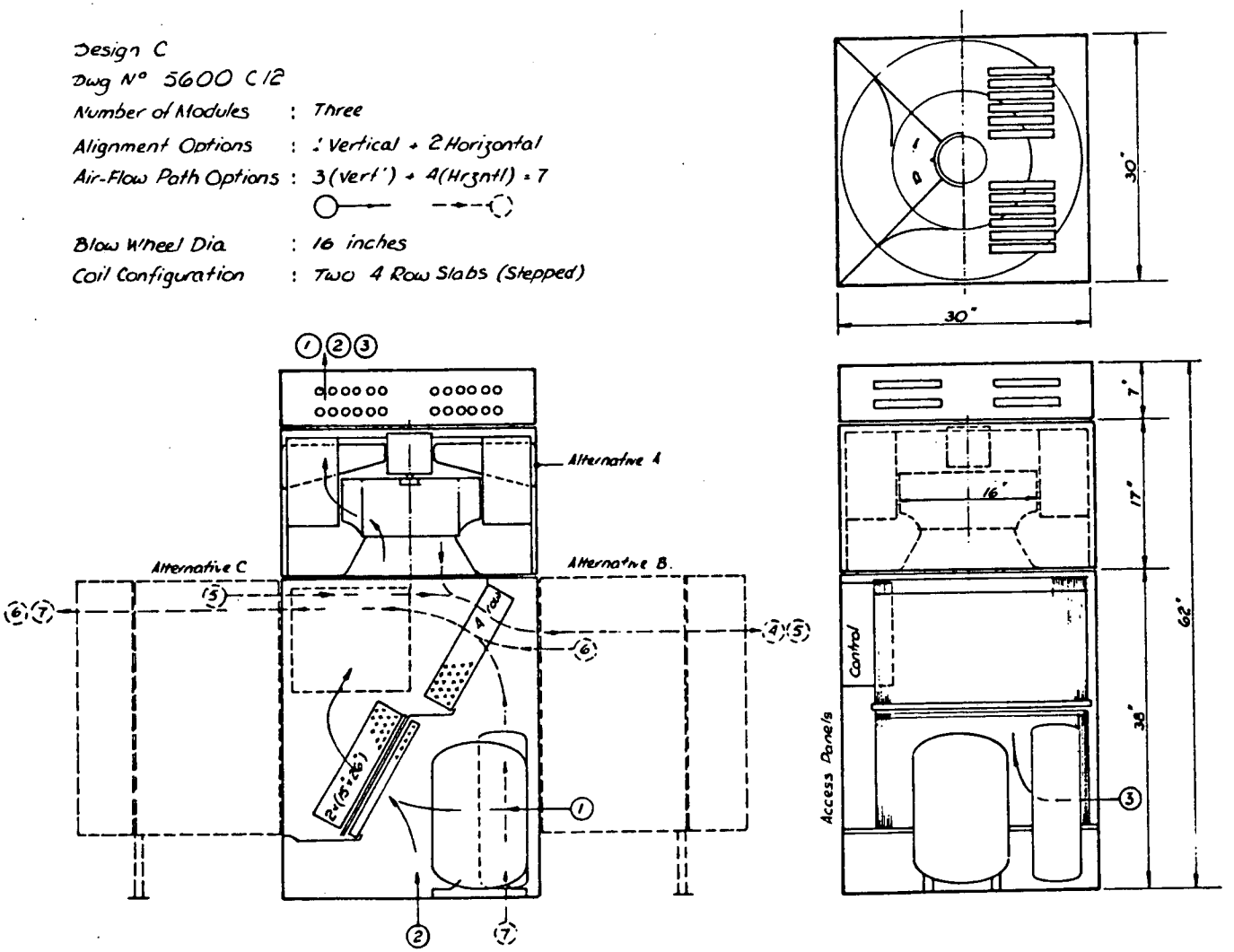

Figure 3.5-13 - Indoor package configuration "C"

5600C12

the three modules are vertically stacked. The air mover in this configuration does not yield its best efficiency and the footprint dimensions are judged entirely too large.

The fourth unit, design "D", is similar to design "B" except that it uses the 16-inch diameter blower wheel in a cylindrical shroud. The increased air mover efficiency attainable with the volute scroll, as well as this unit's large footprint, contribute to its low figure of merit. (See Figure 3.5-14.)

Design "E" is housed in two cabinets, the coils and air mover in one, and the compressor and receiver in another. The coil-air mover section is shown in Figure 3.5-15. This design has the size advantage of a small (28 by 22 inch) footprint, making it attractive for closet installation. Note, however, that the separate compressor module adds complexity to the plumbing and wiring. Further, additional space must be found for the compressor module, with little chance for recovering the compressor shell losses in a useful manner.

Design "F", shown in Figure 3.5-16, is basically design "B" fitted with the high-efficiency air mover. Its principal disadvantage is its large package size.

The final design, design "G", Figure 3.5-17, consists of three separate sections: a coil-compressor section containing a four-row slab coil with compressor and the necessary valving and plumbing, the air mover section housing the blower and controls, and the electric heat section. The compartmenting of the indoor system in this manner allows the flexibility for vertical or horizontal airflow installations. In addition, the resulting packages are conveniently sized for crating and shipping.

Evaluation

Examination of Table 3.5-4 reveals that designs F and G are the most viable. The spread in their respective figures of merit is very small. Design F would undoubtedly be the design of choice if the market

Design D
Dwg No 5600 C 13
Number of Modules : Three
Alignment Options : 1 Vertical + 1 Horizontal
Air-Flow Path Options : 4 (Vert') + 1 (Hrzntl) = 5
Blower Wheel Dia : 16 inches
Coil Configuration : Two 4 Row Slabs forming "V"

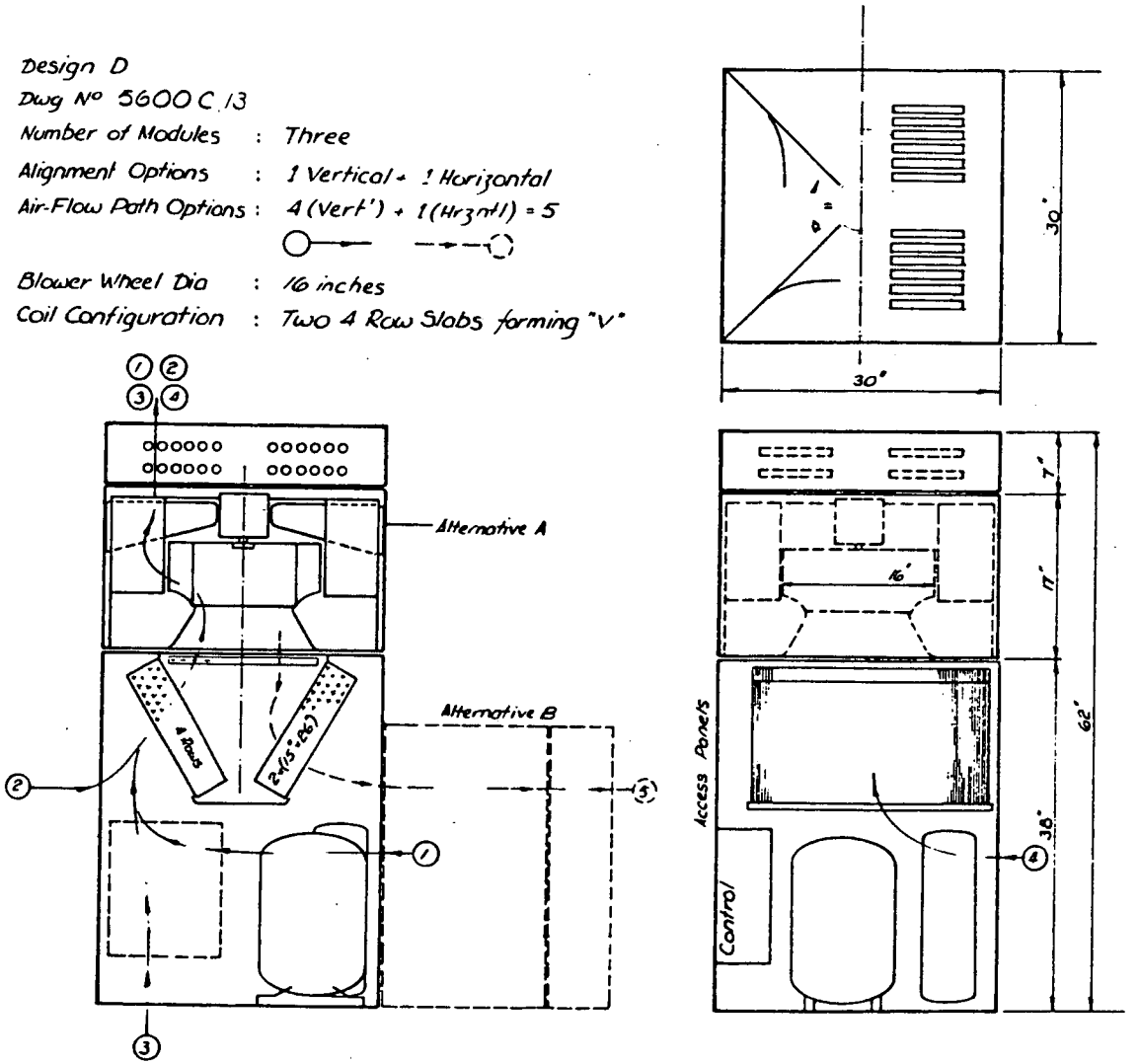

Figure 3.5-14 - Indoor package configuration "D"

5600 C 13

Design E
Dwg N° 5600 C 14
Number of Modules : Four
Alignment Options : Vertical and Horizontal
Air-Flow Path Options : 1(Vert') + 1(Hrzntl) (5 variations on each)

Blower Wheel Dia' : 16 inches
Coil Configuration : Two 4 Row Slabs forming "V"

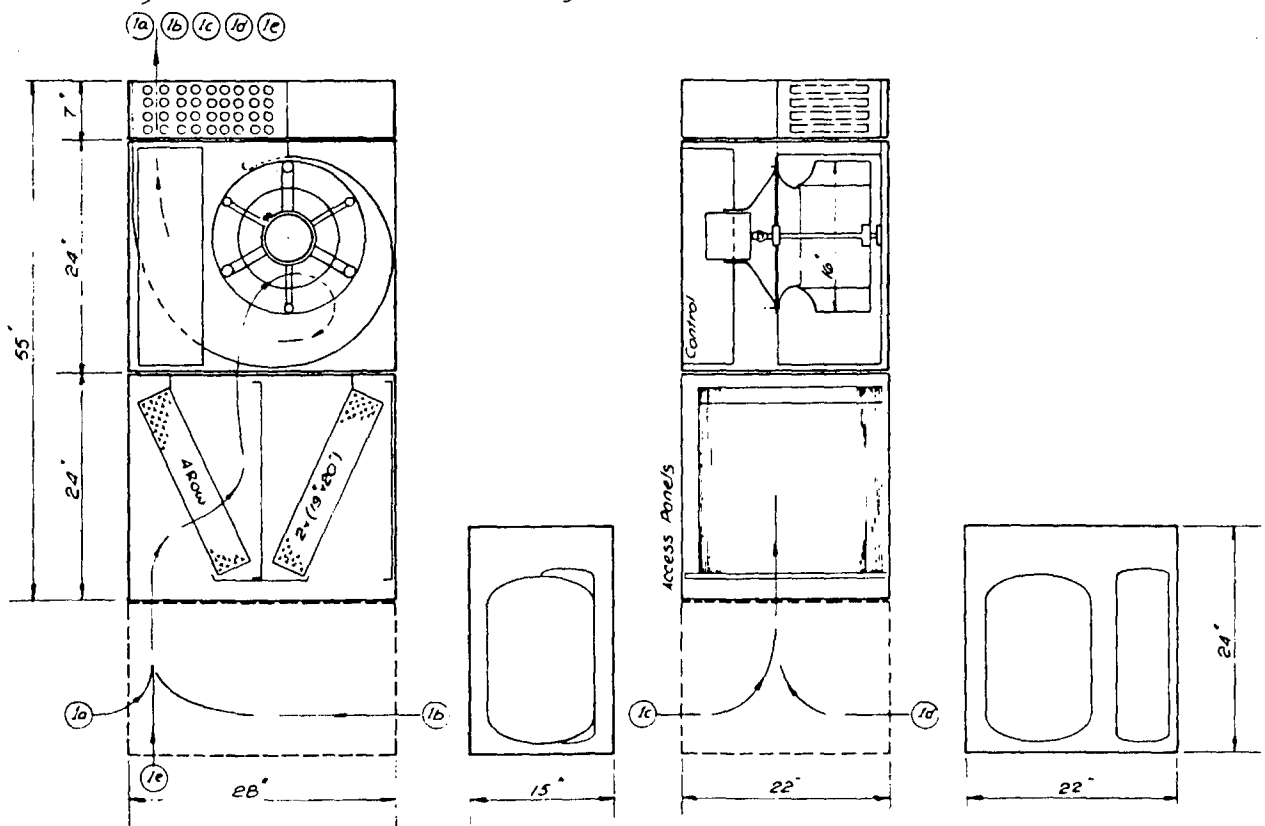

Figure 3.5-15 - Indoor package configuration "E"

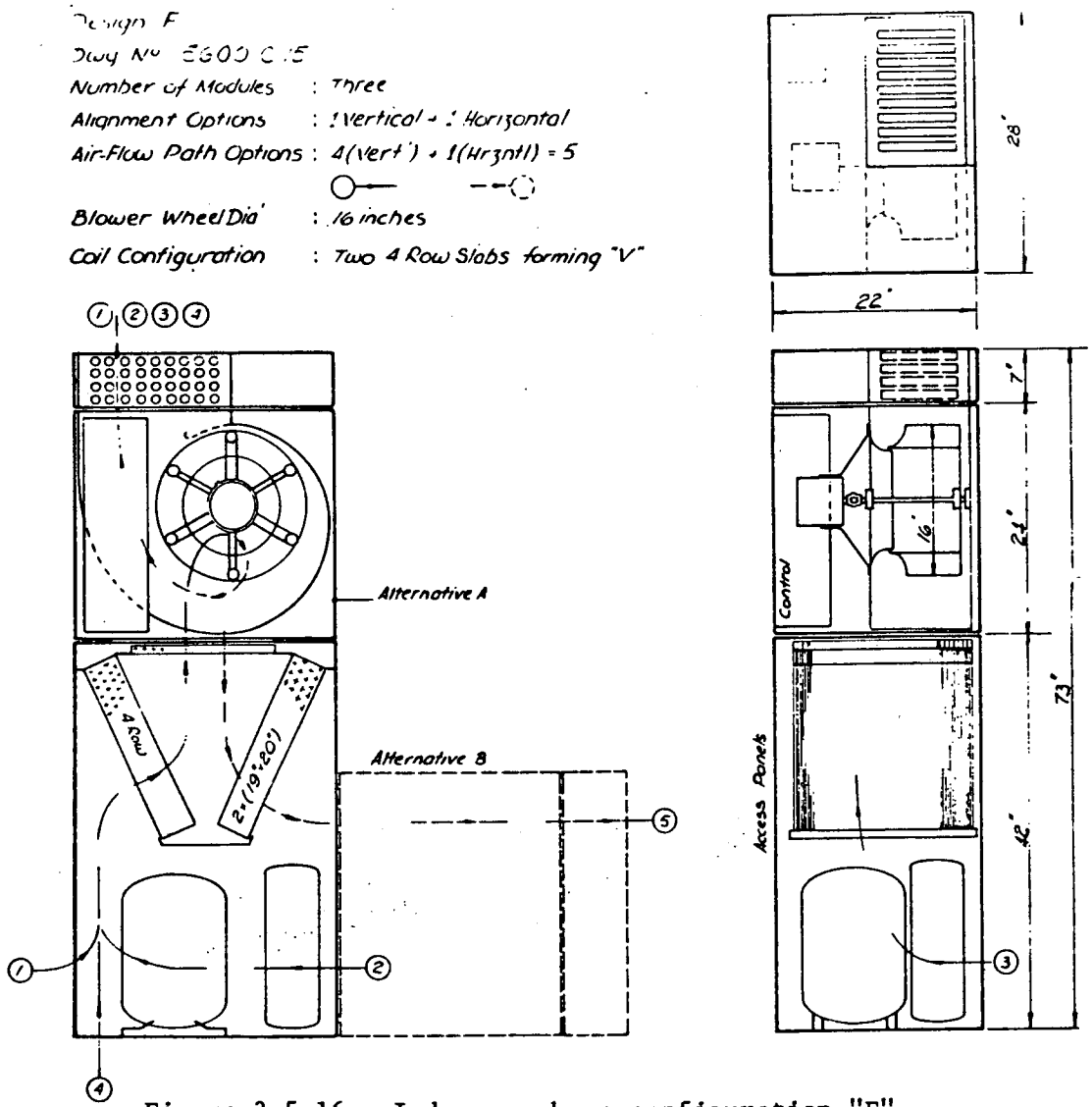

Figure 3.5-16 - Indoor package configuration "F"

5600 C 15

INFORMATION ON THIS PAGE SUBJECT
TO PATENT STATES CLAIRE IN FACT

Design G
Dwg No 5600C16
Number of Modules : Three
Alignment Options : 2 Vertical + 2 Horizontal
Air-Flow Path Options : 4 (Vert') + 4 (Hrzntl) = 8
Blower Wheel Diameter : 16 inches
Coil Configuration : One 4 Row Slab

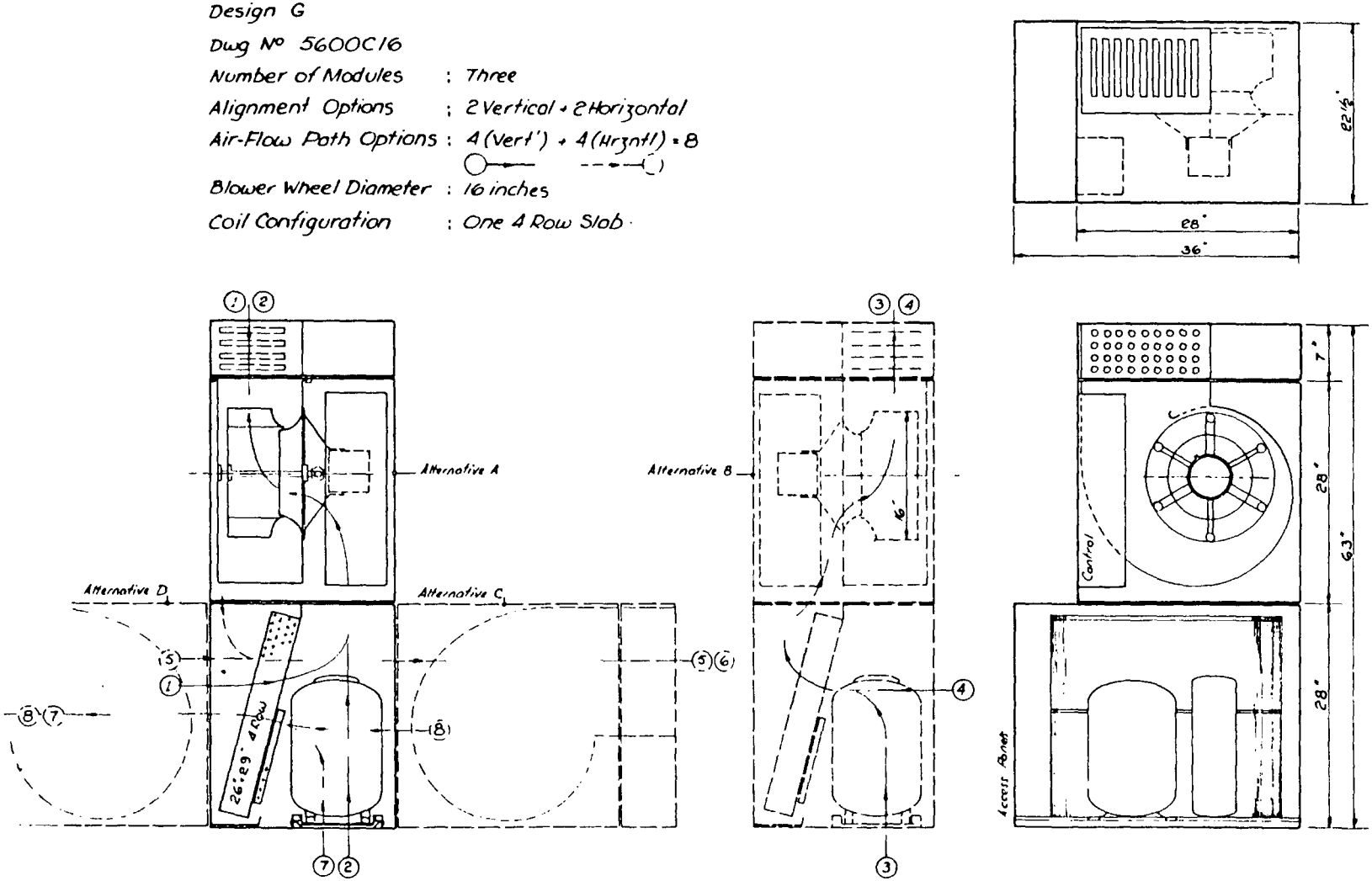

Figure3.5-17 - Indoor package configuration "G"

consisted only of upflow installations. If design F were partitioned into two modules, then design E is also contained. The major disadvantage of design E is that the separate compressor module requires more field connections, and does not permit the full benefit of some of the virtues of our advanced compressor.

Our advanced compressor is well housed in either design F or design G. Design G is the design of choice because it permits a horizontal flow installation and a slightly shorter overall package height, including resistance heat elements.

3.6 Prototype Test Plan

3.6.1 Thermodynamic Performance

A highly instrumented preprototype of the Westinghouse/DOE dual-stroke heat pump will be tested over a wide range of operating conditions in the heat pump test facility.

The planned heating test matrix is shown in Table 3.6-1. In addition to the complete DOE* test series, additional steady-state heating tests will be performed to obtain a complete performance map over an ambient temperature range of -20°F to 62°F. Frost accumulation tests will be performed at several different dry and wet bulb temperatures.

The cooling test matrix is shown in Table 3.6-2. In addition to the complete DOE test series, steady-state cooling tests will be performed at ambient temperatures ranging from 65°F to 115°F to obtain a complete performance map.

---

*10CFR430, "Energy Conservation Program for Consumer Products; Test Procedures for Central Air Conditioners, Including Heat Pumps," Federal Register, Vol. 44, No. 249, Dec. 27, 1979.

Table 3.6-1

Preprototype Heat Pump - Heating Test Matrix

Test No.	Indoors DB/WB	Indoors % Air Flow	Outdoors DB/WB	Outdoors % Air Flow	Capacity Mode	Test Type
H1	70/≤60	Rated	47/43	Rated	High	DOE High Temp. Heat
H2	"	"	47/43	"	Low	"
H3	"	"	62/56.5	"	High	"
H4	"	"	"	"	Low	"
H5	"	"	17/15	"	High	DOE Low Temp. Heat
H6	"	"	"	"	Low	"
H7	"	"	47/43	"	High	DOE Cyclic Heat
H8	"	"	"	"	Low	"
H9	"	Nominal	35/33	Nominal	High	DOE Frost Accumulation
H10	"	"	"	"	Low	"
H11	"	Nominal	35/35	Nominal	High	Capacity Defrost & Frost Accumulation vs Wet Bulb
H12	"	"	35/30	"	"	"
H13	"	"	17/17	"	"	"
H14	"	"	17/13	"	"	"
H15	"	"	35/35	"	Low	"
H16	"	"	35/30	"	"	"
H17	"	"	17/17	"	"	"
H18	"	"	17/13	"	"	"
H19	"	"	0/0	"	High	Capacity & Frost Accumulation vs Outdoor Air Temp.
H20	"	"	-20/-20	"	"	"

Table 3.6-2

Preprototype Heat Pump - Cooling Test Matrix

Test No.	Indoors DB/WB	Indoors % Air Flow	Outdoors DB/WB	Outdoors % Air Flow	Capacity Mode	Test Type
C1	80/67	Rated	95	Rated	High	DOE Test A
C2	"	"	"	"	Low	"
C3	"	"	82	"	High	DOE Test B
C4	"	"	"	"	Low	"
C5	80/57	"	"	"	High	DOE Test C Dry Coil
C6	"	"	"	"	Low	"
C7	"	"	"	"	High	DOE Test D Cyclic
C8	"	"	"	"	Low	"
C9	80/62	"	95	"	High	Capacity & S/T Ratio vs Wet Bulb Temp.
C10	80/56.4	"	"	"	"	"
C11	80/62	"	"	"	Low	"
C12	80/56.4	"	"	"	"	"
C13	80/67	"	115	"		
C14	"	"	65	"	High	"
C15	"	"	115	"	Low	"
C16	"	"	65	"	"	"

The high speed data acquisition and transmission facilities, combined with fully developed and debugged data reduction computer programs and a highly automated test facility, should ensure rapid completion of the test matrix.

3.6.2 Noise Tests

The outdoor unit will be tested for noise emission in the anechoic chamber according to established standards at both high and low fan speeds.

The indoor unit will be coupled to an outdoor unit and operated as a unit in the open laboratory space. Ductwork will be attached, and noise transmitted through the air stream and radiated from the indoor unit will be measured using portable instrumentation.